Characterization of Clade I TGA Transcription Factors in *Arabidopsis thaliana* with Respect to Biotic Stress

Dissertation

zur Erlangung des mathematisch-naturwissenschaftlichen Doktorgrades

„Doctor rerum naturalium“

der Georg-August-Universität zu Göttingen

vorgelegt von

Martin Muthreich

aus Herne

Göttingen 2014

Thesis Committee

Prof. Dr. Christiane Gatz

(Department of Plant Molecular Biology and Physiology)

Prof. Dr. Volker Lipka

(Department of Plant Cell Biology)

Dr. Corinna Thurow

(Department of Plant Molecular Biology and Physiology)

Members of the Examination Board

Reviewer:

Prof. Dr. Christiane Gatz

(Department of Plant Molecular Biology and Physiology)

Second Reviewer:

Prof. Dr. Volker Lipka

(Department of Plant Cell Biology)

Further members of the Examination Board

Prof. Dr. Ivo Feussner (Department of Plant Biochemistry)

Prof. Dr. Andrea Polle (Department of Forest Botany and Tree Physiology)

PD Dr. Thomas Teichman (Department of Plant Cell Biology)

Jr. Prof. Dr. Cynthia Gleason (JP of Molecular Plant Science)

Date of oral examination: 16.04.2014

Contents

1 Summary

Activation of the plant immune system after pathogen attack involves massive transcriptional reprogramming. In *Arabidopsis thaliana*, clade I TGA transcription factors (TFs) TGA1 and TGA4 have been shown to contribute to defense responses against the virulent biotrophic bacterial pathogen *Pseudomonas syringae* pv. *maculicola* ES4326 (*Psm* ES4326). Here, I report that the *tga14* double mutant is also more susceptible towards the avirulent strain *Pseudomonas syringae* pv. *tomato avrRPS4* (*Pst avrRPS4*). When acting within this signaling cascade, which is activated through the plant immune receptor RPS4, clade I TGA TFs function downstream of EDS1 (ENHANCED DISEASE SUSCEPTIBILTY1) and downstream of the plant defense hormone salicylic acid (SA). However, they function independently from NPR1 (NONEXPRESSOR OF PATHOGENESIS-RELATED GENES 1), a transcriptional co-activator of clade II TGA factors within the SA-dependent defense response systemic acquired resistance (SAR). Microarray analysis unraveled that EDS/SA-activated genes were less expressed in mock-infected *tga14* plants as compared to mock-infected wildtype plants. However, these differences disappeared after infection with *Pst avrRPS4*. It is hypothesized that clade I TGA factors might be necessary for the early induction of defense genes, when SA levels are low, whereas at later stages, when SA levels increase, other transcription factors take over.

Furthermore, microarray analysis revealed that clade I TGA TFs are positive regulators of *ROXY9* and negative regulators of *ROXY11*, *ROXY12*, *ROXY13*, and *ROXY15*. ROXYs are plant-specific glutaredoxin-like proteins that are known to interact with TGA TFs. Previous studies had reported that critical cysteines in TGA1 and potentially TGA4 form an internal disulfide bridge, which is reduced in SA-treated plants. Therefore ROXYs are candidate proteins that might transfer the required electrons from glutathione. In this thesis, a direct influence of ROXY9 on the redox state of TGA1 or TGA4 could not be shown. In addition, the *in vivo* importance of these cysteines could not be demonstrated in vivo because *35S:TGA1* constructs failed to complement the *tga14* phenotype. Pathogen assays performed with *ROXY9* RNAi lines turned out to be too variable to answer the question whether ROXY9 has an influence on avrRPS-triggered resistance. Ectopic expression of *ROXY9* leads to reduced plant growth. Since this effect depends on the presence of clade I TGA TFs, it is concluded that ROXY9 influences the activity of TGA TFs.

2 Introduction

Plants are constantly exposed to pathogens, which try to get access to plant-derived nutrients. Due to this continuous pressure, plants have evolved different strategies to cope with a wide range of pathogens and pests such as viruses, bacteria, fungi, oomycetes and insects (Dangl and Jones, 2001). The plant-microbe interactions are a well-studied example for co-evolution and adaptation (Chisholm et al. 2006). The complex multi-layered plant immune system detects attackers at different stages of infection processes and restricts pathogen propagation (Jones and Dangl, 2006)

2.1 Nonhost resistance

Nonhost resistance is a barrier for nonadapted pathogens and facilitates immunity to a group of plant species against all isolates of an attacker that is infective to other plant species (Nürnberger and Lipka, 2005; Senthil-Kumar and Mysore, 2013). It is the most common form of plant defense responses against a wide range of microorganisms (Lipka et al., 2008). The passive and constitutive type I nonhost resistance does not produce visible symptoms. Pathogen invasion is restricted in an early phase by epidermal wax layers, the plant cell wall and constitutively produced antimicrobial compounds in the apoplast (Heath, 2000; Che et al. 2011). In contrast, inducible type II nonhost resistance is established after recognition of pathogen-associated molecular patterns (PAMPs) or pathogen derived effector molecules (Senthil-Kumar and Mysore, 2013).

PAMPs are invariant structures and indispensable for the microorganism (Postel and Kemmerling, 2009). These structures are recognized by pattern recognition receptors (PRRs) predominantly localized at the plasmamembrane. After recognition, a defense response called PAMP triggered immunity (PTI) is induced (Schwessinger and Zipfel, 2008). The best studied recognition mechanism of a PAMP is the perception of the 22-amino-acid epitope of bacteria-derived flagellin, flg22 (Felix et al., 1999). The PRR FLAGELLIN SENSING 2 (FLS2) was identified in a mutant screen of root growth inhibition after flg22 treatment. It encodes a receptor kinase (RK) with an extracellular leucine rich repeat (LRR) and an intracellular signaling domain (Gomez-Gomez and Boller, 2000; Sun et al., 2013). After activation of the PRRs by binding of their cognate PAMP a complex signaling network is

switched on. The earliest events are calcium fluxes in the cytosol and the nucleus, accumulation of reactive oxygen species (ROS) and nitric oxide (NO) production (Garcia-Brugger et al., 2001; Torres et al., 2002). One mechanism for forwarding the signal cascades during PTI is the activation of mitogen-activated protein kinases (MAPK) (Rasmussen *et al*., 2012). Different WRKY TFs are activated by MAPK-dependent phosphorylation (Ishihama and Yoshioka, 2012) which leads to a transcriptional activation of a set of defense-associated genes like *FLG22-INDUCED RECEPTORKINASE 1* (FRK1) and *PATHOGENESIS RELATED* (*PR*) genes (Asai et al., 2002). PR proteins show an antimicrobial function and are grouped to a 17 members containing familiy in *A. thaliana* (Sels et al., 2008) with the most prominent members PR1, PR2 (β-1,3-glucanase) and PR5 (thaumatin-like protein). Other antimicrobial compounds, which are produced after pathogen attack, are secondary metabolites like phytoalexins (Ahuja et al., 2012). Furthermore, callose deposition and the re-organization of the cell wall by the cell wall-plasma membrane-cytoskeleton play a crucial role during PTI (Vogel et al., 2002; Schulze-Lefert, 2004; Battepati et al., 2011)

2.2 Effector triggered susceptibility (ETS) and immunity (ETI)

The first layer of induced plant defense responses (PTI) is a rapid and effective mechanism but it can be overcome by nonadapted and adapted pathogens. Effector proteins were evolved by the pathogen to disturb or block crucial steps in basal defense responses of the plant. The bacterial needle-like nanomachine **t**ype **t**hree **s**ecretion **s**ystem (T3SS) is an effective instrument to inject effectors into the plant. After injection, the effectors can induce effector triggered susceptibility (ETS) (Chatterjee et al., 2013). For example, the *Pseudomonas* derived effector protein AvrPtoB can trigger the degradation of PRRs via an E3 ubiquitin ligase activity (Gohre et al., 2008; Gimenez-Ibanez et al., 2009).

To overcome ETS, plants evolved *resistance* (*R)* genes interfering with pathogen-derived effector proteins (gene-for-gene-hypothesis; Flor, 1971). Plant R proteins, which are often cultivar specific, consist of a central nucleotide binding pocket (NB-ARC-domain), C-terminal LRRs and are distinguished with respect to their variable N-terminal domain into CC (coiled coil) -NB-LRRs and the TIR (Toll-Interleukin-1 receptor) -NB-LRRs (Elmore et al., 2011). These variable N-termini influence the requirement for distinct downstream signaling components. TIR-NB-LRRs require ENHANCED DISEASE SUSCEPTIBILITY 1 (EDS1), a

homolog to eukaryotic lipases, whereas most CC-NB-LRRs require NON-RACE SPECIFIC DISEASE RESISTANCE 1 (NDR1), a plasma membrane-anchored protein (Arts et al., 1998). The recognition of an effector protein by a plant NB-LRR leads to an incompatible interaction. It provokes a rapid and strong defense response that overruns the ETS. In addition, a strong hypersensitive response (HR) with subsequent cell death occurs. Similar to PTI, ETI triggers cytosolic calcium influx, a ROS burst and NO production (Nimchuck et al., 2003; Nürnberger et al., 2004). The recognized effector protein becomes an avirulence (Avr) protein (Chisholm et al. 2006; Jones and Dangl, 2006).

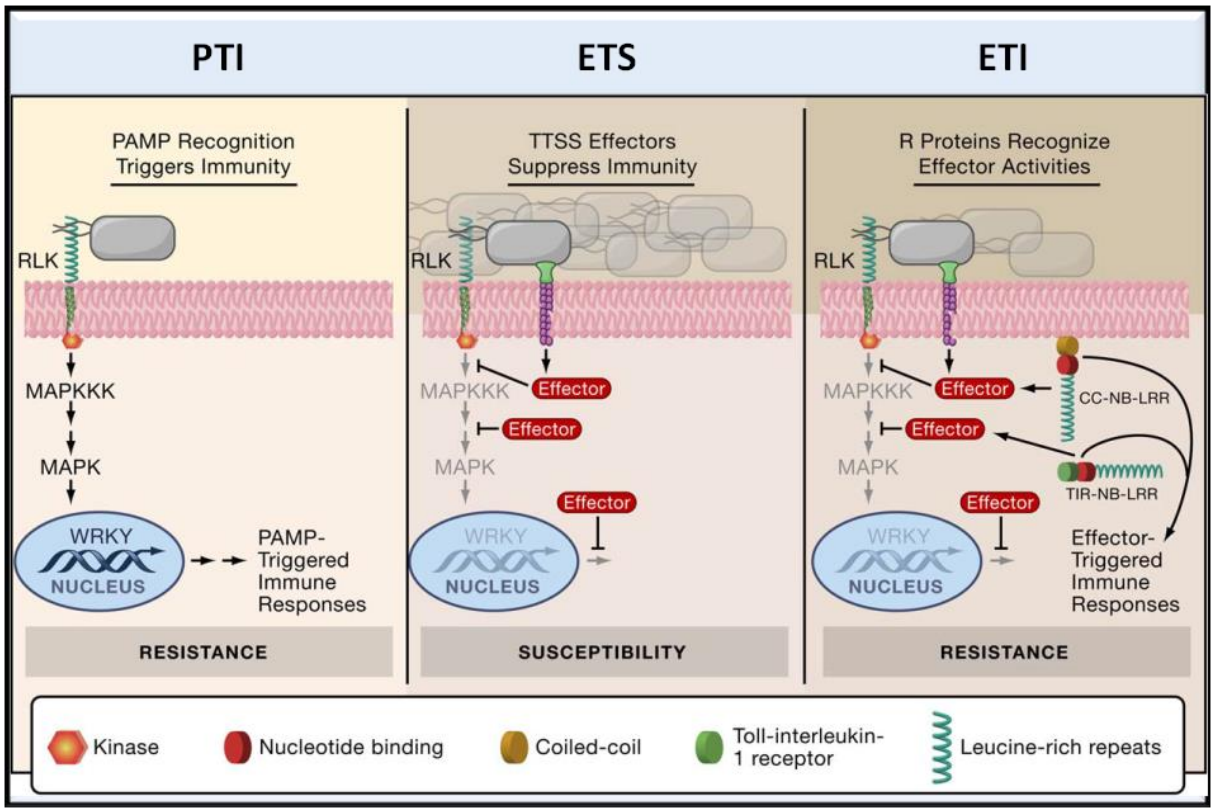

Fig. 2.2: Model for induced plant resistance

PTI: Recognition of PAMPs by RLKs induces basal plant resistance. Signaling is forwarded by MAP kinase cascades and WRKY TFs. **ETS**: Pathogens deliver effectors into the plant affecting basal plant resistance. **ETI**: R proteins recognize pathogen-derived effectors with subsequent activation of plant defense responses. (Chisholm et al., 2006)

Only a few direct interactions of NB-LRRs and Avr proteins are described (Deslandes et al., 2003; Dodds et al., 2006) and two models try to explain how an indirect recognition of effector proteins can lead to R protein-mediated resistance.

An example for the guard hypothesis during ETI is the function of *A. thaliana* RPM1 INTERACTING PROTEIN 4 (RIN4) (Dangl and Jones, 2001; Marathe and Dinesh-Kumar, 2003). RIN4 is a target of different Avr proteins and protects R proteins (Hou et al., 2011). AvrRpt2, a cysteine protease, can cleave RIN4 which leads to the activation of the R protein RPS2 (Axtel and Staskawicz, 2003). Furthermore, AvrRPM1 and AvrB can mediate phosphorylation of RIN4 leading to an activation of the R protein RPM1 (Mackey et al., 2002 & 2003).

In the decoy model a plant protein mimics effector targets (van der Hoom and Kamoun, 2008). The FLS2 protein was revealed as the operative target of AvrPto (Xiang et al., 2008), whereas tomato Pto functions as a decoy for the effector. The Pto protein only functions after being perceived by the effector and does not influence pathogen fitness in the absence of its cognate R protein. To mediate resistance against *P. syringae* strains carrying *avrPto,* the R protein Prf is required. Furthermore, the AvrPto still contributes virulence to tomato in the absence of Pto (Chang et al., 2000).

2.3 Systemic acquired resistance (SAR)

The two layers of induced plant defense response, PTI and ETI, counteract attackers at the local infection site. The recognition of the invaders restricts pathogen development and propagation in an effective way. In addition to these defense responses, plants also evolved a long-lasting, systemic and broad spectrum defense strategy in systemic tissue (systemic acquired resistance (SAR)) (Fu and Dong, 2013). SAR is triggered after PTI and ETS (Mishina and Zeier, 2007) as well as after ETI (Durrant and Dong, 2004). In fact it is rather a "priming" of the plant tissue than an active defense response and allows faster defense activation (Conrath, 2011).

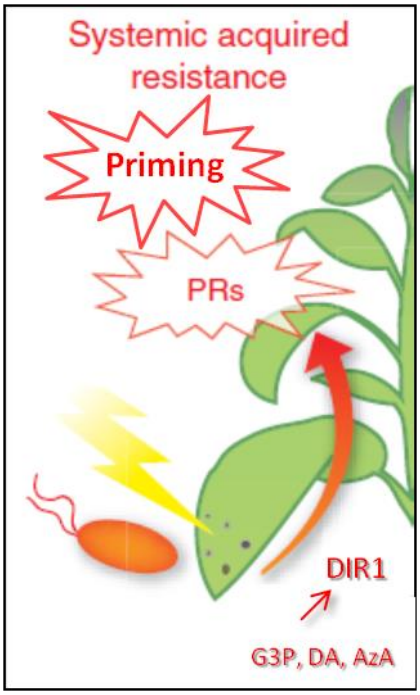

Fig. 2.3: Model for systemic acquired resistance (Pieterse et al., 2009 modified)

Pathogen infection induces mobile signals which travel through the vascular system to activate and prime defense responses in distal and healthy tissue.

After local infection of a plant, a mobile signal is synthesized that establishes the SAR in uninfected tissue. Several candidate mobile signals, like pipecolic acid (Vogel-Adghough et al., 2013), methyl salicylate (MeSA) (Park et al., 2007; Attaran et al., 2009), jasmonic acid (JA) (Truman et al., 2007; Attaran et al., 2009), azelaic acid (Aza) (Jung et al., 2009), glycerol-3-phosphate (G3P) (Chanda et al., 20011) and the abietane diterpenoid dehydroabiential (DA) (Chaturvedi et al., 2011) are described. In addition to these chemical compounds, a lipid transfer protein (LTP), DEFECTIVE IN INDUCED RESISTANCE 1 (DIR1), was found in genetic screens as an important component of the SAR. The *dir1* mutant plants are not affected in local defense response or in perception of a SAR signal. In contrast, a mobile signal is not produced (Maldonado et al., 2002). Remarkably, the DIR1 protein is necessary for AzA, G3P and DA signaling during SAR. Based on these results a possible role in biosynthesis or transport of lipid molecules is discussed (Dempsey and Klessig, 2012).

Because of the long-lasting effect of the SAR, chromatin remodeling of important loci for an enhanced defense response after pathogen attack and a corresponding hereditary immune memory is discussed (van den Burg and Takken, 2009). After infection with the bacterial pathogen *Pseudomonas syringae* pv. *tomato* DC3000 (*Pst* DC3000), the promoters of defense-associated genes *PR1*, *WRKY6* and *WRKY53* display an increased trimethylation at lysine 4 on the histone 3 (H3K4). This methylation is correlated with a subsequent faster

induction of the genes after a second infection and in the following plant generation (Jaskiewicz et al., 2011; Luna et al., 2012).

To monitor a successfully established SAR in the primed systemic tissue, secondary infections, elevated salicylic acid levels or transcription of *PR* genes can be used.

2.4 The role of salicylic acid (SA) in plant defense

Biotrophic and hemibiotrophic plant pathogens need nutrition from living plant tissue to complete their life cycle (Koeck et al., 2011). SA is an important signaling molecule in plant defense response against biotrophic and hemibiotrophic pathogens. The SA-dependent signaling is critical in establishing local and systemic resistance (Chisholm et al., 2006). Upon infection, SA synthesis is induced in local and systemic tissue. Critical enzymatic steps are similar to the bacterial SA biosynthesis. In bacteria, an isochorismate synthase (ICS) converts chorismate to isochorismate followed by SA formation catalyzed by isochorismate pyruvate lyase (IPL) (Mercado-Blanco et al., 2001). In planta, ICS1 is localized in the stroma of chloroplasts. The enzyme shows a high affinity to chorismate derived from the shikimate pathway (Strawn et al., 2007). In contrast, a possible plant IPL was not found until now (Chen et al., 2009). An alternative enzymatic conversion of isochorismate to SA still has to be elucidated.

The mutant *sa induction-deficient 2* (*sid2*), which contains a mutation in the ICS1 protein, produces only 5-10 % of SA after pathogen attack and is affected in local defense response and SAR (Wildermuth et al., 2001). The lack of SA can been overcome by exogenous application of SA or analogs like benzothiadiazole S-methyl ester (BTH) and 2,6-dichloroisonicotinic acid (INA) (Durrant and Dong, 2004). In local leaves, the molecule was excluded as a possible mobile signal initiating SAR (Vernooij et al., 1994).

High concentrations of the electrophilic SA are accumulated after pathogen attack. This property becomes toxic for plants after a while, too. Therefore, SA biosynthesis and SA metabolism are strictly regulated. EDS1 and NDR1 are upstream of SA biosynthesis and affect the accumulation of SA to establish local resistance. After pathogen attack, triggering the TIR-NB-LRR Resistance to Pseudomonas Syringae 4 (RPS4) mediated defense pathway, EDS1 enhances its own expression and SA biosynthesis in a positive feedback loop (Feys et

al., 2001; Heidrich et al., 2011; Bhattacharjee et al., 2011). The interaction of NDR1 with RIN4 mediates multiple SA-dependent disease resistance pathways (Day et al., 2006) and overexpression of NDR1 enhances bacterial disease resistance (Coppinger et al., 2004).

Transcription factors (TF) with a direct influence on *ICS1* expression were identified. In *sar deficient 1-1(sard1-1)/cbp60g* mutants, pathogen-induced up-regulation of *ICS1* and subsequent SA biosynthesis are blocked. These plants are compromised in basal resistance and SAR. Furthermore, a direct binding of SARD1 and CBP60g to the *ICS1* promoter after pathogen attack was shown in electrophoretic mobility shift assays (Zhang et al., 2010).

In addition to the transcriptional regulation of SA biosynthesis, the overall content of active SA *in planta* is modified metabolically. In *A. thaliana*, two SA-inducible SA glucosyl-transferases (SAGT) can detoxify SA via formation of SA glucoside (SAG) (Dean et al., 2005) and salicyloyl glucose ester (SGE) (Vlot et al., 2009). This bioinactive SA stock in the vacuole can be released after pathogen challenge via hydrolysation to become an active signaling molecule.

One major manipulation of cell physiology orchestrated by increased SA levels is an altered intracellular redox homeostasis. After exogenous application of the SA analogon INA, a modification of reduced (GSH) and oxidized (GSSG) glutathione ratio is measurable. This shift results in short oxidizing conditions with subsequent reducing conditions (Mou et al., 2003). The detection of reducing conditions and thereby to increased SA levels is mediated during local resistance and SAR by NPR1 and its paralogs NPR3 and NPR4. In former studies, performed to identify factors acting downstream of SA, NPR1 was found as a central and essential knot responsible for establishing SAR and *PR* gene expression (Cao et al., 1994). NPR1 is characterized by a Broad-Complex, Tramtrack, Brick a Bric/Poxvirus, Zinkfinger (BTB/POZ) protein-protein interaction domain, an ankyrin repeat domain and putative nuclear localization and phosphorylation sites (Cao et al., 1997; Ryals et al., 1997; Kaltdorf and Naseem, 2013). In an uninduced state of the cell, NPR1 forms oligomers in the cytosol and serves as a redox sensor after increased SA levels. Under reducing conditions, the oligomer is released and monomers of NPR1 are shuttled into the nucleus (Mou et al., 2003). After the translocation, *PR* gene expression is activated (Kinkema et al., 2000). Basal NPR1 proteins were also detectable in the nucleus before SA stimulation (Cheng et al., 2009). The conformational change of NPR1 is dependent on one critical cysteine residue at position 156 that forms intermolecular disulfide bridges. A reversible shift of oligomers and monomers is mediated by cytosolic thioredoxins TRX-h3 and TRX-h5 (reduction) and NO driven S-

nitrosylation (oxidation) (Tada et al., 2008). Besides sensing redox changes after increased high SA levels and subsequent NPR1-dependent modification of gene expression in association with TFs, a direct binding of SA to NPR1, NPR3 and NPR4 was described in recent studies.

Fu and colleagues (2012) postulate NPR3 and NPR4 as SA-binding regulators of proteasomal degradation of NPR1 (Figure 2.4). NPR4 shows a higher binding affinity to SA than NPR3. Without its ligand, NPR4 can bind NPR1, followed by subsequent degradation of NPR1 via the proteasome. During basal resistance even low SA concentrations interrupt the interaction of NPR4 and NPR1. Under these conditions, some undegraded NPR1 proteins can still confer resistance. With moderate SA levels, for instance during SAR, the negative effect of NPR4 to NPR1 protein stability is abolished. In this situation, NPR3 proteins binding SA become important for regulation of NPR1 protein stability. SA binding of NPR3 enables the interaction of NPR3 and NPR1, followed by a similar degradation of NPR1 via proteasome. The residual and not degraded NPR1 protein pool can mediate SAR. After local pathogen attack and triggered ETI (incompatible interaction) SA content is increased dramatically. The complete protein pool of NPR1 is subsequently degraded via NPR3 binding SA. In consequence of this lack of NPR1 protein, ETI driven cell death is not suppressed by NPR1 any longer (Rate and Greenberg, 2001). Without suppression the ETI takes place at the infection site for restricting pathogen propagation.

In contrast to these studies, which exclude NPR1 as a SA receptor (Fu et al., 2012), Wu and colleagues (2012) identified the C-terminal transactivation domain (TA) of NPR1 as the SA binding pocket. In plant cells with low SA levels, the BTB domain of NPR1 shows an autoinhibitory function and suppresses the TA domain and therefore NPR1 function. After binding of SA to the TA domain, mediated by copper and the cysteine residues 521 and 529, the autoinhibitory effect is relieved. The conformation of NPR1 protein structure is changed followed by an interaction with TFs via the ankyrin repeats and transcriptional regulation (Figure 2.4).

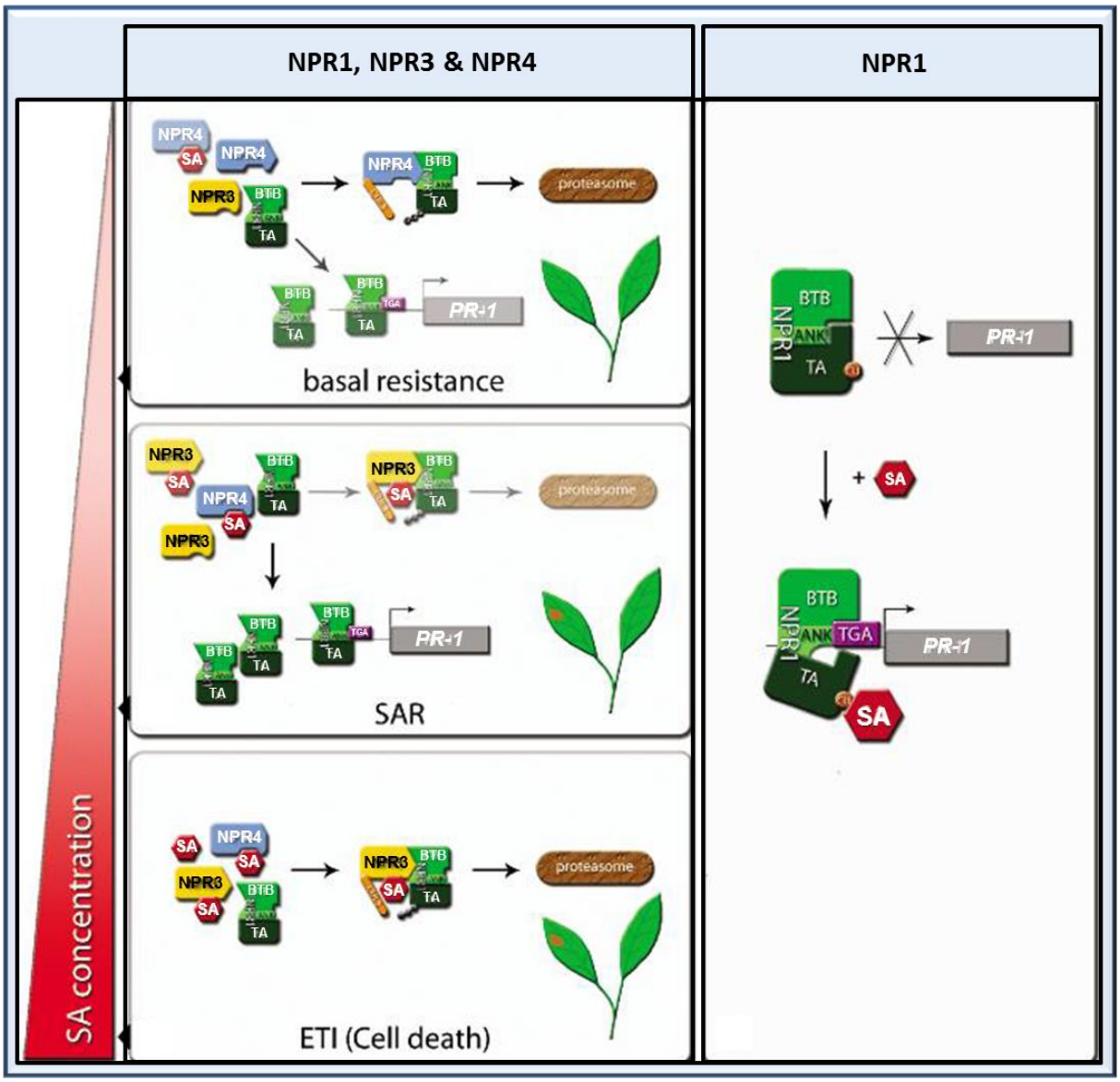

Fig. 2.4: Perception mechanisms of SA in immune signaling (Kaltdorf and Naseem, 2013 modified)

According to Fu et al., 2012: Basal resistance: Low basal SA concentration prefers interaction of NPR1 with unliganded NPR4. Residual unbound NPR1 is not degraded and confers basal resistance. **SAR:** Moderate SA concentrations reduce NPR1-NPR3 interaction. Unbound NPR1 confers SAR. **ETI:** High SA concentrations upon infection promote interaction of NPR1 and NPR3 with fully degraded NPR1 proteins. In the absence of NPR1 ETI with subsequent cell death is triggered. **According to Wu et al., 2012:** NPR1 binds SA directly. Perception relieves repression of the TA domain and interaction with TGA TFs is enabled.

2.5 TGA transcription factors

In *A. thaliana*, the TGA transcription factors (TGA TFs) represent a subgroup of basic leucine zipper domain (bZIP) TFs. The TGA family contains 10 members with different clades (Figure 2.5). TGA1 and TGA4 form clade I, TGA2, TGA5 and TGA6 form clade II, TGA3 and TGA7 form clade III and TGA9 and TGA10 form clade IV (Jakoby et al., 2002; Hepworth et al., 2005). The name of the family is derived from the ability to bind TGACG motifs (Katagiri et al., 1989; Lam et al., 1989). The TGA TFs were highlighted with respect to plant defense response after several members were identified in different yeast two-hybrid screens as interaction partners of NPR1 (Zhang et al., 1999; Zhou et al., 2000). Moreover, direct binding of TGA TFs to the TGACG motif containg *as-1*-like element of the *PR1* promoter was shown (Johnson et al., 2003). Subsequently, several studies gave supporting data for the necessity of TGA TFs for establishing plant defense responses.

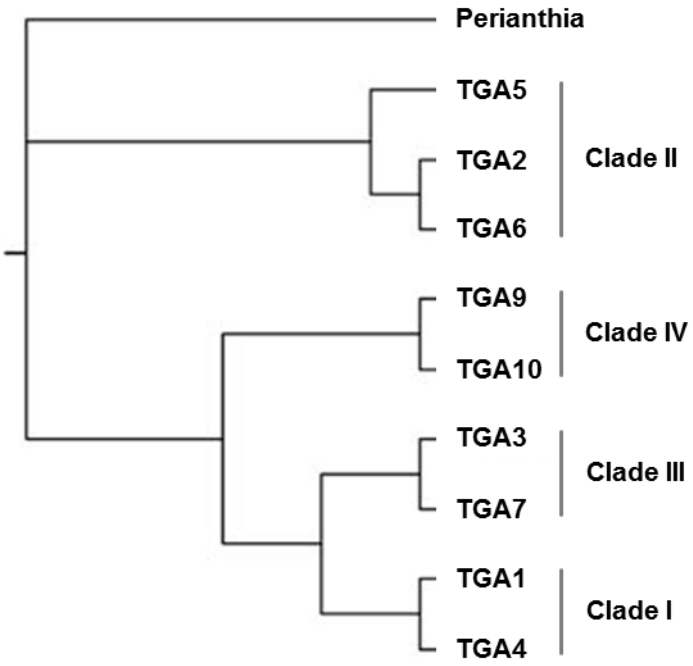

Fig. 2.5: Phylogenetic tree of TGA transcription factor family in *Arabidopsis thaliana* (Hepworth et al., 2005 modified)

TGA TF family consists of 10 members. TGA1 and TGA4 form clade I, TGA2, TGA5 and TGA6 form clade II, TGA3 and TGA7 form clade III and TGA9 and TGA10 form clade IV. Perianthia is not subdivided into a clade.

The clade II TGA TFs can interact with NPR1 directly. They are redundant regulators of SAR and have a dual function in *PR1* gene expression. The triple mutant plant *tga256* shows, similar to the *npr1-1* mutant, a compromised SAR and an increased sensitivity to higher amounts of SA (Zhang et al., 2003), whereas they are not impaired in basal resistance. In contrast to this, *PR1* gene expression is elevated in uninduced *tga2* as well *tga256* mutants. The overexpression of *TGA6* in *tga2* mutant leads to hyperinduction of *PR1*. These results hint at a function of clade II TGA TFs as activators and repressors of *PR* genes (Kesarwani et al., 2007). Supporting data describe the release of TGA2-mediated suppression of *PR1* expression after forming a complex with NPR1 (Boyle et al., 2009).

In addition to the NPR1-dependent involvement in SAR, clade II TGA TFs also execute NPR1-independent functions in *A. thaliana*. The GRAS protein SCARECROW-LIKE 14 (SCL14) interacts with TGA2. Forming a complex is responsible for activation of a broad-spectrum detoxification network after xenobiotic stress. The *scl14* and *tga256* mutants show a similar susceptibility after treatment with the chemicals INA and 2,4,6-triiodobenzoic acid (TIBA), while overexpression of *SCL14* leads to a more tolerant phenotype. Furthermore, SCL14 and TGA proteins are recruited to *as-1*-like sequences containing promoters of detoxification-related genes (Fode et al., 2008).

The function of TGA3, member of clade III TGA TFs and also interactor of NPR1, is assigned to *PR* gene expression. In contrast to clade II TGAs, TGA3 has a positive role in basal defense responses. The *tga3* mutant displays an enhanced susceptibility after infection with the bacterial pathogen *Psm* ES4326. Furthermore, TGA3 seems to be an antagonist of clade II TGA TFs in negative regulation of *PR* gene expression. The elevated *PR1* expression in uninduced *tga256* mutant is abrogated in *tga2356* mutant (Kesarwani et al., 2007), showing the complex regulating network in *PR1* gene expression. The binding capacity of the second clade III TGA TF, TGA7, to cognate promoter elements is enhanced by NPR1 (Shearer et al., 2009). TGA7 recruits the Suppressor of SUPPRESOR OF NPR1, INDUCIBLE 1 (SNI1) (SSN2) to the *PR1* promoter with subsequent release of SNI1-mediated transcriptional repression (Song et al., 2011). Contradictionary results are shown with respect to an affected basal defense response of *tga7* mutants. An increased susceptibility (Song et al., 2011) and a not affected defense response (Kesarwani et al., 2007) are reported.

A special feature of protein modification is described for clade I TGA TFs. In 2000, Despres et al. and Zhou et al. described independently of each other only a weak interaction of TGA1 and TGA4 with NPR1 in yeast two-hybrid (Y2H) assays. In contrast to the other members of

the TGA TF family, both clade I TGAs show conserved cysteine residues at the position 260 and 266 (TGA1) or 256 and 262 (TGA4), which form an internal disulfide bridge. Comparable to NPR1, TGA1 is described as a redox sensor in plant cells and the internal disulfide bridges are sensitive to reducing conditions. While an interaction of clade I TGA TFs with NPR1 is not detectable in yeast, the interaction takes place *in planta* after exogenous application of SA. After an exchange of the conserved cysteine residues of TGA1 and TGA4 an interaction with NPR1 in yeast is enabled (Despres et al., 2003). With respect to modification of the critical cysteine residues in clade I TGAs, Lindermayr et al. (2010) describe a possible S-nitrosylation after treatment with S-nitroglutathione, a physiological NO donor, accompanied with an enhanced NPR1-dependent DNA binding and protection against oxidation.

How these redox modifications of TGA1 and TGA4 are mediated and if they have a biological relevance has to be elucidated. The *tga14* mutant is more susceptible after infection with *Psm* ES4326 (Kersawani et al., 2007). The triple mutant plant *tga14/npr1-1* is more susceptible to *Psm* ES4326 than *npr1-1* and *tga14* mutants (Shearer et al., 2012). These results support a NPR1-independent function of TGA1 and TGA4 in plant defense response. Furthermore, array analysis of SA-treated *tga14* and *npr1-3* mutantss revealed altered expression of NPR1-dependent and NPR1-independent genes in the *tga14* mutant. In addition to NPR1-independent gene expression, *tga14* mutants show *PR* gene expression after infection with *Pst* DC3000 and *Pst avrRpt2* and are not hypersensitive to exogenous SA (Shearer et al., 2012). The most recent study about clade I TGA TFs revealed an impaired PTI. Apoplastic defense responses like an oxidative burst and callose deposition are affected. Interestingly, gene expression of defense-related genes is not impaired, whereas apoplastic PR1 protein accumulation is reduced. Experiments with tunicamycin, an inhibitor of *N*-linked glycosylation that can trigger ER stress and the subsequent unfolded protein response (UPR), revealed a hypersensitivity of *tga14* mutants. These results give hints to an impaired UPR, necessary for decreasing ER stress. Provoked by these results a function of TGA1 and TGA4 as positive regulators of ER-related secretion pathways is proposed (Wang and Fobert 2013).

2.6 Glutaredoxins

After SA and INA treatment or biotrophic pathogen attack the content of reduced glutathione (GSH) is increased and the cellular redox homeostasis is changed (Srivastava and Dwivedi, 1998; Mou et al., 2003). These changes in the GSH:GSSG (oxidized glutathione) ratio can lead to redox modifications of proteins with subsequent regulation of cellular and transcriptional processes (Ghanta and Chattopadhyay, 2011). Possible candidates to mediate protein modifications are thioredoxins (TRXs) and glutaredoxins (GRXs). Interestingly, TGA TFs can interact with a specific group of GRXs.

In *A. thaliana*, 31 GRXs are divided into three groups depending on their active site motifs (Lemaire, 2004). The CPYC and CGFS-type GRXs are found in all species, whereas the CC-type GRXs, also called ROXYs, are specific for land plants. In contrast to thioredoxins, GRXs use GSH as electron donor to regenerate the state of their cysteine residues. Modifications can be mediated by dithiol or monothiol mechanisms. In a dithiol reaction, GRXs reduce disulfides using both active site cysteines. Monothiol mechanisms utilizes only the N-terminal active site cysteine of GRXs for the reduction of GSH mixed disulfides (Lillig and Berndt, 2013).

The land plant-specific ROXYs represent a group of 21 members and they exhibit a conserved C-terminus (Fig. 2.6). A functional relevance of ROXY1, ROXY2, ROXY18 and ROXY19 is described *in planta*. Interestingly, ROXY function is connected to the presence of TGA TFs.

ROXY1 and ROXY2 play a role in floral development (Xing et al. 2005; Xing and Zachgo, 2008). The lack of *ROXY1* results in a reduced initiation of petal primordia and mutant flowers with 2.5 instead of 4 petals (Xing et al., 2005). In contrast, the mutant plants of the TGA TF Perianthia (PAN) initiate five organ primordia with following formation of five petals (Running and Meyerowitz, 1996; Chuang et al., 1999). Studies revealed an interaction between ROXY1 and PAN in the nucleus. Furthermore, a nuclear localization of ROXY1 and an interaction between ROXY1 and PAN are necessary for complementation of petal development. The double mutant plants *roxy1*/*pan* show flowers with five petals, indicating an epistatic role of *PAN* to *ROXY1*. With respect to redox modifications, the mutation C340S in PAN leads to no complementation of the *pan* mutant flowering phenotype. Supported by these results, a modification of PAN by ROXY1 was hypothesized (Li et al., 2009). In

addition, overexpression of *ROXY1* leads to a delayed and stunted plant growth and susceptibility against the necrotrophic pathogen *Botrytis cinerea* (Wang et al., 2008).

For reproductive organ differentiation, ROXY1 and ROXY2 act redundantly. The *roxy1* and *roxy2* mutants are fertile, whereas the double mutant plants *roxy1roxy2* show defects in anther lobe development and microspore production (Xing and Zachgo, 2008). Interestingly, the double mutant plants *tga910* are also male sterile and show defects in anther lobe development, similar to the *roxy1roxy2* mutants. Furthermore, ROXY1/2 and TGA9/10 can interact in the nucleus and loss-of-function mutations of ROXYs and TGAs lead to overlapping changes in the transcriptome. Comparable to the ROXY9/PAN module, a possible modification of TGA9/10 by ROXY1/2 was suggested (Murmu et al., 2010).

While a direct interaction of ROXY1 and ROXY2 with TGA TFs is proven and evidences of a direct effect of GRXs to the TGA function are shown, a direct cysteine modification has not yet been demonstrated.

The expression of *ROXY19/GRX480* is induced by SA and depends on clade II TGA TFs and NPR1. An interaction with TGA2 and TGA6 in Y2H assays was shown. Ectopic expression of *ROXY19/GRX480* in wildtype Col-0 suppresses the jasmonic acid /ethylene (JA/ET) - induced expression of the major regulator of the JA/ET responses, *ORA59* and *PDF1.2*. In contrast, ectopic expression of *ROXY19/GRX480* in the *tga256* plant does not affect *PDF1.2* transcript levels (Ndamunkong et al., 2007). *ROXY19/GRX480* is proposed to mediate the antagonism between the SA and the JA/ET defense pathways (Ndamunkong et al., 2007; Spoel and Dong, 2008).

Zander and colleagues (2012) investigated the redundancy and the functional mechanisms of ROXY-mediated suppression. It was shown that all 21 ROXYs can interact with TGA2 in Y2H assays. In contrast, only ROXYs with a conserved very C-terminal ALWL motif are able to suppress *ORA59* promoter activity in transient assays. Interestingtly, this ALWL motif was also identified as being important for ROXY1 and ROXY2 function with respect to flower development. ROXYs lacking this ALWL motif cannot complement the loss of ROXY1 (Li et al., 2011).

ROXY18/GRXS13 is the closest homolog of ROXY19 and it can also interact with clade II TGA TFs. In contrast to *ROXY19*/*GRX480*, which is induced after SA and JA, *ROXY18*/*GRXS13* is induced by SA and repressed by JA. The *roxy18*/*grxs13* mutant is more susceptible after infection with *Botrytis cinerea*, although induction of *PDF1.2* and *PR1* are

not affected (La Camera et al., 2011). It is not yet known, how ROXY18 contributes to the susceptibility of wildtype Col-0 plants to *B. cinerea*.

Fig. 2.6: Alignment of the conserved C-terminal sequences of CC-type glutaredoxins (Zander et al., 2012)

The C-terminal ALWL motif is shown in orange and the potential interaction motif LxxLL in brown. The sequence of the active site is shown in front of the C-terminal sequences.

2.7 The role of jasmonic acid and ethylene in plant defense

In addition to SA the molecules JA and ET organize the complex defense responses in the plant. The JA pathway is induced after attack of herbivores and the synergistic effect of JA and ET is involved in defense responses against necrotrophic pathogens, which kill plant tissue to take up nutrients.

JA is derived from plastidial α-linolenic acid (Schaller and Stintzi, 2009) and its function is mediated by the JA receptor CORONATINE INSENSITIVE 1 (COI1) (Xi et al., 1998; Chini et al., 2009). In an uninduced state a complex of JASMONATE ZIM-domain (JAZ), TOPLESS (TPL) and NOVEL INTERACTOR of JAZ (NINJA) represses the positive regulator MYC2 (Pauwels et al., 2010). The bioactive (+)-7-iso-jasmonoyl-L-isoleucine (JA-Ile) can bind to JAZ and COI1 (Fonseca et al., 2009). The perception of the signaling molecule initiates the binding of JAZ by the SCF(COI) ubiquitin-ligase complex with subsequent degradation of the protein via the 26S proteasome (Thines et al., 2007). After degradation of JAZ, the repressor complex of JAZ, TPL and NINJA is released from the promoter and the transcriptional activator MYC2 can activate JA-responsive genes like *JAZ10* or *ROXY19/GRX480*.

Together with JA, the gaseous ET is required for plant defense against necrotrophic pathogens. The molecule is perceived at the endoplasmic reticulum (ER) by five ET receptors. ETHYLENE RESPONSIVE1 (ETR1), ETHYLENE RESPONSIVE2 (ETR2), ETHYLENE RESPONSE SENSOR1 (ERS1), ETHYLENE RESPONSE SENSOR2 (ERS2) and ETHYLENE INSENSITIVE4 (EIN4) have an active kinase domain (Stepanova and Alonso, 2009) and act as negative regulators of ET signaling. The ET receptors interact with a second negative regulator of ET signaling, CONSTITUTIVE TRIPLE RESPONSE1 (CTR1), and activate it constitutively (Clark et al., 1998; Gao et al., 2003). CTR1 is a Raf-like protein kinase and it suppresses downstream components of ET signaling. This negative regulation is mediated by SCF(EIN3 BINDING F-BOX1,2) activity (An et al., 2010). After perception of ET the repressive effect of CTR1/ SCF(EBF1,2) to ETHYLENE INSENSITIVE2 (EIN2) and ETHYLENE INSENSITIVE3 (EIN3) is released (Stepanova and Alonso, 2009). The constitutive phosphorylation of EIN2 mediated by CTR1 is blocked in the presence of ET and the C-terminus of EIN2 is translocated into the nucleus to influence gene expression (Ju et al., 2012; Qian et al., 2012; Wen et al., 2012). Stabilized EIN3 promotes the expression of the TFs *OCTADECANOID–RESPONSIVE ARABIDOPSIS AP2/ERF59* (*ORA59*) (Pre et al.,

2008) and *ETHYLENE RESPONSE FACTOR1* (*ERF1*) (Solano et al., 1998). The TF ORA59 is crucial for resistance against the necrotrophic fungus *B.cinerea* (Pre et al., 2008; Berrocal-Lobo et al., 2002) and regulates the expression of defense gene *PDF1.2*.

With respect to JA/ET-signaling the clade II TGA TFs have a dual function. The *tga256* mutant is more susceptible after infection with *B. cinerea* and impaired in JA/ET-induced *PDF1.2* expression. These results indicate a positive role in JA/ET-dependent plant defense responses (Zander et al., 2010). In contrast, TGA2, TGA5 and TGA6 are necessary to integrate the antagonistic effect of SA to the JA/ET-induced *PDF1.2* and *ORA59* expression. This negative effect is suggested to be mediated in cooperation with the SA-inducible GRX ROXY19/GRX480 (Ndamunkong et al., 2007; Zander et al., 2012).

2.8 Aim of the thesis

At the beginning of this work it was known that an interaction between NPR1, crucial for regulating SA-dependent gene expression, and clade I TGA TFs is only enabled in *A. thaliana* leaves after treatment with SA. This interaction comes along with the reduction of clade I TGA TFs specific cysteine residues. Site-directed mutagenesis of the critical residues Cys-260 and Cys-266 in TGA1 also enables interaction with NPR1 in *A. thaliana* and yeast. Furthermore NPR1 enhances the binding of TGA1 to the *as-1* element (Despres et al., 2003).

Since the critical cysteine residues of clade I TGA TFs are reduced by SA and since TGA TFs interact with ROXY-type glutaredoxins (Ndamukong et al., 2007), they have been discussed as being redox-modulated by ROXY oxireductase activity.

Provoked by these data and suggestions, the questions of the relevance and the mechanism of redox modifications at the critical cysteine residues of clade I TGA TFs with respect to plant resistance were addressed:

- ➔ Is the role of clade I TGA TFs in plant defense response dependent on NPR1 and SA?
- ➔ What are possible target genes of clade I TGA TFs?
- ➔ Has the reduction of clade I TGA TFs an importance in gene regulation?
- ➔ What is the mechanism of the redox modification of clade I TGA TFs?

3 Material and Methods

3.1 Materials

3.1.1 Devices

Device	Model	Source
Autoclave	3870 ELV	Tuttnauer
Autoclave	VX95	Systec
Balance	Extend	Sartorius
Balance	SPO51	Scaltec
Blotting Device (semi-dry)		University Göttingen
Blotting Device (wet)	Criterion Blotter	BioRad
Chambers for PAGE		University Göttingen
Chambers for PAGE	Mini-PROTEAN® tetra System	BioRad
Chambers for DNA-gel		University Göttingen
Chemocam		Intas
Cooling centrifuge	Sorvall RC6+	DuPont
Cooling cntrifuge	Rotina 38R	Hettich
Cooling micro centrifuge	Fresco17	Thermo Scientific
Counting chamber	Thoma	
Electroporator	Gene Pulser® II	BioRad
Fluorometer	Centro XS^3 LB 960	Berthold Technologies
Gel documentation device		MWG Biotech
Heating block	TH26	HLC
Heated shaker	MHR11	HLC

Heated stirrer	IKA® RH basic 2	IKA
Ice machine		Ziegra
Incubator	Certomat BS-1	Sartoriusstedim biotech
Microcentrifuge	Pico17	Thermo Scientific
Microscope	DM5000B	Leica
PCR Cycler	MyCycler	BioRad
pH -Meter	pH211	Hanna Instruments
Photometer	Libra S11	Biochrom
Photometer for microtiter plates	Synergy HT	BioTek
qRT-PCR cycler	iCycler	BioRad
RNA-/DNA-Calculator	NanoDrop 2000	Thermo Scientific
Sonication device	Soniprep 150	MSE
Clean bench	Heraguard	Thermo Scientific
Clean bench	SAFE 2020	Thermo Scientific
Water deionization device	arium® pro DI	Sartorius
Vacuum pump	Cyclo 1	Roth
Vortex	Vortex Genie 2	Scientific Industries

3.1.2 Consumables

Product	Source
Blottinge paper 3MM	Whatman
Cover slips	Roth
Filter paper Miracloth	Calbiochem
Leukopor®	BSNmedical
Micotiter plates 96-wells	Greiner bio-one
Microtiter plates 384-wells	Greiner bio-one
Object plates	Roth
Parafilm M	Pechiney Plastic Packaging
Plastic one-way material	Biozym, Eppendorf, Greiner, Roth, Sarstedt
PVDF membrane Immobilon-P	Milipore
Tissue Culture Plate 24-Well	Sarstedt

3.1.3 Chemicals

Chemical	Source
30 % (w/v) Acrylamide: N,N´-methylenebisacrylamide (37.5:1)	Roth
Agarose	Biozym
ammoniumthiocyanate	Sigma Aldrich
Ampicillin (Amp)	AGS
AMS	Sigma Aldrich
APS (Ammonium persulfate)	Biometra
Beef extract	BD Biosciences
Bromophenol blue	Roth

BSA	Serva
diamide	Sigma Aldrich
EDTA	Applichem
Ethidiumbromide	Roth
Fat-free milk powder	commercial
Fluoresceine	BioRad
GELRITE	Duchefa
Gentamycine (Gen)	Duchefa
hypochloric solution	Sigma Aldrich
Kanamycine (Km)	Sigma
luminol	Sigma Aldrich
β-Mercaptoethanol	Roth
Methyl jasmonate (MeJa)	Sigma Aldrich
MES	Roth
Murashige and Skoog medium (MS medium)	Duchefa
NEM	Sigma Aldrich
Orange G	Sigma
Peptone	BD Biosciences
Phenol	Sigma
Rifampicine (Rif)	Duchefa
Salicylic acid (SA)	Merck
Select Agar	Life Technologies
Select yeast extract	Gibco BRL
Sucrose	Roth

SYBR Green I	Cambrex
TCA	Sigma Aldrich
TEMED	Roth
Tetracycline	AGS
Tryptone	Oxoid
Tween20	Roth

3.1.4 Kits

Kit	Source
Advantage® 2 Polymerase Mix	Clontech
BioTaq DNA Polymerase Kit	Bioline
Dual-luciferase reporter assay system	Promega
Ionic Detergent Compatibility Reagent	Thermo Scientific
iProof High-Fidelity PCR kit	BioRad
Luminata™ Forte Western HRT Substrate	Milipore
Nucleo Spin® Gel and PCR Clean-up	Macherey-Nagel
Nucleo Spin® Plasmid	Macherey-Nagel
Nucleo Spin® Plasmid PC500 Maxi Prep Kit	Macherey-Nagel
Nucleo Spin® Plasmid PC100 Midi Prep Kit	Macherey-Nagel
Pierce 660nm Protein Assay Kit	Thermo Scientific
RNeasy Plant Mini Kit (50)	Qiagen
SuperSignal® West Femto	Thermo Scientific

3.1.5 Enzymes

Enzyme	Source
Biotaq DNA polymerase	Bioline
Cellulase Onozuka R-10	Serva
Clonase-Mix (BP, LR)	Invitrogen

DNaseI	Thermo Scientific
iProof high fidelity DNA polymerase	BioRad
Horse radish peroxidase	Sigma-Aldrich
Macerozyme R-10	Serva
Reverse transcriptase H-	MBI Fermentas
Restriction enzymes	MBI Fermentas, New England Bioloabs
RNAse A	Qiagen
T4 DNA-ligase	MBI Fermentas

3.1.6 Standards

Standard	**Source**
GeneRuler DNA Ladder Mix	MBI Fermentas
Prestained Protein Ladder	MBI Fermentss

3.1.7 Antibodies

Antibody	**Source**
Goat-anti-rabbit	Pierce
HA-tag antibody ChIP grade	Abcam

3.1.8 Nucleic Acids

3.1.8.1 Plasmids

Plasmid	Description	Reference
pDONOR201-TGA1	*TGA1* CDS was amplified by PCR from cDNA with specific primers exhibiting GW sequences. The PCR product was cloned into pDONR201 by BP reaction.	M. Zander
pDONOR201-TGA1red	Critical cysteine residues in TGA1 CDS were exchanged to serines with specific primers and a full length fragment was created by overlapping PCR. The PCR product was cloned into pDONR201 by BP reaction.	this thesis
pDONOR223-TGA4	*TGA4* CDS was amplified by PCR from cDNA with specific primers exhibiting GW sequences. The PCR product was cloned into pDONR223 by BP reaction.	this thesis
pDONOR223-TGA4red	Critical cysteine residues in TGA1 CDS were exchanged to serines with specific primers and a full length fragment was created by overlapping PCR. The PCR product was cloned into pDONR223 by BP reaction.	this thesis
pDONR223-ROXY9	*ROXY9* CDS was amplified by PCR from cDNA with specific primers exhibiting GW sequences. The PCR product was cloned into pDONR223 by BP reaction.	M. Zander
pDONR201-ROXY13	*ROXY13* CDS was amplified by PCR from cDNA with specific primers exhibiting GW sequences. The PCR product was cloned into pDONR201 by BP reaction.	this thesis
pDEST-GAD-HA-TGA1	LR reaction was performed using pDEST-GAD-HA and pDONR201-TGA1.	this thesis
pDEST-GAD-HA-TGA1red	LR reaction was performed using pDEST-GAD-HA and pDONR223-TGA1red.	this thesis
pDEST-GAD-HA-TGA4	LR reaction was performed using pDEST-GAD-HA and pDONR223-TGA4.	this thesis
pDEST-GAD-HA-TGA4red	LR reaction was performed using pDEST-GAD-HA and pDONR223-TGA4red.	this thesis

pDEST-GAD-HA-TGA2	LR reaction was performed using pDEST-GAD-HA and pDONR223-TGA2.	M. Zander
pDEST-GBKT7-Myc-NPR1	LR reaction was performed using pDEST-GAD-HA and pDONR201-NPR1.	C. Thurow
pDEST-GBKT7-Myc-ROXY9	LR reaction was performed using pDEST-GAD-HA and pDONR223-ROXY9.	M. Zander
pDEST-GBKT7-Myc-ROXY13	LR reaction was performed using pDEST-GAD-HA and pDONR201-ROXY13.	this thesis
pDEST-GBKT7-Myc-ROXY19	LR reaction was performed using pDEST-GAD-HA and pDONR201-ROXY19.	M. Zander
pCU425-CTR1-HA-TGA1	LR reaction was performed using pCU425-CTR1-HA and pDONR201-TGA1.	this thesis
pCU425-CTR1-HA-TGA1red	LR reaction was performed using pCU425-CTR1-HA and pDONR201-TGA1red.	this thesis
pCU425-CTR1-HA-TGA4	LR reaction was performed using pCU425-CTR1-HA and pDONR201-TGA4.	this thesis
pCU425-CTR1-HA-TGA4red	LR reaction was performed using pCU425-CTR1-HA and pDONR201-TGA4red.	this thesis
pCU423-CTR1-HA-ROXY9	LR reaction was performed using pCU425-CTR1-HA and pDONR223-ROXY9.	this thesis
pCU423-CTR1-HA-ROXY9C24A	Cysteine residue 24 in ROXY9 (pDONR223-ROXY9) was exchanged to alanine with specific primers and a full length fragment was created by overlapping PCR. The PCR product was cloned into pCU423-CTR1 by LR reaction.	this thesis
pE-SPYNE-TGA1	LR reaction was performed using pE-SPYNE and pDONR201-TGA1.	this thesis
pE-SPYNE-TGA1red	LR reaction was performed using pE-SPYNE and pDONR201-TGA1red.	this thesis
pE-SPYNE-TGA4	LR reaction was performed using pE-SPYNE and pDONR221-TGA4.	this thesis
pE-SPYNE-TGA4red	LR reaction was performed using pE-	this thesis

	SPYNE and pDONR201-TGA1red.	
pE-SPYCE-ROXY9	LR reaction was performed using pE-SPYCE and pDONR223-ROXY9.	this thesis
pE-SPYCE-ROXY13	LR reaction was performed using pE-SPYNE and pDONR201-ROXY13.	this thesis
pB2GW7.0-HA-TGA1	LR reaction was performed using pB2GW7.0-HA and pDONR201-TGA1.	this thesis
pB2GW7.0-TGA1	LR reaction was performed using pB2GW7.0 and pDONR201-TGA1.	this thesis
pB2GW7.0-HA-TGA1red	LR reaction was performed using pB2GW7.0-HA and pDONR201-TGA1red.	this thesis
pB2GW7.0-TGA1red	LR reaction was performed using pB2GW7.0 and pDONR201-TGA1red	this thesis
pB2GW7.0-HA-TGA4	LR reaction was performed using pB2GW7.0-HA and linearised pDONR223-TGA4.	this thesis
pB2GW7.0-TGA4	LR reaction was performed using pB2GW7.0 and linearised pDONR223-TGA4.	this thesis
pB2GW7.0-HA-TGA4red	LR reaction was performed using pB2GW7.0-HA and linearised pDONR223-TGA4red.	this thesis
pB2GW7.0-TGA4red	LR reaction was performed using pB2GW7.0 and linearised pDONR223-TGA4red.	this thesis
pB2GW7.0-HA-ROXY9	LR reaction was performed using pB2GW7.0-HA and linearised pDONR223-ROXY9.	M. Zander
pUBQ10-HA-TGA1	LR reaction was performed using pUBQ10-HA and pDONR201-TGA1.	this thesis
pUBQ10-TGA1	LR reaction was performed using pUBQ10 and pDONR201-TGA1.	this thesis
pUBQ10-HA-TGA1red	LR reaction was performed using pUBQ10-HA and pDONR201-TGA1red.	this thesis
pUBQ10-TGA1red	LR reaction was performed using pUBQ10 and pDONR201-TGA1red.	this thesis
pUBQ10-HA-TGA4	LR reaction was performed using pUBQ10-HA and linearised pDONR223-TGA4.	this thesis
pUBQ10-TGA4	LR reaction was performed using pUBQ10 and linearised pDONR223-TGA4.	this thesis

pUBQ10-HA-TGA4red	LR reaction was performed using pUBQ10-HA and linearised pDONR223-TGA4red.	this thesis
pUBQ10-TGA4red	LR reaction was performed using pUBQ10 and linearised pDONR223-TGA4red.	this thesis

3.1.8.2 Oligonucleotides for qRT-PCR

Gene	**fwd Primer** **sequence 5´→ 3´**	**rev Primer** **sequence 5´→ 3´**
CRK7	CACAGGACTTGGTGACACATGC	ACCACTTCACTCTTCCGGCAAC
CRK36	AACATGGATGAGACTCGAGGAGAG	TCCGGAGCCATATATCCGTAGG
CRK37	AGACGCGGAGATGAACCCTAAG	GTCCATATCGAACAGCCTTGCC
EDS1	QuantiTect	QuantiTect
ICS1	QuantiTect	QuantiTect
JAZ7	QuantiTect	QuantiTect
JAZ8	QuantiTect	QuantiTect
JAZ10	QuantiTect	QuantiTect
NUDT5	CTGAGATCCATGCTGCTAAGTGG	CCCTCCTTGTTGTGATAGGGTTGG
NUDT6	CCTAGTACTCTTCCTGCCAATGCG	AATCTCCTGGACCACAAGCACCTC
PAD4	AGATACGCGAGCACAACGCAAG	TTCTCGCCTCATCCAACCACTC
PDF1.2	CTTGTTCTCTTTGCTGCTTTC	CATGTTTGGCTCCTTCAAG
PR1	CTGACTTTCTCCAAACAACTTG	GCGAGAAGGCTAACTACAACTAC
ROXY1	AGCTTAGGATTCGGCGGTTTGG	AGCCAGGGACTCTATACGAAGCAG
ROXY2	ATGCCATCAAGCGTCTCTTCCG	TTCAACTCCGTAAGGGAGGAGGTC

ROXY3	TTAGGCTGTAGCCCTACGGTTC	TGGCCGTTCCTACGAATTTCCC
ROXY4	CTTTCTTGACCATCGCAAATGGAG	TGTGAATATCACCGCCGCTTTC
ROXY5	GCTCGTGTTGCATGTGTCATAGC	TCAAGCTCATGGATGGCAGGAC
ROXY8	AGAAGGCCTTAGTTCGTCTTGGC	AACCCACGAGCTTGCCACTTAC
ROXY9	TTGTCGGAGGCAAGCTTGTTGG	TGGGACAAGAGAGCCACTAAGGTG
ROXY10	AGCCAACGAGGTCATGAGTCTAC	AGCCCGCTTAAGCATGGGAATC
ROXY11	GCGTGAACCCGACGATCTATGAAC	CCTATGAACACCACTGGCACTGTC
ROXY12	ACTTTGGCGTGAACCCGACTATC	CCAATGCTTGCTCTATCTCCCTTC
ROXY13	TCCATCTCAATCGCTCTCTGGTTC	ATCAAAGCCATAGTGCTCCAACCC
ROXY14	TTCATAGGAGGGCAGCTTGTCG	AGCATTGGAATGAGAGAACGGTTG
ROXY15	TTGGCGTGAACCCGACAATC	GCCAAGCTGAGCCAATGCATAC
ROXY16	AGAGCTCGTAGGTGGTGCAAATC	GCAACGAAGCTAGTTGGTTCCTG
ROXY17	GGGCAACAATTCATCGGTGGTG	TTGCGGCTAGCTGGTTCTTGAC
ROXY18	QuantiTect	QuantiTect
ROXY19	QuantiTect	QuantiTect
ROXY21	TAGCAACGATCGGCGTAATCCC	TGGGAAGAGAGGAAACCTCGTG
TGA1	ACGAACCTGTCCATCAATTCGG	CCATGGGAAGTATCCTCTGACACG
TGA4	AAAGTCGTTTGCGCAAGAAAGC	AGCATTGGTATCTACTCCGTTCCC
VSP2	CAAACTAAACAATAAACCAT ACCATAA	GCCAAGAGCAAGAGAAGTGA
WRKY38	QuantiTect	QuantiTect
WRKY54	QuantiTect	QuantiTect
WRKY70	QuantiTect	QuantiTect

3.1.8.3 Oligonucleotides for cloning

Construct	fwd Primer sequence 5´→ 3´	rev Primer sequence 5´→ 3´
TGA1	GGGGACAAGTTTGTACAAAAAA GCAGGCTCCATGAATACAACCTC GACACATTTTG	GGGGACCACTTTGTACAAGAAAGC TGGGTCTAACTCAAACCTACGTTGG TTCACG
TGA1red	GTAAATAATCTAAAACAATCGAG TCAGCAAGCAGAAGACGCG	GCTTGCTGACTCGATTGTTTTAGAT TATTTACATCTAGAAGT
TGA4	GGGGACAAGTTTGTACAAAAAA GCAGGCTCCATGAATACAACCTC GACACATTTTG	GGGGACCACTTTGTACAAGAAAGC TGGGTCCATCTAAACACCTTAATTA CGTTGG
TGA4red	GTAAATAATCTGAGGCAATCAAG TCAACAAGCAGAAGATGCG	GTTGACTTGATTGCCTCAGATTATT TACATCCAAAAGTTGTTGATCCG
ROXY9C24A	CTCATGTTGTCTCGCTTACGCCGT TCAAATCC	GTAAGCGAGACAACATGAGCTCTTC GTGAAGATCACC
ROXY13	GGGGACAAGTTTGTACAAAAAA GCAGGCTCCATGGATAAGCTACA GAAGATGATCTCCGAG	GGGGACCACTTTGTACAAGAAAGC TGGGTCTGAAATCAAAGCCATAGTG CTCC
ROXY9 Promoter	GGGGACAAGTTTGTACAAAAAA GCAGGCTTAAACACCACACCAGT CAACACC	GGGGACCACTTTGTACAAGAAAGC TGGGTCGCATGTAAAAAGCTTGACA TTTGCTCG
ROXY13 Promoter	GGGGACAAGTTTGTACAAAAAA GCAGGCTAAGGATAGATTATGA GGCAGGGTAC	GGGGACCACTTTGTACAAGAAAGC TGGGTCGCATGTAGTGAAGGGTCTC TAAGGGTCC

3.1.8.4 Oligonucleotides for sequencing

Plasmid	fwd Primer sequence 5´→ 3´	rev Primer sequence 5´→ 3´
pDONR201	TCGCGTTAACGCTAGCATGGATCTC	GTAACATCAGAGATTTTGAGACAC
pDONR223	ACGACGTTGTAAAACGACGGCCAG	TAATACGACTCACTATAGGG

3.1.8.5 Oligonucleotides for genotyping

Mutant	fwd Primer sequence 5´→ 3´	rev Primer sequence 5´→ 3´
eds1-2	ACACAAGGGTGATGCGAGACA	GGCTTGTATTCATCTTCTATCC
eds1-2		GTGGAAACCAAATTTGACATT
npr1-1	AGGCACTTGACTCGGATGAT	ATGCACTTGCACCTTTTTCC
sid2-2	CTCAATTAGGTGTCTGCAGTGAAGC	GTTGTAGCAAAAACCGTAATGATCG
tga1	GCGTGGACCGCTTGCTGCAACT	
tga4	GCGTGGACCGCTTGCTGCAACT	GTTCCACCGAGAAGGTTTG

3.1.9 Organisms

3.1.9.1 Bacteria

Species	Properties	Reference
Agrobacterium tumefaciens GV3101	PMP90RK *rifr, gmr*	(Koncz and Schell, 1986)
Escherichia coli DB3.1	F-, *gyr*A 462, *end*A1, D(*sr*1-*rec*A), *mcr*B, *mrr*, *hsd*S20 (rB-	(Bernard et al. 1993)

	m_{B^-}), *sup*E44, *ara*-14, *gal*K2, *lac*Y1, *pro*A2, *rps*L20(Sm_r), *xyl*-S, λ-leu, *mtl*-1	
Escherichia coli DH5α	F-, *gyr*A 96 (Nalr), *rec*A1, *end*A1, *thi*-1, *hsd*R17 (rk-mk+), *gln*V44, *deo*R, D (*lac*ZYA-*arg*F) U169 [p80dD(*lac*Z)M15]	(Hanahan 1983)
Pseudomonas syringae pv. tomato DC3000	pVSP61 rif, km	(Hinsch and Staskawicz, 1996)
Pseudomonas syringae pv. tomato DC3000 avrRPS4	pVSP61 expressing *Pseudomonas syringae* pv. *pisi* effector AvrRps4 rif, km	(Hinsch and Staskawicz, 1996)
Pseudomonas syringae pv. maculicola ES4326	rif	(Whalen et al., 1991)
Pseudomonas syringae pv. maculicola ES4326 avrRPM1	rif, tetra	(Ritter and Dangl, 1995)

3.1.9.2 Yeast

Strain	**Properties**	**Reference**
PJ69-4A	*MATa trp1-901 leu2-3, 112 ura3-52 his3-200 LYS2::GAL1-HIS3 GAL2-ADE2 met2::GAL7-lacZ*	(James et al., 1996)
YPH499	*MATa ura3-52 lys2-801_amber ade2-101_ochre trp1-Δ63 his3-Δ200 leu2-Δ1*	(Terziyska et al., 2005)

YPH499 *Δgrx1Δgrx2*	*MATa ura3-52 lys2-801_amber ade2-101_ochre trp1-Δ63 his3-Δ200 leu2-Δ1URA3 KanMX4*	(Terziyska et al., 2005)

3.1.9.3 Fungal cultivars

Strain	**Reference**
Botrytis cinerea BMM	Provided by Brigitte Mauch-Mani (University of Neuchatel, Switzerland)

3.1.9.4 Plant genotypes

Genotype	**Description**	**Reference**
Columbia, Col-0	Wildtype	NASC stock no. N1902
tga14 mutant	knockout line lacking two class I TGA transcription factors, impaired in basal defense	Y. Zhang, (Kesarwani et al., 2007)
tga1 mutant	single knockout of TGA1	this thesis
tga4 mutant	single knockout of TGA4	this thesis
tga256 mutant	knockout line lacking all three class II TGA transcription factors, impaired in systemic acquired resistance	(Zhang et al. 2003); X.Dong (Duke University, Durham, USA)
sid2-2 mutant	SA-induced deficient	(Wildermuth et al., 2001)
tga14/sid2-2 mutant	double cross of *tga14* and *sid2-2*	this thesis
npr1-1 mutant	Knock out line lacking functional NPR1	(Cao et al., 1994)
tga14/npr1-1 mutant	double cross of *tga14* and *npr1-1*	this thesis

tga14::35S:HA-TGA1	overexpression line, expressing the *TGA1* gene under the control of the CaMV *35S* promoter, n-terminal 3xHA-tag	this thesis
tga14::35S:TGA1	overexpression line, expressing the *TGA1* gene under the control of the CaMV *35S* promoter	this thesis
tga14::35S:HA-TGA1red	overexpression line, expressing the *TGA1* gene under the control of the CaMV *35S* promoter, n-terminal 3xHA-tag	this thesis
tga14::35S:TGA1red	overexpression line, expressing the *TGA1* (C260/266S) gene under the control of the CaMV *35S* promoter	this thesis
tga14::35S:HA-TGA4	overexpression line, expressing the *TGA4* gene under the control of the CaMV *35S* promoter, n-terminal 3xHA-tag	this thesis
tga14::35S:TGA4	overexpression line, expressing the *TGA4* gene under the control of the CaMV *35S* promoter	this thesis
tga14::35S:HA-TGA4red	overexpression line, expressing the *TGA4* gene (C256/262S) under the control of the CaMV *35S* promoter, n-terminal 3xHA-tag	this thesis
tga14::35S:TGA4red	over-expression line, expressing the *TGA4* (C256/262S) gene under the control of the CaMV *35S* promoter	this thesis
Col-0*::35S:HA-ROXY9*	overexpression line, expressing the *ROXY9* gene under the control of the CaMV *35S* promoter,n-terminal 3xHA-tag	this thesis
tga14::35S:HA-ROXY9	overexpression line, expressing the *ROXY9* gene under the control of the CaMV *35S* promoter, n-terminal 3xHA-tag	this thesis

3.1.10 Growing Media

Medium	Content
dYT medium for bacteria	20 g/L tryptone, 10 g/L yeast extract, 10 g/L NaCl
King´s B medium for bacteria	10 g/L Proteose-Pepton No 3, 1,5 g/L K_2HPO_4, 15 g/L glycerol (86%), pH 7.0, after autoclaving 2 mM $MgSO_4$
LB medium for bacteria	10 g/l tryptone, 5 g/L Yeast extract, 10 g/L NaCl
MS-MES medium for plants	4.4 g/L MS medium, 1.0 g/L MES, pH 5.7 with KOH, 6.8 g/L select agar
YEB medium for bacteria	10 g/L beef extract, 2 g/L yeast extract, 5 g/L peptone, 5 g/L sucrose, pH 7.0 with NaOH, after autoclaving 2 mM $MgSO_4$
YPAD medium for yeast	6 g/L yeast extract, 12 g/L peptone, 12 g/L glucose
PDA for fungi	Merck
PDB for fungi	Fulda
SD medium for yeast	4 g/L Yeast Nitrogen Base, 12 g/L glucose, appropriated synthetic complete drop out mix, pH 5.6 with NaOH

3.1.11 Standard Buffers

Buffer	Content
Buffer B+	10 mM Tris-HCl (pH 7.5 at 37°C), 10 mM MgCl2, 0.1 mg/mL BSA

Buffer G+	10 mM Tris-HCl (pH 7.5 at 37°C), 10 mM MgCl2, 50 mM NaCl, 0.1 mg/mL BSA
Buffer O+	50 mM Tris-HCl (pH 7.5 at 37°C), 10 mM MgCl2, 100 mM NaCl, 0.1 mg/mL BSA
Buffer R+	10 mM Tris-HCl (pH 8.5 at 37°C), 10 mM MgCl2, 100 mM KCl, 0.1 mg/mL BSA
Buffer Y+	33 mM Tris-acetate (pH 7.9 at 37°C), 10 mM magnesium acetate, 66 mM potassium acetate, 0.1 mg/mL BSA
TAE (20x)	0.8 M Tris, 2.3 % (v/v) acetic acid, 20 mM EDTA
TBS (10x)	24.2 g Tris, 80 g NaCl, pH 7.6
TBS-T (1x)	1× TBS + 0.1 % Tween 20
SDS-PAGE running buffer	250 mM Tris, 2 M glycine, 1 % SDS
Westernblot buffer	25 mM Tris, 188 mM glycine, 20 % methanol

3.2 Methods

3.2.1 Standard molecular methods

3.2.1.1 Isolation of plasmid DNA from bacteria

3.2.1.1.1 Alkaline lysis of *E.coli*

For isolation of plasmid DNA 2 mL of an *E. coli* o/n culture was centrifuged for 1 min at 13000 rpm. The supernatant was discarded and the pellet was resuspended in 100 µL buffer I (50 mM Tris-HCl pH 8.0, 10 mM EDTA, 100 µg/ µL RNase A). After adding 200 µL buffer II (0.2 M NaOH, 1% SDS (w/v)) the cells were lysed on ice for 5 min. The suspension was neutralized with 150 µl buffer III (29.6 g potassium acetate, 5 mL formic acid and water to 100 mL) and the reaction tube was inverted for 6-8 times. After centrifugation for 10 min at 13000 rpm (RT) the aqueous solution (400 µL) was transferred into a new reaction tube and the DNA was precipitated with 1 mL of ice cold ethanol (96 %, v/v) for 15 min. The precipitated DNA was centrifuged for 20 min at 13000 rpm (4°C) and the pellet was washed with ethanol (70 %, v/v). The air dried pellet was dissolved in 25 µl water.

3.2.1.1.2 Alkaline lysis of *A. tumefaciens*

Before an *Agrobacterium*-mediated gene transfer to *A. thaliana* was performed, 5 mL of the pre-culture of transformed *A. tumefaciens* cells GV3101 were centrifuged for 1 min at 13000 rpm. The pellet of the pre-culture was dissolved with 300 µL buffer I (50 mM Tris-HCl pH 8.0, 10 mM EDTA, 100 µg/ µL RNase A) and the cells were lysed with additional 300 µL buffer II (0.2 M NaOH, 1% SDS (w/v)) for 5 min at RT. Neutralization was achieved with addition of 300 µl buffer III (29.6 g potassium acetate, 5 mL formic acid and water to 100 mL) and incubation on ice for 5 min. The solution was centrifuged at 13000 rpm for 10 min (RT) and the supernatant (600 µL) was mixed with 500 µL PCI-mix (phenol/ chloroform I-mix). The mixture was vortexed for 3 sec and after centrifugation at 13000 rpm for 1 min the aqueous supernatant (500 µL) was mixed with 500 µL PCI-mix again. After vortexing (3 sec) and centrifugation for 1 min at 13000 rpm the DNA in the aqueous supernatant (700 µL) was

precipitated with 500 µL 2-propanol. The pellet was washed after centrifugation for 15 min at 13000 rpm with 1 mL ethanol (70 %, v/v) and air dried at RT. The dry pellet was dissolved with 15 µL water.

3.2.1.1.3 Isolation of high-quality plasmid DNA

High-purity plasmid DNA was isolated for sequencing, cloning and transformation. According to requirements the manufacturer instructions of Macherey-Nagel Mini, Midi and Maxi Kit were followed.

3.2.1.2 Measurement of DNA and RNA concentrations

The concentration of nucleic acids was determined by measuring their absorption in a NanoDrop 2000 at a wave length of 260 nm (maximum nucleic acid absorption value, due to the π-electron systems of the heterocycles of the nucleotides). Absorption at 280 nm (due to the presence of aromatic rings from amino acids and phenol compounds) was used for references of the purity of the DNA or RNA samples. The optimal ratio of OD_{260}/OD_{280} for RNA is from 1.9-2.0 and for DNA 1.8.

3.2.1.3 Separation of DNA on agarose gels

The DNA was separated electrophoreticly in horizontal 1 % agarose gels with 1x TAE buffer. With respect to the size of estimated DNA fragments the run was performed in 2 % agarose gels (< 500 kb) or 1.0 % agarose gels (< 4000 bp). DNA samples were mixed with 1/10 volume of 10x DNA loading buffer, loaded in separate lanes and run at 120 V for 45 min. The gels were stained in ethidiumbromide solution (0.1 % w/v) for 15 min and the detection of the DNA was performed on an UV-transilluminator (260 nm). The signals were documented with a gel-documentation station. For elution of DNA fragments the visualization was done with larger wavelength UV-light (320 nm) and the cut DNA fragments were eluted with the NucleoSpin® Gel and PCR Clean-up Kit (Macherey-Nagel).

3.2.1.4 Digestion of DNA

For analytical and cloning purpose type II endonucleases were used for digestion of double stranded DNA molecules. The incubation of the digestion was done at the temperature and in the optimized buffer systems with respect to the manufacturer instructions. The enzymes cut the DNA either as 5´or 3´ "sticky" overhangs or as blunt ends. 1 U of the restriction enzymes cutting completely 1 µg of λ DNA (48000 bp) in 60 minutes at optimal conditions, whereupon the required amount of enzyme was determined for every reaction according to the following formula:

U = (bp[λ] x number of restriction sites in target DNA) / (number of restriction sites in [λ] x bp of target DNA)

3.2.1.5 Ligation of DNA fragments

For conventional cloning the T4-DNA ligase enzyme was used. The enzyme is able to catalyze the formation of a phosphodiester chemical bond between free 5´-phosphate and 3´-OH groups of double stranded DNA fragments and vectors. The vector DNA was incubated with 10x accessed donor DNA fragment, 2 µL of ligation buffer and 1 µL of T4-DNA ligase for 2 hours at room temperature. Blunt ended DNA fragments were incubated in the presence of 5 % (w/v) PEG 4000. To stop ligase activity the solution was heated up to 65°C for 10 min and following it was used for transformation.

3.2.1.6 Gateway cloning

The gateway® technology is based on the site specific recombination of bacteriophage lambda and thereby provides a fast method to exchange DNA fragments between multiple vectors without the use of conventional cloning strategies (Landy 1989, Hartley et al. 2000). All cloning steps done with the gateway® system were performed as described in the Invitrogen manual, Version E, September 22, 2003.

3.2.1.7 Sequencing of DNA

Sequencing of plasmid DNA was performed with SeqLab. Minimum 600 ng plasmid DNA was mixed with 20 pmol required primer and water was added to a final volume of 7 µL.

3.2.1.8 Gene transfer into *E. coli*

The transformation of chemical competent *E. coli* cells was done with the heat shock method according to Hanahan (1983). An aliquot of competent cells (200 µL) was thawed for 10 min on ice, 50 ng of plasmid DNA were added and the mixture was incubated for 30 min on ice. Afterwards the cells were shocked at 42°C for 90 sec, 800 µl dYT medium were added and the transformed cells were incubated for 1h at 37°C. The cells were streaked on plates containing LB medium and the required antibiotics. Incubation took place o/n at 37°C.

3.2.1.9 Gene transfer into *A. tumefaciens*

Electrocompetend *A. tumefaciens* GV3101 cells were transformed by electroporation method. On ice thawed cells were mixed with high-quality plasmid DNA, an electric pulse (2.5 kV, 25 µF, 400 Ω) was applied for 5 s and the cells were immediately incubated with 1 mL YEB medium for 2 h at 30°C. Different amounts of transformation mix were spreaded on selective YEB plates and incubated for 2-3 days at 30°C. Transformed cells from plate were grown o/n in 25 mL YEB liquid medium with appropiate antibiotics at 30°C. 5 mL of the pre-culture were used for plasmid extraction (3.2.1.1.1.2) and the rest was transferred into a selective 400 mL YEB liquid main-culture for *Agrobacterium*-mediated gene transfer to *A. thaliana*.

3.2.1.10 *Agrobacterium*-mediated gene transfer to *A. thaliana*

For transformation of *A. thaliana* flowering plants were dipped into an *Agrobacterium* solution (OD600 = 0.8) according to Clough (2005). A 400 mL selective YEB liquid culture were harvested by centrifugation (2500 rpm, 30 min) and the cells were dissolved in 5 %

sucrose solution mixed with 0.05 % Silwet-L77. The dipped plants were covered o/n with a hood. After seed development selection was performed with integrated selection markers on transgenic DNA.

3.2.1.11 Isolation of genomic DNA from *A. thaliana* for genotyping

Genomic DNA was isolated to perform PCR-based genotyping of F2 generation plants after crossing of different plant genotypes and to amplify promoter sequences. To avoid contaminations the lid of a 1.5 mL reaction tube was used to cut discs from leaf tissue. With a small pestle the plant tissue was homogenized with 100 µL of extraction buffer (200 mM Tris-HCl pH 7.5, 250 mM NaCl, 25 mM EDTA, 0.5 % SDS) in the reaction tube and the mixture was filled up with 300 µL extraction buffer. After centrifugation for 5 min at 13000 rpm and 4°C the supernatant was mixed with 300 µl 2-propanol for precipitation of the DNA. After centrifugation for 5 min at 13000 rpm and RT the pellet was washed with 200 µL 70 % ethanol and dissolved in 100 µl water (ultra-pure, 65°C, 10 min).

3.2.2 Plant growth conditions

3.2.2.1 Plant growth conditions on soil

Surface sterilized seeds were sown on steamed soil (Archut, Fruhstorfer Erde, T25, Str1 fein) supplemented with Confidor (50 mg/L) and fertilizer (0,5 ml/L Wuxal) and stratificated at 4°C for two days. The plants were grown under short day conditions (22°C/ 18°C, 80-100 µmol Photones/m^2/s, 8h light/16h dark, 60 % humidity), long day conditions (22°C/ 18°C, 80-100 µmol photones/m^2/s, 16h light/8h dark, 60 % humidity) or 12h/12h-light cycle conditions (22°C/ 18°C, 80-100 µmol photones/m^2/s, 12h light/12h dark, 60 % humidity).

3.2.2.2 Plant growth conditions on axenic plates

Surface sterilized seeds were sown on MS-MES plates under the clean bench and sealed with Leukopor®. After stratification of 2 days at 4°C the plants grown under 14h/10h-light cycle conditions (22°C/ 18°C, 80-100 µmol Photones/m^2/s, 14h light/10h dark, 60 % humidity) for 12 to 14 days.

3.2.3 Surface sterilization of *A. thaliana* seeds

Seeds were sterilized in an exsiccator with a mixture of 100 mL hypochloric solution and 5 mL hydrochloric acid. The exsiccator was closed with a weak vacuum. After 2h (soil grown plants) or 4 h (axenic plates) the vacuum and the gaseous phase were released under a clean bench.

3.2.4 Generation of *A. thaliana* triple mutants

To get the *tga14/sid2-2*, *tga14/npr1-1* and *tga14*/*eds1-2* triple mutants the F1 plants of crossed genotypes *tga14* and *sid2-2* or *npr1-1* were allowed to self-fertilize. The F2 populations were screened for homozygosity by using PCR. The *tga1* and the *tga4* alleles were identified according to Kesarwani et al (2007) and the *sid2-2* allele was identified according to Wildermuth et al (2001). The *npr1-1* mutation was identified by using PCR and additional digestion of PCR products according to Cao et al (1994).

3.2.3 Transcript analysis

3.2.3.1 RNA extraction

TRIZOL method (Chomczynski 1993) was used to extract RNA from plant tissue. Phenol/chloroform (dichloromethane) extraction dissolves RNA in the aqueous phase while other compounds like chlorophyll or proteins are solved in the hydrophobic chloroform phase.

RNAse activity is inhibited by two thiocyanate compounds in the extraction buffer. Deep frozen fine powder (~200 mg) of grinded plant tissue (2 mL reaction tube) was dissolved in 1.3 mL extraction buffer (380 mL/L phenol saturated with 0.1 M citrate buffer pH 4.3, 0.8 M guanidinthiocyanate, 0.4 M ammoniumthiocyanate, 33.4 mL 3 M Na-acetate pH 5.2, 5 % glycerol) and shaked for 15 min at RT. Chloroform (260 µL) was added to every sample and after an additional shaking step of 15 min at RT the samples were centrifuged for 30 – 40 min at 12.000 rpm and 4°C. The clear supernatant (~ 900 µL) was transferred into a new 1.5 mL reaction tube and 325 µL of precipitation buffer (HSB, 1.2 M NaCl, 0.8 M Na-citrate) and 325 µl of 2-propanol were added, the samples inverted and incubated for 10 min at RT. After centrifugation for 20 min at 12.000 rpm and 4°C the supernatant was discarded, the pellets were washed two times with 70 % ethanol and afterwards dried at RT. The pellets were dissolved in 20-60 µL water (ultra pure) and the concentration was measured after freezing and thawing (65°C, 5 min) of the samples as described in 3.2.1.2.

3.2.3.2 Preparation of cDNA

RNA was digested with DNase I to prevent gDNA contamination of cDNA. 1 µg of RNA, 1 µL of 10x DNase I reaction buffer and 1 µL DNase I were added with RNase-free water to a final reaction volume of 10 µL and incubated at 37°C for 30 min. For denaturation of the Dnase I 1 µl 25 mM EDTA was added to the reaction and incubated at 65°C for 10 min. cDNA synthesis was performed with 1 µg RNA (DNA-free), 20 pmol of oligo-dT primer, 200 pmol random nonamer oligonucleotides and a final volume of 12.5 µl (water). After annealing for 10 min at 70°C, 20 nmol dNTPs, 4 µL RT 5x reaction buffer and 60 U reverse transcriptase H- were added and the reaction with a final volume of 20 µL was incubated at 42°C for 70 min and afterwards at 70°C for 10 min.

3.2.3.3 Quantitative Realtime RT-PCR (qRT-PCR)

For quantification of cDNA qRT-PCR was performed with *Ubiquitin 5* (*UBQ5*) as reference gene and the fluorescence intensity was measured with the iCycler from BioRad. The reaction consisted of 1 µL of 1:10 diluted cDNA, 1x NH_4-reaction buffer, 2 mM $MgCl_2$, 100 µM dNTPs, 0.4 µM primers, 0.25 U BIOTaq DNA polymerase, 10 nM fluoresceine, 100000 times

diluted SYBR Green I solution and 17.2 µL water. PCR started with a denaturation for 6 min and 95°C followed by 40 cycles of 20 s at 95°C, 20 s at 55°C and 40 s at 72°C. For melting curve analysis the samples were finaly incubated at 72°C for 4 min. Calculation of relative gene expression was done with the $2^{-[C_T(\text{gene of interest})-C_T(\text{reference gene})]}$ method (Schmittgen and Livark 2008).

3.2.3.4 Microarray analysis

The transcriptomes of Col-0 and *tga14* plants after infection with *Pst avrRPS4* (OD_{600} = 0.02) for 3h, 6h 11h and 24 h were compared by microarray analysis. Plants were grown for 4 weeks in 12 h light/ 12 h light – cycle conditions and were infiltrated as described in 3.2.5.1.2. Total RNA was extracted according to the TRIZOL method (3.2.3.1) and purified using the RNeasy Plant Mini Kit (50). Quality control and hybridization were done by the Integrierte Funktionelle Genomik of the Westfälische-Universität Münster. For every sample the leaf material of 9 plants was pooled.

3.2.4 Protein analysis

3.2.4.1 Protein extraction from plant tissue

Proteins were extracted from ground plant tissue under denaturing conditions. The deep frozen plant powder (~ 200 µL) was thawn in 600 µl extraction buffer (4 M urea, 16.6 % glycerol, 5 % SDS, 0.5 % β-mercaptoethanol) while shaking at 65°C for 10 min. Afterwards the solution was centrifuged for 20 min at 13000 rpm and RT and the supernatant was used for SDS-PAGE.

3.2.4.2 Protein extraction form yeast cells

For protein extraction of yeast cells 2 mL of an o/n culture were centrifuged for 1 min at 13000 rpm and RT and the pellet was frozen in liquid nitrogen twice. The deep frozen pellet

was supplemented with 40 µl extraction buffer (8 M urea, 5 % SDS, 40 mM Tris-HCl pH 6.8, 0.1 mM EDTA, 0.4 mg/ L bromophenol blue, 0.01 % β-mercaptoethanol) and incubated in a thermomixer for 10 min and 70°C. After centrifugation for 1 min at 13000 rpm at RT the supernatant was used for SDS-PAGE.

3.2.4.3 Determination of protein concentrations

Due to the high concentrations of detergents in the extraction buffers the protein concentration was measured with the Pierce 660 nm protein assay kit and the ionic detergent compatibility reagent according to the manufacturer instructions.

3.2.4.4 SDS-PAGE

Proteins were separated on the basis of their polypeptide length in sodium dodecyl sulfate-polyacrylamide gel electrophoresis (SDS-PAGE) using a discontinuous buffer system. The stacking gel (5% (w/v) acrylamide/ bisacrylamide (37.5:1), 125 mM Tris-HCL pH 6.8, 0.1 % (w/v) SDS, 0.2 % (w/v) TEMED, 0.1 % (w/v) APS) with a non-restrictive pore size was followed by the resolving gel (10-12 % (w/v) acrylamide/ bisacrylamide (37.5:1), 400 mM Tris-HCL pH 8.8, 0.1 % (w/v) SDS, 0.1 % (w/v) TEMED, 0.1 % (w/v) APS). The denatured protein samples (3.2.4.1) were load to the stacking gel and the electrophoresis was performed at 80 V with 1x SDS-running buffer (250 mM Tris, 2M glycine, 1% SDS) for 30 min. After formation of an equal and straight sample layer in the stacking gel the run was performed for additional 2-4 h at 140 V until bromophenol blue band exit the lower end of the gel. A prestained ladder (6µl) was used for estimating the size of the protein signals.

3.2.4.5 Immunoblot analysis

In order to detect proteins that had been separated by SDS-PAGE a western blot was performed at which the proteins were transferred to a PVDF membrane using a semi-dry or wet-blot method. The stacking gel of the PAA gels was removed with a scalpel and resolving gel was released from the glass plates into 1x transfer buffer for equilibration of 10 min.

Afterwards PVDF membrane was activated in 100 % MeOH, three layers of Whatman paper (pre-soaked with 1x transfer buffer) were placed in the blot chamber and the activated PVDF membrane, the equilibrated PAA gel and three additional layers of pre-soaked Whatman paper were stacked. The transfer of the proteins was performed at a current rating of 1 mA/ cm^2 for 2 h. After blotting, the membrane was blocked for 1 h at RT with TBS-T containing 5 % (w/v) non-fat dry milk. Incubation with primary antibody (TBS-T/ 5 % MP) was done over night at 4°C on a shaking platform and after washing the membrane 3 x 15 min with TBS-T the primary antibody was detected using horseradish peroxidase (HRP)-conjugated goat anti-rabbit secondary antibody diluted 1:25000 in TBS-T/ 5 % MP at RT for 2 h on a shaking platform. The membrane was washed 5 x 10 min with TBS-T, incubated with chemilumenescence kits according to manufacturer instructions and fixed between to plastic sheets. The prestained protein ladder was marked on top of the plastic sheet and the luminescence was detected in a chemocam (Intas).

3.2.4.6 Coomassie staining

The membranes were stained with coomassie staining solution for 1 h at RT and destained with water until the background was gone. Coomassie staining solution consists of 400 mL solution A 840 g ammonium sulfate and 8 ml phosphoric acid) and 10 mL solution B (0.5 g Coomassie Brilliant Bue G-250).

3.2.5 Pathogen assays

3.2.5.1 Infection of *A. thaliana* with *Pseudomonas syringae*

3.2.5.1.1 Cultivation of *Pseudomonas syringae*

Glycerol stocks frozen at -80°C were used for preparing freshly grown colonies on King´s B agar plates with appropriate antibiotics. The streaked bacteria were incubated o/n at 30°C and the plates were stored at 4°C for maximum 2 weeks. For infection of *A. thaliana* plants 20 mL King´s B were supplemented with 100 µL 1 M $MgSO_4$ and the required antibiotics. The bacteria were incubated o/n at 30°C and 220 rpm. The o/n cultures were centrifuged for 10 min at 4000 rpm and the pellet was washed 2 times with 20 mL 10 mM $MgCl_2$. The OD_{600} of the washed cells were measured and the required OD_{600} was prepared by dilution with 10 mM $MgCl_2$.

3.2.5.1.2 Infiltration of plants with *Pseudomonas syringae*

For infection of *A. thaliana* with *P. syringae* fully expanded leaves of plants grown under SD- or 12h light/ 12h darkness-conditions were infiltrated with a needleless syringe. The blunt end of the syringe was pressed carefully onto the abaxial side next to the midnerve and the leaves were fixed with the finger tip. The infiltration with slide pressure was stopped until 75 % of the leaf tissue was soaked with the bacterial solution. Drops of residual bacterial solution were removed with tissue and the petioles of the infiltrated leaves were labeled with a pen. The plants were incubated for 1 h at the bench until the dark soaked pattern of the leaves was gone. Control plants were infiltrated with $MgCl_2$. The plants were placed back into the climate chambers for incubation.

3.2.5.1.3 Bacterial growth assay

For the determination of the bacterial growth 3 leaves per plant were infiltrated with bacterial solution (virulent strains OD_{600} = 0.0001, avirulent strains OD_{600} = 0.002) and three leaf discs (4 mm diameter) per leaf were cut at 0 dpi and 3 dpi. The 9 leaf discs per plant were transferred into a 2.0 mL reaction tube filled with 10 mM $MgCl_2$/ 0.2 % Silwett L77 and the reaction tubes were shaked for 10 min on a vortex. Afterwards appropriate dilutions were prepared with 10 mM $MgCl_2$ and 10 µL of every dilution were dropped to King´s B agar plates with the appropriate antibiotics. The plates were incubated at 28°C for 2-3 days and the colony-forming units (CFU) per cm^2 leaf surface area were calculated.

3.2.5.1.4 Induction of the systemic acquired resistance

For SAR experiments three local (lower) leaves were infiltrated with *Psm* (OD_{600} = 0.2) and control plants were infiltrated with $MgCl_2$. For a successful experiment the contact of other plant tissue with any drops of the bacterial solution should be circumvented. After incubation of the plants for 48 h in the climate chamber three systemic (upper) leaves were harvested for gene expression analysis.

3.2.5.2 Infection of *A. thaliana* with *Botrytis cinerea*

For infection of *A. thaliana* with *B.cinerea* plants were grown under 12h light/ 12h darkness-conditions. 5 fully expanded leaves per plant were drop inoculated with 4 µl of *B. cinerea* spore solution (5 x 10^4 spores/ ml) or ¼ PDB media as mock control. For high humidity conditions infection was performed in sealed gas-proofed tanks. The lesion size was determined with a caliper.

3.2.6 Chemical treatments of *A. thaliana*

3.2.6.1 Salicylic acid

Soil grown plants or axenic plates were sprayed with 1 mM SA until the surfaces were equally moistened and incubated for different times. Control plants were sprayed with water.

3.2.6.2 Methyl jasmonate

MeJA treatment was done in a gas-proof tank. Pieces of filter paper were soaked with MeJA (1 µL MeJA/ $L_{air\ volume}$) and sticked to the inner surface of the tank. The soil grown plants or the axenic plates were incubated for different times in the sealed tank (grease). Control plants were incubated in sealed tanks without MeJA.

3.2.6.3 Flagellin 22

Axenic plates with 12-14 days old seedlings were moistened with 1 µM flg22 solved in water. Control plants were sprayed with water.

3.2.6.4 N-depletion of *A. thaliana* seedlings

Experiment was done according to Scheible et al (2004) and composition of media was changed with respect to available chemicals and microelements. Seeds were surface sterilized for 4 h and sterile flasks with 30 ml liquid FN medium were supplemented with 100 seeds. Flasks were agitated at 30 rpm for 2 days and at 80 rpm for 6 additional days under constant light (50 µmol photons/cm^2/min). After over all 8 days medium was exchanged against fresh FN or FN- medium. Flasks were agitated for 1 additional day and seedlings were harvested.

Compounds	FN medium	FN- medium
KNO_3	2 mM	0,1 mM
NH_4NO_3	1 mM	50 µM
Glu	1 mM	
KCl		3 mM
KH_2PO_4/K_2HPO_4 pH 5.8	3 mM	3 mM
$CaCl_2$	4 mM	4 mM
$MgSO_4$	1 mM	1 mM
K_2SO_4	2 mM	2 mM
Sucrose	0,5 %	0,5 %
FeEDTA	40 µM	40 µM
H_3BO_3	60 µM	60 µM
$MnSO_4$	14 µM	14 µM
$ZnSO_4$	1 µM	1 µM
$CuSO_4$	0,6 µM	0,6 µM
$NiSO_4$	0,4 µM	0,4 µM
$HMoO_4$	0,3 µM	0,3 µM
$CaCl_2$	20 nm	20 nM

3.2.7 Transient promoter activity studies by protoplast transformation

3.2.7.1 Protoplast isolation

Protoplast isolation was performed according to the method described by Sheen (2001). The lower surface of leaves of 4-6 week old plants grown in 12h/ 12h light cycle was lightly scratched with a razor blade and scored leaves were placed in a petri dish containing 10 mL enzyme solution. After incubation over night in 12/ 12 light cycle the digested solution was filtrated (75 µM mesh) and the protoplasts were centrifuged (2 min, 780 rpm, soft start and stop). The pellet was washed two times with 10 mL W5 solution (10 min, 780 rpm, soft start and stop) and afterwards the protoplasts were subsequently incubated for 4-6 h on ice.

3.2.7.2 Protoplast transformation

The W5 solution covering the protoplasts was discarded carefully and the pellet was dissolved in MMg solution (250 µL/ transformation). For every transformation 200 µL of protoplasts were added to a mixture of at least 13.5 µg DNA (5 µg promoter:*Firefly luciferase* plasmid, 1 µg UBQ10:*Renilla luciferase* plasmid, 7.5 µg effector plasmid) in a 2 mL reaction tube. The reaction tubes were carefully inverted, 220 µl PEG solution was added and after further half turn of the reaction tubes the mixture was incubated for 30 min at RT. Afterwards the transfected protoplasts were diluted with 800 µl W5 buffer and sediment stepwise by 3x centrifugation (2 min, 780 rpm, soft start and stop). In between centrifugation the supernatant was discarded stepwise and the pellet was subsequently dissolved in 200 µl WI solution. The protoplasts were incubated overnight in 12h/ 12h light cycle and after discarding the supernatant the pellet was frozen in liquid nitrogen. During protoplast preparation cut tips were used.

3.2.7.3 Measurement of luciferase activity

For luciferase activity measurement the Centro XS^3 LB 960 plate reader (Berthold technologies) and the Dual-luciferase reporter assay system (Promega) were used. Before the protoplasts were lysed, the plate reader was primed with the necessary substrates for renilla (Stop&Glo buffer + substrate, 1:50 diluted) and firefly (LARII) luciferase. Afterwards the frozen protoplasts were supplemented with 20 µl PassivLysisBuffer (diluted 1:5 with water), thawn on ice and 3 µl of every reaction tube were transferred into a single well of a 348 well-plate. The plate was covered with parafilm and stored on ice. Every single measurement was done as followed: 30 sec waiting time, injection of 15 µl LARII, 5 sec waiting time, measurement of firefly activity for 5 sec, injection of 15 µl Stop&Glo, measurement of firefly activity for 5 sec.

3.2.7.4 Buffers used for protoplast isolation and transformation

Solution	**Content**
Enzyme solution	1-1.5 % cellulose R10, 0.2-0.4 % macerozyme R10, 0.4 M mannitol, 20 mM KCl, 20 mM MES pH 5.7
PEG solution (40 %, v/v)	4 g PEG4000, 3 ml H_2O, 2.5 mL 0.8 M mannitol, 1 mL 1 M $CaCL_2$
Washing and incubation solution (WI)	0.5 M mannitol, 4 mM MES pH 5.7, 20 mM KCl
W5 solution	154 mM NaCl, 125 mM CaCl2, 5 mM KCl, 2 mM MES pH 5.7
MMg solution	0.4 M mannitol, 15 mM MgCl2, 4 mM MES pH 5.7

3.2.8 Analysis of protein-protein interactions

3.2.8.1 Yeast-Two-Hybrid

3.2.8.1.1 Transformation of Yeast

Yeast transformation was done according to Gietz and Woods (2002). The yeast strains were inoculated in a 20 µL o/n culture of liquid YPAD medium at 220 rpm and 30°C. Next day 50 mL (10 transformations) of a fresh liquid YPAD culture with an OD_{600} = 0.5 was prepared and incubated at 220 rpm and 30°C until an OD600 = 1.8 was reached. Afterwards the cells were washed in 25 mL sterile water (4000 rpm, 5 min) and resuspended in 1 mL of sterile water. The cells were transferred into a 1.5 mL reaction tube and centrifuged for 30 sec at 13000 rpm. After the supernatant was discarded sterile water was added to a final volume of 1.0 mL and 100 µl aliquots were pipetted into 1.5 mL reaction tubes. The reaction tubes were centrifuged for 30 sec at 13000 rpm, the supernatant was discarded and the pellets were dissolved in 360 µl transformation mix (240 µl 50 % (w/v) PEG 3500, 36 µl 1 M LiAc, 50 µl boiled HSP, 1 µg per plasmid in 34 µl sterile water). After incubation for 40 min at 42°C the transformation mix was centrifuged and the pellets dissolved in 1.0 mL sterile water. Appropriate aliquots of the cells were plated onto SD selection medium and the plates were incubated for 2-3 days at 30°C.

3.2.8.1.2 ONPG-Assays

With the ONPG-assay the strength of protein-protein interaction in yeast cells was quantified. The used yeast strain PJ69-4A contains the *lacZ* gene form *E. coli* which codes for β-galactosidase. The expression is controlled by the GAL4 factor protein which is assembled after protein-protein interaction (pDEST-GAD-HA, pDEST-GBKT7-Myc). The activity of the GAL4 factor can be quantified by photometric measurement of the product ONP (420 nm) after cleavage of ONPG by the GAL4 controlled β-galactosidase. For the ONPG-assay transformed yeast cells were grown over night in 5 mL liquid selective SD medium at 30°C and 220 rpm and afterwards 3 mL were centrifuged for 1 min at 13000 rpm at RT. The pellets were washed in 1 mL Z-buffer (60 mM Na_2HPO_4, 40 mM NaH_2PO_4, 10 mM KCl, 1.0 mM

$MgSO_4$, pH 7.0) and finally dissolved in 300 µl Z-buffer. An aliquot of 100 µl was transferred into a new 1.5 ml reaction tube and frozen (liquid nitrogen) and thawn at 37°C for three times. The broken yeast cells were supplemented with Z-buffer + 27% (v/v) β-mercaptoethanol and inverted and subsequently 160 µl of the ONPG solution (4 mg/mL o-nitrophenyl-β-D-galactopyranoside in Z-buffer) were added. The reaction was stopped after the solution turns from clear to yellow colour with 400 µl 1 M Na_2CO_3. After centrifugation (10 min, 13000 rpm, RT) of the samples, 200 µl supernatant were transferred into a 96-well plate and the OD_{420} was measured in a plate reader. For calculation of the enzymatic reaction the time of incubation and the OD of the remaining 200 µl yeast cells were determined. The enzymatic reaction was calculated as followed: β-galactosidase activity [u] =1000 x OD_{420} / reaction time in min x OD_{600}.

3.2.8.2 Bimolecular fluorescence complementation (BiFC)

3.2.8.2.1 Transformation of protoplasts

The isolation and the transformation of protoplasts were done as described in 3.2.7.1 and 3.2.7.2. In contrast, the protoplasts were incubated on top of round cover slips supplied with short parts of rubber hose as spacers in tissue culture plates (24-well) filled with WI buffer (700 µL) and were transformed with the required plasmids (pE-SPYNE, pE-SPYCE, 7.5 µg). After the pellet was dissolved with 40 µl WI buffer the protoplasts were transferred (cut tips) to the cover slips already submerged in WI buffer. During incubation overnight in 12h/ 12h light cycle the protoplasts settled down and stick to the surface of the cover slip.

3.2.8.2.2 Microscopy

The microscopy was done with the microscope DM5000B (Leica). After incubation of the protoplasts over night the cover slips were lifted carefully with a forceps out of the 24-well plate and the spacers were removed. The cover slips were transferred to object slides and the interspace was filled with 10 µl WI buffer. The borders were sealed with two-component

gluten. The samples were excited at a wavelength of 495 to 510 nm and the emission was detected at 520 to 550 nm.

3.2.9 AMS-shift assays

For determination of the redox state of proteins expressed in yeast cells AMS was used according to Kojer (2012). Transformed yeast cells (3.2.8.1.1) were inoculated from plate in selective liquid SD medium overnight and afterwards 1.0 mL of yeast cells with an O_{D600} = 1 were centrifuged (30 sec, 13000 rpm, RT). The supernatant was discarded and the cells were dissolved in buffer B +/- diamide (0.1 M sorbitol, 0.1 M NaCl, 0.1 M Tris-HCl pH 7.4). The cells were treated with 32 µl 72 % (v/v) TCA directly or after incubation with diamide (oxidation) at RT for 20 min. All samples were kept on ice after addition of TCA. Yeast cells were broken using 2 x 30 sec sonification (cycle 0.6, amplitude 80 %) and the crude extract was incubated at -20°C for at least 1 h. The completely thawn samples were centrifuged at 13000 rpm and 4°C for 30 min. The pellets were washed with 500 µl 5 % TCA and centrifuged at 13000 rpm and 4°C for 30 min again. The supernatant was removed completely and 2 µl 1 M Tris-HCl pH 7.4 were added. The pellets were dissolved in 40 µl buffer A (+/- 3.75 mM TCEP, +/- 15 mM AMS). Before AMS was added to all samples, TCEP treated samples were incubated for 5 min at 95°C (strong reduction) or for 30 min at 30°C (mild reduction). For the modification with AMS the samples were incubated with AMS for 1 h at RT in the dark. The proteins were boiled for 2 min at 96°C and separated and detected as described in 3.2.4.4 and 3.2.4.5.

3.2.10 Root length determination

For observation of flg22-induced root growth reduction *A. thaliana* seeds were placed on 1 MS-MES (+/ - flg22) medium plus GELRITE (5g/L) in square petri dishes. The plants were grown for 10 days in a vertical position and the root length was quantified with ImageJ software.

3.2.11 ROS-burst assay

The production of ROS after application of flg22 was detected with a luminol based assay. Leaf discs from 4 weeks old soil grown plants (8 h/ 16 h light cycle) were placed in 96-well microtiter plates filled with 100 µL water o/n until the wound response was gone. The water was removed and 100 µl luminol solution (10 mM Tris/ HCl pH 9.5, 10 µg/ mL horse radish perocidase, 17 µg/ mL luminol) +/ - 1 µM flg22 were added to the leaf discs. After adding the solution with a multichannel pipette the horseradish peroxidase catalyses immediately the oxidation of luminol to 3-aminophthalate and a weak chemiluminescence is emitted at 428 nm. The chemiluminescence was measured in a plate reader every minute after starting the reaction.

4 Results

4.1 Clade I TGA TFs are not important for known NPR1-dependent functions in *A. thaliana*

TGA1 mutant proteins that cannot adopt the oxidized state interact with NPR1 in yeast. Based on these results it was postulated that a reduction of clade I TGA TFs facilitates interaction with NPR1 (Depres et al., 2003). However, the in vivo relevance of the redox-induced TGA/NPR1 interaction is not known. Therefore, the interaction between clade I TGA TFs and NPR1 was re-investigated and the influence of TGA1 and TGA4 on known NPR1-dependent processes (*PR1* gene expression, basal resistance, SAR) was tested.

4.1.1 The interaction between NPR1 and clade I TGA TFs is not enhanced after mutation of conserved cysteine into serine residues

To mimic constitutively reduced forms of clade I TGA TFs, the redox-modulated cysteine residues of TGA1 and TGA4 (Despres et al., 2003) were changed to serines by site-directed mutagenesis (Figure 4.1.1.1).

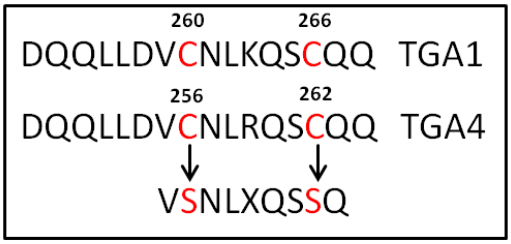

Fig. 4.1.1.1: Redox-modulated cysteine residues in clade I TGA TFs

Exchange of cysteine residues to serines in TGA1 and TGA4 is indicated in red.

The interaction of NPR1 with wildtype and mutated clade I TGA TFs was tested by yeast two-hybrid (Y2H) assays (M&M 3.2.8.1). NPR1 was fused to the GAL4 binding domain and wildtype and mutated clade I TGA TFs were fused to the GAL4 activation domain. The interaction between BD-TGA2 and AD-NPR1was used as positive control. Co-expression of BD-TGA2 and AD-NPR1 led to a clear increase of β-galactosidase activity, reflecting a strong interaction of both proteins. Co-expression of wildtype and mutated clade I TGA TFs

and NPR1 showed less but distinct galactosidase activity**.** The mutation of the cysteine residues did not influence the interaction. Furthermore, no interaction between clade I TGA TFs and NPR1 was observed in BiFC assays (Fig. S1).

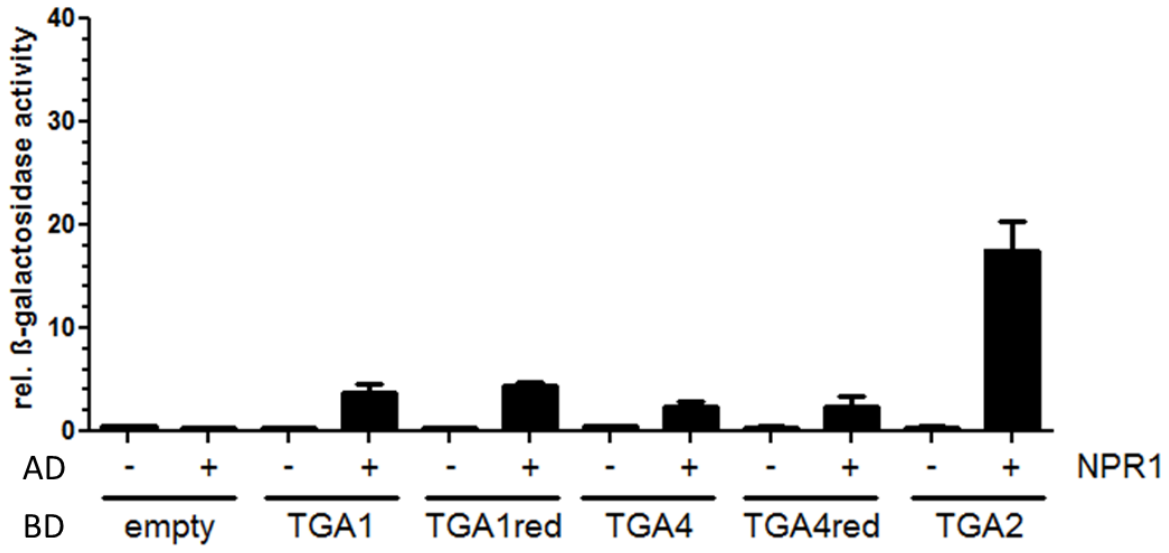

Fig. 4.1.1.2: Interaction between NPR1 and clade I TGA TFs

Protein-protein interaction in yeast cells was quantified with ONPG assays. Prey plasmids encode clade I TGA TFs fused to the GAL4 transactivation domain, bait plasmid encodes NPR1 fused to the GAL4 binding domain. β-galactosidase activity was measured in yeast strain PJ69-4A. Bars represent the average ± SEM of 5-8 independent clones.

Next, we investigated the redox state of wildtype TGA TFs expressed in yeast with AMS shift assays (Kojer et al., 2012; M&M 3.2.9**)**. The chemical compound AMS binds to reactive cysteine residues in the reduced state and changes the mobility of proteins during SDS-PAGE. Protein extracts from yeast were treated with AMS and the TFs were identified by western blot analysis (Figure 4.1.1.3).

After treatment of yeast cells with diamide, the protein was oxidized and the AMS treatment did not influence the mobility. In contrast, HA-TGA1 protein in the untreated sample was affected in mobility and shifted to a higher molecular weight. This result suggests that the HA-TGA1 protein is reduced in yeast, explaining the constitutive interaction with NPR1.

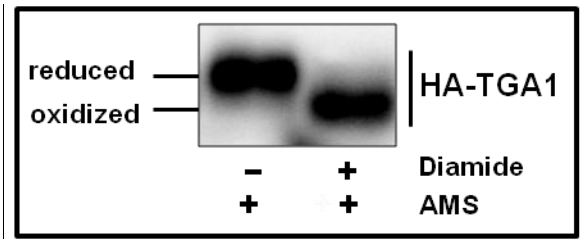

Fig. 4.1.1.3: Redox state of HA-TGA1 expressed in yeast

The yeast strain YPH499 was transformed with the plasmid pCU425-CTR1-HA-TGA1. Yeast cultures were treated with or without 20 mM diamide for 10 min. After sonification, proteins were precipitated with 10 % TCA and treated with AMS for 1 h. Protein was separated by SDS-PAGE and the HA-TGA1 signal was detected by western blot analysis with α-HA.

4.1.2 The expression of the NPR1-dependent gene *PR1* is not affected in the *tga14* mutant

NPR1 plays a crucial role in *PR1* gene expression after exogenous application of SA and infection with virulent *Pseudomonas syringae* (Cao et al., 1994). To investigate the importance of clade I TGA TFs in *PR1* gene expression, 14-day old seedlings of the *tga14* mutant grown on MS-MES medium were sprayed with 1 mM SA and total RNA was extracted. The transcript levels of *PR1* were monitored with specific primers by qRT-PCR (Figure 4.1.2.1). Within 5 h post SA treatment, *PR1* expression was increased in Col-0. Maximal expression was detected at 10 h, whereas expression already declined at 24 h. The kinetics and strength of SA-induced *PR1* transcript levels in the *tga14* mutant were similar to those observed in wildtype Col-0.

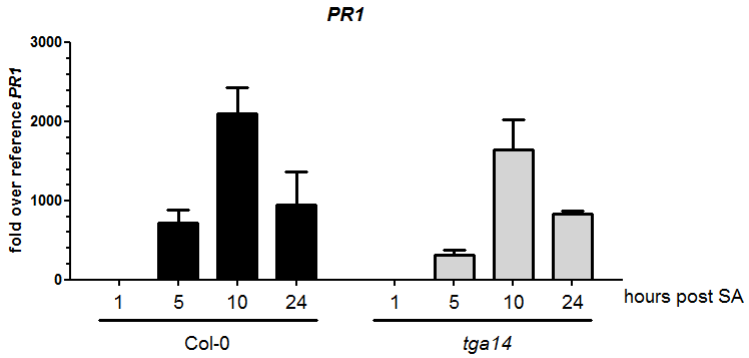

Fig. 4.1.2.1: *PR1* expression after exogenous SA application in axenically grown seedlings

Wildtype Col-0 and *tga14* mutant plants were grown axenically on MS-MES for 14 days under LD conditions. The seedlings were sprayed with 1 mM SA and harvested 1, 5, 10 and 24 hours after treatment. RNA was extracted and the transcript levels of *PR1* were measured with specific primers by qRT-PCR and normalized to *UBQ5* expression. Bars represent average ± SEM with n = 2-3

Next, we aimed to analyze the functional relevance of clade I TGA TFs in soil-grown plants. To exclude processes influenced by endogenous SA which may fluctuate in soil-grown plants, the SA biosynthesis mutant *sid2-2* was crossed with the *tga14* mutant. The *sid2-2* and *tga14/sid2-2* mutants were grown for 4 weeks on soil and sprayed with 1 mM SA (Figure 4.1.2.2). As described for axenically grown seedlings, *PR1* transcript levels were similar in both genotypes at 24 hours after treatment.

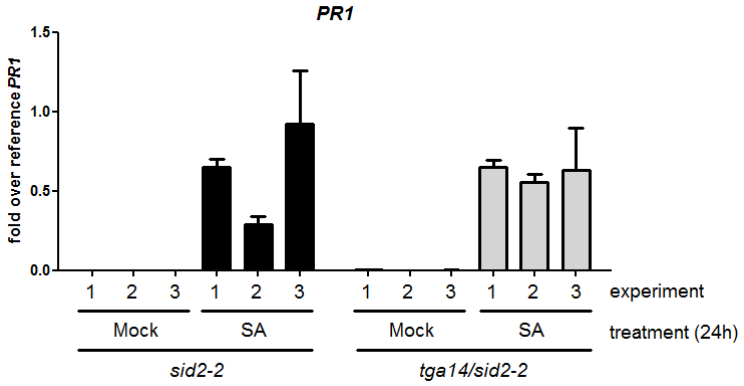

Fig. 4.1.2.2: *PR1* expression after exogenous SA application in soil grown *sid2-2* and *tga14/sid2-2* mutant plants

sid2-2 and *tga14/sid2-2* mutant plants were grown on soil for 4 weeks under 12h/12h-light cycle. Plants were sprayed with 1 mM SA and harvested at 24 hours after treatment. RNA was extracted and the transcript levels of *PR1* were measured with specific primers by qRT-PCR and normalized to *UBQ5* expression. Every experiment displays the average ± SEM with 3 independent samples. For every sample plant material of 7 individual plants was combined.

To investigate the role of clade I TGA TFs in *PR1* expression after pathogen-induced SA biosynthesis, wildtype Col-0 and the *tga14* mutant were infiltrated with a bacterial *Psm* ES4326 suspension or 10 mM $MgCl_2$. (Figure 4.1.2.3). Again, *PR1* expression was not affected in the *tga14* mutant.

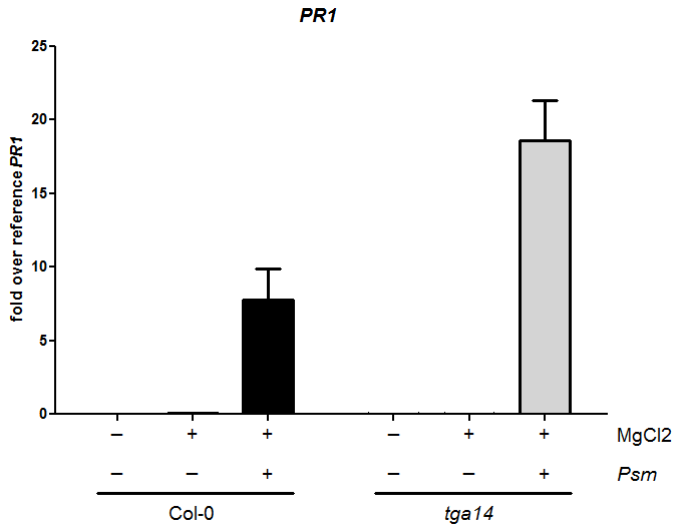

Fig. 4.1.2.3: *PR1* expression after infection with *Psm* E4326

Wildtype Col-0 and *tga14* mutant plants were grown on soil for 5 weeks under SD conditions. Three leaves per plant were inoculated with a *Psm* E4326 suspension (OD600 = 0.01) and 10 mM $MgCl_2$, respectively. Total RNA was extracted at 2 days post inoculation (dpi). Transcript levels of *PR1* were measured with specific primers by qRT-PCR and normalized to *UBQ5* expression. Bars represent average ± SEM with n = 3.

4.1.3 The *tga14* mutant is not impaired in perception of SAR signals in systemic tissue

The NPR1-dependent SAR is established in planta after generation of a mobile signal at the local infection site and its perception in the systemic tissue. This process leads to a long-lasting and broad spectrum defense against further pathogen attack. The *npr1-1* and the *tga256* mutants show compromised *PR1* expression in systemic tissue (Zhang et al., 2003). Furthermore, SA accumulation in systemic tissue is impaired in the *npr1-1* mutant (Attaran et al., 2009). To investigate the role of clade I TGA TFs with respect to NPR1-dependent SAR, the SA content and the expression of *ICS1* and *PR1* in systemic tissue after local infection were measured.

4.1.3.1 The SAR-induced SA biosynthesis in systemic leaves of the *tga14* mutant is not affected

Three leaves of wildtype Col-0, *tga14* mutant and *tga256* mutant were infiltrated with a *Psm* ES4326 suspension or with 10 mM $MgCl_2$. Two days later, three systemic leaves were harvested and the levels of free SA were determined (Figure 4.1.3.1.1). Local infection of

Col-0 and the *tga14* mutant led to an increase of free SA in uninfected systemic leaves. In contrast, the *tga256* mutant accumulated nearly no free SA in systemic tissue.

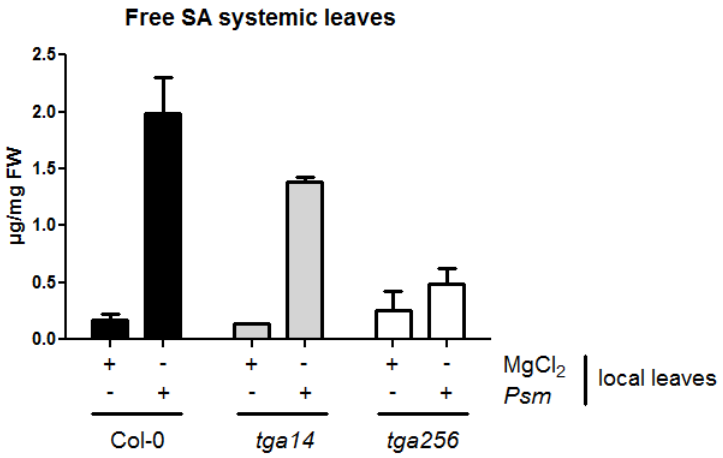

Fig. 4.1.3.1.1: *Psm* ES4326-induced SA accumulation in systemic tissue

Three fully expanded leaves of 3 wildtype Col-0, *tga14* and *tga256* mutant plants were infiltrated with a *Psm* ES4326 suspension (OD_{600} = 0.01). As control, 10 mM $MgCl_2$ was infiltrated. Systemic leaf tissue was harvested two days after infection and free SA was determined by vapor-phase extraction and subsequent GC-MS analysis according to Mishina and Zeier, 2006. Measurement was performed by Thomas Griebel. Bars represent mean values ± SEM of two to three independent samples.

4.1.3.2 The *tga14* mutant shows no impaired expression of SAR-related genes in systemic tissue

Elevated SA levels in systemic tissue during SAR lead to an NPR1-dependent expression of the marker gene *PR1*. To investigate a role of clade I TGA TFs in *ICS1* and *PR1* expression during SAR, transcript levels were measured in systemic tissue (Figure 4.1.3.2.1). The expression of the SA- and NPR1-dependent gene *PR1* was increased in the *tga14* mutant. The expression of *ICS1* was also not affected, supporting the wildtype-like SA accumulation (Fig. 4.1.3.1.1).

These results hint at a negative function of clade I TGA TFs in *PR1* expression in systemic tissue during SAR. This contrasts with the induction after SA treatment, where a deregulation of *PR1* expression after exogenous application of SA was not observed (Chapter 4.1.2). Therefore, we did not investigate this result in more detail.

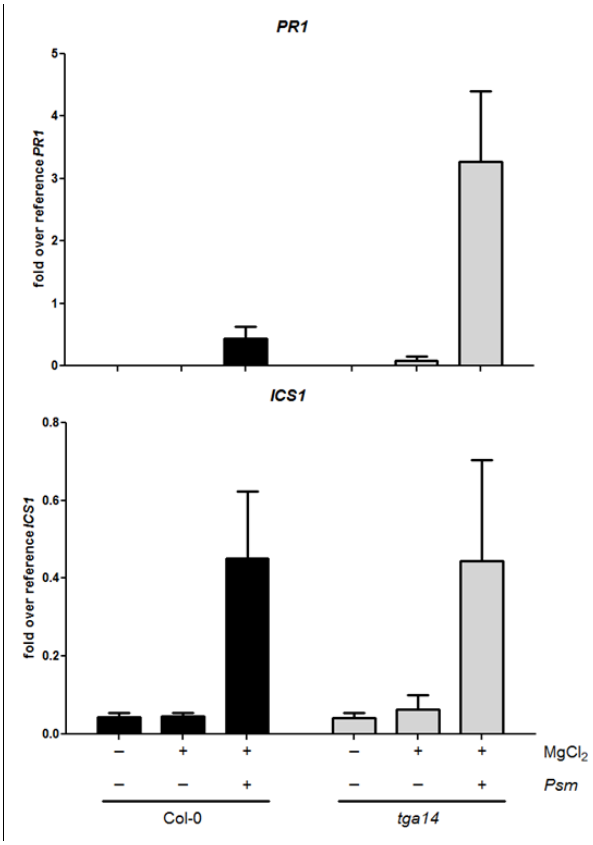

Fig. 4.1.3.2.1: *Psm* ES4326-induced expression of defense-related genes in systemic tissue

Systemic expression of defense-related genes in wildtype Col-0 and *tga14* mutant plants after infection with *Psm* ES4326 (OD_{600}=0.01) were detected. Systemic leaf tissue was harvested two days after local infection and total RNA of three leaves per plant was extracted. The transcript levels of *ICS1* and *PR1* were monitored by qRT-PCR with specific primers and normalized with *UBQ5* expression. Bars represent the average ± SEM with n = 5.

4.1.4 Clade I TGA TFs play no general role in basal resistance

After having excluded that clade I TGA TFs contribute to the SA-induced regulation of *PR1*, we also investigated the importance of TGA1 and TGA4 in basal resistance. It has been reported before that the *tga14* mutant shows similarity to the *npr1-1* mutant with respect to a higher bacterial titer after infection with virulent *Psm* ES4326 (Kersawani et al., 2007). To address a general function of clade I TGA TFs in basal resistance against virulent *Pseudomonas syringae*, we infected the *tga14* mutant with virulent *Pst* DC3000. The *tga14* mutant showed only a slight increase in bacterial titer at 3 dpi (Figure 4.1.4.1). In addition, the analysis of plant responses triggered by the PAMP flg22 (ROS burst, stunted root growth, gene expression) did not reveal a function of clade I TGA TFs in PTI (Supplemental figures

S2, S3, S4). An influence of an impaired basal resistance towards defense responses against the necrotrophic pathogen *B. cinerea* were also not observed (Fig. S25).

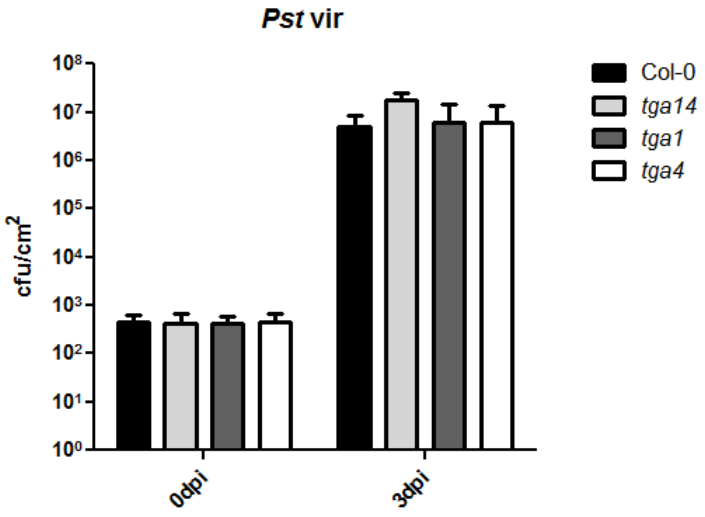

Fig. 4.1.4.1: Propagation of *Pst* DC3000 in Col-0 and *tga14* mutant

Three fully expanded leaves per wildtype Col-0 and *tga14*, *tga1* and *tga4* mutant plant were infiltrated with a bacterial suspension of vir *Pst* DC3000 (OD600 = 0.0001). One hour or three days after treatment the bacteria were extracted and appropriate dilutions were incubated on King´s B medium. Bars represent the average ± SEM with 5 biological replicates.

An importance of clade I TGA TFs in known NPR1-dependent functions in *A. thaliana* could not be demonstrated. Moreover, TGA1 and TGA4 do not seem to play a major role in basal resistance. To continue to investigate the role of clade I TGA TFs in SA-dependent plant defense responses, we took a closer look to the ETI.

4.2 The *tga14* mutant shows a partially impaired ETI

In contrast to basal defense responses and SAR, the role of TGA TFs during ETI has been unexplored. Therefore we investigated a possible function of clade I TGA TFs in ETI.

4.2.1 The *tga14* mutant is defective in avrRPS4-triggered defense responses

ETI is established after recognition of pathogen-derived effector proteins by plant R proteins. To analyze the plant resistance mediated by TIR-NB-LRR RPS4 and CC-NB-LRR RPM1, wildtype Col-0 and the *tga14* mutant were infiltrated with a bacterial suspension of *Pst* avrRPS4 and *Psm avrRPM1* (M&M 3.2.5.1; Figure 4.2.1.1).

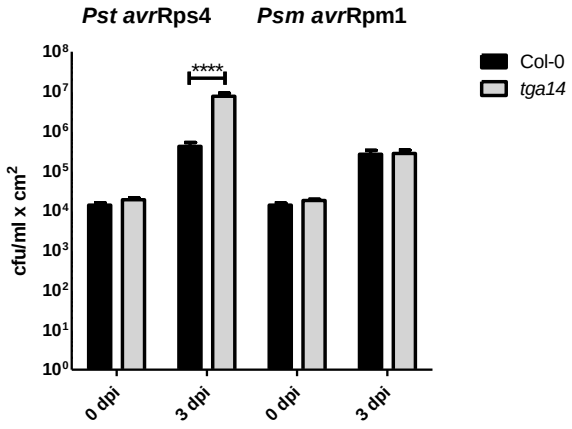

Fig. 4.2.1.1: Propagation of *Pst avrRPS4* and *Psm avrRPM1* in Col-0 and *tga14* mutant plants

Three fully expanded leaves of 5 wildtype Col-0 and *tga14* mutant plants were infiltrated with a bacterial suspension of *Pst avrRPS4* or *Psm avrRPM1* (OD600 = 0.002). Bacterial growth was measured 1 hour and 3 days after treatment. Bars represent the average ± SEM with 5 individual plants. Statistical significance was calculated by Two-Way ANOVA with $P < 0.0001$.

After infection with *Pst avrRPS4*, the *tga14* mutant was more susceptible than wildtype Col-0 and the infiltrated leaves showed clear different symptoms (Fig. S5). In contrast, no differences between wildtype Col-0 and the *tga14* mutant were measurable after infection with *Psm avrRPM1*. This susceptibility of the *tga14* mutant indicates a role of clade I TGA TFs in avrRPS4-triggered but not in avrRPM1-triggered resistance.

4.2.2 TGA1 and TGA4 are redundant with respect to avrRPS4-triggered resistance

To elucidate the specific roles of TGA1 and TGA4 in avrRPS4-triggered resistance, the single mutants *tga1* and *tga4* were infected with *Pst avrRPS4* (Figure 4.2.2.1). The single mutants

were not more susceptible than wildtype Col-0. As already displayed in figure 4.2.1.1, the *tga14* mutant had a higher bacterial titer at 3dpi. In conclusion, clade I TGA TFs are redundant with respect to conferring resistance upon infection with *Pst avrRPS4*.

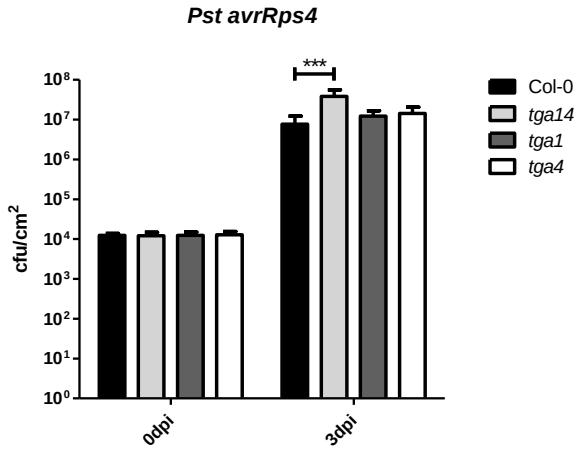

Fig. 4.2.2.1: Redundancy of TGA1 and TGA4 with respect to *Pst avrRPS4* infection

Three fully expanded leaves of 5 wildtype Col-0, *tga14* mutant, *tga1* mutant and *tga4* mutant plants were infiltrated with a bacterial suspension of *Pst avrRPS4* (OD600 = 0.002). Bacterial growth was measured 1 hour or 3 days after treatment. Bars represent the average ± SEM with 5 individual plants. Statistical significance was calculated by Two-Way ANOVA with $P < 0.001$.

4.2.3 Clade I TGA TFs-dependent resistance after infection with *Pst avrRPS4* is independent of NPR1, NPR3 and NPR4

Next, we investigated the role of NPR1 in avrRPS4-triggered resistance. The triple mutant *tga14/npr1-1* was created and infected with a bacterial suspension of *Pst avrRPS4*. Three independent experiments were performed (Figure 4.2.3.1 (A)), in which the *tga14* mutant was more susceptible than wildtype Col-0. The *npr1-1* mutant was also more susceptible than wildtype Col-0, but significantly less than the *tga14* mutant in 2 of 3 experiments. This result indicates a minor important role of NPR1 in avrRPS4-triggered resistance. Moreover, the triple mutant *tga14/npr1-1* was significantly more susceptible than the *tga14* mutant in 2 of 3 experiments. This result indicates a NPR1-independent function of TGA1 and TGA4. The average of all three experiments, displayed in figure 4.2.3.1 (B), did not reflect that the additive effect in the *tga14*/*npr1-1* mutant in comparison to the *tga14* mutant is significant.

Because of a minor role of NPR1 in avrRPS4-triggered resistance and only a slight increased susceptibility of the *tga14/npr1-1* mutant, it is hard to judge whether TGA1 and TGA4 act independently of NPR1. Based on the additive effect of *tga14* mutant and *npr1-1* mutant in 2 single experiments, we assumed a NPR1-independent function of TGA1 and TGA4 in mediating resistance after infection with *Pst avrRPS4*.

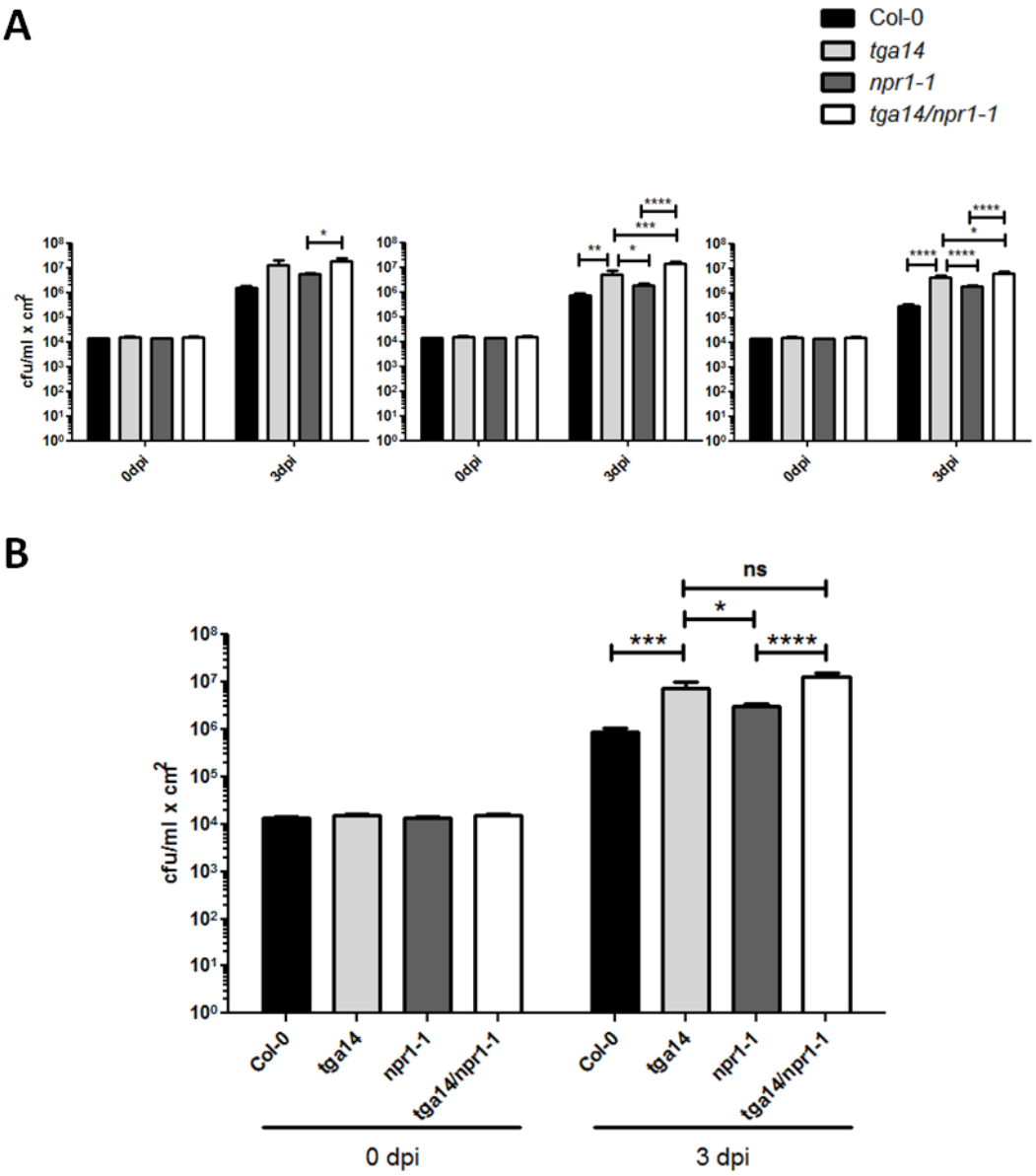

Fig. 4.2.3.1: The role of NPR1 in TGA1 and TGA4-mediated resistance after recognition of avrRPS4

Three fully expanded leaves of 5 wildtype Col-0, *tga14* mutant, *npr1-1*mutant and *tga14/npr1-1* mutant plants were infiltrated with a bacterial suspension of *Pst avrRPS4* (OD600 = 0.002). Bacterial growth was measured one hour or three days after treatment. (A) Three independent experiments are shown. Bars represent the average ± SEM with 5 individual plants. (B) The mean of the three independent experiments shown in (A). Statistical significance was calculated by Two-Way ANOVA with $P < 0.05$.

In recent studies, NPR3 and NPR4 were described as SA receptors mediating NPR1 protein degradation (Fu et al., 2012). A weak interaction between NPR4 and TGA1 was shown in previous studies (Zhang et al., 2004). To investigate the importance of NPR3/4 in clade I TGA TFs-dependent resistance, wildtype Col-0, *tga14* mutant and *npr3/4* mutant were infected with *Pst avrRPS4* (Figure 4.2.3.2).

In contrast to the *tga14* mutant, the *npr3/4* mutant was more resistant than wildtype Col-0. These results exclude NPR3 and NPR4 as positive factors in TGA1- and TGA4-dependent immunity.

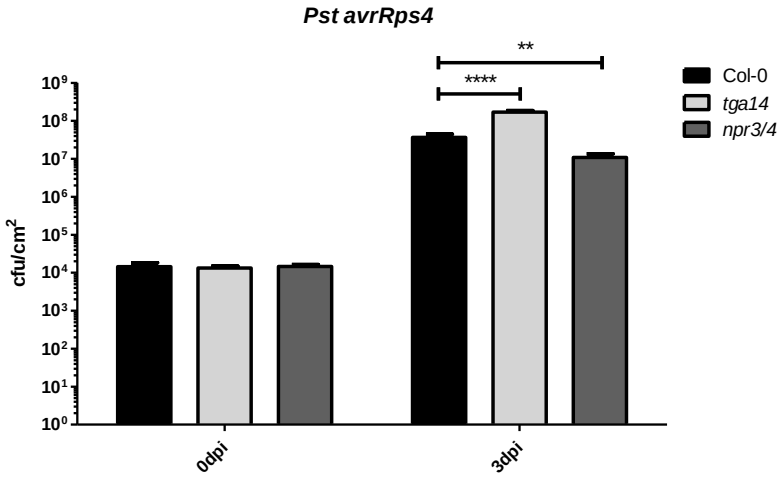

Fig. 4.2.3.2: The role of NPR3 and NPR4 in TGA1- and TGA4-dependent resistance after recognition of avrRPS4

Three fully expanded leaves of 5 wildtype Col-0, *tga14* mutant and *npr3/4* mutant plants were infiltrated with a bacterial suspension of *Pst avrRPS4* (OD600 = 0.002). Bacterial growth was measured 1 hour or 3 days after treatment. Bars represent the average ± SEM with 5 individual plants. Statistical significance was calculated by Two-Way ANOVA with $P < 0.01$.

4.2.4 Clade I TGA TFs-dependent resistance after infection with *Pst avrRPS4* is dependent on SA

Because two redox-modified cysteine residues of clade I TGA TFs are reduced after SA treatment (Depres et al., 2003), we analyzed the importance of SA in TGA1- and TGA4-dependent resistance after infection with *Pst avrRPS4*. Wildtype Col-0 and the *tga14*, *sid2-2* and *tga14/sid2-2* mutants were infiltrated with a *Pst avrRPS4* suspension (Figure 4.2.4.1). In figure 4.2.4.1 (A) three independent experiments are displayed, in which the *tga14* mutant was more susceptible than wildtype Col-0. In 2 of 3 experiments the *sid2-2* mutant was

slightly more susceptible than the *tga14* mutant. Furthermore, the *tga14/sid2-2* mutant was significantly more susceptible than the *tga14* mutant, but not more than the *sid2-2* mutant. These results indicate an SA-dependent function of TGA1 and TGA4 in avrRPS4-triggered resistance. The average of all 3 experiments is displayed in figure 4.2.4.1 (B). In contrast, the similarly susceptible phenotypes of *tga14*, *sid2-2* and *tga14/sid2-2* mutants suggest, that all SA-mediated functions are dependent on clade I TGA TFs.

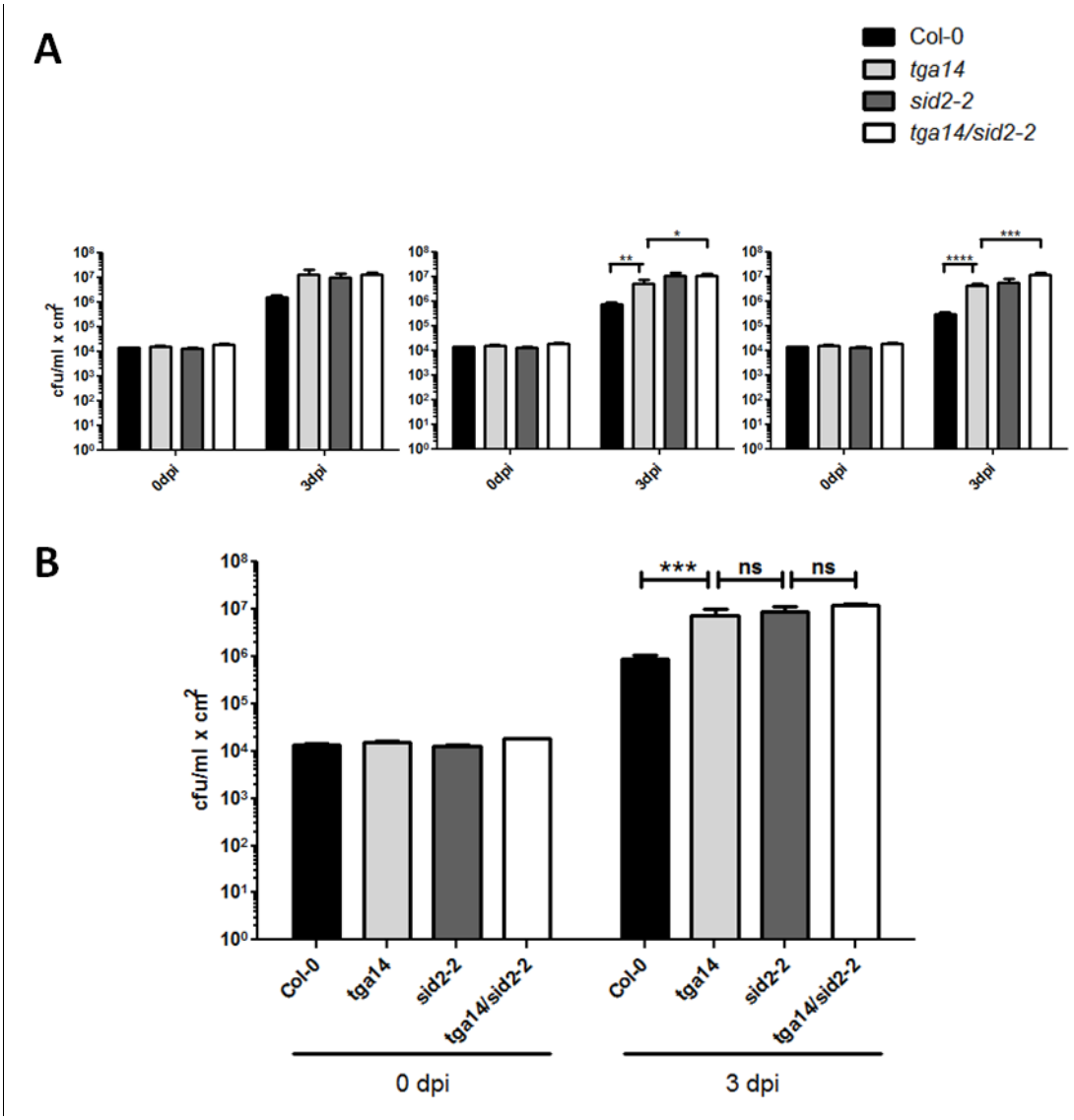

Fig. 4.2.4.1: The role of SA in TGA1 and TGA4-mediated resistance after recognition of avrRPS4

Three fully expanded leaves of 5 wildtype Col-0, *tga14* mutant, *sid2-2* mutant and *tga14/sid2-2* mutant plants were infiltrated with a bacterial suspension of *Pst avrRPS4* (OD600 = 0.002). Bacterial growth was measured one hour or three days after treatment. (A) Three independent experiments are shown. Bars represent the average ± SEM with 5 individual plants. (B) The mean of the three independent experiments shown in (A). Statistical significance was calculated by Two-Way ANOVA with $P < 0.05$.

4.2.5 The *tga14/eds1-2* triple mutant is slightly more resistant than the *eds1-2* mutant after infection with *Pst avrRPS4*

EDS1 is indispensable for defense responses mediated by TIR-NB-LRR receptors. Complexes of RPS4 and EDS1 and avrRPS4 and EDS1 were detected in soluble *A. thaliana* leaf extracts after resistance activation (Heidrich et al., 2011). This crucial function of EDS1 in avrRPS4-triggered immunity prompted us to cross the *tga14* mutant with the *eds1*-2 mutant plant. Next, wildtype Col-0 and the mutants *tga14*, *eds1-2* and *tga14/eds1-2* were infiltrated with a bacterial suspension of *Pst avrRPS4* (Figure 4.2.5.1).

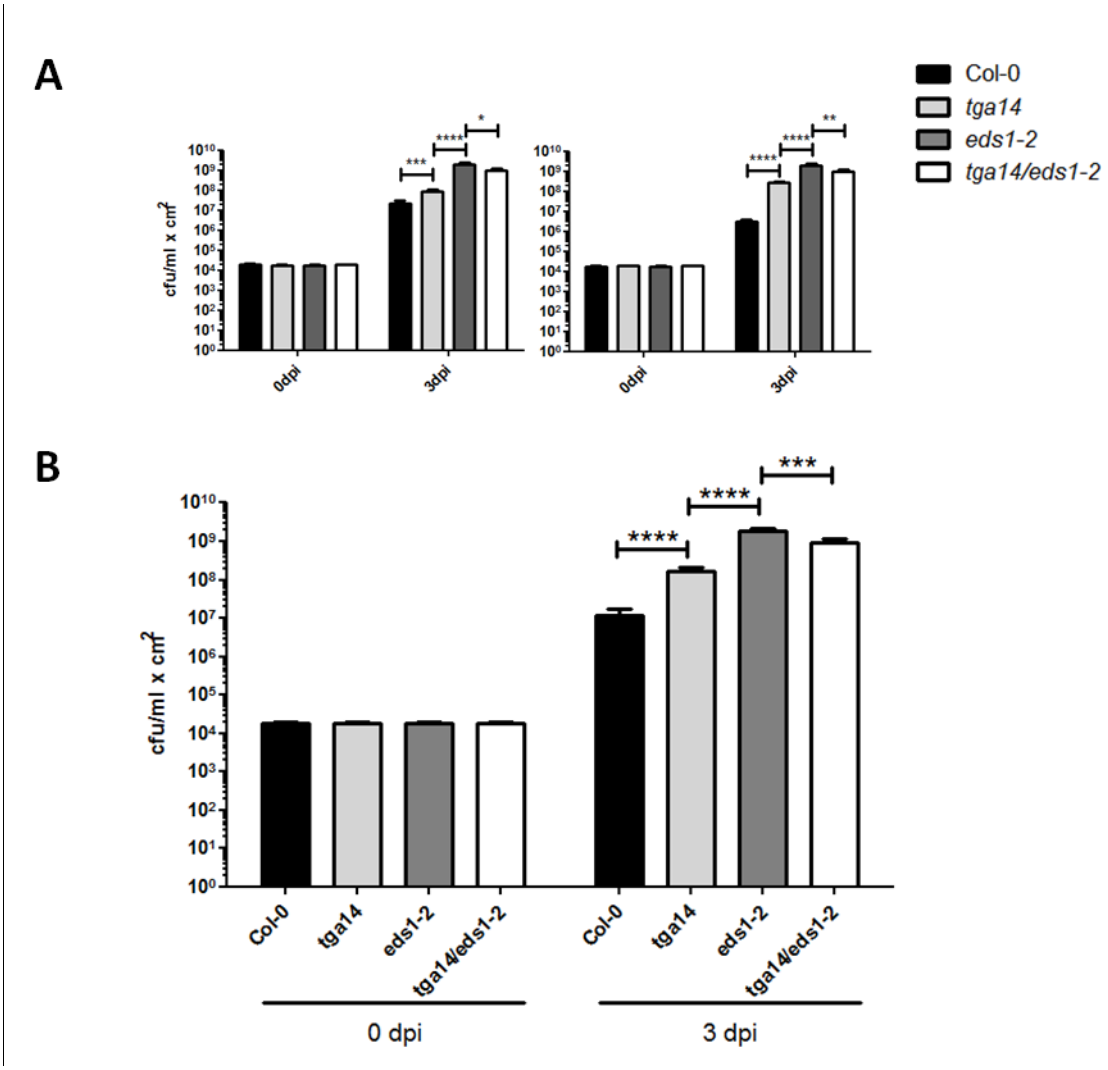

Fig. 4.2.5.1: The role of EDS1 in TGA1 and TGA4-mediated resistance after recognition of avrRPS4

Three fully expanded leaves of 5 wildtype Col-0, *tga14* mutant, *eds1*-2 mutant and *tga14/eds1-2* mutant plants were infiltrated with a bacterial suspension of *Pst avrRPS4* (OD600 = 0.002). Bacterial growth was measured 1 hour or 3 days after treatment. (A) Two independent experiments are shown. Bars represent the average ± SEM with 5 individual plants. (B) The mean of the two independent experiments shown in (A). Statistical significance was calculated by Two-Way ANOVA with $P < 0.05$.

The *tga14* mutant and the *eds1-2* mutant were more susceptible than wildtype Col-0. This susceptibility was more pronounced in the *eds1-2* mutant. The triple mutant *tga14/eds1-2* was more susceptible than the *tga14* mutant but less than the *eds1-2* mutant. These results suggest a complex connection between EDS1-dependent and TGA1- and TGA4-dependent resistance.

4.3 Microarray analysis of the *tga14* mutant infected with *Pst avrRPS4*

In order to reveal direct target genes of clade I TGA TFs that might be affected during ETI, microarray analysis after infection with *Pst avrRPS4* was performed. Wildtype Col-0 and *tga14* mutant were infiltrated with *Pst avrRPS4* (OD_{600} = 0.2) and harvested at 3, 6 and 11 hpi. For every sample, 3 infected leaves of 9 individual plants were combined. For every time point 3 samples were collected.

In order to find suitable and equal conditions the upregulation of SA-related defense genes was monitored. Transcript levels of *EDS1*, *WRKY70* and *PR1* were monitored by qRT-PCR. *EDS1* and *WRKY70* expression was increased in wildtype Col-0 and *tga14* mutant to similarly levels already at 6 and 11 hpi (Figure 4.3.1). Transcript levels of *PR1* were induced after 11 hpi to comparable amounts in wildtype Col-0 and *tga14* mutant (Figure 4.3.2). This result shows a TGA1- and TGA4-independent *PR1* expression also after infection with *Pst avrRPS4*.

The induction of *EDS1*, *WRKY70* and *PR1* confirmed a SA response after infection already at 11 hpi. For microarray analysis only the samples of infected tissue were used. At 3 hpi only small transcriptomal changes were detected after infection with avr *Pseudomonas* strains (de Torres et al., 2003; Bartsch et al., 2006) and the samples were used as reference for induced genes at 6 and 11 hpi with *Pst avrRPS4*

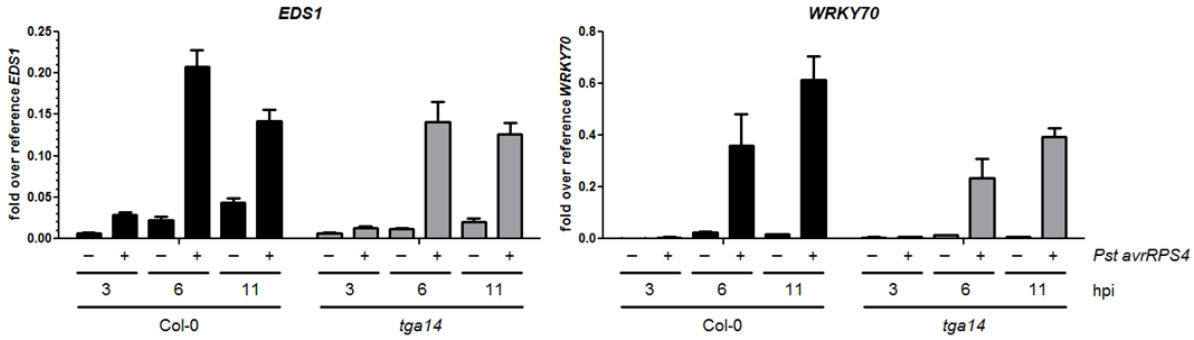

Fig. 4.3.1: Expression of *EDS1* and *WRKY70* after infection with *Pst avrRPS4*

Wldtype Col-0 and *tga14* mutant plants were grown under 12h/ 12h light conditions for 4 weeks and three leaves per plant were infiltrated with a *Pst avrRPS4* suspension (OD600 = 0.02) or 10 mM $MgCl_2$. At 3, 6 and 11 hpi the leaf tissue was harvested and total RNA extracted. Transcript levels were measured with specific primers by qRT-PCR and normalized to *UBQ5* expression. Bars represent average ± SEM with 3 independent samples. For every sample the leaf tissue of 9 plants was combined.

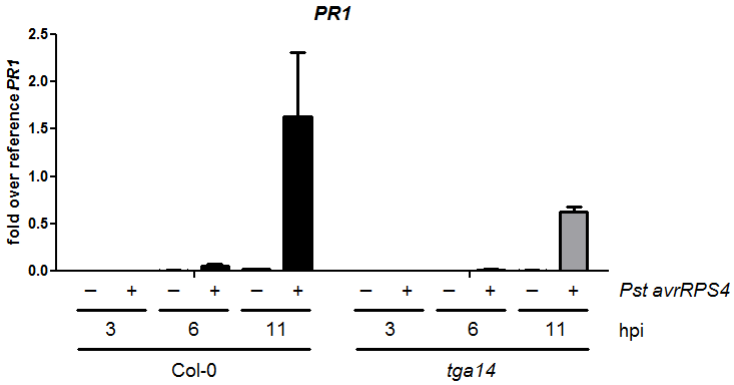

Fig. 4.3.2: Expression of *EDS1* and *WRKY70* after infection with *Pst avrRPS4*

Wildtype Col-0 and *tga14* mutant plants were grown under 12h/ 12h light conditions for 4 weeks and three leaves per plant were infiltrated with a *Pst avrRPS4* suspension (OD600 = 0.02) or 10 mM $MgCl_2$. At 3, 6 and 11 hpi the leaf tissue was harvested and total RNA extracted. Transcript levels were measured with specific primers by qRT-PCR and normalized to *UBQ5* expression. Bars represent average ± SEM with 3 independent samples. For every sample the leaf tissue of 9 plants was combined.

4.3.1 Microarray analysis did not reveal affected expression of defense related genes in the *tga14* mutant

The microarray revealed 1023 up-regulated and 1252 down-regulated genes at 6 hpi and 1407 up-regulated and 1715 down-regulated genes at 11 hpi in wildtype Col-0. Because we were interested in clade I TGA TFs-controlled genes induced after infection with *Pst avrRPS4*, we focused on genes that were induced in wildtype Col-0 between 3 hpi and 6 hpi and 11 hpi respectively (> 2fold change, P value < 0.05) and differentially regulated in *tga14* mutant at the same time (> 2fold change, P value < 0.05) (Figure 4.3.1.1). In the *tga14* mutant 165 genes were differentially expressed at 3 hpi, 140 genes at 6 hpi and 41 genes at 11 hpi (Figure 4.3.1.1). These genes were categorized into 4 classes: induced in wildtype Col-0 and less or stronger expressed in the *tga14* mutant and repressed in wildtype Col-0 and stronger or less expressed in the *tga14* mutant (Fig. S6 - S17). For only 9 genes consistently altered expression of *Pst avrRPS4*-induced genes was detectable in the *tga14* mutant at 3, 6 and 11 hpi. The observed deregulation of defense-related genes at early single time-points was not confirmed with independent experiments consistently (Fig. S18). Remarkably, differences in the transcriptome were larger at the beginning of the infection.

Gene class	3hpi	6hpi	11hpi	over all
Col-0 induced - *tga14* less expressed	**78**	**41**	**8**	**0**
Col-0 induced - *tga14* stronger expressed	**30**	**9**	**5**	**2**
Col-0 repressed - *tga14* stronger expressed	**32**	**87**	**23**	**7**
Col-0 repressed - *tga14* less expressed	**25**	**3**	**5**	**0**

Fig. 4.3.1.1: Differentially induced genes in the *tga14* mutant after infection with *Pst avrRPS4*

Only genes induced in wildtype Col-0 after infection with *Pst avrRPS4* between 3 and 6 hpi , respectively 11 hpi, were used for the identification of deregulation in the *tga14* mutant. Threshold was a minimum difference of 2fold with a P value < 0.5. Four different classes of deregulated genes at 3, 6 and 11 hpi are displayed: induced in Col-0 and less or stronger expressed in the *tga14* mutant (Col-0 induced – *tga14* less expressed and Col-0 induced – *tga14* stronger expressed) and repressed in Col-0 and stronger or less expressed in the *tga14* mutant (Col-0 repressed – *tga14* stronger expressed and Col-0 repressed – *tga14* less expressed). Threshold was a minimum difference of 2fold with a P value < 0.5.

In order to identify genes that are affected in the *tga14* mutant at later time points, a second microarray analysis was done with *Pst avrRPS4* at 24 hpi. For this analysis, 3 independent experiments were performed. For every experiment, 3 leaves of 9 individual plants of wildtype Col-0 and *tga14* mutant were infiltrated with *Pst avrRPS4* (OD_{600} = 0.2) or 10 mM $MgCl_2$. To confirm the susceptibility of the *tga14* mutant, the bacterial titer of side by side grown plants was determined at 3 dpi (Fig. 4.3.1.2). The *tga14* mutant was more susceptible than wildtype Col-0 in all 3 independent experiments.

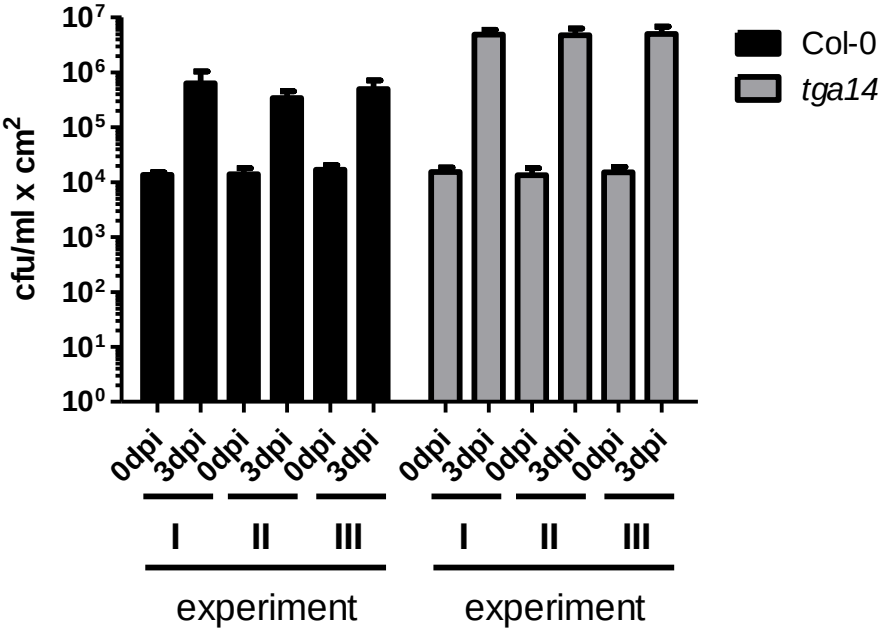

Fig. 4.3.1.2: Bacterial propagation in plants used for microarray analysis 24 hpi with *Pst avrRPS4*

Plants were grown in 12h/12h-light cycle on soil for 5 weeks. Three fully expanded leaves of 10 wildtype Col-0 and *tga14* mutant plants were infiltrated with a bacterial suspension of *Pst avrRPS4* (OD600 = 0.002). Bacterial growth was measured one hour or three days after treatment. Three independent experiments are shown. Bars represent the average ± SEM with 5 individual plants.

After microarray analysis, 1660 up-regulated and 1440 down-regulated genes were identified in wildtype Col-0 at 24 hpi. Comparable to the results of the first microarray, only small differences were detectable in the transcriptomes of wildtype Col-0 and the *tga14* mutant after infection with *Pst avrRPS4*. Only 5 of the *Pseudomonas*-induced and 23 of the *Pseudomonas*-repressed genes were differentially expressed in the *tga14* mutant (> 2fold change, P value < 0.05) (Fig. 4.3.1.3; S18; S19). Again, genes were categorized into 4 classes. After a

correlation with gene classes I-IV after 3, 6 and 11 hpi only expression of *MPL1* (*MYZUS PERSICAE-INDUCED LIPASE 1*) was influeneced by the lack of TGA1 and TGA4 consistently.

Gene class	24hpi	3, 6, 11 hpi	Over all
Col-0 induced - *tga14* less expressed	**4**	**0**	**0**
Col-0 induced - *tga14* stronger expressed	**1**	**2**	**0**
Col-0 repressed - *tga14* stronger expressed	**23**	**7**	**1**
Col-0 repressed - *tga14* less expressed	**0**	**0**	**0**

Fig. 4.3.1.3: Differentially induced genes in the *tga14* mutant after infection with *Pst avrRPS4* at 3, 6, 11 and 24 hpi

Only genes induced in wildtype Col-0 plants after infection with *Pst avrRPS4* at 3, 6, 11 and 24 hpi were used for the identification of deregulation in the *tga14* mutant. Threshold was a minimum difference of 2fold with a P value < 0.5. Four different classes of deregulated genes are displayed: induced in Col-0 and less or stronger expressed in the *tga14* mutant (Col-0 induced – *tga14* less expressed and Col-0 induced – *tga14* stronger expressed) and repressed in Col-0 and stronger or less expressed in the *tga14* mutant (Col-0 repressed – *tga14* stronger expressed and Col-0 repressed – *tga14* less expressed). Threshold was a minimum difference of 2fold with a P value < 0.5.

4.3.2 The *tga14* mutant shows constitutively deregulated expression independently of the induction in wildtype Col-0

Next, we analyzed affected gene expression in the *tga14* mutant in both microarrays independently of induced expression after infection with *Pst avrRPS4*. In the *tga14* mutant 7 genes were down-regulated and 30 genes up-regulated at 3, 6 and 11 hpi and in mock treated samples 152 genes were down-regulated and 75 genes were up-regulated.

In comparison, overall 7 genes were down-regulated (Fig. 4.3.2.1) and 10 genes were up-regulated (Fig. 4.3.2.2) constitutively in the *tga14* mutant in all samples. Conspicuously, the expression of different *GRXs* belonging to the ROXY-family was altered in the *tga14* mutant. One single *ROXY* (*ROXY9*) was less and 5 *ROXYs* (*ROXY13*, *ROXY12*, *ROXY11*, *ROXY16* and *ROXY15*) were higher expressed.

Gene	Description	3h	6h	11h	Mock 24h	Inf 24h
TGA4 (AT5G10030)	bZIP transcription factor family	0,12	0,25	0,29	0,44	0,44
ROXY9 (AT2G47880)	Glutaredoxin family protein	0,18	0,26	0,22	0,50	0,33
not assigned (AT1G64360)	Unknown function	0,20	0,21	0,23	0,35	0,25
not assigned (AT1G68600)	Unknown function	0,22	0,42	0,30	0,29	0,15
DUR3 (AT5G45380)	symporter family protein	0,30	0,38	0,50	0,27	0,31
NAP3 (AT1G67940)	transporter	0,33	0,31	0,42	0,22	0,19
not assigned (AT1G22160)	Senescence-associated protein	0,44	0,47	0,44	0,36	0,24
not assigned (AT5G05960)	lipid transfer protein (LTP) family protein	0,45	0,41	0,42	0,21	0,26
TGA1 (AT5G65210)	bZIP transcription factor family	0,48	0,24	0,16	0,45	0,22

Fig. 4.3.2.1: Constitutively less expressed genes in the *tga14* mutant

Genes constitutively less expressed in the *tga14* mutant are displayed. Threshold was a minimum difference of 2fold with a P value < 0.05.

Gene	Description	3h	6h	11h	Mock 24h	Inf 24h
ROXY13 (AT4G15680)	Glutaredoxin family protein	10,46	14,06	6,94	6,43	9,46
RAM1 (AT4G15210)	BETA-AMYLASE	5,37	5,68	2,69	3,70	1,56
ROXY12 (AT4G15690)	Glutaredoxin family protein	5,23	4,97	5,80	4,66	6,32
ROXY11 (AT4G15700)	Glutaredoxin family protein	4,75	6,61	4,87	4,38	2,89
ROXY16 (AT1G03020)	Glutaredoxin family protein	4,66	3,15	2,65	3,96	3,52
MPL1 (AT5G14180)	Lipid metabolism, lipase	4,14	2,23	2,42	2,85	2,54
ASN1 (AT3G47340)	asparagine synthase	3,34	2,90	2,55	6,51	1,15
NAI2 (AT3G15950)	10 EFE repeats	3,24	2,82	2,64	3,88	5,32
LTP4 (AT5G59310)	lipid binding	3,10	5,48	3,57	6,21	3,63
SPL4 (AT1G53160)	DNA binding / transcription factor	3,05	2,68	2,31	5,03	4,75

ROXY15 (AT4G15660)	Glutaredoxin family protein	2,99	7,00	2,55	3,14	2,29

Fig. 4.3.2.2: Constitutively higher expressed genes in the *tga14* mutant

Genes constitutively higher expessed in the *tga14* mutant are displayed. Threshold was a minimum difference of 2fold with a P value < 0.05.

Since ROXYs can interact with TGA TFs (Ndamukong et al., 2007) and a redox modification of clade I TGA TFs was suggested (Despres et al., 2003), we focused on a possible common function of the TFs and ROXYs.

4.4 Expression of ROXY-type glutaredoxins is altered in the *tga14* mutant

A constitutively affected expression of *ROXY*s was observed in microarray analysis. ROXY proteins can interact physically with TGA TFs (Ndamukong et al., 2007) and are involved in TGA-regulated processes like flower development (Xing et al., 2005; Xing and Zachgo, 2008) and cross-talk between hormone-controlled defense pathways (Ndamukong et al., 2007). Furthermore, expression of *ROXY19*, which is involved in clade II TGA TF-controlled processes, depends on clade II TFs. Therefore, we were interested in a functional relationship of clade I TGA TFs and *ROXY9*. *ROXY13* belongs to a co-regulated subset of genes (*ROXY11-15*) arranged in tandem on chromosome 4 (tandem-*ROXYs*) and was analyzed in parallel.

Expression of *ROXY*s was differentially regulated in all samples in the *tga14* mutant and did not change upon infection with *Pst avrRPS4*. Only expression of *ROXY15* was slightly up-regulated after 6 and 11 hpi when compared to 3 hpi (Figure 4.4.1).

A

Name	3 hpi	6 hpi	11 hpi	Mock 24h	Inf 24h
TGA1	0,48	0,24	0,16	0,45	0,22
TGA4	0,12	0,25	0,29	0,44	0,44
ROXY9	0,18	0,26	0,22	0,50	0,33
ROXY15	4,66	3,15	2,65	3,14	2,29
ROXY13	9,91	20,76	8,15	6,43	9,46
ROXY12	4,75	6,61	4,87	4,66	6,32
ROXY11	3,10	5,48	3,57	4,38	2,89

B

Name	3 vs 6 hpi	3 vs 11 hpi	6 vs 11 hpi	Mock vs 24hpi
ROXY9	0,63	0,69	1,09	1,28
ROXY15	2,35	2,67	1,13	1,52
ROXY13	0,63	1,23	1,98	0,65
ROXY12	0,88	0,95	1,07	0,73
ROXY11	0,77	0,97	1,26	1,94

Fig. 4.4.1: Deregulated basal expression of glutaredoxins in the *tga14* mutant

Expression of *ROXY9* and *ROXY11*, *ROXY12*, *ROXY13* and *ROXY15* in wildtype Col-0 and *tga14* mutant is listed. (A) Direct comparison of *TGA1*, *TGA4*, *ROXY9*, *ROXY11*, *ROXY12*, *ROXY13* and *ROXY15* expression in Col-0 and *tga14* mutant at 3, 6 and 11 hpi with *Pst avrRPS4*. The values represent the average of three independent samples ($P < 0.05$). (B) Induction of *ROXY9*, *ROXY11*, *ROXY12*, *ROXY13* and *ROXY15* expression in Col-0 after infection with *Pst avrRPS4*. The induction from 3 – 6 hpi, 3 – 11 hpi and 6 – 11 hpi are displayed. The values represent the average of three independent samples.

Next, we tested whether the expression is already influenced in untreated plants and if the expression of other *ROXYs* is affected. Total RNA of 6 week-old wildtype Col-0 and *tga14* mutant was analyzed by qRT-PCR (Figure 4.4.2).

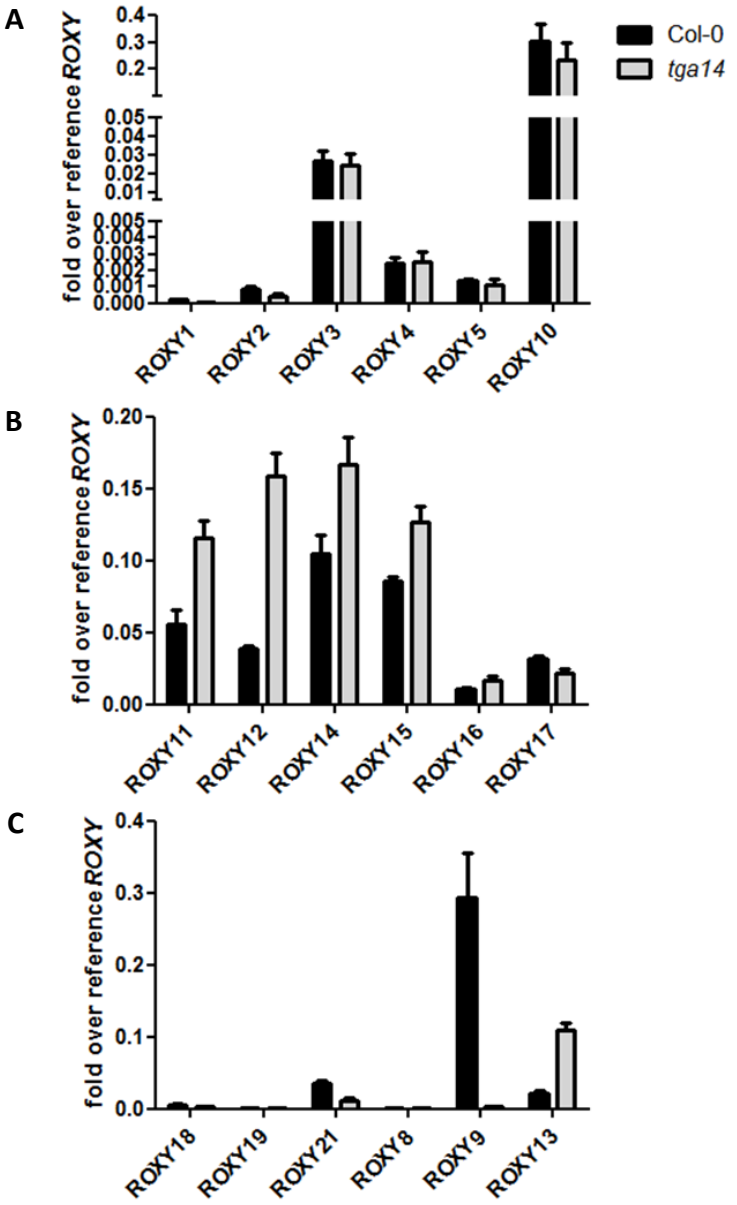

Fig. 4.4.2: Basal expression of *ROXYs* in Col-0 and *tga14* mutant

Total RNA of 6 week-old wildtype Col-0 and *tga14* mutant plants grown under short day conditions was extracted and the expression of *ROXYs* was tested with specific primers by qRT-PCR and normalized to *UBQ5* transcript levels. Bars represent the average ± SEM with n = 6. (A) Expression of *ROXY1*, *ROXY2*, *ROXY3*, *ROXY4*, *ROXY5* ans *ROXY10*. (B) Basal expression of *ROXY11*, *ROXY12*, *ROXY14*, *ROXY15*, *ROXY16* and *ROXY17*. (C) Basal Expression of *ROXY18*, *ROXY19*, *ROXY21*, *ROXY8*, *ROXY9* and *ROXY13*.

Again, *ROXY9* transcripts were absent in the *tga14* mutant background. Expression of its closest homolog *ROXY8* was not affected by clade I TGA TFs. In contrast, expression of *ROXY13* and all tandem-*ROXY* genes was increased (Figure 4.4.2 (C) & (B)). Expression of all other tested *ROXYs* was not affected in the *tga14* mutant under these conditions.

4.4.1 Deregulated expression of *ROXY9* and *ROXY13* is detected from the seedling stage onwards

To monitor whether the deregulated expression of *ROXY9* and *ROXY13* in the *tga14* mutant was consistent and robust during growth from seedlings to mature plants, wildtype Col-0 and *tga14* mutant were grown under SD conditions and harvested 1 to 6 weeks after sowing.

Transcript levels of *ROXY9* were consistently lower in the *tga14* mutant background, whereas *ROXY13* expression was up-regulated.

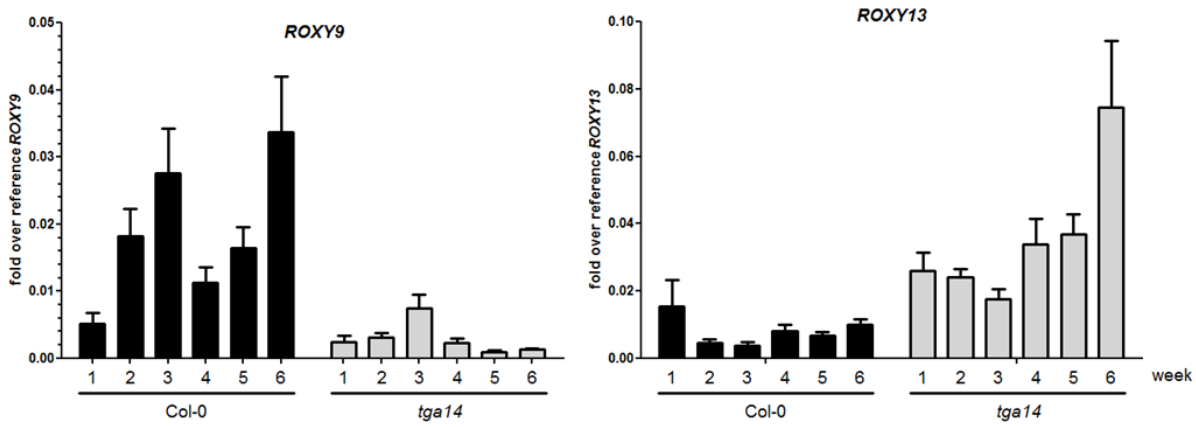

Fig. 4.4.1.1: Expression of *ROXY9* and *ROXY13* at different plant developmental stages

Total RNA of 1 to 6 week-old wildtype Col-0 and *tga14* mutant plants grown under short day conditions on soil was extracted. The expression of *ROXYs* was tested with specific primers by qRT-PCR and normalized to *UBQ5* transcript levels. Bars represent the average ± SEM with n = 6.

4.4.2 TGA1 and TGA4 control *ROXY9* and *ROXY13* expression redundantly

To analyze whether TGA1 and TGA4 act redundantly in controlling *ROXY9* and *ROXY13* expression, the single mutants *tga1* and *tga4* were grown with wildtype Col-0 and *tga14* mutant under SD conditions for 6 weeks. The transcript levels of *ROXY9* and *ROXY13* were analyzed by qRT-PCR (Figure 4.4.2.1). The reciprocal basal expression of both *ROXYs* was detected in *tga14* mutant. In contrast, the single *tga1* and *tga4* mutants were not affected in *ROXY9* and *ROXY13* expression. It is concluded that TGA1 and TGA4 act redundantly with regard to the expression of these genes.

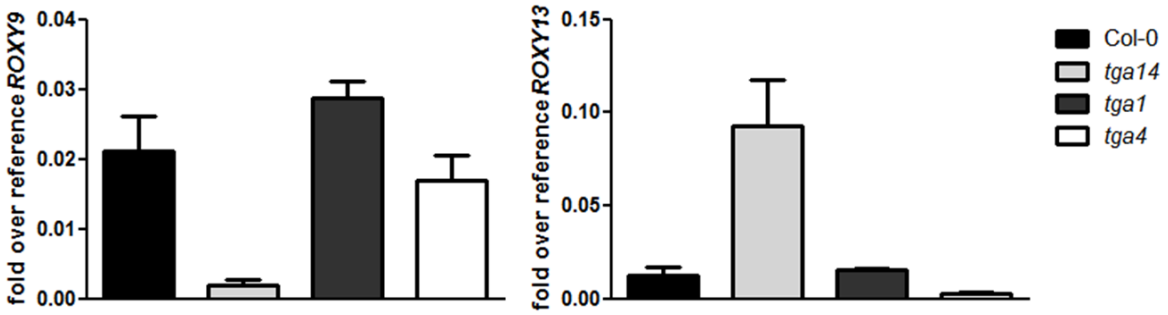

Fig. 4.4.2.1: Basal ROXY expression in the single mutant plants *tga1* and *tga4*

Total RNA of 6 weeks-old Col-0, *tga14*, *tga1* and *tga4* mutant plants grown under short day conditions was extracted. The expression of *ROXYs* was tested with specific primers by qRT-PCR and normalized to *UBQ5* transcript levels. Bars represent the average ± SEM with n = 4-5.

4.4.3 *ROXY* expression is not influenced by N-depletion

In order to find stimuli influencing the expression of *ROXY9* and *ROXY13* we searched available expression databases (https://www.genevestigator.com/gv/). Interestingly, only N-depletion influenced the expression of both *ROXYs*. Transcript levels of *ROXY9* were decreased and ROXY13 expression was elevated (Scheible et al., 2004). These reciprocal changes in expression reflected the constitutive deregulation of *ROXYs* in the *tga14* mutant. Therefore, we tried to repeat this observation and grew seedlings of wildtype Col-0 and the *tga14* mutant in liquid culture. After 8 days the medium was exchanged against medium with

(FN) or without (FN-) nitrogen. After 1 day incubation seedlings were harvested and the expression of *ROXY9* and *ROXY13* was monitored by qRT-PCR (Figure 4.4.3.1).

In contrast to other experiments, the reciprocal expression of *ROXYs* in the *tga14* mutant was not detectable in samples supplemented with a nitrogen source. A less pronounced effect was also observed in 1 week-old seedlings grown on soil (Fig. 4.4.1.1). Interestingly, the total amount of *ROXY13* transcripts was very low in this experiment. However, a strong influence of N-depletion on the expression of both *ROXYs* was not detected.

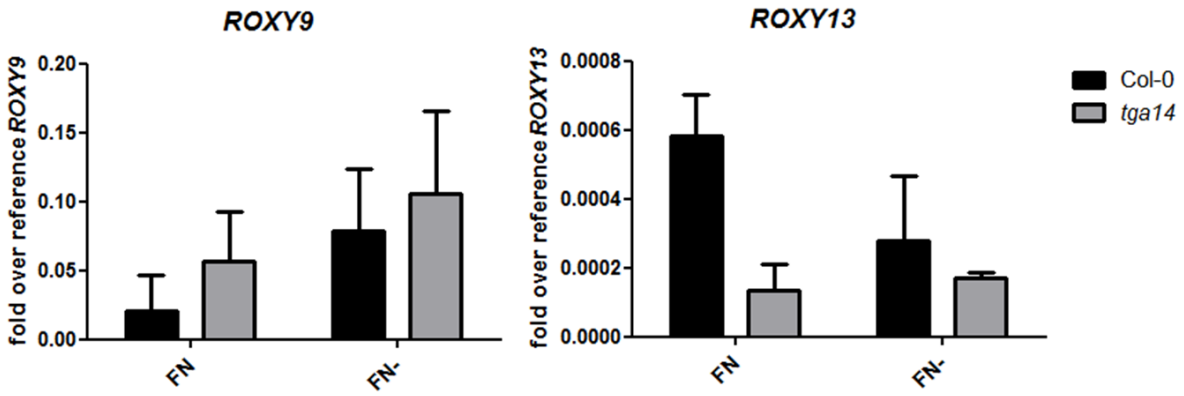

Fig. 4.4.3.1: ROXY expression in seedlings suffering N-depletion

Wildtype Col-0 and *tga14* mutant seedlings were grown for 8 days (30 rpm, 50 µM photones/cm^2/min) in six flasks with 30 ml of FN medium. The medium was exchanged against medium supplemented with (FN) or without (FN-) nitrogen. The seedlings were grown for 1 additional day and total RNA was extracted. ROXY9 and ROXY13 expression was analyzed by qRT-PCR. The bars represent the average ± SEM of 3 individual replicates.

4.4.4 *ROXY* expression is not influenced after exogenous application of SA or MeJA

In order to analyze whether exogenously applied plant defense-related hormones can influence the expression of both *ROXYs*, plants grown on soil were treated with SA or MeJA. To exclude processes influenced by endogenous SA which may fluctuate in soil-grown plants, the SA treatment was done with the *sid2-2* and *tga14/sid2-2* mutants. Total RNA was extracted 24 hours after application and analyzed by qRT-PCR (Figure 4.4.4.1). The affected expression of *ROXY9* and *ROXY13* in the *tga14/sid2-2* mutant was detectable in mock and SA

treated samples. After 24 h post SA application, the transcription was not influenced in the *sid2-2* and *tga14/sid2-2* mutants.

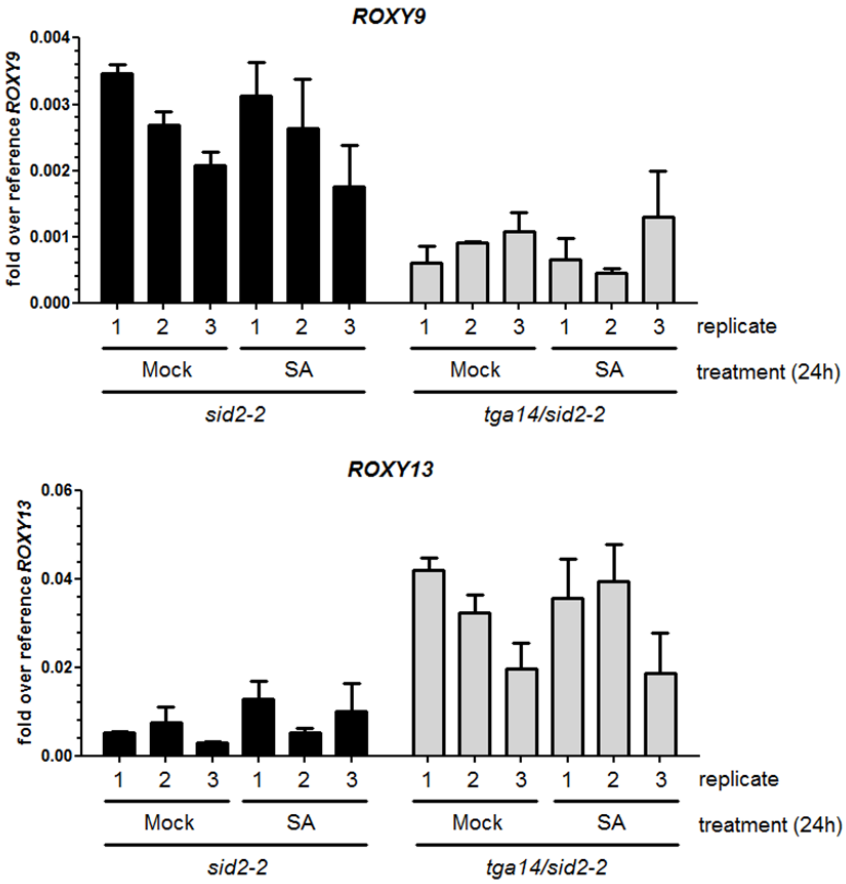

Fig. 4.4.4.1: *ROXY* expression after exogenous SA application in soil grown *sid2-2* and *tga14/sid2-2* mutant plants

sid2-2 and *tga14/sid2-2* mutant plants were grown on soil for 4 weeks under 12h/12h-light cycle. Plants were sprayed with 1 mM SA and harvested at 24 hours after treatment. RNA was extracted and the transcript levels of *ROXY9* and *ROXY13* were measured with specific primers by qRT-PCR and normalized to *UBQ5* expression. Every experiment displays the average ± SEM with 3 independent samples. For every sample plant material of 7 individual plants was combined.

Wildtype Col-0 and *tga14* mutant were grown on soil for 4 weeks and treated with MeJA (M&M 3.2.6.2). After 1, 4, 8 and 24 hpi total RNA was extracted and analyzed by qRT-PCR (Figure 4.4.4.2). Expression of *ROXY9* was constantly reduced in mock and MeJA treated *tga14* mutant. Incubation with MeJA did not affect the transcript levels in wildtype Col-0 and *tga14* mutant. However, transcript levels of *ROXY9* were elevated in all samples harvested at 8 hpi. Expression of *ROXY13* was slightly increased in wildtype Col-0 plants 8 h after MeJA application, whereas transcript levels were constitutively up-regulated in the *tga14* mutant in

all samples. Transcription in the mutant background was not influenced by MeJA. However, transcript levels of *ROXY13* were lowered in all samples harvested at 24 hpi.

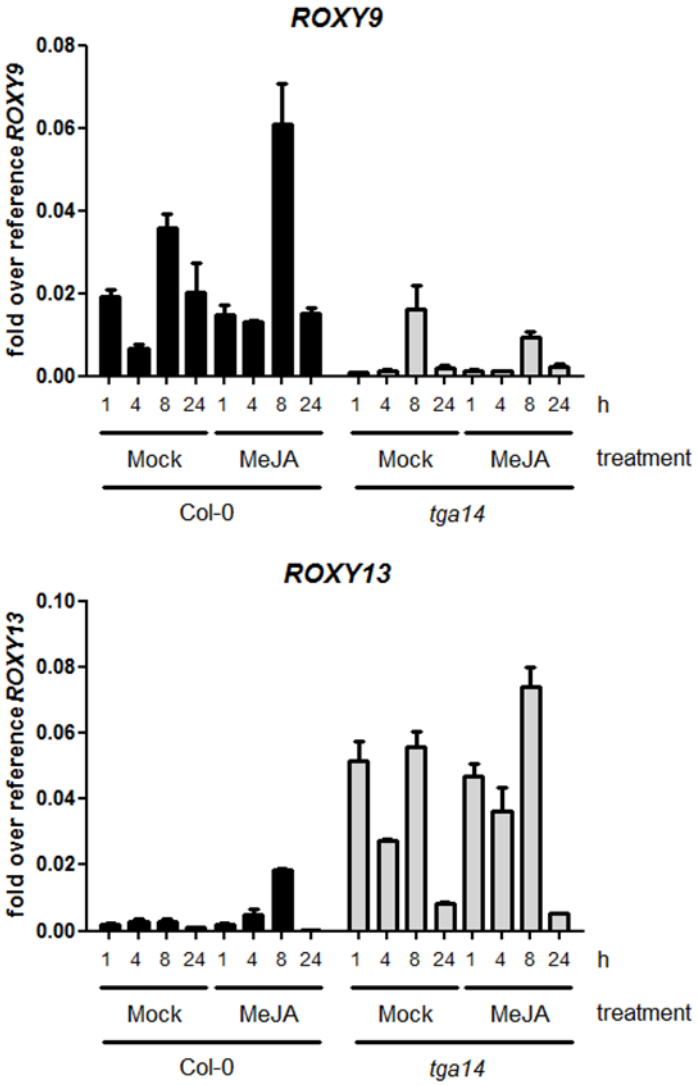

Fig. 4.4.4.2: *ROXY* expression after exogenous MeJA application in soil grown wildtype Col-0 and *tga14* mutant plants

Wildtype Col-0 and *tga14* mutant plants were grown on soil for 4 weeks under LD conditions. Plants were incubated in glass tanks aerated with or without 48 µl MeJA. RNA was extracted after 1, 4, 8 and 24 hours post treatment and the transcript levels of *ROXY9* and *ROXY13* were measured with specific primers by qRT-PCR and normalized to *UBQ5* expression. Every bar displays the average ± SEM with 3 independent samples.

4.5 ROXY9 and ROXY13 can physically interact with TGA1 and TGA4

To address the question whether a functional context between ROXY9 and ROXY13 and clade I TGA TFs is also possible on protein level, the interaction of the proteins was tested by Y2H and BiFC assays.

For Y2H assays ROXYs were fused to the GAL4 binding domain and tested with regard to its potential to interact with TGA1, TGA1red, TGA4, TGA4red, all fused to the GAL4 activation domain. As a positive control also the interaction of TGA2 with ROXY9 and ROXY13 was tested (Figure 4.5.1)

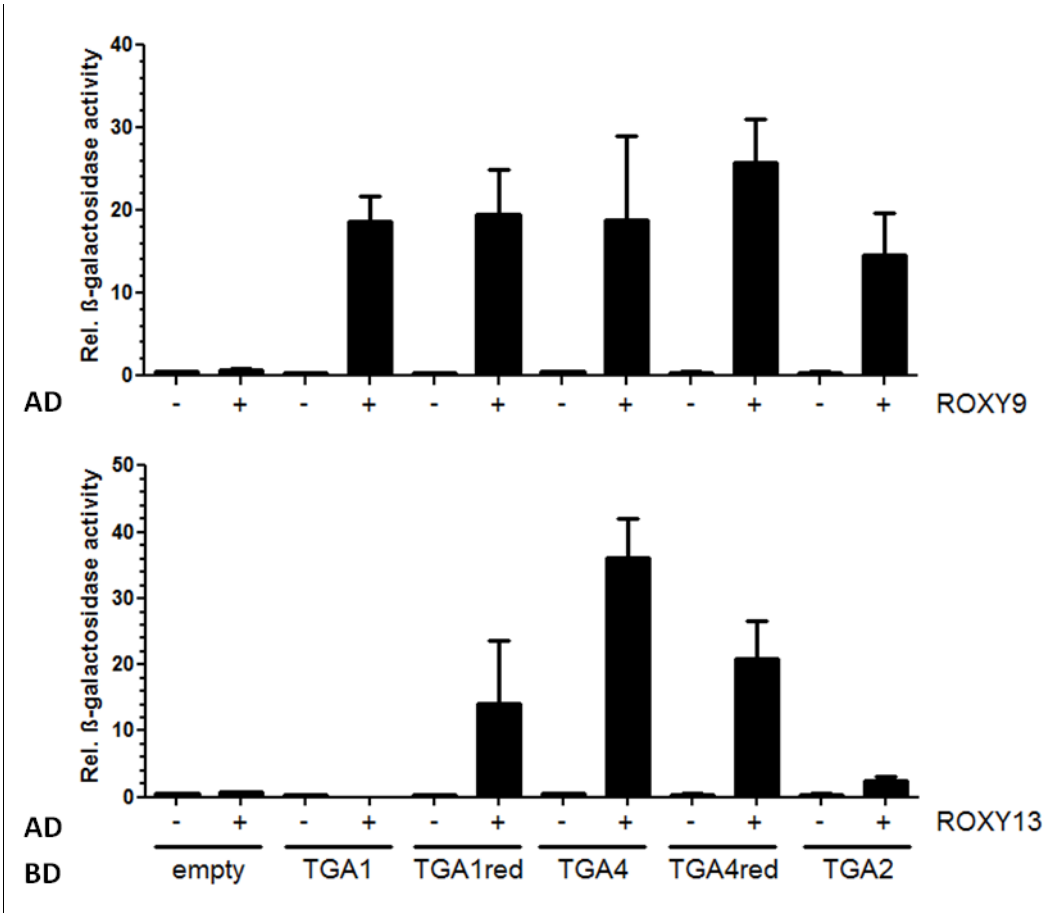

Fig. 4.5.1: Interaction of ROXYs and clade I TGA TFs in Y2H assays

Quantification of protein-protein interaction in yeast cells by ONPG assays. Prey plasmids encode TGA TFs fused to the GAL4 transactivation domain, bait plasmids encode ROXYs fused to the GAL4 binding domain. β-galactosidase activity was measured in yeast strain PJ69-4A. Bars represent the average ± SEM of 5-8 independent clones.

Co-expression of BD-TGA2 and AD-ROXY9 led to a clear increase of β-galactosidase activity. In direct comparison, co-expression of wildtype or mutated clade I TGA TFs and ROXY9 displayed similarly interaction intensity. The mutation of the critical cysteine residues of clade I TGA TFs did not influenced the interaction.

The ß-galactosidase activity after co-expression of ROXY13 and TGA2 was weaker than after co-expression of TGA1red, TGA4, and TGA4red with ROXY13. After co-expression of TGA1 and ROXY13 no ß-galactosidase activity was detectable. This was probably due to technical problems. To confirm these results and to elucidate the interaction of TGA1 and ROXY13, also BiFC assays were performed.

For BiFC assays TGA1, TGA1red, TGA4 and TGA4red were fused to the N-terminal part of YFP and the ROXYs to the C-terminal part. Wildtype Col-0 protoplasts were co-transformed with clade I TGA TFs and ROXYs (Figure 4.5.2).

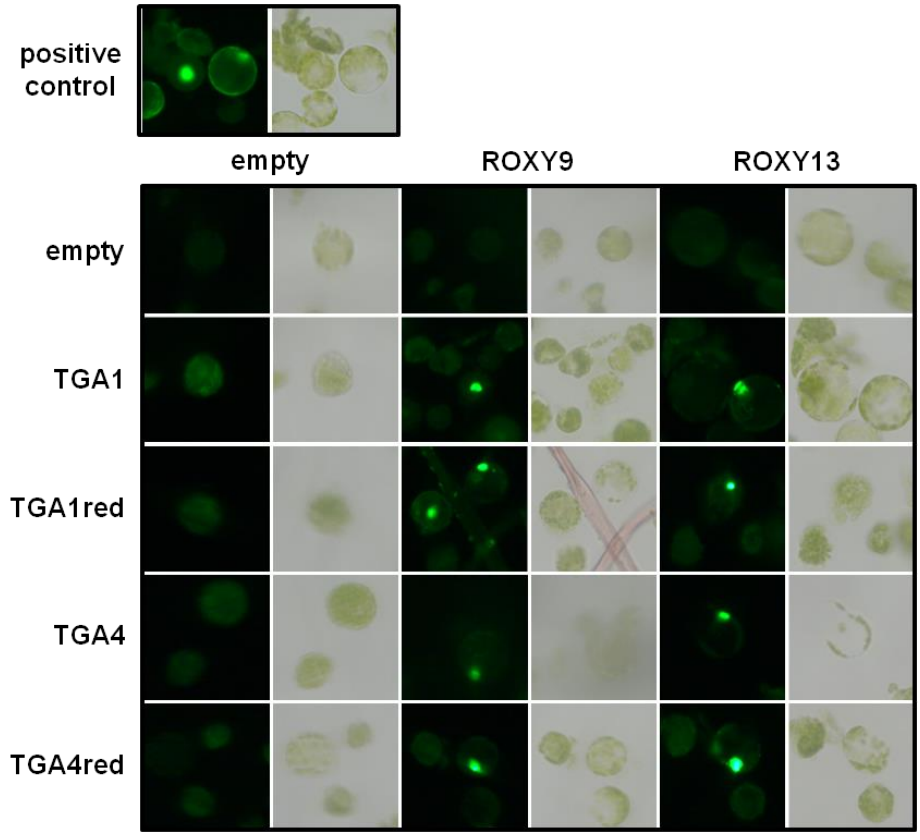

Fig. 4.5.2: Interaction of ROXYs and clade I TGA TFs in BiFC assays

The interaction of ROXY9 and ROXY13 with wildtype and constitutively reduced clade I TGA TFs was investigated with BiFC assays in *A. thaliana* protoplasts. Clade I TGA TFs are encoded with the N-terminal part of YFP, NPR1 with the C-terminal part. Successful complementation is shown by positive nuclear localization of BZI and ANK1 (positive control). Transformed protoplasts were incubated over night.

In protoplasts, co-transformed with wildtype or mutated clade I TGA TFs and the corresponding empty vector, no YFP signal was detectable. The expression of ROXY9 and ROXY13 without a clade I TGA TF also displayed no YFP signal. In contrast, co-expression of ROXY9 as well ROXY13 and TGA1, TGA1red, TGA4 and TGA4red led to a nuclear localized YFP signal.

The results of the Y2H assays and the BiFC assays show a clear interaction of clade I TGA TFs with ROXY9 and ROXY13. These interactions are independent of the mutation of the critical cysteine residues in TGA1 and TGA4. Furthermore the BiFC assays revealed an interaction in the nucleus.

4.6 ROXY9 cannot modify the redox status of critical cysteine residues in clade I TGAs in yeast

Since a direct redox modification of TGA1/TGA4 was suggested (Despres et al., 2003) and after an interaction between clade I TGA TFs with ROXY9 was detected in the nucleus (Fig. 4.5.2), a role of ROXY-dependent modification of TGA1 and TGA4 became more plausible. Therefore, we monitored a possible ROXY9-dependent protein modification of TGA1 by AMS-Shift assays (Kojer et al., 2012; M&M 3.2.9). Briefly, proteins were expressed in yeast and living cells were treated with AMS, in which AMS bound to reduced reactive cysteine residues in proteins.

First, we investigated whether the redox state of the HA-TGA1 protein is influenced by endogenous yeast GRXs. The yeast strains *YPH499* and *YPH499Δgrx1Δgrx2* were transformed with *pCU425-CTR1-HA-TGA1* and additionally with or without *pCU423-CTR1-HA-ROXY9*. Moreover, the binding of AMS to reactive cysteine residues was verified by treatment with NEM that blocks reactive cysteine residues in the reduced state without causing size shifts (Figure 4.6.1).

AMS treatment of HA-TGA1 led to a clear size shift, showing an already reduced HA-TGA1. Treatment with NEM did not lead to a size shift and it blocked an AMS-dependent shift of HA-TGA1. The pattern of proteins expressed in *YPH499Δgrx1Δgrx2* was similar to the pattern of proteins expressed in *YPH499*. It is concluded that the endogenous yeast GRXs were not responsible for the reduced status of HA-TGA1. Co-expression of HA-TGA1 with HA-ROXY9 displayed the same pattern.

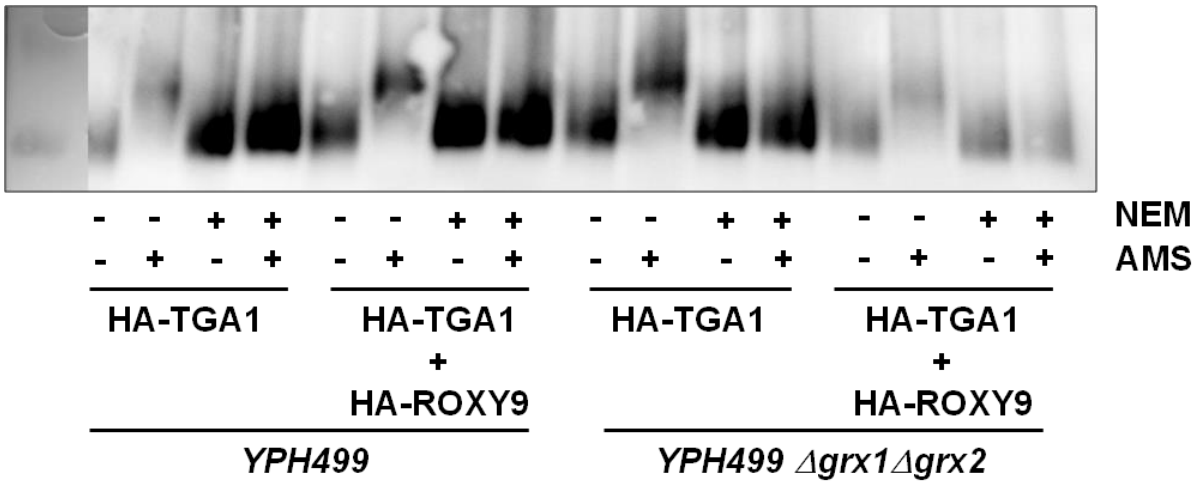

Fig. 4.6.1: Redox state of HA-TGA1 in the presence of endogenous yeast GRXs and ROXY9

Yeast strains *YPH499* and *YPH499Δgrx1Δgrx2* were transformed with pCU425-CTR1-HA-TGA1 with or without pCU423-CTR1-HA-ROXY9. First treatment was done with or without 100 mM NEM for 60 min at RT. After precipitation with 10 % TCA and washing 2 times, samples were treated with or without 75 mM AMS for 60 min at RT. Both incubation steps were done in darkness. Finally, samples were heated to 96°C for 2 min and proteins were separated by SDS-PAGE. HA-TGA1 protein signal was detected by western blot analysis with α-HA.

Next, we investigated the function of ROXY9 in mediating reduction of TGA1 in recovery assays. In order to oxidize the critical cysteine residues in HA-TGA1 proteins, *YPH499* yeast cells expressing HA-TGA1 with or without HA-ROXY9 were treated with the oxidizing reagent diamide for 10 min. Subsequently, yeast cells were washed and after a recovery time of 0 to 16 min the samples were treated with AMS. The mobility of the HA-TGA1 was monitored with SDS-PAGE and Westernblot analysis (Figure 4.6.2).

Again, the HA-tagged TGA1 protein was reduced in samples not treated with diamide. The diamide led to an oxidation of the HA-TGA1 protein and treatment with AMS did not result in a size shift. The ratio of a shifted and un-shifted signal of HA-TGA1 increased slightly over a period of 16 minutes recovery time (Figure 4.6.2 (A)). Whether this was due to a reduction of TGA1 or newly synthesized proteins cannot be answered. Additional expression of HA-ROXY9 did not result in a faster or more distinct reduction of the HA-TGA1 protein (Figure 4.6.2 (B)). These results show no evidence of functional ROXY9 activity for a reduction of TGA1 in yeast.

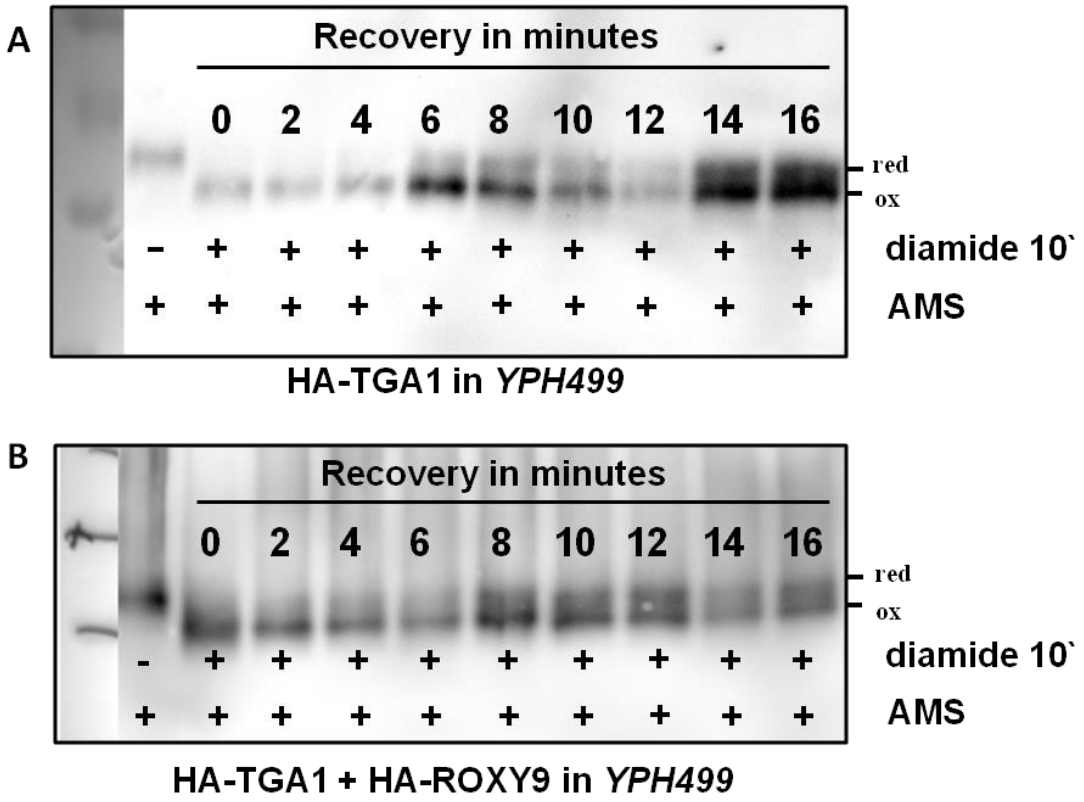

Fig. 4.6.2: Influence of the ROXY9 active site to the interaction with and modification of TGA TFs

Yeast cells transformed with pCU425-CTR1-HA-TGA1 and with or without pCU423-CTR1-HA-ROXY9 were treated with 20 mM diamide for 10 min at 30°C. After washing the cells 2 times, samples were incubated at 30°C. At 0, 2, 4, 8, 10, 12, 14, 16 min after washing cells were treated with 10% TCA. After sonification, proteins were precipitated with 10 % TCA and treated with AMS for 1 h. Proteins were separated by SDS-PAGE and the HA-TGA1 signal was detected by western blot analysis with α-HA. (A) Yeast cells transformed with pCU425-CTR1-HA-TGA1. (B) Yeast cells transformed with pCU425-CTR1-HA-TGA1 and pCU423-CTR1-HA-ROXY9.

Furthermore, we analyzed a possible formation of a mixed disulfide between HA-TGA1 and HA-ROXY9 to elucidate a functional ROXY9 activity. The presence of cysteine residues at N-terminal position 21 and C-terminal position 24 in the hypothetical active site of ROXY9 would favor a dithiol reaction. Exchange of cysteine 24 to alanine in ROXY9 would still allow a possible nucleophilic attack of the critical cysteine residues of HA-TGA1, whereas a completed reduction of HA-TGA1 and a release of HA-ROXY9 C24A would be blocked. This blocked release would result in a stable mixed sulfide between HA-TAG1 and HA-ROXY9. The yeast strain *YPH499* was transformed with *pCU425-CTR1-HA-TGA1*, *-HA-TGA1red*, *-HA-TGA4*, *-HA-TGA4red* and in addition with or without *pCU423-CTR1-HA-ROXY9* or *HA-ROXY9C24A*. The protein extracts were separated by SDS-PAGE and a

possible size shift of clade I TGA TFs mediated by a mixed disulfide was monitored by Westernblot analysis (Figure 4.6.3).

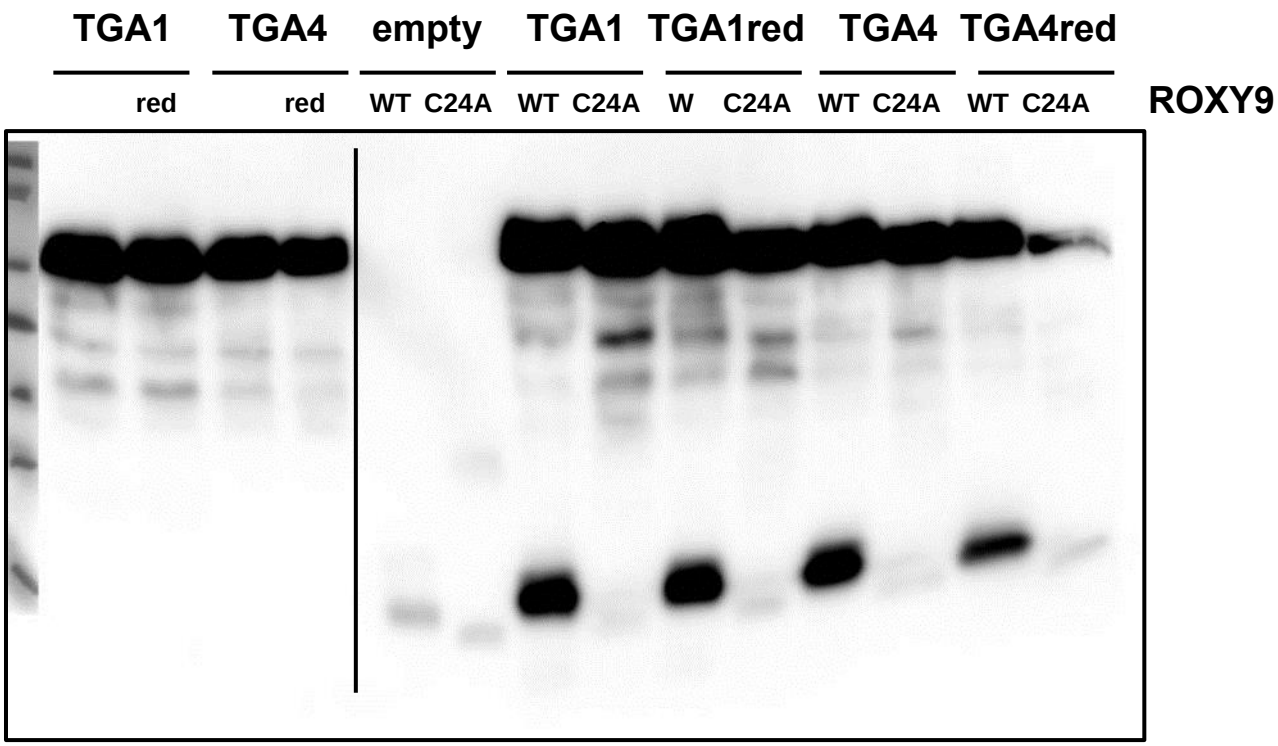

Fig. 4.6.3: Influenec of the ROXY9 active site to the interaction with and modification of TGA TFs

Yeast strain *YPH499* was transformed with *pCU425-CTR1-HA*-TGA1, *-HA-TGA1red*, *-HA-TGA4*, *-HA-TGA4red* and additionaly with or without *pCU423-CTR1-HA-ROXY9* and *-HA-ROXY9C24A*. Proteins were extracted from o/n cultures and separated by SDS-PAGE. Protein signals were detected by western blot analysis with α-HA.

All clade I TGA TFs were detected at the same size in extracts of transformed yeast cells. Also expression of HA-ROXY9 and HA-ROXY9C24A was similar, in which the mutation led to a size shift downwards. Co-expression of clade I TGA TFs and HA-ROXY9 and HA-ROXY9C24A did not led to any size shift of the TFs. Remarkably, the weak signal of HA-ROXY9 is increased after co-expression of clade I TGA TFs. In contrast, the signal of HA-ROXY9C24A was not enhanced.

These results do not support a possible role of ROXY9 in protein modification of clade I TGA TFs. However, a mutation of ROXY9 cysteine residue C24 led to a size shift of the protein and influences a displayed stabilization of HA-ROXY9 after co-expression with clade I TGA

TFs. Whether this was due to affected modifications of ROXY9 at the hypothetical active site has to be elucidated.

4.7 *ROXY9* and *ROXY13* promoter activities upon ectopic expression of clade I TGA TFs

Microarray analysis had revealed that *ROXY9* is constitutively less expressed in the *tga14* mutant. In order to analyze the potential of TGA1 and TGA4 in regulating *ROXY* promoter activities, clade I TGA TFs were expressed transiently in protoplasts along with *ROXY:LUC* reporter constructs. Furthermore, they were expressed stably in the *tga14* mutant and complementation of *ROXY* gene expression was monitored by qRT-PCR.

4.7.1 TGA1 and TGA4 activate the *ROXY9* promoter in transiently transformed *A. thaliana* protoplasts

To test whether clade I TGA TFs can stimulate *ROXY9* promoter activity, a fragment of 2086 bps upstream of the transcriptional start site (TSS) was fused to the firefly luciferase reporter gene. This fragment encodes TGA binding sites at -280, -947 and -1462 bps. Luciferase activity was measured after transfection of *A. thaliana* protoplasts with wildtype and mutated clade I TGA TFs driven by the *UBQ10* promoter (M&M 3.2.7).

In the experiment displayed in figure 4.7.1.1 (A), untagged clade I TGA TFs mediated slight increases of *ROXY9* promoter activities in wildtype Col-0 and *tga14* mutant protoplasts, whereby the TGA4 TFs were more effective. Mutation of the critical cysteine residues of TGA1 and TGA4 did not affect transcription of the luciferase gene. The 3xHA-tagged TFs failed to activate the *ROXY9* promoter (Figure 4.7.1.1 (B)).

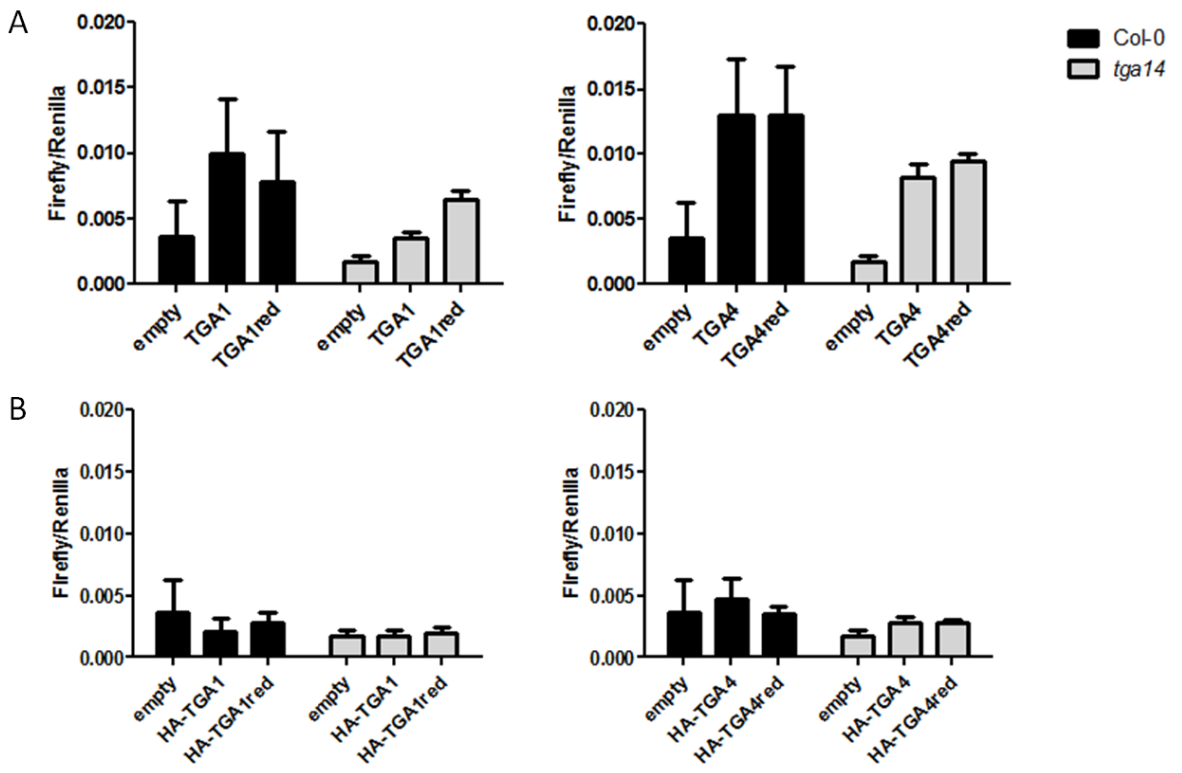

Fig. 4.7.1.1: Activation of the *ROXY9* promoter by clade I TGA TFs in transient protoplast assays

Wildtype Col-0 and *tga14* mutant protoplasts were transfected with 5 µg *ROXY9:Firefly luciferase* plasmid, 1 µg *UBQ10:Renilla luciferase* plasmid and 7.5 µg effector plasmid (*UBQ10:TGAs*). The untagged (A) and 3xHA-tagged (B) clade I TGA TFs were expressed under the control of the *UBQ10* promoter. Bars represent the average of 4 independent samples.

4.7.2 Co-expression of *ROXYs* and application of SA cannot enhance TGA activity in transient protoplast assays

Endogenous Clade I TGA TFs are described to be reduced after application of SA (Depres et al., 2003) and ROXYs are suggested to mediate modifications of TGA TFs, whereas we found no evidence for this in yeast. In order to analyze a possible activation or an increase of clade I TGA TFs function at the *ROXY9* promoter, protoplasts were treated with SA or co-transfected with *ROXYs* (Figure 4.7.2.1). The wildtype and mutated TGA4 activated the *ROXY9* promoter more effectively than TGA1 (Figure 4.7.1.1). Hence TGA4 was used for analysis.

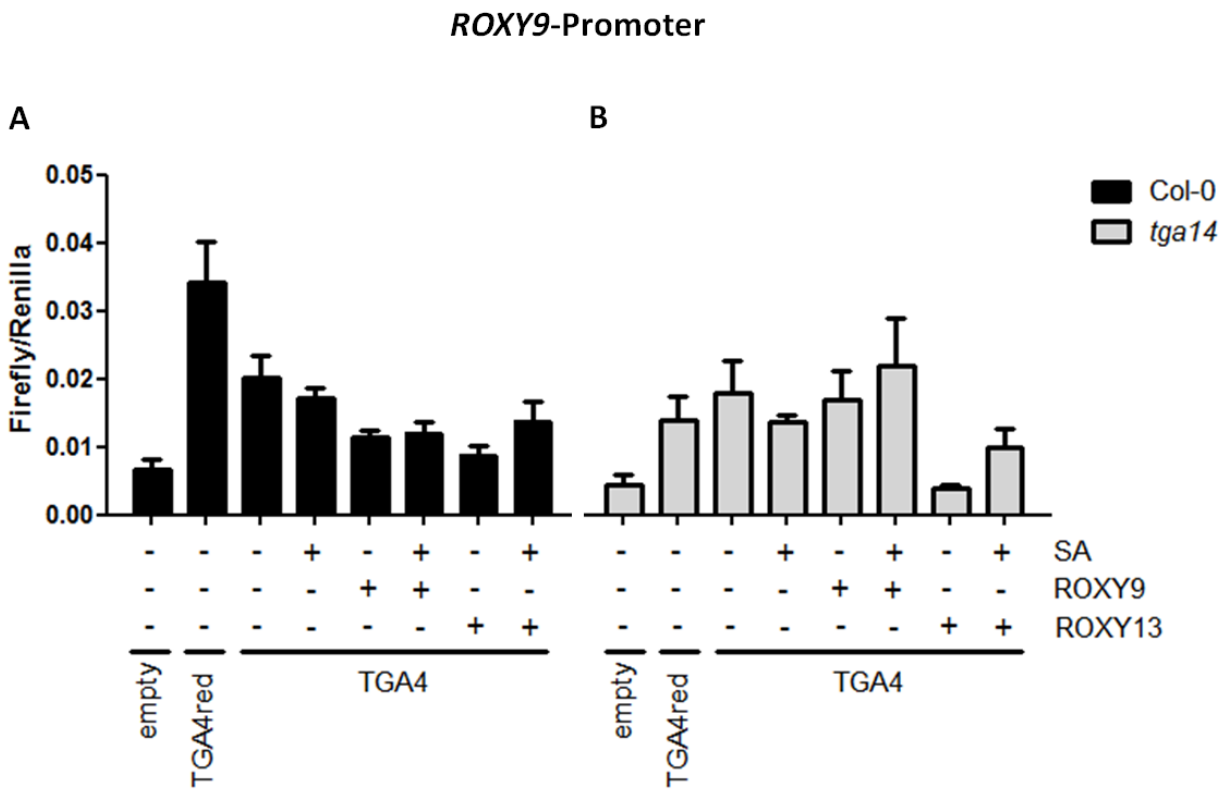

Fig. 4.7.2.1: Activation of *ROXY9* promoter by TGA4 TFs after SA treatment and co-transfection with ROXYs in transient protoplast assays

Wildtype Col-0 and *tga14* mutant protoplasts were transfected with 5 µg *ROXY9:Firefly luciferase* plasmid, 1 µg *UBQ10:Renilla luciferase* plasmid and 7.5 µg effector plasmid. The untagged clade I TGA TFs and *ROXYs* were expressed under the control of the *UBQ10* promoter. Samples were incubated over night with or without 5 µM SA. Bars represent the average of 4 independent samples.

Mutated TGA4red and TGA4 were able to activate the *ROXY9* promoter in wildtype Col-0 and *tga14* mutant protoplasts. The different combinations of SA treatment and co-transfection with ROXY9 and ROXY13 did not affect the function of TGA4.

In addition, the function of wildtype and mutated TGA4 at the *ROXY13* promoter was analyzed (Figure 4.7.2.2). The promoter fragment 2035 bps upstream of the TSS encodes two possible single binding sites at -800 and -1126 bps.

Surprisingly, *ROXY13* promoter was activated by the mutated TGA4red in wildtype Col-0 protoplasts but only slightly by TGA4. SA treatment and co-transfection did not activate TGA4 function at the promoter. However, the *ROXY13* promoter was only slightly activated in *tga14* mutant protoplasts by TGA4 and TGA4red.

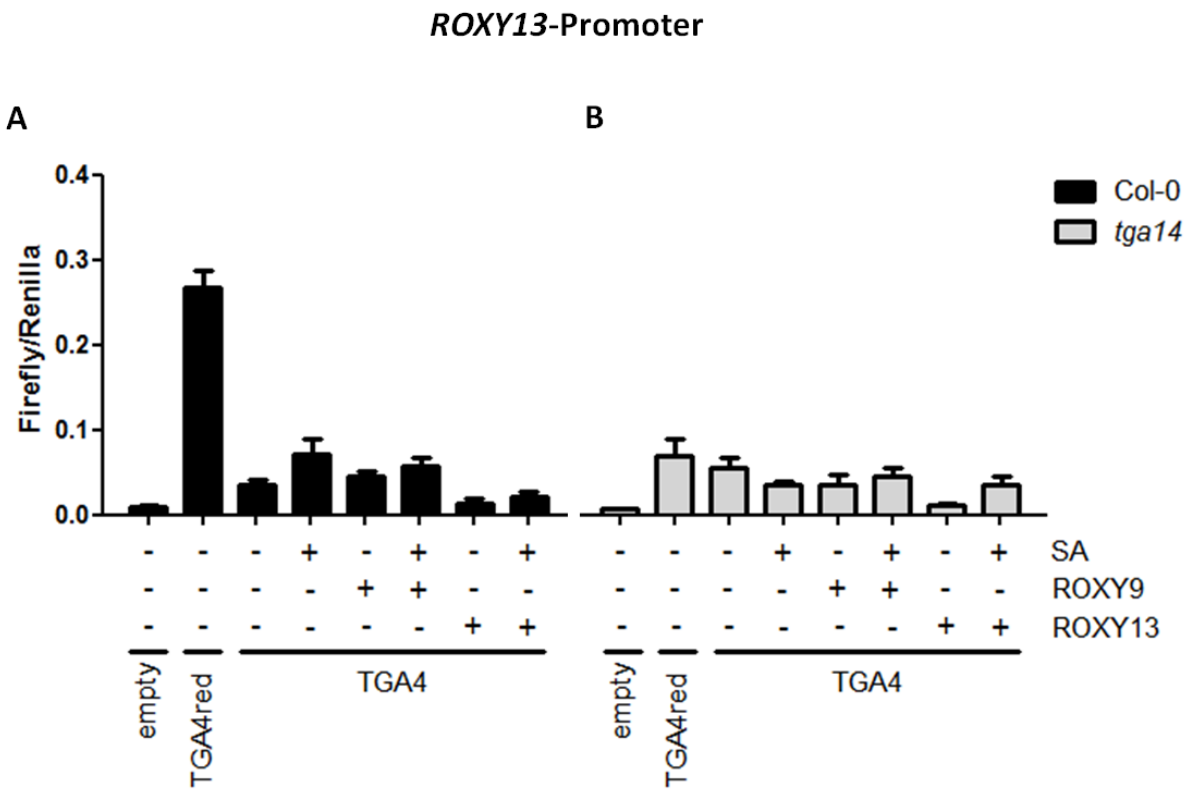

Fig. 4.7.2.2: Activation of *ROXY13* promoter by TGA4 after SA-treatment and co-transfection with ROXYs in transient protoplast assays

Wildtype Col-0 and *tga14* mutant protoplasts were transfected with 5 µg *ROXY9:Firefly luciferase* plasmid, 1 µg *UBQ10:Renilla luciferase* plasmid and 7.5 µg effector plasmid. The untagged clade I TGA TFs and *ROXYs* were expressed under the control of the *UBQ10* promoter. Samples were incubated over night with or without 5 µM SA. Bars represent the average of 4 independent samples.

4.7.3 Deregulated expression of *ROXYs* is not complemented after ectopic expression of clade I TGA TFs in the *tga14* mutant

Next, we analyzed the complementation of *ROXY* gene expression by qRT-PCR in *tga14* mutant plants expressing wildtype and mutated clade I TGA TFs. The cDNAs of the TFs were driven by the *35S:* promoter and the proteins were expressed with or without a 3xHA-tag. Seed batches of 10 independent lines per construct were used for analysis.

As expected, transcripts of *TGA1* and *TGA4* were not detectable in the *tga14* mutant. Expression levels of the four different transgenes were in the same range in all samples (Figure 4.7.3.1) and ectopically expressed 3xHA-tagged proteins were detectable by western blot analysis (Fig S23).

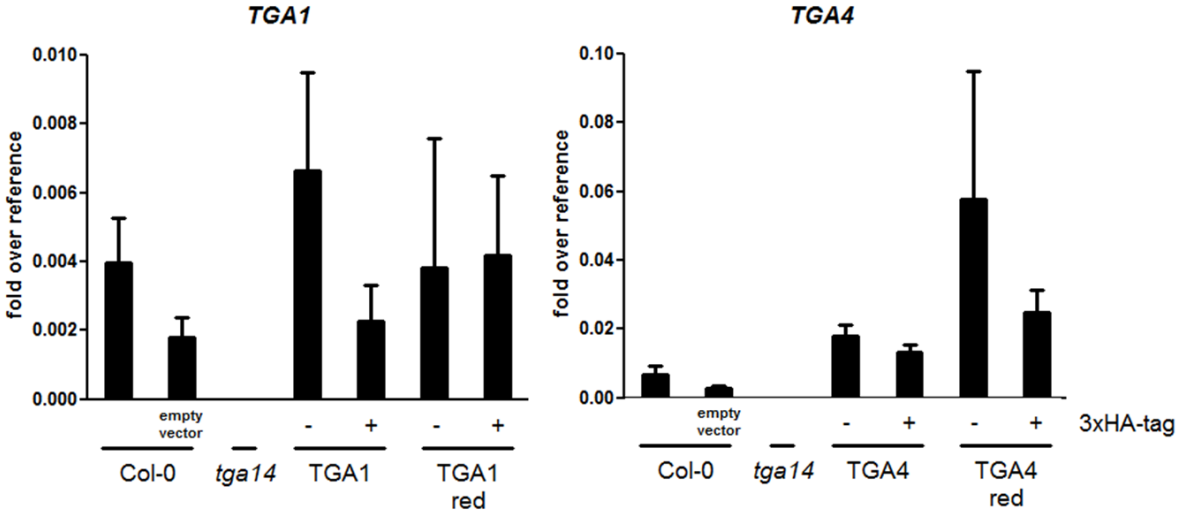

Fig. 4.7.3.1: *TGA1* and *TGA4* expression in *tga14* mutant plants transformed with untagged and 3xHA-tagged wildtype and mutated clade I TGA TFs

Clade I TGA TFs were expressed under the control of the *35S*:promoter with or without a 3xHA-tag in *tga14* mutant plants. The progenies of 40 T2 lines per construct were combined and used for analysis. For every replicate (4), 10 individual plants per combined seed batch were harvested. Plants were grown under LD-conditions for 3 weeks and transcript levels were analyzed by qRT-PCR.

Unexpectedly, the expression of *ROXY9* and *ROXY13* was not complemented (Figure 4.7.3.2). As shown before, the *tga14* mutant was affected in *ROXY* expression.

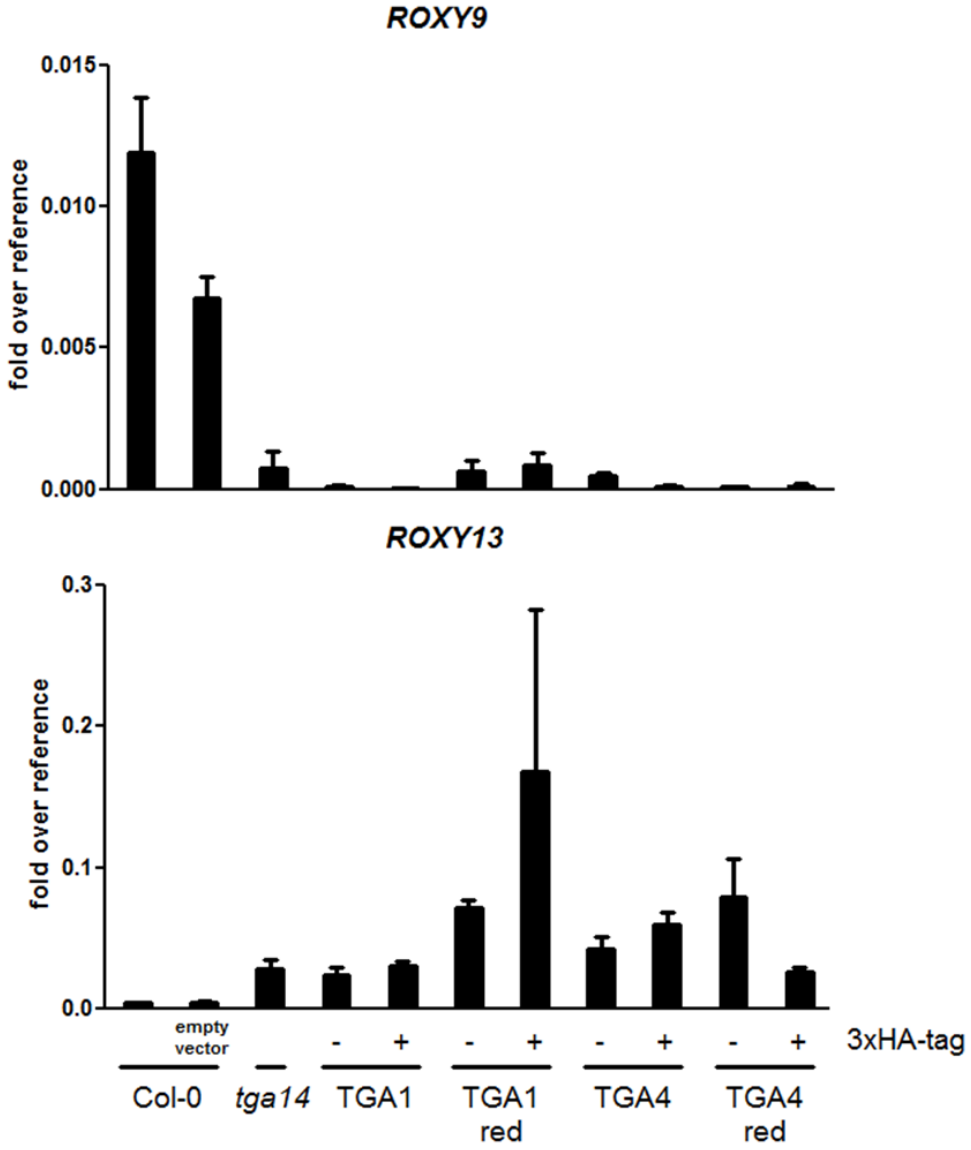

Fig. 4.7.3.2: *ROXY9* and *ROXY13* expression in *tga14* mutant plants transformed with untagged and 3xHA-tagged wildtype and mutated clade I TGA TFs

Clade I TGA TFs were expressed under the control of the *35S*:promoter with or without a 3xHA-tag in *tga14* mutant plants. In total, the progenies of 10 T2 lines per construct were combined and used for analysis. Bars represent 4 biological replicates. For every replicate, 10 individual plants per combined seed batch were harvested. Plants were grown under LD-conditions for 3 weeks and transcript levels were analyzed by qRT-PCR.

4.8 RNAi lines of *ROXY9* do not show *tga14*-like susceptibility after infection with *Pst avrRPS4*

In order to identify a possible role of *ROXY9* in avrRPS4-triggered resistance, we compared bacterial propagation in the *tga14* mutant and *ROXY9*-RNAi-plants.

First, we ordered a set of 10 individual seed stocks (N275884, CATMA2a46300) at the European Arabidopsis Stock Centre (NASC). All lines were transformed with the same clone that contains gene-specific tags (GSTs) for *ROXY9* developed by the CATMA (Complete *Arabidopsis* Transcriptome MicroArray) project (Hilson et al., 2004). These GSTs had been cloned into binary hairpin RNA vectors by the AGRIKOLA (Arabidopsis Genomic RNAi Knock-down Line Analysis) project and transgenic plants had been created (http://www.agrikola.org/index.php?o=/agrikola/main).

ROXY9 transcript levels in the 10 individual heterozygous lines were monitored by qRT-PCR (Figure 4.8.1). Lines 2821 and 2825 showed the lowest *ROXY9* expression compared to expression in wildtype Col-0 plants.

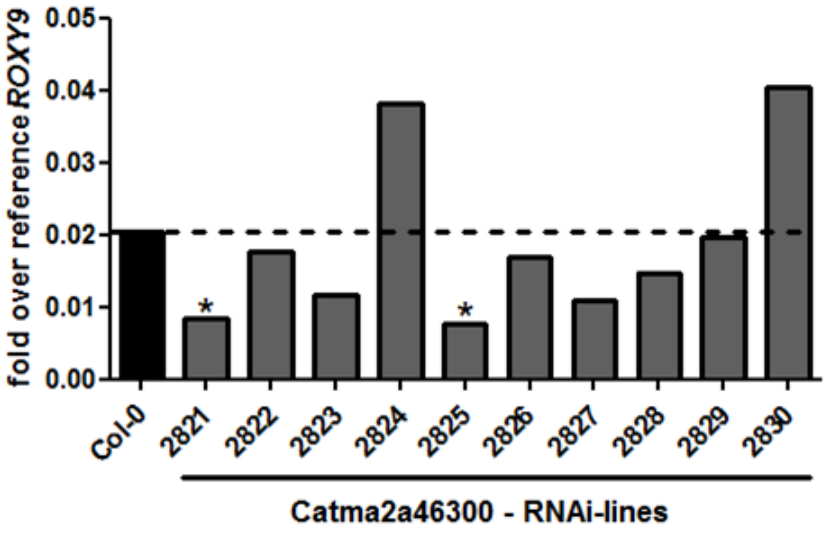

Fig. 4.8.1: Analysis of *ROXY9* expression in *ROXY9*-RNAi-lines

30 - 40 single plants per *ROXY9*-RNAi line and wildtype Col-0 were grown under SD conditions on soil for 3 weeks. A single leaf per plant was harvested and the plant tissue combined in one sample. RNA was extracted and the *ROXY9* transcript levels were detected by qRT-PCR and normalized to *UBQ5* expression.

Based on the reduced expression in the heterozygous seed batches of lines 2821 and 2825, we used single plants grown under SD conditions for a pre-characterization after 3 weeks (Figure 4.8.2) with subsequent infection with *Pst avrRPS4* after 6 weeks of growth under SD conditions (Figure 4.8.3).

Again, the *tga14* mutant displayed an impaired *ROXY9* expression and it was used as threshold for the selection of individual plants, indicated by the broken lines (Figure 4.8.2). Asterisks indicate plants used for the titer experiment at 3dpi shown in figure 4.8.3. In the case of RNAi-line 2821, less individual plants displayed a decreased *ROXY9* expression than for RNAi-line 2825.

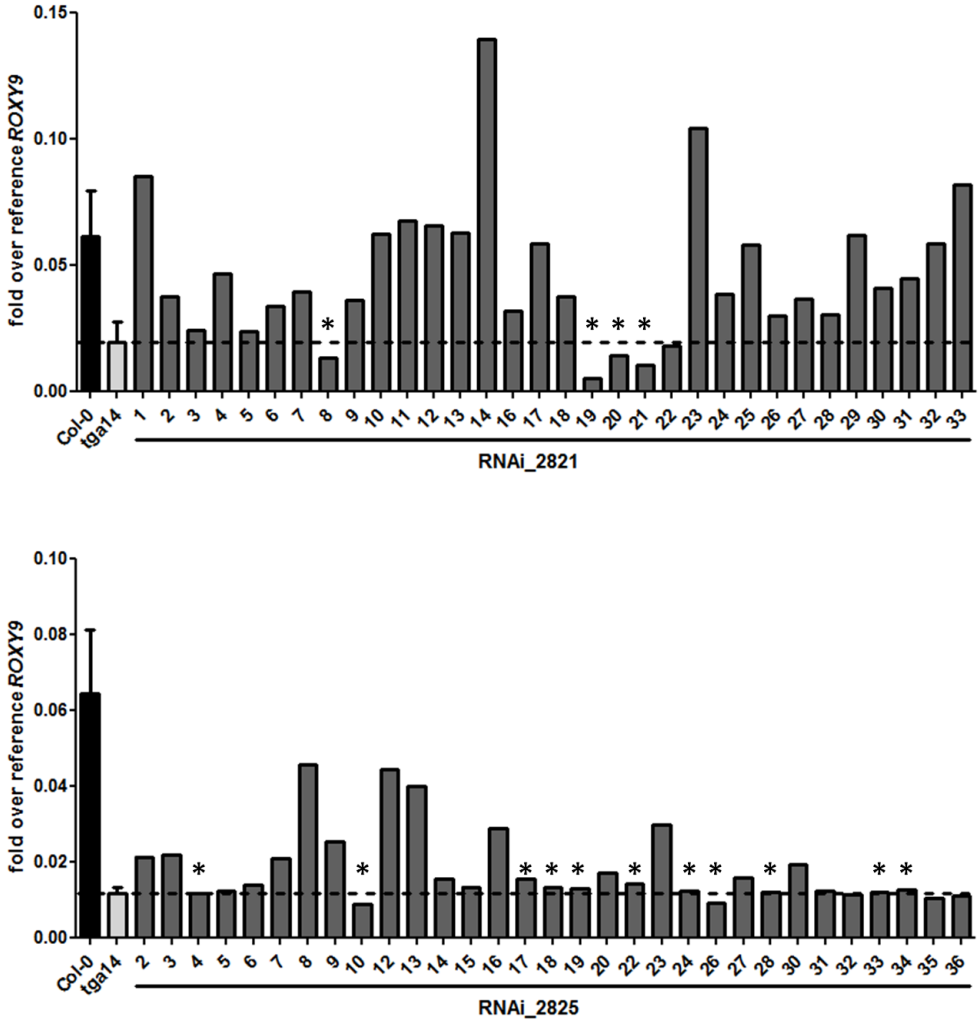

Fig. 4.8.2: Pre-characterization of individual plants of *ROXY9*-RNAi-lines 2821 and 2825

Plants were grown under SD conditions on soil for 3 weeks. RNA of a single leaf per plant of *ROXY9*-RNAi-lines 2821 and 2825 was extracted. Transcript levels of *ROXY9* were analyzed by qRT-PCR and normalized to *UBQ5* expression. The bars of wildtype Col-0 and the *tga14* mutant represent the average of 2 individual plants.

After selection of suitable candidate plants, leaf tissue was infiltrated with a bacterial suspension of *Pst avrRPS4* 3 weeks later and the propagation was determined at 3 dpi (Figure 4.8.3).

As observed before, the *tga14* mutant was more susceptible after infection with *Pst avrRPS4*. Moreover, the individual plants of RNAi-lines 2821 and 2825 allowed a *tga14*-like bacterial growth.

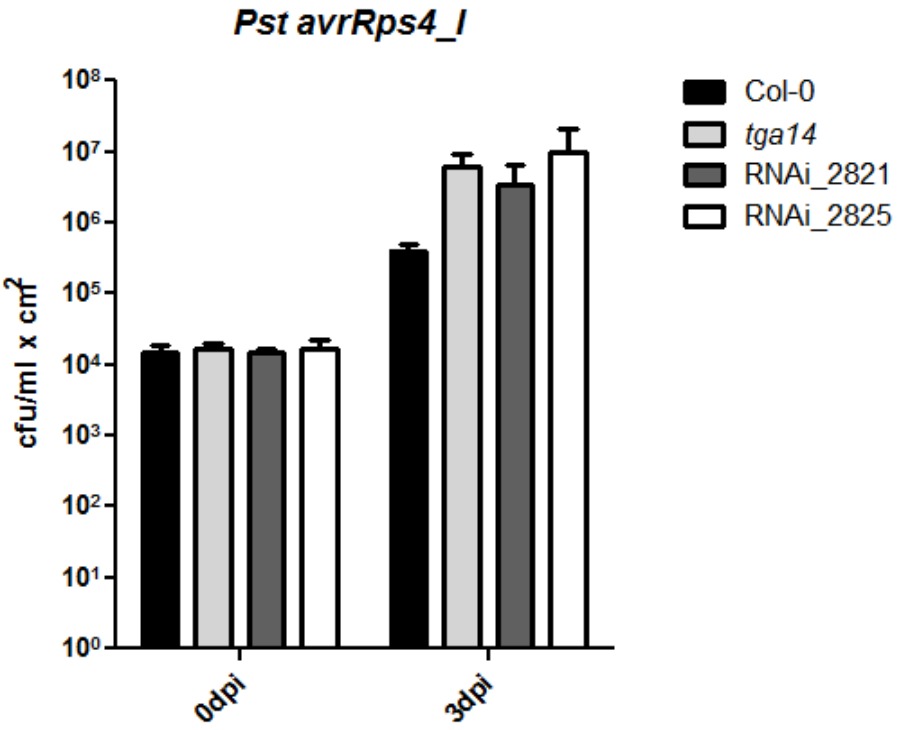

Fig. 4.8.3: Propagation of *Pst avrRPS4* in pre-characterized plants of *ROXY9*-RNAi-lines 2821 and 2825

Plants were grown under SD conditions on soil for 6 weeks. Three fully expanded leaves of wildtype Col-0, *tga14* mutant and pre-characterized plants of ROXY9-RNAi-lines 2821 and 2825 were infiltrated with a bacterial suspension of *Pst avrRPS4* (OD600 = 0.002). Bacterial growth was measured 1 hour and 3 days after treatment. Bars represent the average ± SEM of minimal 5 individual plants.

To confirm these results, we repeated this experiment with single plants of RNAi-line 2821. For an internal wildtype control in the heterozygous seed batch also plants with wildtype like *ROXY9* expression were infiltrated with *Pst avrRPS4* (Figure 4.8.4).

Unexpectedly, RNAi plants with WT-like *ROXY9* expression were more susceptible than RNAi plants with *tga14*-like *ROXY9* expression.

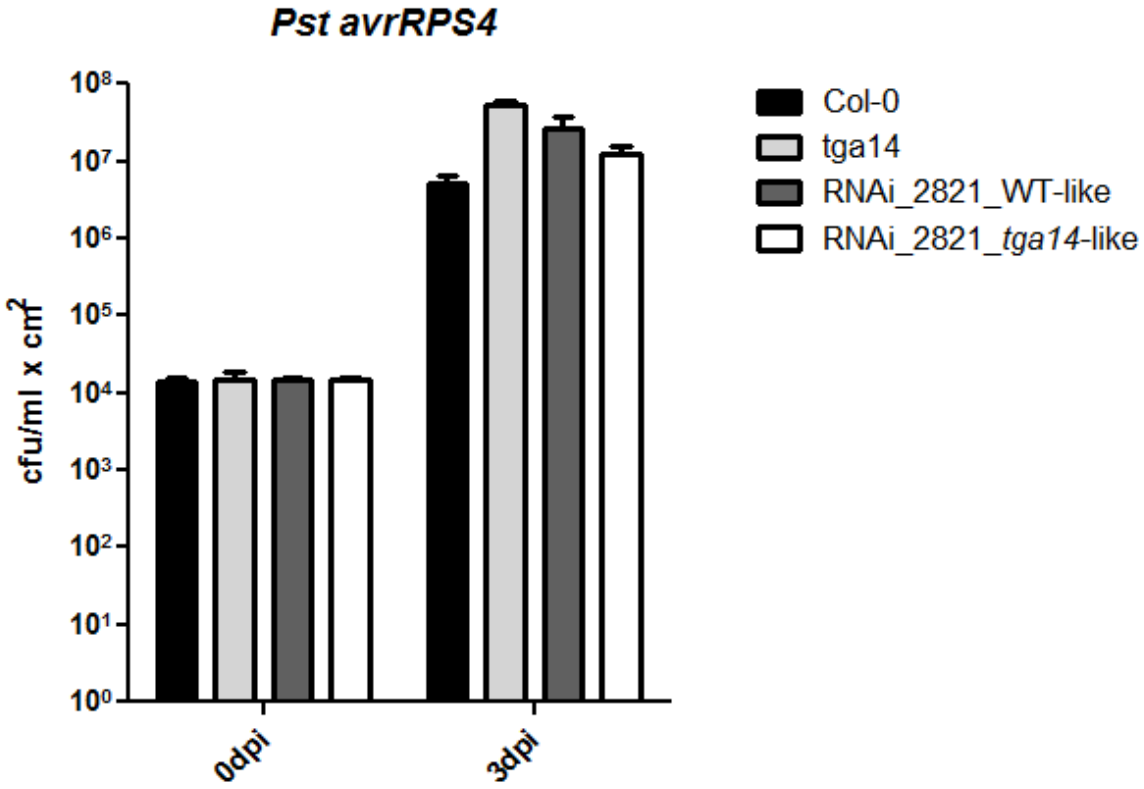

Fig. 4.8.4: Propagation of *Pst avrRPS4* in pre-characterized plants of *ROXY9*-RNAi-lines 2821

Plants were grown under SD conditions on soil for 6 weeks. Three fully expanded leaves of wildtype Col-0, *tga14* mutant and pre-characterized plants of ROXY9-RNAi-line 2821 were infiltrated with a bacterial suspension of *Pst avrRPS4* (OD600 = 0.002). Bacterial growth was measured 1 hour and 3 days after treatment. Bars represent the average ± SEM of minimal 5 individual plants.

In order to analyze a possible increased susceptibility of *ROXY9*-RNAi-lines in more detail, the bacterial propagation in the single plants was correlated to the *ROXY9* expression detected by qRT-PCR and the presence of the specific RNAi construct amplified by PCR (Figure 4.8.5). The bacterial propagation in the single plants of RNAi-line 2821 are displayed in figure 4.8.5 (A), the expression of *ROXY9* in figure 4.8.5 (B) and the presence of the specific RNAi construct in figure 4.8.5 (C).

For the single plants 1, 2, 6, 18, 19 and 32 a correlation of decreased *ROXY9* expression, presence of the specific RNAi-construct and susceptibility of the plants after infection with *Pst avrRPS4* was possible. In contrast, the plants 3 and 4 displayed a decreased *ROXY9* expression, whereas no increased bacterial propagation was measurable. In the plants 5, 10, 11, 16, 24, 26 and 28 no RNAi-construct was detectable. The *ROXY9* expression was, in average, comparable to the expression in wildtype Col-0.

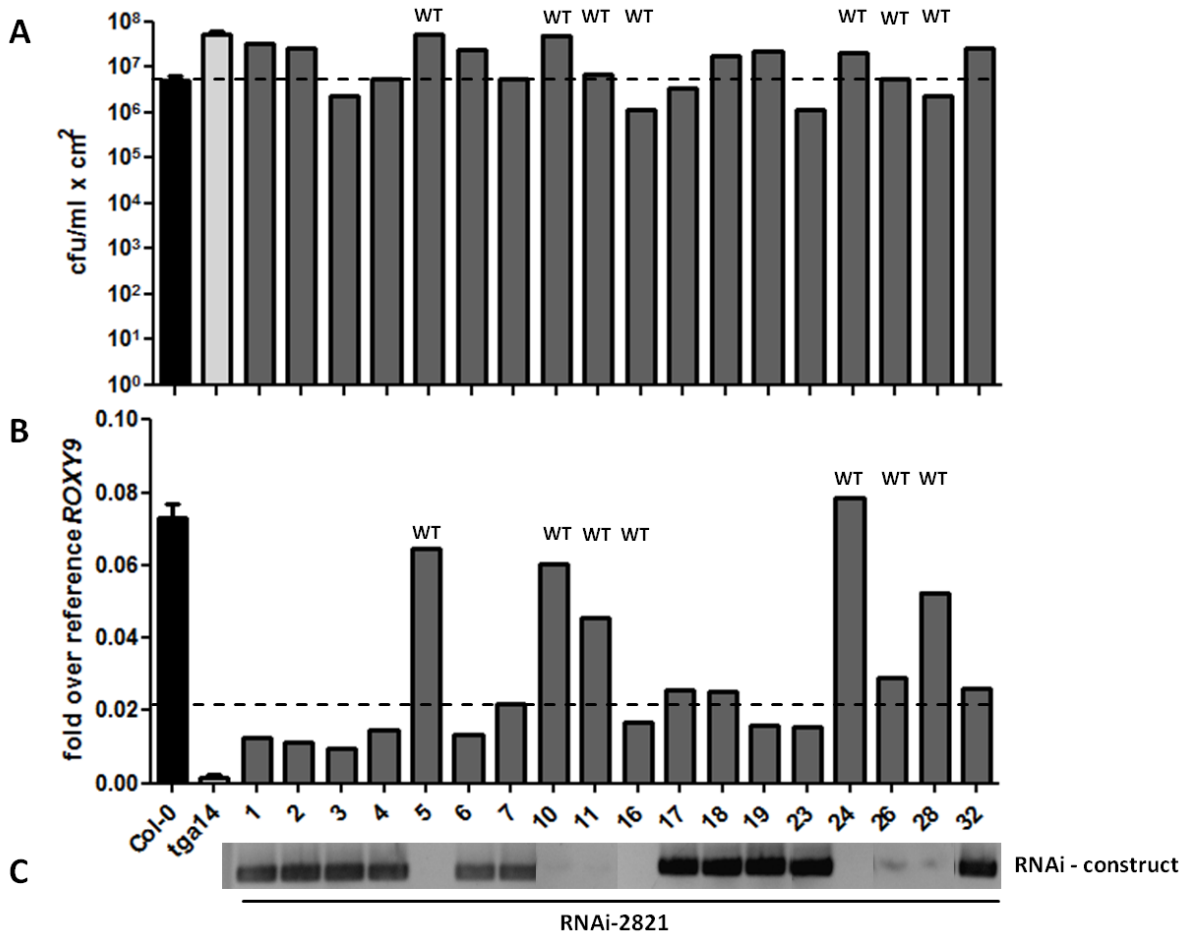

Fig. 4.8.5: Characterization of individual plants of *ROXY9*-RNAi-lines 2821

Bacterial propagation of individual plants of RNAi-line 2821 was correlated with *ROXY9* gene expression and the presence of the specific RNAi-construct. Wildtype plants are labeled with WT. (A) Bacterial propagation after infection with *Pst avrRPS4* in single plants analyzed in figure 3.9.3 (B). *ROXY9* expression was detected by qRT-PCR and normalized to *UBQ5* transcript levels. RNA was extracted from plants used in (C). *ROXY9*-RNAi-construct was detected with specific primers by PCR. Genomic DNA was extracted from leaf tissue.

However, these plants showed different bacterial propagations. Because of these fluctuations, the progenies of the plants 1, 2, 6, 11 and 24 were used for further pathogen assays (Figure 4.8.6).

Lines 1 and 2 reflected the overall correlation seen in figure 4.8.5, whereas line 6 showed wildtype-like bacterial propagation. The line 11 displayed an internal wildtype control. However, line 24 showed still a slight increase of bacterial propagation. To confirm the overall correlation of lines 1, 2 and 11, the experiment was repeated. Contradictorily, all lines displayed wildtype-like bacterial propagation.

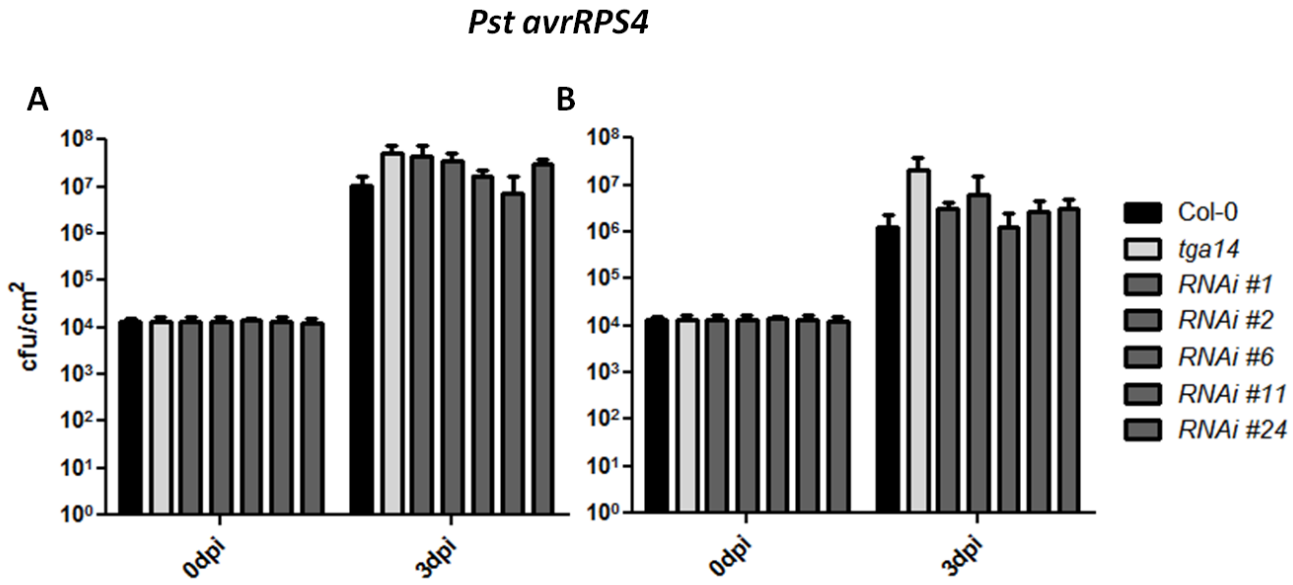

Fig. 4.8.6: Propagation of *Pst avrRPS4* in *ROXY9*-RNAi-lines 2821 #1, #2, #6, #11 and #24

Plants were grown under SD conditions on soil for 6 weeks. Three fully expanded leaves of wildtype Col-0, *tga14* mutant and *ROXY9*-RNAi-lines 2821 #1, #2, #6, #11 and #24 were infiltrated with a bacterial suspension of *Pst avrRPS4* (OD600 = 0.002). Bacterial growth was measured 1 hour and 3 days after treatment. Bars represent the average ± SEM of 5 individual plants. Two independent experiments are displayed in (A) and (B).

In order to analyze *ROXY9* expression in the tested lines, transcript levels were detected by qRT-PCR (Figure 4.8.7). Only lines 1 and 2 displayed in figure 4.8.6 (A) showed a correlation of decreased ROXY9 expression and increased susceptibility.

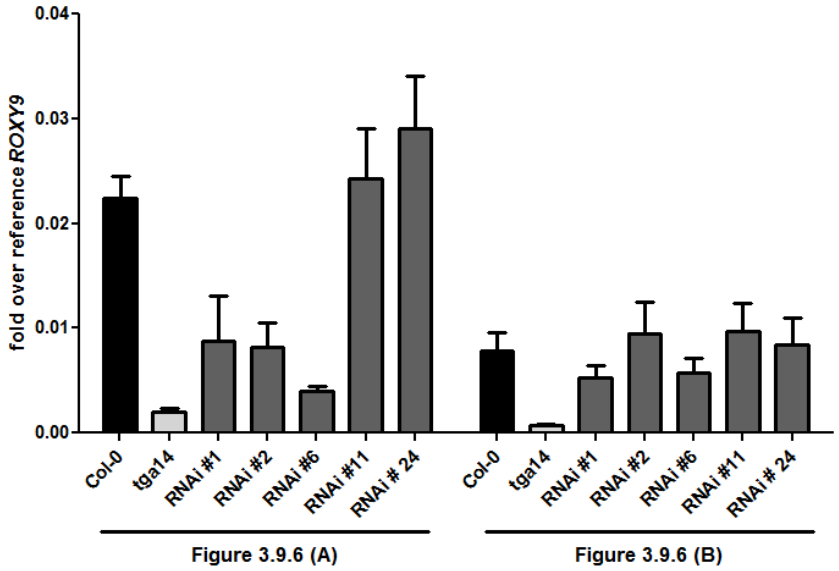

Fig. 4.8.7: ROXY9 expression in tested RNAi-lines 1, 2, 6, 11 and 24

Total RNA of plants used in figure 3.9.5 or infiltrated with 10 mM $MgCl_2$ was extracted and ROXY9 transcript levels were analyzed by qRT-PCR and normalized to *UBQ5* expression. Bars represent the average ± SEM of 5 individual plants.

The variability in susceptibility of tested single lines indicates that these results are not reliable. However, the loss of susceptibility of lines #1 and #2 in the experiment displayed in figure 4.8.6 (B) came along with wildtype-like transcript levels of *ROXY9* (Fig. 4.8.7).

4.9 Overexpression of *ROXY9* leads to clade I TGA TF-dependent developmental phenotypes

Next, we created wildtype Col-0 and *tga14* mutant plants expressing *HA-ROXY9* ectopically under the control of the *35S:* promoter (Figure 4.9.1)

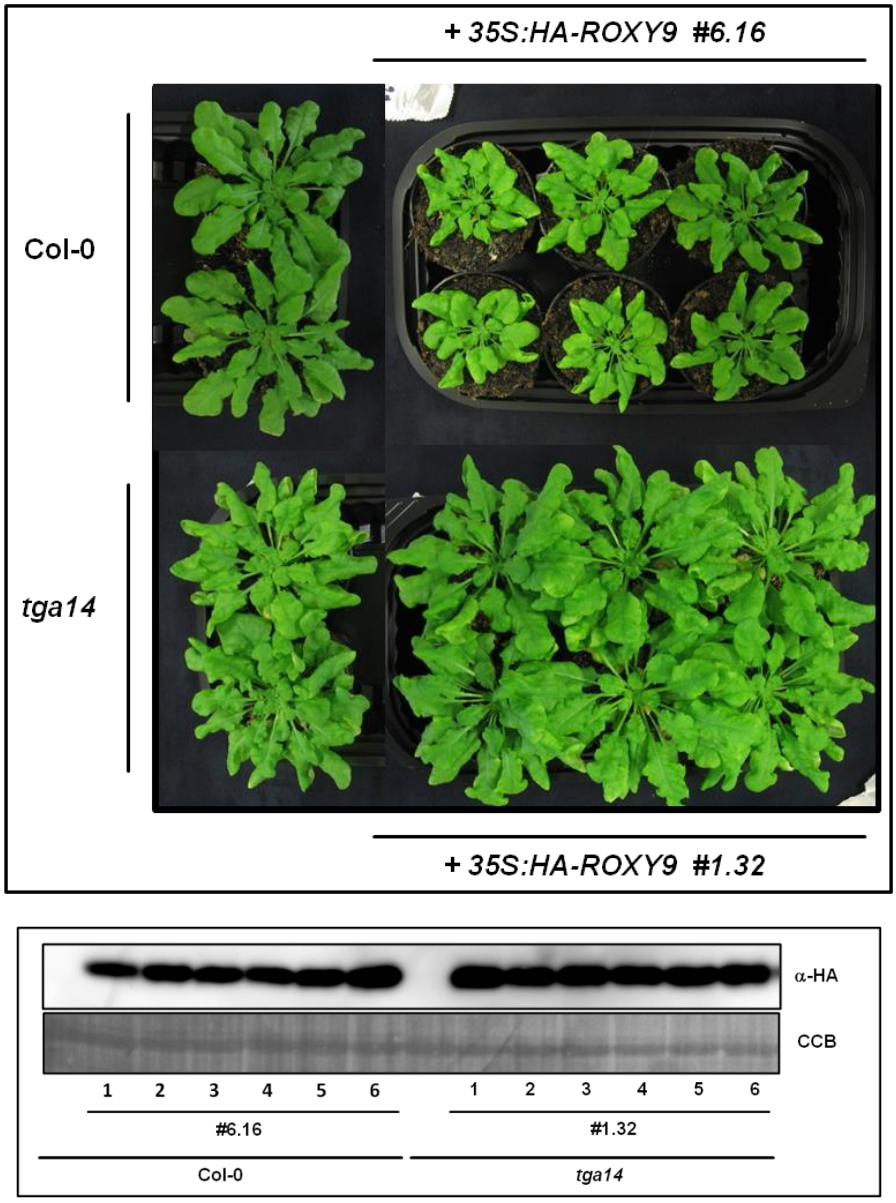

Fig. 4.9.1: Ectopic expression of *HA-ROXY9* in wildtype Col-o and tga14 mutant plants

Homozygous plants of Col-0 + *HA-ROXY9* and *tga14* + *HA-ROXY9* were grown on soil under SD conditions for 8 weeks. The ectopic expression of the 3x HA-tagged *ROXY9* is driven by the *35S:* promoter. Protein levels in Col-0 + *HA-ROXY9* and *tga14* + *HA-ROXY9* were detected by westernblot analysis using an α-HA antibody.

Interestingly, expression of *HA-ROXY9* in wildtype Col-0 led to reduced growth under SD conditions. Furthermore, the stunted growth was associated with crinkled and yellowing leaves. In contrast, ectopic expression in *tga14* mutant plants did not affect plant growth. Westernblot analysis revealed comparable protein levels of HA-ROXY9 in wildtype Col-0 and *tga14* mutant background.

In order to analyze further developmental phenotypes of plants overexpressing *HA-ROXY9*, flowering time and plant heigth were monitored. The identical plants from figure 4.10.1 were grown under SD conditions for overall 4 months (Figure 4.9.2). The ectopic expression of *HA-ROXY9* in wildtype Col-0 caused a reduction in plant height. Furthermore, seed development was delayed. In contrast, overexpression in the *tga14* mutant did not affect plant height or seed production.

Fig. 4.9.2: Analysis of flowering and seed development in wildtype Col-0 and *tga14* mutant plants expressing *HA-ROXY9* ectopically

Plants were grown on soil under SD conditions for 4 months. The ectopic expression of the 3x HA-tagged *ROXY9* was driven by the *35S:* promoter. The homozygous lines Col-0 + *HA-ROXY9 #6.16* and *tga14 + HA-ROXY9 #1.32* were compared with wildtype Col-0 and *tga14* mutant plants.

To test whether the dramatic phenotype of Col-0 + *35S:HA-ROXY9* occurs also under different growth conditions, a comparison of transgenic plants grown under LD conditions was done (Figure 4.9.3). A second wildtype Col-0 plant expressing *HA-ROXY9* ectopically was analyzed (Col-0 + *35S:HA-ROXY9* #7.18). Col-0 - *35S:HA-ROXY9* #7.19, lacking the transgene because of segregation, was used as an internal control. The lines Col-0 + *35S:HA-ROXY9* #6.16 and *tga14* + *35S:HA-ROXY9* #1.32 which had been analyzed before, were included for the experiments shown in figures 4.9.1 and 4.9.2.

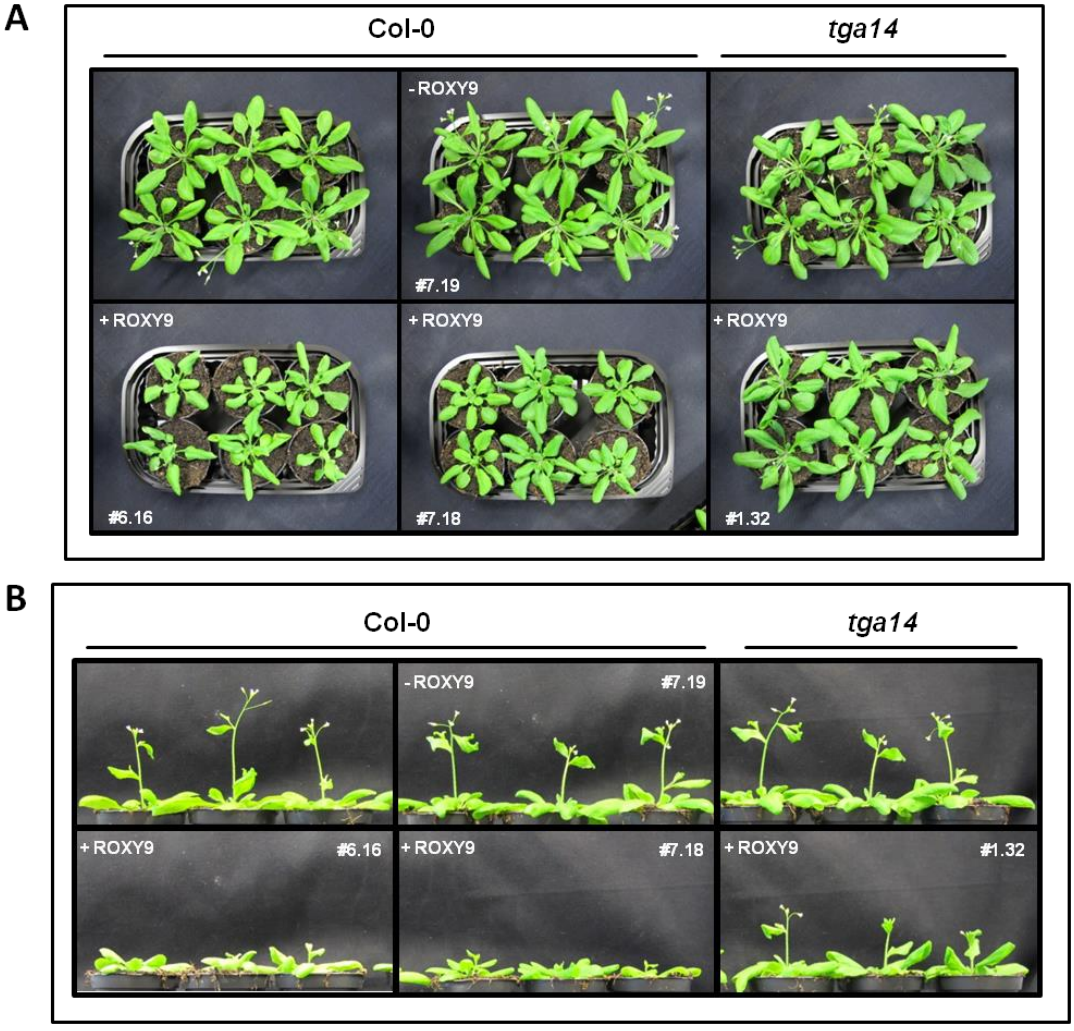

Fig. 4.9.3: The clade I TGA TF-dependent growth reduction induced by ectopic expression of *HA-ROXY9* under LD conditions

Homozygous plants of Col-0 + 35:S:*HA-ROXY9* and *tga14 + 35:S:HA-ROXY9* were grown on soil under LD conditions for 5 weeks. (A) Comparison of the growth. (B) Comparison of the flowering.

Again, the line Col-0 + *35S:HA-ROXY9* #6.16 showed a stunted growth with crinkled leaves (4.9.3 (A)). Furthermore, flowering was delayed in comparison to wildtype Col-0 and *tga14* mutant (4.9.3 (B)). In contrast, *tga14* + *35S:HA-ROXY9* #1.32 was not affected in growth or flowering. Col-0 + *35S:HA-ROXY9* #7.18 showed also the distinct phenotypes, whereas the internal control Col-0 - *35S:HA-ROXY9* #7.19 was not affected (4.9.3 (A) + (B)).

These results support a common function of clade I TGA TFs and ROXY9 *in planta*. Under SD conditions and under LD conditions the ectopic expression of *HA-ROXY9* in wildtype Col-0 led to alterations in plant development. To substantiate a clade I TGA TF-dependent mechanism triggered by ectopic expression of *HA-ROXY9,* an independent line expressing *HA-ROXY9* ectopically in the *tga14* mutant has to be tested.

4.10 Overexpression of *ROXY9* does not affect basal expression of defense related genes

In order to investigate a possible constitutive activation of plant defense signaling in the stunted Col-0 + *35S:HA-ROXY9* plants, we monitored the basal expression of the SA-dependent gene *PR1*, the JA-dependent gene *VSP2* and the JA/ET-dependent gene *PDF1.2* (Figure 4.10.1). Transgenic Col-0 + *35S:HA-ROXY9* #6.16 and *tga14* + *35S:HA-ROXY9* #1.32 plants were grown on soil for 8 weeks under SD conditions until the growth phenotype was visible. Total RNA was extracted and the transcript levels were detected with specific primers by qRT-PCR and normalized to *Actin8* expression (Figure 4.11.1).

The expression of *PR1* was not affected by overexpressing *HA-ROXY9*. All four genotypes showed similar transcript levels. Furthermore, the JA/ET-dependent gene *PDF1.2* was also not deregulated by high HA-ROXY9 protein levels. In contrast, the overexpression of *HA-ROXY9* in the *tga14* mutant background decreased elevated *VSP2* expression that was monitored in the *tga14* mutant plants (Figure 4.10.1).

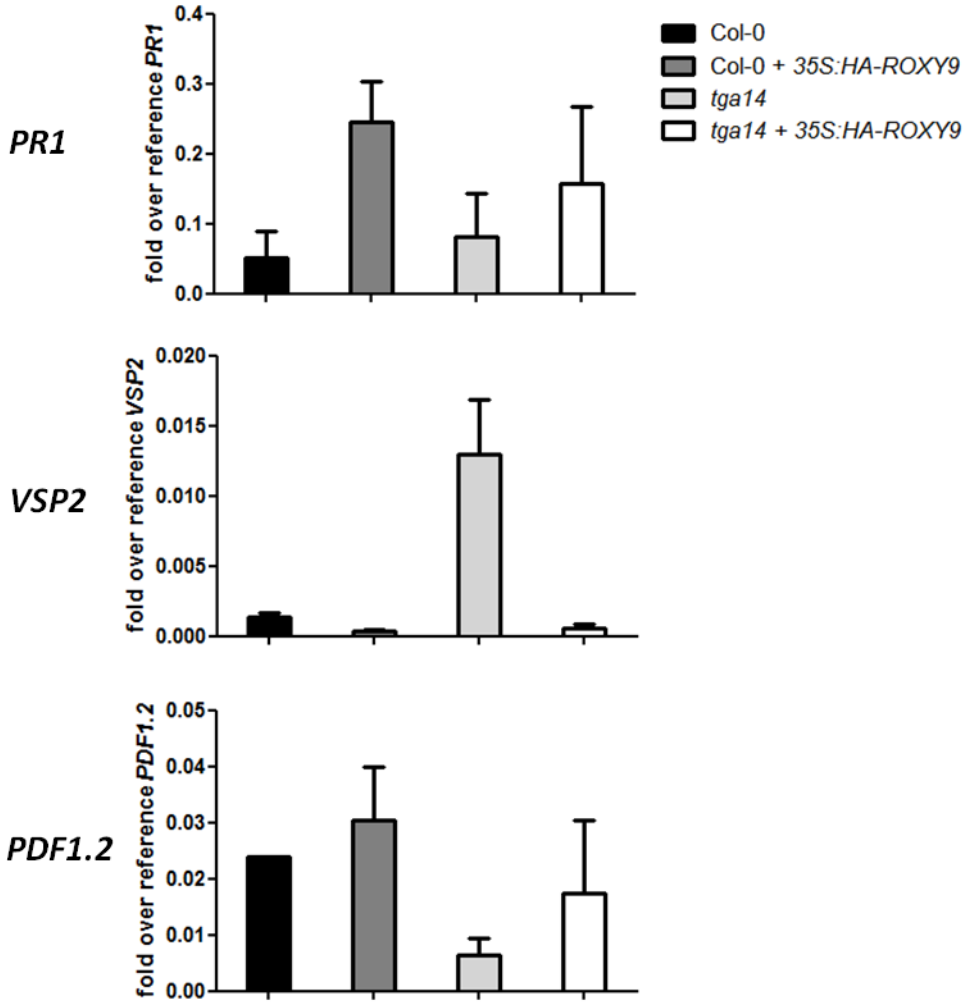

Fig. 4.10.1: Defense related genes are not constitutively influenced by ectopic expression of *HA-ROXY9*

Total RNA of wildtype Col-0, *tga14* mutant, transgenic Col-0 + *35S:HA-ROXY9* #6.16 and transgenic *tga14* + *35S:HA-ROXY9* #1.32 plants grown under short day conditions for 8 weeks was extracted. The expression of *PR1, VSP2 and PDF1.2* was tested with specific primers by qRT-PCR and normalized to *Actin8* transcript levels. Bars represent the average ± SEM with n = 1-6.

The high amounts of *VSP2* transcripts in the *tga14* mutant background prompted us to investigate a negative role of clade I TGA TFs in the regulation of JA-dependent genes. Wildtype Col-0 and *tga14* mutant were wounded with forceps and *VSP2* transcript levels were detected with specific primers and normalized with *UBQ5* expression at 0, 2, 6 and 24 hours after treatment (4.10.2).

Already 2 hours after wounding the expression of *VSP2* in Col-0 was increased. The treatment resulted in a peak 6 hours after treatment, whereas 24 hours after treatment *VSP2* expression was nearly on a level of an untreated plant. Similarly expression kinetics and strength were monitored in *tga14* mutant. Interestingly, basal *VSP2* expression was slightly elevated in wounding experiment I.

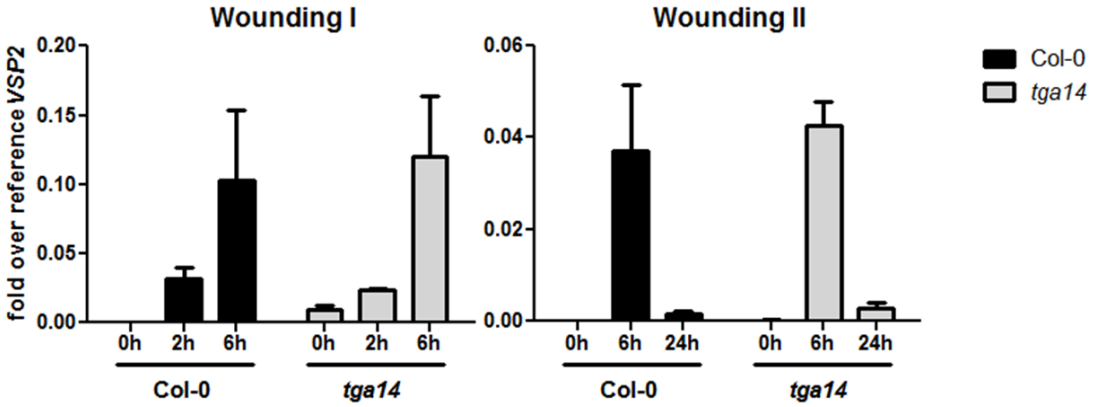

Fig. 4.10.2: The mutation of TGA1 and TGA4 does not influence *VSP2* induction

Leaves of 4 weeks-old Col-0 and *tga14* mutant plants grown under long day conditions were wounded with a forceps. 0, 2, 6 and 24 hours after wounding the total RNA was extracted. The expression of *VSP2* was measured with specific primers by qRT-PCR and normalized to *UBQ5* transcript levels. Bars represent the average ± SEM with n = 5-6.

Supported by the similar *VSP2* expression in wildtype Col-0 and *tga14* mutant, the negative effect of HA-ROXY9 towards *tga14*-dependent elevated *VSP2* transcript levels was strongly damped. Consequently, we assumed no influence of ectopic expression of *HA-ROXY9* with respect to *PR1*, *VSP2* and *PDF1.2* expression.

4.11 Overexpression of *ROXY19* cannot mimic *ROXY9* overexpressing phenotype

In order to analyze a general influence of ROXYs to plant growth and flowering, the effects of HA-ROXY9 and HA-ROXY19 in wildtype Col-0 were compared. ROXY19 is suggested to mediate the negative cross talk between the SA- and JA/ET-pathway (Ndamukong et al., 2007) and exhibits the conserved ALWL-motif at the C-terminus (Fig. 2.6). In contrast, ROXY9 lacks this conserved motif that is suggested to mediate a negative influence to promoter activities (Zander et al., 2012).

First, the interaction between clade I TGA TFs and ROXY19 was analyzed by Y2H assays (Figure 4.11.1). ROXY19 was fused to the GAL4 binding domain and TGA1, TGA1red, TGA4, TGA4red and TGA2 were fused to the GAL4 activation domain. All clade I TGA TFs could interact with ROXY19 as well as the clade II TGA TF TGA2 did.

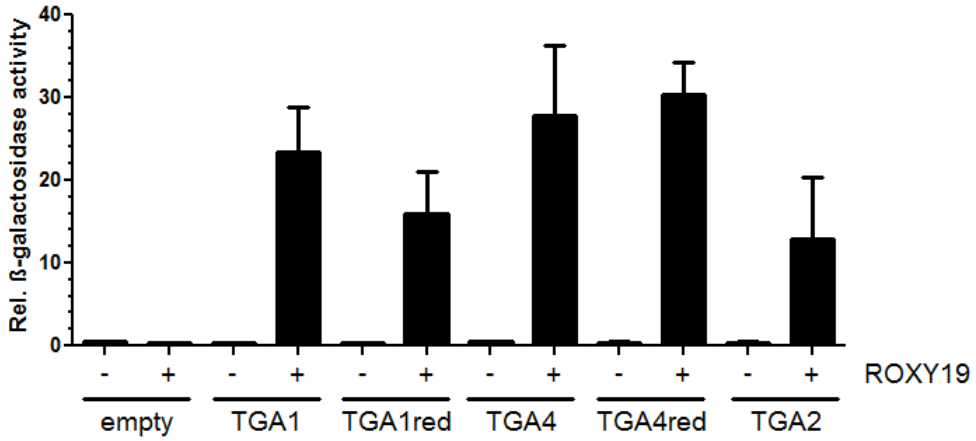

Fig. 4.11.1: Interaction of ROXY19 and clade I TGA TFs

The interaction of ROXY19 with wildtype and constitutively reduced clade I TGA TFs. Quantification of protein-protein interaction in yeast cells by ONPG-assay. Prey plasmids encode clade I TGA TFs fused to the GAL4 transactivation domain, bait plasmid encode ROXY19 fused to the GAL4 binding domain. β-galactosidase activity was measured in yeast strain PJ69-4A. Bars represent the average ± SEM with n = 5-8.

Transgenic Col-0 + *35S:HA-ROXY9* and Col-0 + *35S:HA-ROXY19* plants were grown on soil under SD conditions until the stunted growth of Col-0 + *35S:HA-ROXY9* was well pronounced (Figure 4.11.2). Overexpression of *HA-ROXY9* and *HA-ROXY19* in wildtype Col-0 did not result in similar growth phenotypes. The high protein levels of HA-ROXY9 went

along with reduced plant size and crinkled leaf shape. The constitutive expression of *ROXY19* in wildtype Col-0 did not show a visible growth phenotype. These observations hint at a specific function of ROXY9 in *A. thaliana*.

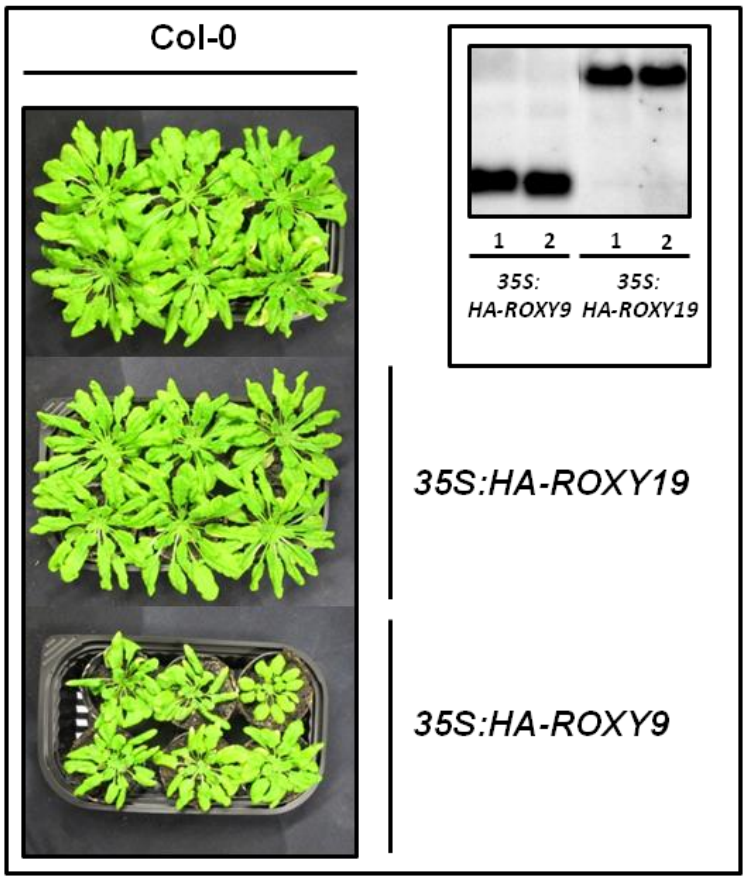

Fig. 4.11.2: Comparison of wildtype Col-0 plants expressing *HA-ROXY19* or *HA-ROXY9*

Plants were grown on soil for 10 weeks under short day conditions (A) Representative pictures of Col-0 *35S:HA-ROXY9* and Col-0 *35S:HA-ROXY19* plants. (B) Westernblot analysis of the protein levels in Col-0 + *35:S:HA-ROXY9* and Col-0 + *35:S:HA-ROXY9.* The proteins were detected with α-HA antibody.

Next, we compared the influence of HA-ROXY9 and HA-ROXY19 to gene expression in planta. The transcript levels of *PDF1.2*, *VSP2* and *PR1* in untreated plants grown for 10 weeks under short day conditions were quantified by qRT-PCR (Figure 4.11.3). In comparison to Col-0 + *35S:HA-ROXY9*, the ectopic expression of HA-ROXY19 suppressed the basal *PDF1.2* expression. Oppositional, the basal expression of *VSP2* and *PR1* was elevated in Col-0 + *35S:HA-ROXY19* plants.

These results reflect the negative effect of ROXY19 to JA/ET-dependent gene expression, whereas ROXY9 cannot influence basal expression of *PDF1.2*, *VSP2* and *PR1*.

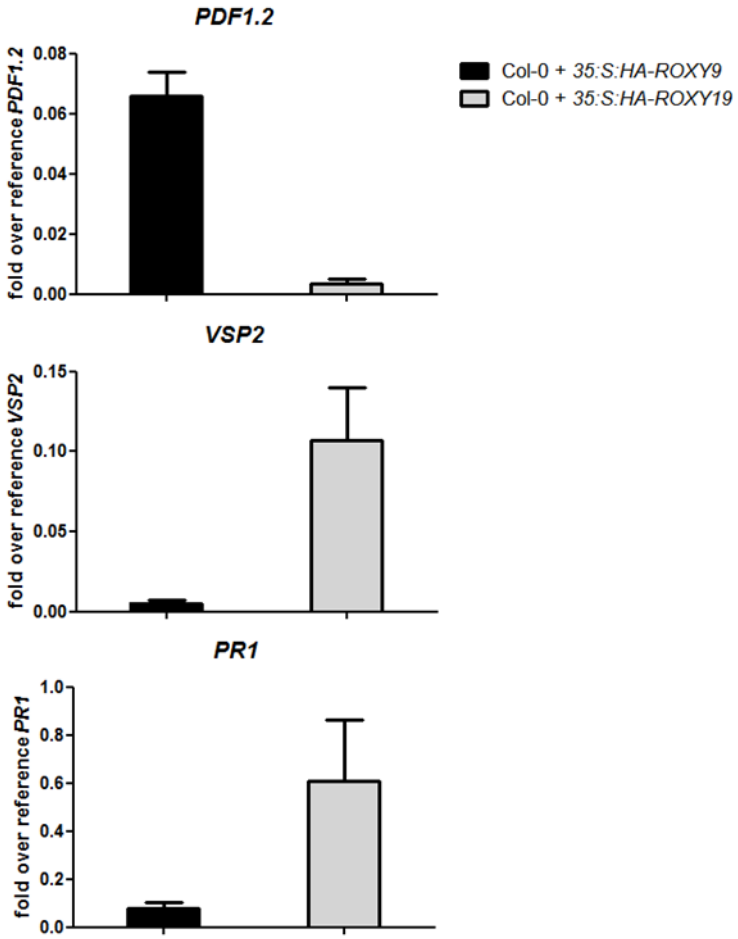

Fig. 4.11.3: Defense related genes are influenced by ectopic expression of *HA-ROXY19*

Total RNA of 10 weeks-old Col-0, *tga14* mutant, transgenic Col-0 + *35:S:HA-ROXY9* and transgenic Col-0 + *35:S:HA-ROXY19* plants grown under short day conditions was extracted. The expression of *PR1, VSP2 and PDF1.2* was tested with specific primers by qRT-PCR and normalized to *Actin8* transcript levels. Bars represent the average ± SEM with n = 4-5.

5 Discussion

TGA TFs interact with NPR1 (Zhang et al., 1999; Zhou et al., 2000), a key regulator of SA-dependent basal and systemic acquired resistance. Moreover, TGA TFs can bind *in vivo* to *as-1*-like elements of promoters (Johnson et al., 2003; Fode et al., 2008) and are involved in establishing plant defense responses (Zhang et al., 2003; Kesarwani et al., 2007).

TGA1 and TGA4 represent the clade I TGA TFs and an interaction with NPR1 is only enabled after mutation of two conserved cysteine residues (Despres et al., 2003). Based on the findings that these cysteines are reduced in SA-treated tissues and that TGA1 and NPR1 interact *in planta* only after SA treatment, it was hypothesized that the *in planta* reduction of the critical cysteines is a prerequisite for the TGA1/NPR1 interaction. Furthermore, a contribution of TGA1 and TGA4 to basal resistance after infection with *Psm* ES4326 was shown (Kersawani et al., 2007). The mechanism of redox modification at the critical cysteine residues of TGA1 and TGA4 and whether this modification has an impact on NPR1-mediated defense processes is not known. Since ROXY-type glutaredoxins interact with TGA TFs (Ndamukong et al., 2007; Li et al., 2009; Murmu et al., 2010), they have been discussed as possible candidates for protein modifications at TGA TF proteins.

These findings prompted us to investigate the role of TGA1 and TGA4 in plant defense responses with respect to SA, NPR1 and redox modifications in more detail.

5.1 Clade I TGA TFs do not play a major role in basal defense under our conditions

In 2003, it was described that a mutation of critical cysteine residues in clade I TGA TFs enabled the interaction with NPR1 (Despres et al., 2003). However, an *in vivo* relevance of the potentially redox-induced TGA/NPR1-interaction was not proven. To re-investigate the functional importance of the conserved cysteines for the TGA/NPR1 interaction, I mutated the critical cysteine residues of TGA1 and TGA4 (Fig. 4.1.1.1). Despres and colleagues had exchanged the cysteine residues to asparagine and serine, because the strongly NPR1-interacting TGA factor TGA2 contains these residues in the corresponding position. Indeed, these mutations enabled TGA1 to interact with NPR1. Since the model of redox-regulated TGA1 implicated that only the reduced form of TGA1 interacts with NPR1 in plants, I

mutated both cysteines to the most related amino acid serine. In the yeast two-hybrid assay used in our lab, co-expression of wildtype BD-TGA1 (and BD-TGA4) with AD-NPR1 yielded weaker ONPG activities than co-expression of BD-TGA2 with NPR1, which is consistent with previous results. Mutation of the critical cysteine residues to serines did not enhanced the interaction (Fig.4.1.1.2). AMS-shift assays revealed that reactive cysteines in TGA1 are already reduced in yeast (Fig. 4.1.1.3), which can explain the constitutive interaction between clade I TGA TFs and NPR1. Therefore, mutation of the first cysteine into an asparagine might enhance the interaction with NPR1. Since we cannot mimic the oxidized state by site-specific amino acid exchanges, we cannot investigate whether the oxidized form of TGA1 does not interact with NPR1. However, clade I TGA TFs can be oxidized after treatment with diamide in yeast (Fig. 4.7.2). Thus, it may be analyzed in the future, whether this oxidation compromises the interaction with NPR1. Our data can be reconciled with data published by Despres and colleagues by assuming that oxidized TGA1 might not interact with NPR1, that reduced TGA1 weakly interacts with NPR1 and that TGA1 containing asparagine instead of the first critical cysteine interacts more strongly with NPR1.

However, a redox modification with subsequent interaction between TGA1/TGA4 and NPR1 seemed probable since also an SA-induced interaction between TGA1 and NPR1 was described (Despres et al., 2003). Moreover, if the critical cysteines are mutated to asparagine and serine, respectively, the interaction becomes constitutive (Rochon et al., 2006). Therefore, to study the impact of a possible regulatory role of clade I TGA TFs on NPR1-controlled gene regulation, expression of the NPR1-dependent and SA-inducible marker gene *PR1* was monitored in the *tga14* mutant. Here I show that expression of *PR1* was not affected by the lack of clade I TGA TFs after application of SA to axenically or soil grown plants or after infection with *Psm* ES4326 (Fig. 4.1.2.1; 4.1.2.2; 4.1.2.3). These observations are in line with results that described a wildtype-like induction of *PR1* after infection with *Pst* DC3000 or *Pst avrRpt2* in the *tga14* mutant (Shearer et al., 2012). Furthermore, my studies of SAR did not reveal a decreased *PR1* expression in systemic leaves after local infection with *Psm* E4326 (Fig. 4.1.3.1). These results exclude clade I TGA TFs as regulators of *PR1* expression. In previous studies it was shown, that class II TGA TFs can bind to the TGACG motif within the *as-1*-like element of the *PR1* promoter (Johnson et al., 2003) and that the induction of *PR1* failed in the *npr1-1* and *tga256* mutant (Cao et al., 1994; Zhang et al., 2003b).

Although I could not find evidence for a common function of clade I TGA TFs and NPR1 in regulating *PR1* gene expression after SA treatment or in SAR leaves, I aimed to identify a link

between the lack of TGA1 and TGA4 and NPR1 in the process of impaired basal resistance after infection with *Psm* E4326 (Kersawani et al., 2007). Analysis of flg22-induced plant responses with respect to ROS burst, gene expression or root growth did not reveal a function of clade I TGA TFs in PTI (Supplemental figures S2, S3, S4). This contrasts with recent studies revealing an impaired flg22-induced ROS burst in the *tga14* mutant (Wang and Fobert, 2013). After infection with *Pst* DC3000 (Fig. 4.1.4) the *tga14* mutant was not as susceptible as described after infection with *Psm* ES4326 (Kersawani et al., 2007).

Based on all these results, I assume no relevance of clade I TGA TFs in known NPR1-dependent functions and that the TFs do not play a major role in PTI.

5.2 Clade I TGA TFs play a role in avrRPS4-triggered resistance

Until now, the function of TGA1 and TGA4 was attributed to basal defense mechanisms only (Kesarwani et al., 2007). My studies provide evidence that clade I TGA TFs additionally contribute to defense responses triggered by the bacteria-derived effector protein avrRPS4 (Fig. 4.2.1.1). Infection of the single *tga1* and *tga4* mutants with *Pst avrRPS4* showed that TGA1 and TGA4 have redundant functions with respect to this response (Fig 4.2.2.1). In contrast, TGA1 and TGA4 seem to have different functions in the defense response against *Psm* E4326 (Kersawani et al., 2007). The single mutation of *TGA4* did not lead to increased susceptibility after infection with *Psm* E4326, whereas the *tga1* mutant exhibited more bacterial growth.

The effector avrRPS4 is recognized by the *A. thaliana* TIR-type NB-LRR receptor RPS4, which then triggers ETI (Gassmann et al., 1999). In this process, nuclear localization of RPS4 is necessary and full resistance is dependent on nuclear localized EDS1 (Wirthmüller et al., 2007; Garcia et al., 2010). EDS1 is a key-regulator of defense responses determined by TIR-type NB-LRR receptor proteins (Parker et al., 1996; Aarts et al., 1998). Though the *eds1-2* mutant was twofold more susceptible than the *tga14* mutant after infection with *Pst avrRPS4*, a slight reduction of bacterial propagation in the *tga14*/*eds1-2* mutant was observed (Fig. 4.2.5.1). Nevertheless, since the mutations in the *tga14* and the *eds1-2* mutant did not show an additive effect, I assume a function of TGA1 and TGA4 downstream of EDS1 in mediating resistance against *Pst avrRPS4*. Analysis of the *tga14*/*eds1-2* mutant provided evidence for a complex regulatory network in mediating avrRPS4-triggered resistance.

Consistent with my results, a contribution of clade I TGA TFs to TIR-type NB-LRR receptor-triggered defense was recently reported by Shearer et al (2012). The defense pathways triggered by the constitutively activated function of the TIR-type R protein SNC1 (Suppressor of *npr1-1*, constitutive1) was partially blocked in the *tga14*/*snc1*/*npr1-1* mutant. The constitutively activated defense response of the *snc1/npr1-1* mutant is due to a single mutation in *SNC1* (Li et al., 2001; Zhang et al., 2003a). *SNC1* was mapped to the *RPP5* R gene cluster (Parker et al., 1997; van der Biezen et al., 2002) and the function of SNC1 is dependent on EDS1 (Li et al., 2001) and partially dependent on SA (Zhang et al., 2003a). My infection of the *tga14* mutant with *Psm avrRPM1* that is recognized by the CC-type NB-LRR RPM1 showed wildtype-like bacterial propagation (Fig. 4.2.1.1). These observations support my assumption that TGA1 and TGA4 function in resistance determined by TIR-type NB-LRR and not CC-type NB-LRR.

In this thesis, I provide evidence for an NPR1-independent but SA-dependent function of TGA1 and TGA4 in avrRPS4-triggered resistance. An additive negative effect of NPR1- and TGA1/4-dependent signaling pathways was observed after infection of the *tga14/npr1-1* mutant with *Pst avrRPS4* (Fig. 4.2.3.1 (A)). In 2 of 3 experiments the *tga14*/*npr1-1* mutant was significantly more susceptible than the *tga14* mutant. However, the average of all three experiments did not confirm this significance (Fig 4.2.3.1 (B)), which is probably due to the minor role of NPR1 in avrRPS4-mediated resistance. In general, the function of NPR1 is attributed to basal resistance, ETS and SAR (Fu and Dong, 2013). In the course of this thesis, supporting data for a possible NPR1-independent function of clade I TGA TFs were published (Shearer et al., 2012), which showed a higher bacterial titer in *tga14*/*npr1-1* plants after infection with *Psm* ES4326 than in the *tga14* and *npr1-1* mutants.

The function of TGA1 and TGA4 in mediating resistance to *Pst avrRPS4* is dependent on SA (Fig. 4.2.4.1), which has been shown previously to be necessary for resistance mediated by both, NPR1 and EDS1. The *sid2-2* and the *tga14*/*sid2-2* mutants allowed similar bacterial propagation, whereas the *tga14* mutant was significantly less susceptible than the *tga14*/*sid2-2* mutant in 2 of 3 experiments (Fig. 4.2.4.1 (A)). Interestingly, the *tga14* mutant was nearly as susceptible as the *sid2-2* (Fig. 4.2.4.1) but clearly less susceptible than the *eds1-2* mutant (Fig. 4.2.5.1) after infection with *Pst avrRPS4*. EDS1 acts up-stream of SA promoting its biosynthesis (Wiermer et al., 2005), therefore I assume that clade I TGA TFs functions down-stream of EDS1-driven SA to fulfill SA-dependent mechanisms after recognition of avrRPS4.

In contrast to the *tga14* mutant, the *npr3/4* mutant was significantly more resistance than wildtype Col-0 after infection with *Pst avrRPS4* (Fig. 4.2.3.2), which excludes the SA-receptors NPR3 and NPR4 (Fu et al., 2013) as positive factors in clade I TGA TF-dependent immunity against *Pst avrRPS4*. An enhanced resistance of the *npr3/4* mutant was also observed after infection with virulent *Psm* ES4326, in which increased basal *PR* transcript level were monitored (Zhang et al., 2006). This enhanced resistance is probably due to constitutively enriched basal NPR1 levels and activated basal defense responses.

5.3 Induction of defense-related genes is not affected in the *tga14* mutant after infection with *Pst avrRPS4*

In order to identify a set of defense-related genes that is dependent on the clade I TGA TFs microarray analysis of wildtype Col-0 and *tga14* mutant was performed (Chapter 4.3). Though expression of a large number of genes was altered in wildtype Col-0 after infection with *Pst avrRPS4*, no transcriptional differences of induced genes were detected in the *tga14* mutant (Fig. 4.3.2.1; 4.3.2.3). TGA1 and TGA4 are bZIP TF and bind preferentially to TGACGtca motifs in promoters (Lam & Lam, 1995). Considering that the function of TGA1 and TGA4 in avrRPS4-triggered resistance is dependent on SA, I expected a set of SA-dependent genes to be regulated by clade I TGA TFs. However, no possible target genes were identified after infection. Interestingly, it was recently reported that SA-dependent gene expression in the *sid2-2* mutant can be regulated in the absence of SA after recognition of bacterial effector proteins (Tsuda et al., 2013). For instance, *PR1* expression was triggered after recognition of avrRPS4 and in avrRpt2- and avrRpm1-triggered ETI. This SA-independent induction of *PR1* was not observed after infection with virulent *Pseudomonas* strains. Regulation of most SA-responsive genes was attributed to a prolonged activation of MAPK cascades (MPK3 and MPK6), whereas the MAPK cascades were only activated transiently during PTI. Based on these observations I assume, that SA- and clade I TGA TF-dependent gene expression was restored by MAPK. Whether a single SA stimulus would lead to more distinct transcriptional differences between wildtype Col-0 and *tga14* mutant has to be tested. Whether clade I TGA TFs have an SA-dependent function beside gene regulation has to be discussed since TGA1 and TGA4 contribute to total and apoplastic PR1 protein accumulation (Wang and Fobert, 2013).

The microarray analysis revealed that the largest transcriptional differences were detected in the *tga14* mutant at 3 hpi, whereas differences faded away at 6, 11 and 24 hpi (Fig. 4.3.2.1; 4.3.2.3). These results are consistent with a possible restoration of TGA-dependent function by MAPK cascades resulting in robustness of innate immunity (Tsuda et al., 2013). If this restoration would comprise all functions of clade I TGA TF, the *tga14* mutant should not be more susceptible after infection with *Pst avrRPS4*. Therefore, I assume a possible role of TGA1 and TGA4 in mediating starting expression levels of genes that are involved in plant defense. Already in mock-treated plants, transcript levels of SA- and EDS1-related genes (*FMO1*, *NUDT5*, *NUDT6*, *EDS1*) were slightly decreased (Fig S21), whereas all differences were gone at 24 hpi (Fig 4.3.2.3). Therefore I hypothesize that decreased starting expression levels in the *tga14* mutant is a disadvantage that cannot be fully overcome during infection with *Pst avrRPS4*.

Based on all results, I assume two possible roles of clade I TGA TFs in avrRPS-triggered ETI that do not exclude each other (Figure 5.2).

(I) TGA1 and TGA4 control starting levels of genes that are involved in EDS1-mediated resistance.

(II) TGA1 and TGA4 function in SA-dependent mechanisms downstream of EDS1 in resistance determined by RPS4, in which possible target genes or defense mechanisms are not known.

5.4 Clade I TGA TFs influence basal gene expression

Comparison of genes constantly affected in the *tga14* mutant at 3, 6, 11 and 24 hpi and in mock-treated plants identified 7 down-regulated (Fig. 4.3.3.1) and 10 up-regulated (Fig. 4.3.3.2) genes.

A function of 3 up-regulated genes was predicted based on amino acid sequences and the role of two proteins was already described. DUR3 (Degradation of Urea 3) has a high affinity to urea and it serves as the major transporter for urea up-take in *A. thaliana* (Kojima et al., 2007). The *atdur3-1* and *atdur3-3* mutants grew less vigorously on media with urea as the main nitrogen source. Moreover, expression of *DUR3* was stimulated by urea and repressed by ammonium and nitrate and an increased *DUR3* promoter activity was detected under low

nitrogen conditions in the rhizodermis. Therefore, DUR3 function is suggested to be an adaptation to low urea levels in unfertilized soils (Kojima et al., 2007). Due to one potential TGA binding site in the *DUR3* promoter a direct regulation of the gene by clade I TGA TFs could be possible. Since my experiments were done on fertilized soil I assume that lower levels of *DUR3* expression should not have an impact on avrRPS4-triggered defense response in the *tga14* mutant.

The ABC transporter *NAP3* was suggested to be involved in the detoxification of Al (Huang et al., 2010). It was shown that *nap3* mutants (*atstar1*) were more sensitive to Al and an earlier flowering was observed. The increased sensitivity to Al was complemented after expression of a *NAP3* rice ortholog (*OSSTAR1*) that was also implicated in Al tolerance (Huang et al., 2009). *NAP3* expression occurs at outer cell layers of root tips and in developing leaves (Huang et al., 2010). A binding site for TGA TFs in the promoter is missing. Since my plants grew without Al stress I assume no impact of low *NAP3* transcript levels to resistance mediated by TGA1 and TGA4.

The third down-regulated gene with a predicted function as a glutathione-dependent oxireductase was *ROXY9*, which is described later (Chapter 5.4).

The functions of 5 of the 10 genes that were consistently higher expressed in the *tga14* mutant were already described.

MPL1 plays an important role in defense against the green peach aphid and is highly induced after attack (Louis et al., 2010). Interestingly, it is the only TGA1/TGA4-suppressed gene that was induced after *Pst avrRPS4* in wildtype Col-0 (Fig. 4.4.1.3). The *mpl1* mutant showed an increased number of green peach aphids in infection studies, whereas over-expression under the control of the *35S* promoter led to a lower number of attackers. The MPL1 protein exhibits lipase activity and MPL1-dependent lipids were suggested to have a positive influence on resistance against green peach aphids (Louis et al., 2010). Whether clade I TGA TFs play a role in defense against aphids remains to be tested. In order to find a possible link between increased susceptibility of the *tga14* mutant after infection with *Pst avrRPS4* and an elevated *MPL1* expression, infection of the *mpl1* mutant and *35S:MPL1* plants with *Pst avrRPS4* has to be performed. With respect to ETI triggered by avrRPS4 I have to propose that MPL1 interferes with this defense response. The *MPL1* promoter exhibits 1 potential binding site for TGAs and might therefore be a direct target gene of TGA1 and TGA4. For *MPL1*, it has to be postulated that clade I TGA TFs can repress promoters of genes.

The β-amylase RAM1 was shown to account for the major part of β-amylase activity in rosette leaves and inflorescences. The *ram1* mutant has normal starch levels, indicating that only small activities of *RAM1* homologs are sufficient for starch degradation (Laby et al., 2001). The promoter of *RAM1* exhibits 3 possible binding sites for TGA TFs.

ASN1 encodes an asparagine synthase and overexpression of the gene under the control of the *35S* promoter increased the nitrogen levels in seeds. It is suggested that increased asparagine levels lead to a higher source to sink flux of the amino acid resulting in high amounts of nitrogen in seeds (Lam et al., 2003). The promoter of *ASN1* shows 4 possible TGA TF binding sites.

The NAI2 protein is localized to endoplasmic reticulum (ER) bodies and a lack of *NAI2* resulted in abnormal formation and a low number of these bodies. Therefore, a crucial function of NAI2 in the formation of ER bodies was implicated (Yamada et al., 2009). The promoter of NAI2 exhibits one potential TGA binding site.

Transcripts of *LTP4* (*Lipid Transfer Protein 4*) were found specifically in guard cells, whereas they were up-regulated in all tissues in seedlings after NaCl treatment (Chae et al., 2010). The plant LTP proteins exhibit four conserved disulfide bonds with eight cysteine residues (Douliez et al., 2000) and can interact with phospholipid molecules and fatty acids in vitro (Zachowski et al., 1998). Two possible TGA binding sites are present in the *LTP4* promoter.

Transcription factor *SPL4* (*SPL3*, *SPL5*) is important in regulating flowering (Wang et al., 2009). The expression of *SPLs* is increased in the center of the shoot during the transition from juvenile to adult plants (Schmid et al., 2003; Wu and Poething et al., 2006) and overexpression results in early flowering (Wu and Poething, 2006). An early flowering of the *tga14* mutant was not observed. The *SPL4* promoter exhibits three possible binding sites for TGA TFs.

Furthermore, 5 *ROXYs* arranged in a tandem on chromosome 4 were constitutively co-regulated to higher transcript levels in the *tga14* mutant and are described later (Chapter 5.4).

Taken together, it cannot be decided whether this basal deregulation of different genes influences the interaction with *Pst avrRPS4*. Since an interaction of ROXYs and TGA TFs was shown (Ndamukong et al., 2007) and a redox modification of clade I TGA TFs was

suggested (Depres et al., 2003), the reciprocal changes in *ROXY* gene expression were the most promising alterations with respect to defense mechanisms.

5.5 Clade I TGA TFs influence basal *ROXY* expression

Microarray analysis revealed that the glutaredoxin *ROXY9* was less expressed in the *tga14* mutant, whereas *ROXY11-15*, which are located in a tandem arrangement on chromosome 4, were expressed to higher levels. Expression of these *ROXYs* was not influenced by infection with *Pst avrRPS4* (Fig 4.5.1). The differences concerning expression of the *ROXY* genes were less pronounced in one week old seedlings, but from week two on (Fig. 4.4.1.1). *ROXY* expression was controlled by TGA1 and TGA4 redundantly (4.4.2.1). ROXYs are land plant-specific GRXs and a function of ROXY1, ROXY2 and ROXY19 in connection with TGA TFs is known (Fig. 5.1).

A TGA-dependent positive regulation of *ROXY* gene expression was also reported for *ROXY19*, which expression is triggered by SA in dependency to clade II TGA TFs (Ndamukong 2007). TGA2, TGA5 and TGA6 are important for the activation of SA- and ET-dependent defense genes (Zhang et al., 2003; Zander et al., 2010). Interestingly, ectopic expression of *ROXY19* leads to suppression of the ET-dependent defense pathway (Ndamukong et al., 2007; Zander et al., 2012), which is strongly antagonized by SA (Spoel et al., 2007) and JA (Lorenzo et al., 2004). Since *ROXY19* expression is induced by SA (Ndamukong et al., 2007), ROXY19 was suggested to be an important factor for the negative cross-talk between the defense pathways. In contrast, I could not monitor an induced expression of *ROXY9* (*ROXY13*) after SA- or MeJA-treatment (Fig. 4.4.4.1; 4.4.4.2), which indicates that ROXY9 has a different function *in planta*.

Whether *ROXY1* and *ROXY2* expression is influenced by TGA TFs PAN, TGA9 and TGA10 is not known, but functional connections between PAN and ROXY1 and TGA9/10 and ROXY1/2 were reported. The *roxy1* mutant develops in average only 2.5 instead of 4 petals (Xing et al., 2005), whereas the mutant plant of the TGA TF *PAN* is characterized by 5 petals (Running and Meyerowitz, 1996; Chuang et al., 1999). The *roxy1/pan* double mutants show flowers with five petals, indicating an epistemic role of *PAN* to *ROXY1* (Li et al., 2009). The *roxy1roxy2* and the *tga910* mutants are male sterile and are affected in anther development, reflected in overlapping changes in expression of genes that are involved in early and middle tapetal development in the two double mutants (Xing and Zachgo, 2008; Murmu et al., 2010). Partially overlapping expression domains of *ROXY1* and *PAN* (Li et al., 2009) and *ROXY1/2* and *TGA9/10* (Murmu et al., 2010) in the specific cells of the flower meristem were described.

A ubiquitous interaction between TGA2 and ROXYs were described in yeast (Zander et al., 2012). Furthermore it was shown that the interaction between ROXY1 and the TGA TF PAN in the nucleus is necessary for the developmental initiation of 4 petals (Li et al., 2009) and that ROXY1/2 and TGA9/10 can interact in the nucleus (Murmu et al., 2010). In this thesis I could identify an interaction between clade I TGA TFs and ROXY9 and ROXY13 respectively (Fig. 4.5.1; 4.5.2). Since clade I TGA TFs were described as redox modifiable proteins (Despres et al., 2003), ROXYs are discussed as possible mediators of direct redox modifications at critical cysteine residues in TGA1 and TAG4.

I could not provide evidence for a direct influence of ROXY9 to the redox state of TGA1 in yeast (Fig. 4.6.1; 4.6.2; 4.6.3). Interestingly, the TGA1 protein was already reduced in all experiments. Oxidation of the protein could be achieved by diamide treatment and a reduced form reappeared after diamide had been washed out. Whether this was due to a reduction of the oxidized protein or to newly synthesized proteins cannot be judged. However, ROXY9 had no influence on the ratio of reduced to oxidized TGA1 (Fig. 4.6.2). Also the formation of a stable mixed disulfide of mutated ROXY9 (ROXY9C24A) and TGA1 was not detectable, questioning a redox reaction between both proteins via the hypothetical active motif of ROXY9 (**C**CL**C**) and the critical cysteine residues of TGA1 (**C**NLKQS**C**). However, co-expression of TGAs with wildtype ROXY9 stabilized ROXY proteins. This was not the case for mutated ROXY9C24A. This observation confirms a relevance of the interaction of both proteins and that this interaction might be influenced by the CCLC-motif of ROXY9 (Fig. 4.6.3).

Likewise, a possible modification of PAN by ROXY1 was suggested. The PAN protein exhibits 5 cysteine residues and one single cysteine (C340) was identified to be crucial for PAN activity (Li et al., 2009). The exchange of C340 to serine abolished the ability of PAN to complement the flowering phenotype of the *pan* mutant (Li et al., 2009). These results indicated that the reduction of C340 in PAN by ROXY1 could block PAN activity. This hypothesis would support the epistemic role of *PAN* to *ROXY1* in flower development (Li et al., 2009). However, the redox state of PAN *in planta* has never been addressed and a direct modification on PAN C340 by ROXY1 has not yet been demonstrated.

Furthermore, TGA10 exhibits a corresponding cysteine residue to PAN C340 and TGA1 C260 and TGA9/10 show a unique cysteine residue at the C-terminus (TGA9 C429; TGA10 C435). Therefore, a redox modification of TGA9/10 by ROXY1/2 was suggested (Murmu et al., 2010), but a direct modification of TGAs has not yet been demonstrated.

The hypothesis of a ROXY9 function in redox modifications of critical cysteine residues in clade I TGA TFs was not supported by my results. Nevertheless, a possible redox-modulation of other proteins *in planta* cannot be excluded. A comparison of different working models for the ROXY/TGA modules is depicted in Figure 5.1.

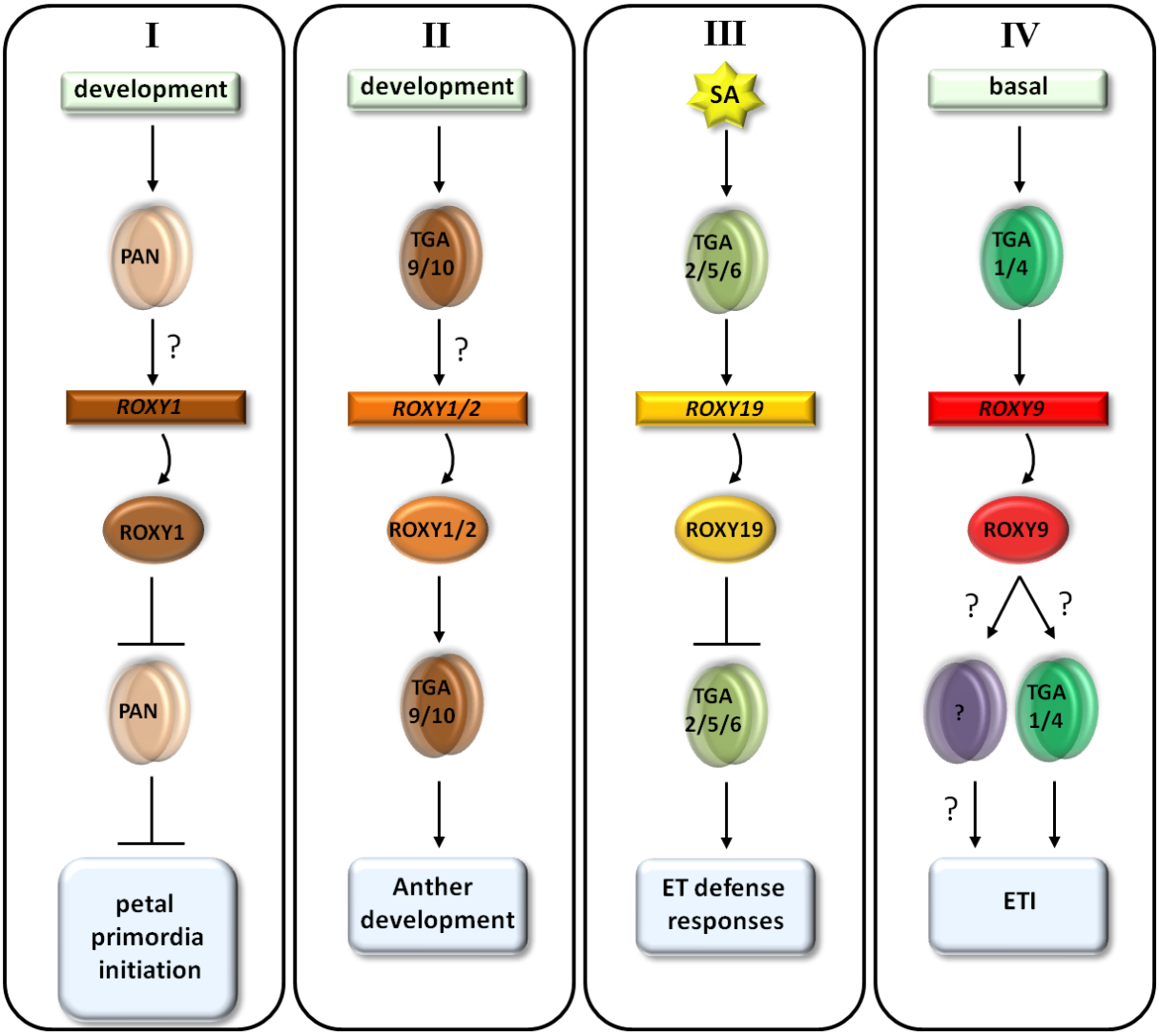

Fig. 5.1: Known and proposed functions of different TGA/ROXY units in planta

Four different functional TGA/ROXY units are shown. The upper part shows known and hypothesized TGA-dependent regulation of *ROXY* gene expression. The lower part shows known and possible functional connections of TGA and ROXY proteins.

(I) The epistatic function of *PAN* to *ROXY1* in regulation of primordial initiation (Xing et al., 2005; Li et al., 2009)

(II) The redundant function of TGA9/10 and ROXY1/2 in anther development (Xing and Zachgo, 2008; Murmu et al., 2010)

(III) The role of a TGA2/5/6 in relationship to *ROXY19*/ROXY19 in ET defense responses (Ndamukong et al., 2007; Zander et al., 2009)

(IV) The hypothetical function of ROXY9 in TGA1/4-mediated ETI (This thesis)

5.6 Clade I TGA TFs can activate *ROXY* promoters in transient protoplast assays

I could show that the *ROXY9* promoter is activated by clade I TGA TFs in wildtype Col-0 and *tga14* mutant protoplasts in transient gene transfer experiments (Fig. 4.7.1.1). However, TGA activity was not influenced by mutation of the critical cysteine residues. This is mostly due to already reducing conditions in protoplasts, as observed in yeast (Fig. 4.6.1; 4.6.2; 4.6.3). The N-terminal 3xHA-tag completely abolished TGA function. An influence of SA, of co-expressed ROXY9 or ROXY13 or a combination of SA and co-expression of ROXYs did not enhance the activity of TGA4 (Fig. 4.7.2.1). Unexpectedly, the *ROXY13* promoter, which is negatively regulated by clade I TGA TFs *in planta*, was activated by TGA4 in protoplasts (4.7.2.2). At this promoter, TGA4red was more efficient in activating *ROXY13* than TGA4. Additional application of SA or co-expression of ROXYs did not result in an enhanced activity of TGA4. The unexpected positive influence of TGA4 to the *ROXY13* promoter in transient protoplast assays might be due to a co-repressing factor that is lacking in this system. Although many aspects of these data set cannot be explained and do not seem to be consistent with the role of clade I TGA TFs *in planta*, my results indicate a possible function of clade I TGA TF at the *ROXY* promoters.

5.7 Ectopic expression of clade I TGA TFs in the *tga14* mutant cannot complement *ROXY* gene expression

The ectopic expression of untagged and 3xHA-tagged TGA TFs in the *tga14* mutant background did not complement the reciprocal changes in *ROXY* expression (4.7.3.2). Transcript levels of all TGA-derivates were similar (Fig. 4.7.3.1) and the proteins of 3xHA-tagged were detectable by western blot analysis (Fig. S23). With respect to transient protoplast assays I assume that also the untagged proteins are synthesized. However *cDNAs* of the clade I TGA TFs are not sufficient to rescue *ROXY* expression *in planta*. Likewise, transgenic plants expressing different *cDNA* derivates of *TGA1* failed to complement increased susceptibility after infection with *Pst* DC3000 (Lindermayr et al., 2010), whereas a successful complementation with genomic *TGA1* was shown (Shearer et al., 2012). The reasons for synthesis of a non-functional protein when translated from *cDNA*-derived *mRNA* have remained elusive.

5.8 *ROXY9* knock down plants show varying levels of susceptibility after infection with *Pst avrRPS4*

Basal and effector triggered resistance in the *tga14* mutant is impaired after infection with *Psm* ES4326 (Kersawani et al., 2007) and with *Pst avrRPS4* (Fig 4.2.1.1), respectively. Furthermore, it was suggested that the activities of TGA1 and TGA4 are influenced by SA with subsequent reduction of critical cysteine residues (Depres et al., 2003), However, no defense-related target genes were revealed by microarray analysis, but affected basal *ROXY9* expression that is controlled by clade I TGA TFs was identified (Fig. 4.4.2). Therefore, I performed pathogen assays with *ROXY9*-RNAi lines to investigate whether ROXY9 has a function in avrRPS4-triggered resistance,

In my infection studies of RNAi-lines knocking down *ROXY9* expression, I could not correlate an increased susceptibility to decreased *ROXY9* transcript levels (Chapter 4.9). In single experiments or single plants a correlation was possible, but in other cases, plants which had lost the RNAi construct due to segregation of the transgene were also susceptible. The RNAi-lines #1 and #2 showed decreased *ROXY9* transcript levels and an increased susceptibility, whereas in an independent experiment the phenotypes were gone (Fig. 4.8.6; 4.8.7). The increased susceptibility of the *tga14* mutant was consistent in all experiments and fluctuations in wildtype Col-0 and *tga14* mutant were not detected.

ROXY functions in plant defense responses are described. For *roxy18* mutant an increased resistance against *B. cinerea* was shown (La Camera et al., 2011) and *ROXY1*-overexpressing plants were more susceptible against *B. cinerea* (Wang et al., 2009). A function of the SA-inducible *ROXY19* is speculated in mediating the negative crosstalk between the SA- and JA/ET-pathway (Ndamukong et al., 2007), whereas a direct involvement of *ROXY9* in SA-triggered resistance is not known.

Because of inconsistent results of investigated *ROXY9*-RNAi-lines I can neither confirm not exclude a function of ROXY9 in avrRPS4-triggered resistance.

5.9 *ROXY9* overexpressing lines exhibit TGA1/4-dependent growth phenotypes

Overexpression of *ROXY9* in wildtype Col-0 led to impaired plant development. Rosettes of *ROXY9* overexpressors were smaller and had crinkled and yellowing leaves, inflorescent stems were shorter and seed development was delayed. In contrast, ectopic expression in the *tga14* mutant did not lead to similar effects (Fig. 4.9.1; 4.9.2; 4.9.3). Similar protein amounts in wildtype Col-0 and *tga14* mutant background were confirmed by westernblot analysis (4.9.1). These observations supports a common function of ROXY9 and clade I TGA TFs downstream of TGA1/4-controlled basal expression of *ROXY9* (Fig 4.4.1). *ROXY9* transcript levels of the plants tested in this thesis were on average 30 fold higher than transcript levels in wildtype Col-0, reflecting a strong overxpression of *ROXY9* (Figure S24).

Severe growth phenotypes were also described after overexpression of *ROXY1*. The plants were smaller in size, the edges of rosette leaves were rolled downwards and the flowering time was delayed by one week. Furthermore, a reduced fertility was observed (Wang et al., 2009). ROXY1 represses the function of TGA TF PAN in petal organ initiation (Xing et al., 2005; Li et al., 2009). Endogenous expression of *ROXY1* and *PAN* is limited to buds and flowers and nearly no transcripts of *ROXY1* were detectable in leaf tissue (Fig 4.4.2). Similar growth phenotypes of plants overexpressing *ROXY9* or *ROXY1* indicate that they can influence similar processes when present in higher amounts. To elucidate a ROXY-TGA specifity in plant development, overexpression of *ROXYs* in different mutant plants of TGA TFs has to be performed.

In contrast to overexpression of *ROXY9*, ectopic expression of *ROXY19* did not lead to affected plant growth. Similar protein levels of tested lines were detected excluding that the phenotype is due to different expression levels (Fig 4.11.2). ROXY19 and ROXY1 exhibit the conserved very c-terminal ALWL-motif that is described be to cruical for a negative effect to promoter activities (Zander et al., 2012), wheras this motif is lacking in ROXY9 (Fig. 2.6). Because of similar phenotypes of ROXY1 and ROXY9 overexpressor, I assume that the presence of an ALWL-motif is not important to influence plant growth observed in transgenic plants.

Overall only ROXY6, ROXY7, ROXY8 and ROXY9 do not encode this ALWL-motif, in which ROXY7 does not show a C-terminal cysteine residue in the hypothetical active site (ROXY9 CCLC → ROXY7 CCMS). Transcript levels of *ROXY9*-closest homolog, *ROXY8*,

were nearly not detectable in leaf tissue and also not influenced in the *tga14* mutant (Fig. 4.4.2). Furthermore, transcriptional differences of *ROXY6*, *ROXY7* and *ROXY8* expression were not detected by microarray analysis in the *tga14* mutant (Fig. 4.4.1).

It is known that constitutively activated defense pathways can result in dwarfism. In order to observe an influence of *ROXY9* onto defense-related genes, expression of SA-dependend *PR1*, JA-dependent *VSP2* and JA/ET-dependent *PDF1.2* was monitored in plants expressing *ROXY9* ectopically. Transcript levels of the three tested genes were not affected (Fig. 4.10.1). In contrast, ectopic expression of *ROXY19* led to suppression of the *PDF1.2* expression (Ndamukon et al., 2007; 4.11.3), in which this repressive effect is dependent on clade II TGA TFs (Ndamukong et al., 2007).

The wildtype-like basal expression of defense-related genes in plants overexpressing *ROXY9* indicates no relevance of *ROXY9* in regulating the expression of *PR1*; *VSP2* and *PDF1*.2. Whether overexpression of *ROXY9* leads to an affected interaction with *Pst avrRPS4* has to be tested. Due to the influence of TGA1 and TGA4 on apoplastic PR1 protein accumulation but not on total protein amount (Wang and Fobert, 2013), a common function of ROXY9 and clade I TGA TFs besides transcriptional regulation has to be discussed.

ROXYs can ubiquitously interact with TGA TFs in yeast (Zander et al., 2012) and a common function of the the very c-terminal ALWL-motif in ROXYs is suggested. Complementation studies revealed that ROXYs containing this motif, for instance ROXY1 and ROXY19 (Fig. 2.6), can be functionally exchanged. In contrast, ROXY9 was not able to complement observed phenotypes (Li et al., 2011; Zander et al., 2012) (Fig. S26).

Taken together, I identified a dual role of clade I TGA TFs with respect to ROXY9 and propose that TGA1/4 and ROXY9 form a new functional unit in *A. thaliana*.

(III) Clade I TGA TFs regulate basal *ROXY9* expression.

(IV) ROXY9 plays a role in plant responses in a common function with clade I TGA TFs, in which a relevance of ROXY9 in plant defense cannot be excluded.

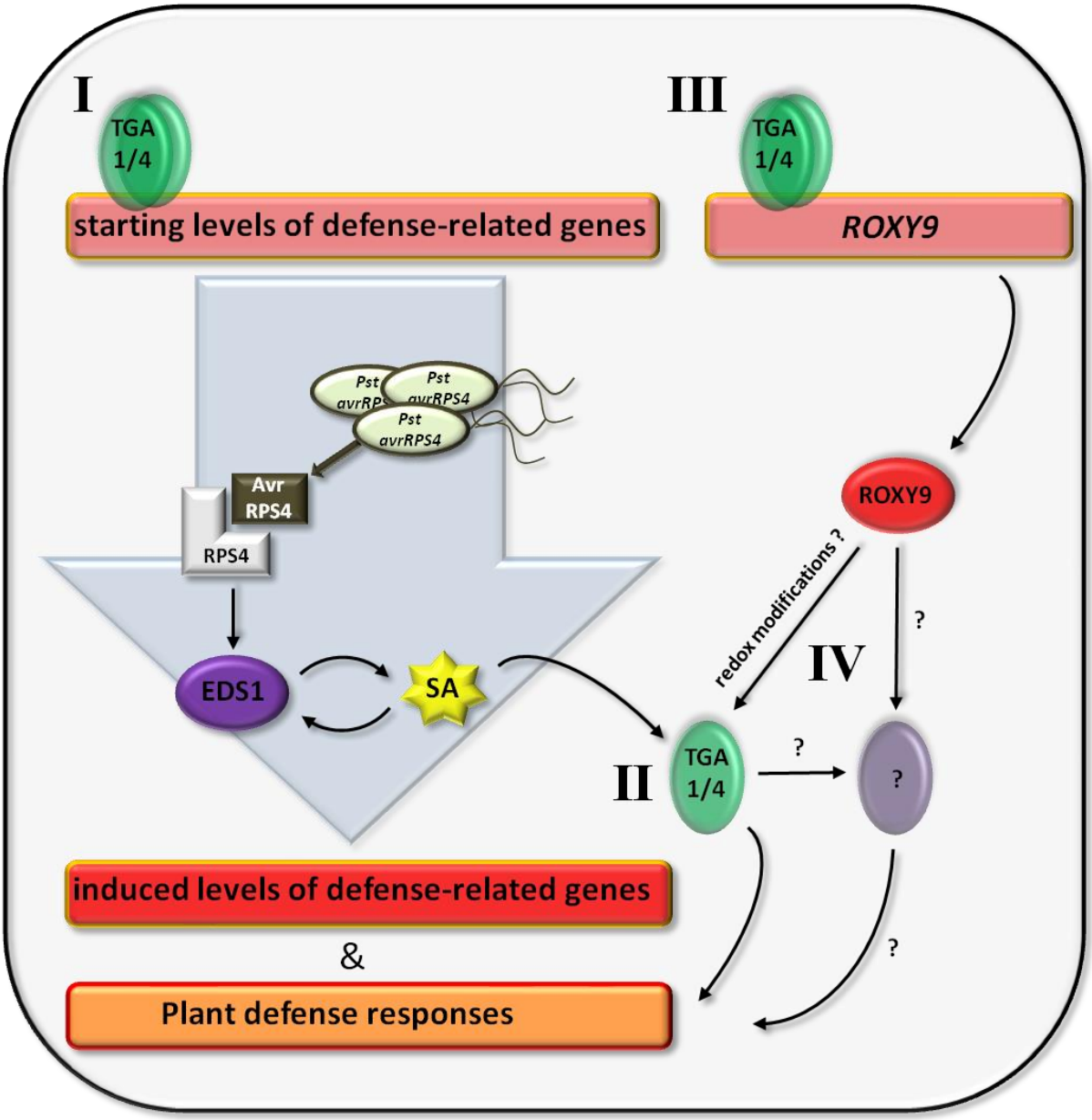

Fig. 5.2: Possible functions of clade I TGA TFs and ROXY9 in avrRPS-triggered resistance

I. TGA1 and TGA4 control starting levels of genes that are involved in EDS1-mediated resistance.

II. TGA1 and TGA4 function in SA-dependent mechanisms downstream of EDS1 in resistance determined by RPS4. Whether this is due to transcriptional regulation of *ROXY* gene expression or other mechanisms remain to be shown.

III. Clade I TGA TFs regulate basal *ROXY9* expression.

IV. ROXY9 plays a role in plant responses in a common function with clade I TGA TFs, in which a relevance of ROXY9 in plant defense cannot be excluded. Whether TGA1 and TGA4 are redox modified by ROXY9 remains questionable Furthermore, an influence of ROXY9 to other proteins involved in defense responses cannot be excluded.

6 Supplemental data

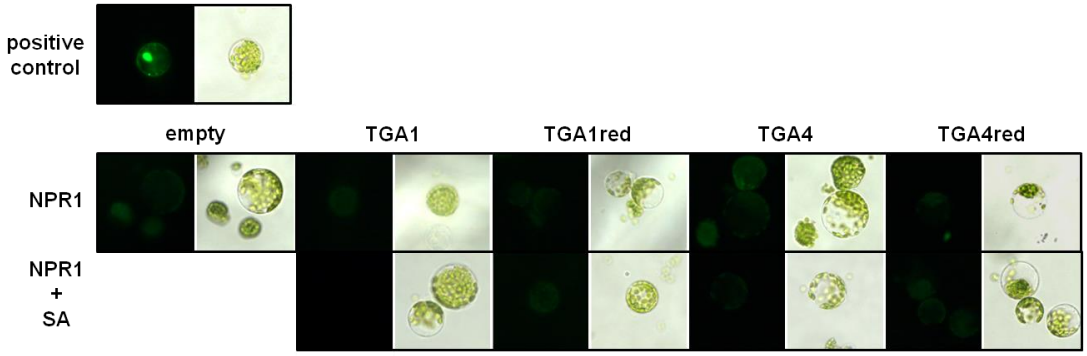

Fig. S1: Interaction between NPR1 and clade I TGA TFs in BiFC assays

The interaction of NPR1 with wildtype and constitutively reduced clade I TGA TFs. Representative pictures of BiFC studies in *A. thaliana* protoplasts. Clade I TGA TFs are encoded with the N-terminal part of YFP, NPR1 with the C-terminal part. Successful complementation is shown by positive nuclear localization of BZI and ANK1 (positive control). Transformed protoplasts were incubated over night ± 5 µM SA.

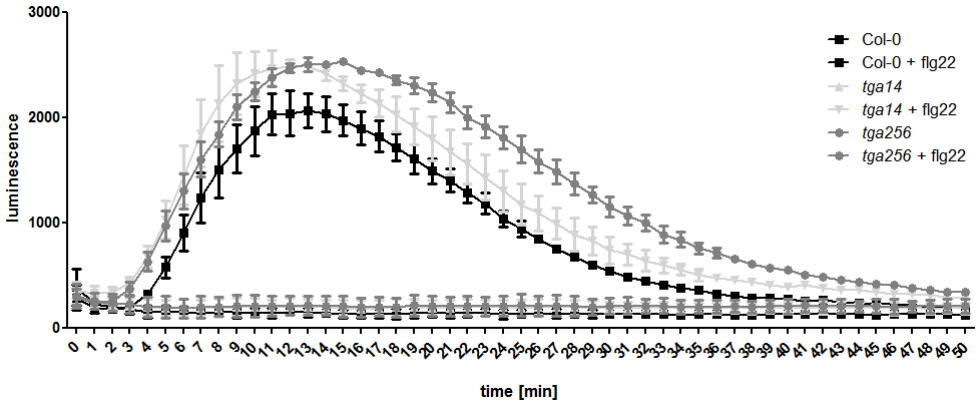

Fig. S2: flg22-induced oxidative burst in Col-0, *tga14* mutant and *tga256* mutant leaf tissue

Chemiluminescence of *A. thaliana* leaf tissue after treatment with 1 µM flg22 was monitored with luminol and peroxidase in a solution. The graph represents the average of two independent experiments ± SEM, in which twelve leaf discs for every data point were measured for a single experiment.

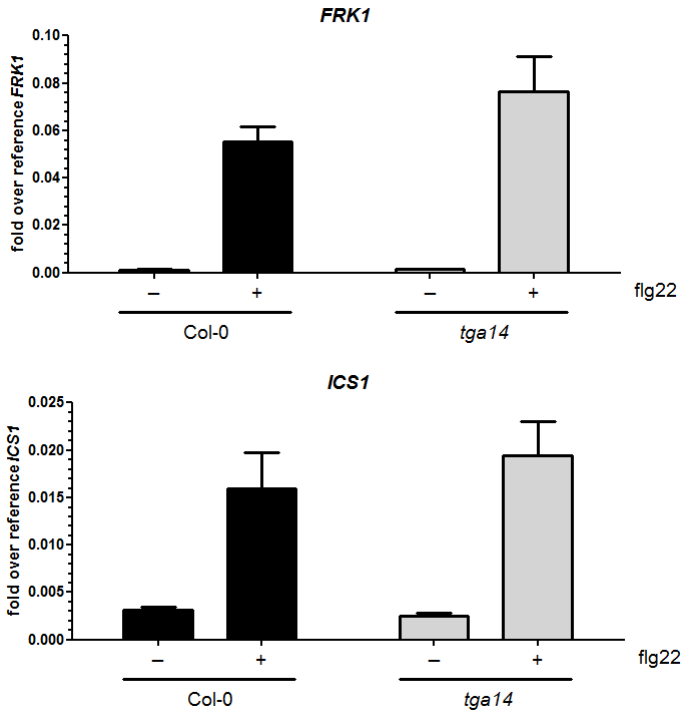

Fig. S3: flg22-induced gene expression in wildtype Col-0 and *tga14* mutant

A. thaliana seedlings grown on MS-MES plates for two weeks were sprayed with 100 nM flg22. Total RNA of approximately 40 seedlings was extracted after eight hours and the transcript levels of *FRK1* and *ICS1* were quantified by qRT-PCR and normalized to expression of *UBQ5*. The average (SEM) of n = 5 samples is shown.

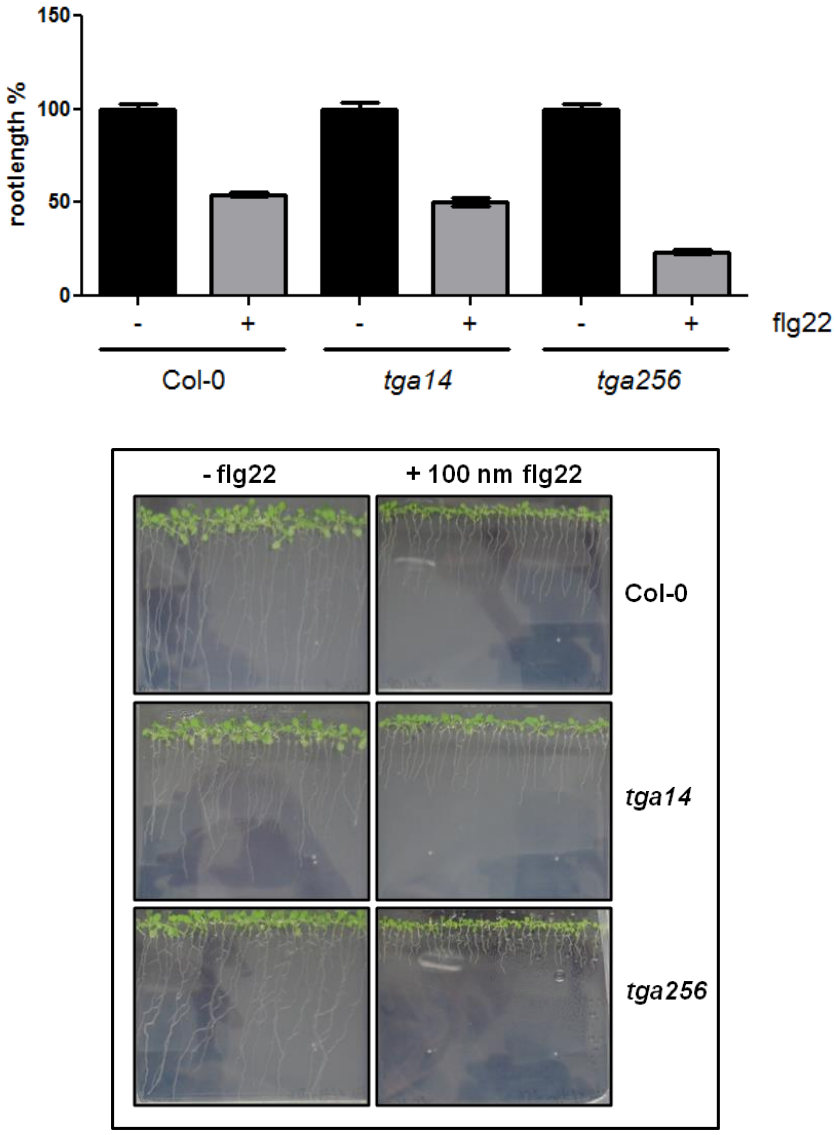

S4: flg22-induced reduction of root length in wildtype Col-0, *tga14* mutant and *tga256* mutant

A. thaliana seedlings of wildtype Col-0, *tga14* mutant and *tga256* mutant were grown vertically for 14 days on MS-MES medium supplemented with 100 nM flg22. (A) For quantification root length of 30 seedlings per genotype was measured and the reduction is displayed in %. Every bar represents the average ± SEM. (B) Representative pictures of 14 days-old wildtype Col-0 and *tga14* mutant seedlings grown on vertical MS-MES plates with or without 100 nM flg22.

S5: Symptoms after infection with *Pst avrRPS4* in wildtype Col-0 and the *tga14* mutant at 3dpi

Plants grown under 12h/12h light cycle conditions on soil for 4 weeks were infiltrated with a bacterial suspension of *Pst avrRPS4* (OD_{600} = 0.002).

S6: Table of gene class I (Col-0 induced – *tga14* less expressed) at 3 hpi

Affected expression of *Pst avrRPS4*-induced genes in the *tga14* mutant at 3 hpi relative to expression in wildtype Col-0 (Col-0 induced – *tga14* less expressed). Only genes with minimum 2 fold change and a P value < 0.005 are listed.

Description	3 hpi Col-0 vs. tga14	P value
(at4g04500): protein kinase family protein	2,44	9,86E-07
(at4g10500): oxidoreductase, 2OG-Fe(II) oxygenase family protein	2,33	2,28E-02
(at2g14560): LURP1 (LATE UPREGULATED IN RESPONSE TO HYALOPERONOSPORA PARASITICA)	2,31	3,60E-03
(at2g18660): EXLB3 (EXPANSIN-LIKE B3 PRECURSOR)	2,29	2,78E-03
(at2g04450): ATNUDT6 (Arabidopsis thaliana Nudix hydrolase homolog 6); ADP-ribose diphosphatase/ NAD or NADH binding / hydrolase	2,28	9,60E-07
(at5g64530): ANAC104, XND1; transcription factor	2,23	7,95E-10

(at4g17670): senescence-associated protein-related	2,12	1,77E-12
(at4g00700): C2 domain-containing protein	2,11	3,39E-06
(at4g23150): protein kinase family protein	2,02	2,27E-04
(at1g67810): SUFE2 (SULFUR E 2); enzyme activator	1,91	2,30E-09
(at4g04490): protein kinase family protein	1,87	2,30E-05
(at5g13320): PBS3 (AVRPPHB SUSCEPTIBLE 3)	1,86	3,29E-08
(at5g55450): protease inhibitor/seed storage/lipid transfer protein (LTP) family protein	1,84	8,11E-07
MULTIPLE HITS: (at1g14870,at1g14880). at1g14870: FUNCTIONS IN: molecular_function unknown; INVOLVED IN: response to oxidative stress; LOCATED IN: plasma membrane; EXPRESSED IN: callus; CONTAINS InterPro DOMAIN/s: EGF-type aspartate/asparagine hydroxylation conserved site (InterPro:IPR000152), Protein of unknown function Cys-rich (InterPro:IPR006461); BEST Arabidopsis thaliana protein match is: unknown protein (TAIR:AT5G35525.1); Has 492 Blast hits to 491 proteins in 78 species: Archae - 0; Bacteria - 0; Metazoa - 93; Fungi - 76; Plants - 297; Viruses - 0; Other Eukaryotes - 26 (source: NCBI BLink). | chr1:5128375-5129523 REVERSE at1g14880: unknown protein | chr1:5132535-5133716 REVERSE	1,83	1,43E-04
(at3g54150): embryo-abundant protein-related	1,78	1,82E-08
(at5g59670): leucine-rich repeat protein kinase, putative	1,78	9,24E-06
(at1g74710): isochorismate synthase 1 (ICS1) / isochorismate mutase	1,73	1,22E-09
(at1g02450): NIMIN1 (NIM1-INTERACTING 1); protein binding	1,70	1,35E-04
(at1g19960): FUNCTIONS IN: molecular_function unknown; INVOLVED IN: biological_process unknown; LOCATED IN: cellular_component unknown; EXPRESSED IN: 21 plant structures; EXPRESSED DURING: 13 growth stages; BEST Arabidopsis thaliana protein match is: transmembrane receptor (TAIR:AT2G32140.1); Has 41 Blast hits to 41 proteins in 16 species: Archae - 0; Bacteria - 2; Metazoa - 25; Fungi - 0; Plants - 9; Viruses - 0; Other Eukaryotes - 5 (source: NCBI BLink). | chr1:6928039-6928463 FORWARD	1,68	5,40E-04
(at3g18250): unknown protein	1,68	4,31E-03
(at5g43910): pfkB-type carbohydrate kinase family protein	1,67	3,01E-09
(at4g35180): LHT7 (Lys/His transporter 7); amino acid transmembrane transporter	1,64	2,16E-06
(at1g21240): WAK3 (wall associated kinase 3); kinase/ protein serine/threonine kinase	1,62	1,14E-03
(at3g13610): oxidoreductase, 2OG-Fe(II) oxygenase family protein	1,62	4,00E-02
(at5g22570): WRKY38; transcription factor	1,60	2,96E-03
(at1g33960): AIG1 (AVRRPT2-INDUCED GENE 1); GTP binding	1,60	2,51E-04
(at5g60280): lectin protein kinase family protein	1,59	1,75E-07
(at3g52430): PAD4 (PHYTOALEXIN DEFICIENT 4); lipase/ protein binding / triacylglycerol lipase	1,57	6,98E-08
(at1g75040): PR5 (PATHOGENESIS-RELATED GENE 5)	1,56	6,91E-03
(at4g23700): ATCHX17 (CATION/H+ EXCHANGER 17); monovalent cation:proton antiporter/ sodium:hydrogen antiporter	1,54	4,05E-05
(at5g22530): unknown protein	1,53	1,88E-07
(at3g60420): LOCATED IN: cellular_component unknown; EXPRESSED IN: 17 plant structures; EXPRESSED DURING: 10 growth stages; CONTAINS InterPro DOMAIN/s: Phosphoglycerate mutase (InterPro:IPR013078); BEST Arabidopsis thaliana protein match is: unknown protein (TAIR:AT3G60450.1); Has 196 Blast hits to 165 proteins in 65 species: Archae - 0; Bacteria - 41; Metazoa - 2; Fungi - 34; Plants - 58; Viruses - 0; Other Eukaryotes - 61 (source: NCBI BLink). | chr3:22334431-22337494 FORWARD	1,48	7,92E-09
(at2g04430): atnudt5 (Arabidopsis thaliana Nudix hydrolase homolog 5); hydrolase	1,47	6,90E-07
(at2g26400): ATARD3 (ACIREDUCTONE DIOXYGENASE 3);	1,46	1,05E-02

acireductone dioxygenase [iron(II)-requiring]/ heteroglycan binding / metal ion binding		
(at3g51330): aspartyl protease family protein	1,45	4,76E-08
(at3g21080): ABC transporter-related	1,45	1,98E-09
(at1g13470): unknown protein	1,42	1,59E-04
(at5g60800): heavy-metal-associated domain-containing protein	1,37	1,41E-06
(at1g03850): glutaredoxin family protein	1,36	1,53E-02
(at2g47130): short-chain dehydrogenase/reductase (SDR) family protein	1,36	2,22E-06
(at3g48080): lipase class 3 family protein / disease resistance protein-related	1,34	2,28E-03
(at1g35230): AGP5 (ARABINOGALACTAN-PROTEIN 5)	1,33	8,36E-06
(at5g48400): ATGLR1.2; intracellular ligand-gated ion channel	1,32	2,19E-06
(at1g13340): unknown protein	1,30	1,03E-07
(at3g26470): FUNCTIONS IN: molecular_function unknown; INVOLVED IN: biological_process unknown; LOCATED IN: cellular_component unknown; EXPRESSED IN: 8 plant structures; EXPRESSED DURING: 4 anthesis, LP.04 four leaves visible, petal differentiation and expansion stage; CONTAINS InterPro DOMAIN/s: Disease resistance, plant (InterPro:IPR014011); BEST Arabidopsis thaliana protein match is: ADR1-L1 (ADR1-like 1); ATP binding / protein binding (TAIR:AT4G33300.2); Has 27 Blast hits to 27 proteins in 3 species: Archae - 0; Bacteria - 0; Metazoa - 0; Fungi - 0; Plants - 27; Viruses - 0; Other Eukaryotes - 0 (source: NCBI BLink). | chr3:9686098-9687642 FORWARD	1,30	1,12E-07
(at2g47000): MDR4, ABCB4 (ATP BINDING CASSETTE SUBFAMILY B4); ATPase, coupled to transmembrane movement of substances / xenobiotic-transporting ATPase	1,28	3,94E-06
(at3g17690): ATCNGC19; calmodulin binding / cyclic nucleotide binding / ion channel	1,28	7,05E-07
(at3g55470): C2 domain-containing protein	1,26	2,41E-08
(at1g74590): GSTU10 (GLUTATHIONE S-TRANSFERASE TAU 10); glutathione transferase	1,22	3,58E-02
(at4g26120): ankyrin repeat family protein / BTB/POZ domain-containing protein	1,21	3,26E-09
(at3g56400): WRKY70; transcription factor/ transcription repressor	1,21	2,89E-05
(at3g09010): protein kinase family protein	1,20	5,67E-05
(at3g14470): disease resistance protein (NBS-LRR class), putative	1,20	5,57E-06
(at3g60470): unknown protein	1,19	3,70E-04
(at2g35980): YLS9 (YELLOW-LEAF-SPECIFIC GENE 9)	1,18	1,36E-04
(at4g02550): unknown protein	1,18	2,45E-09
(at5g17760): AAA-type ATPase family protein	1,18	4,73E-05
(at3g13950): unknown protein	1,17	1,05E-02
(at1g01340): ATCNGC10 (CYCLIC NUCLEOTIDE GATED CHANNEL 10); calmodulin binding / cyclic nucleotide binding / ion channel	1,15	4,69E-07
(at5g64780): FUNCTIONS IN: molecular_function unknown; INVOLVED IN: biological_process unknown; LOCATED IN: cellular_component unknown; EXPRESSED IN: 21 plant structures; EXPRESSED DURING: 15 growth stages; CONTAINS InterPro DOMAIN/s: Uncharacterised conserved protein UCP009193 (InterPro:IPR016549); BEST Arabidopsis thaliana protein match is: unknown protein (TAIR:AT4G09830.1); Has 56 Blast hits to 56 proteins in 10 species: Archae - 0; Bacteria - 0; Metazoa - 0; Fungi - 0; Plants - 56; Viruses - 0; Other Eukaryotes - 0 (source: NCBI BLink). | chr5:25900559-25902127 REVERSE	1,14	1,28E-05
(at4g11840): PLDGAMMA3; phospholipase D	1,14	1,98E-04
(at5g42380): CML37 (CALMODULIN LIKE 37); calcium ion binding	1,12	6,80E-06
(at1g61800): GPT2; antiporter/ glucose-6-phosphate transmembrane	1,12	4,87E-05

transporter		
(at5g45090): AtPP2-A7 (Phloem protein 2-A7); carbohydrate binding	1,12	6,47E-05
(at1g12200): flavin-containing monooxygenase family protein / FMO family protein	1,11	3,24E-06
(at5g47130): Bax inhibitor-1 family / BI-1 family	1,11	3,60E-06
(at5g11920): AtcwINV6 (6-&1-fructan exohydrolase); hydrolase, hydrolyzing O-glycosyl compounds / inulinase/ levanase	1,10	1,14E-03
(at5g51630): disease resistance protein (TIR-NBS-LRR class), putative	1,10	4,82E-07
(at5g24210): lipase class 3 family protein	1,09	5,44E-06
(at4g12490): protease inhibitor/seed storage/lipid transfer protein (LTP) family protein	1,09	3,78E-05
(at1g21250): WAK1 (CELL WALL-ASSOCIATED KINASE); kinase	1,09	6,97E-04
(at5g45110): NPR3 (NPR1-LIKE PROTEIN 3); protein binding	1,08	6,53E-09
(at1g05570): CALS1 (CALLOSE SYNTHASE 1); 1,3-beta-glucan synthase/ transferase, transferring glycosyl groups	1,07	4,90E-06
(at3g47780): ATATH6; ATPase, coupled to transmembrane movement of substances / transporter	1,07	7,26E-07
(at5g65210): TGA1; DNA binding / calmodulin binding / transcription factor	1,06	1,70E-07
(at3g14840): leucine-rich repeat family protein / protein kinase family protein	1,06	3,92E-07
(at3g28580): AAA-type ATPase family protein	1,05	2,40E-04
(at1g15790): unknown protein	1,05	1,82E-03
(at1g33950): avirulence-responsive family protein / avirulence induced gene (AIG1) family protein	1,03	3,09E-03
(at3g09270): ATGSTU8 (GLUTATHIONE S-TRANSFERASE TAU 8); glutathione transferase	1,00	3,74E-02
(at3g13100): ATMRP7; ATPase, coupled to transmembrane movement of substances	1,00	4,26E-04

S7: Table of gene class II (Col-0 induced – *tga14* higher expressed) at 3 hpi

Affected expression of *Pst avrRPS4*-induced genes in the *tga14* mutant at 3 hpi relative to expression in wildtype Col-0 (Col-0 induced – *tga14* higher expressed). Only genes with minimum 2 fold change and a P value < 0.005 are listed.

Description	**3h Col-0 vs. tga14**	**P value**
(at4g21680): proton-dependent oligopeptide transport (POT) family protein	-2,90	6,10E-08
(at2g34600): JAZ7 (JASMONATE-ZIM-DOMAIN PROTEIN 7)	-2,45	1,80E-09
(at5g14180): MPL1 (MYZUS PERSICAE-INDUCED LIPASE 1); catalytic	-2,36	3,81E-07
(at4g15660): glutaredoxin family protein	-2,22	1,05E-11
(at1g30135): JAZ8 (JASMONATE-ZIM-DOMAIN PROTEIN 8)	-2,19	4,09E-08
(at3g46660): UGT76E12 (UDP-GLUCOSYL TRANSFERASE 76E12); UDP-glycosyltransferase/ quercetin 3-O-glucosyltransferase/ quercetin 7-O-glucosyltransferase/ transferase, transferring glycosyl groups	-2,08	1,68E-06
(at1g44800): nodulin MtN21 family protein	-1,79	1,22E-07
(at5g13220): JAZ10 (JASMONATE-ZIM-DOMAIN PROTEIN 10)	-1,68	2,31E-09
(at2g39030): GCN5-related N-acetyltransferase (GNAT) family protein	-1,66	1,55E-08

(at5g51060): RHD2 (ROOT HAIR DEFECTIVE 2); NAD(P)H oxidase	-1,58	3,71E-06
(at5g13330): Rap2.6L (related to AP2 6L); DNA binding / transcription factor	-1,52	9,89E-08
(at5g67080): MAPKKK19; ATP binding / kinase/ protein kinase/ protein serine/threonine kinase	-1,43	8,78E-08
(at5g59220): protein phosphatase 2C, putative / PP2C, putative	-1,40	6,64E-05
(at5g23820): MD-2-related lipid recognition domain-containing protein / ML domain-containing protein	-1,34	4,87E-04
MULTIPLE HITS: (at1g51760,at1g51780). at1g51760: Symbols: IAR3, JR3 | IAR3 (IAA-ALANINE RESISTANT 3); IAA-Ala conjugate hydrolase/ metallopeptidase | chr1:19199419-19201642 FORWARD at1g51780: Symbols: ILL5 | ILL5; IAA-amino acid conjugate hydrolase/ metallopeptidase | chr1:19204512-19206586 FORWARD	-1,30	4,98E-08
(at3g28007): nodulin MtN3 family protein	-1,28	1,69E-04
(at1g69880): ATH8 (thioredoxin H-type 8)	-1,26	1,63E-04
MULTIPLE HITS: (at3g44860,at3g44870). at3g44860: Symbols: FAMT | FAMT (farnesoic acid carboxyl-O-methyltransferase); S-adenosylmethionine-dependent methyltransferase/ farnesoic acid O-methyltransferase | chr3:16379633-16381070 FORWARD at3g44870: S-adenosyl-L-methionine:carboxyl methyltransferase family protein | chr3:16382219-16383605 FORWARD	-1,25	1,98E-09
(at5g23660): MTN3 (Arabidopsis homolog of Medicago truncatula MTN3)	-1,24	1,73E-05
(at1g52890): ANAC019 (Arabidopsis NAC domain containing protein 19); transcription factor	-1,23	2,73E-07
(at3g48360): BT2 (BTB AND TAZ DOMAIN PROTEIN 2); protein binding / transcription factor/ transcription regulator	-1,19	2,00E-06
(at4g27410): RD26 | RD26 (RESPONSIVE TO DESICCATION 26); transcription activator/ transcription factor	-1,16	1,95E-05
(at4g02360): unknown protein	-1,09	8,87E-07
(at1g06620): 2-oxoglutarate-dependent dioxygenase, putative	-1,08	1,19E-04
(at3g57520): AtSIP2 (Arabidopsis thaliana seed imbibition 2); hydrolase, hydrolyzing O-glycosyl compounds	-1,06	1,31E-06
(at5g03210): unknown protein |	-1,06	1,42E-03
MULTIPLE HITS: (at1g72510,at2g09970). at1g72510: unknown protein | chr1:27303389-27304850 FORWARD at2g09970: unknown protein | chr2:3779992-3780691 REVERSE	-1,05	1,81E-08
(at2g22760): basic helix-loop-helix (bHLH) family protein	-1,03	5,33E-04
(at1g76790): O-methyltransferase family 2 protein	-1,03	1,50E-03
(at1g17020): SRG1 (SENESCENCE-RELATED GENE 1); oxidoreductase, acting on diphenols and related substances as donors, oxygen as acceptor / oxidoreductase, acting on paired donors, with incorporation or reduction of molecular oxygen, 2-oxoglutarate as one donor, and inc	-1,01	8,01E-03

S8: Table of gene class III (Col-0 repressed – *tga14* higher expressed) at 3 hpi

Affected expression of *Pst avrRPS4*-induced genes in the *tga14* mutant at 3 hpi relative to expression in wildtype Col-0 (Col-0 repressed – *tga14* higher expressed). Only genes with minimum 2 fold change and a P value < 0.005 are listed.

Description	3h Col-0 vs. tga14	P value
(at5g65390): AGP7	-2,02	7,85E-09
(at4g16563): aspartyl protease family protein	-1,84	5,18E-08
(at5g24030): SLAH3 (SLAC1 HOMOLOGUE 3); transporter	-1,67	3,85E-05
(at1g23205): invertase/pectin methylesterase inhibitor family protein	-1,61	1,03E-09
(at5g50915): basic helix-loop-helix (bHLH) family protein	-1,58	1,99E-06
(at1g02205): CER1 (ECERIFERUM 1); octadecanal decarbonylase	-1,53	9,35E-04
(at5g44050): MATE efflux family protein	-1,50	3,72E-04
(at4g22620): auxin-responsive family protein	-1,45	2,25E-07
(at1g16370): OCT6 (ORGANIC CATION/CARNITINE TRANSPORTER 6); carbohydrate transmembrane transporter/ sugar:hydrogen symporter	-1,43	4,60E-05
(at1g21910): AP2 domain-containing transcription factor family protein	-1,40	1,26E-07
(at5g03120): unknown protein	-1,39	2,28E-04
(at3g27170): CLC-B (CHLORIDE CHANNEL B); anion channel/ voltage-gated chloride channel	-1,35	1,01E-06
(at2g23130): AGP17 (ARABINOGALACTAN PROTEIN 17)	-1,34	1,98E-04
(at2g34930): disease resistance family protein	-1,33	4,35E-07
(at2g20670): unknown protein	-1,32	1,26E-07
(at3g62950): glutaredoxin family protein	-1,28	2,42E-06
(at5g37300): WSD1; diacylglycerol O-acyltransferase/ long-chain-alcohol O-fatty-acyltransferase	-1,23	3,48E-03
(at3g45060): ATNRT2.6; nitrate transmembrane transporter	-1,22	1,26E-02
(at3g62930): glutaredoxin family protein	-1,22	1,76E-05
(at3g28200): peroxidase, putative	-1,21	1,14E-06
(at5g01740): FUNCTIONS IN: molecular_function unknown; INVOLVED IN: biological_process unknown; LOCATED IN: cellular_component unknown; EXPRESSED IN: 18 plant structures; EXPRESSED DURING: 9 growth stages; CONTAINS InterPro DOMAIN/s: Wound-induced protein, Wun1 (InterPro:IPR009798); BEST Arabidopsis thaliana protein match is: SAG20 (SENESCENCE ASSOCIATED GENE 20) (TAIR:AT3G10985.1); Has 49 Blast hits to 49 proteins in 12 species: Archae - 0; Bacteria - 4; Metazoa - 0; Fungi - 0; Plants - 45; Viruses - 0; Other Eukaryotes - 0 (source: NCBI BLink). | chr5:280722-281445 FORWARD	-1,21	3,78E-07
(at1g02205): CER1 (ECERIFERUM 1); octadecanal decarbonylase	-1,19	1,01E-02
(at1g35140): PHI-1 (PHOSPHATE-INDUCED 1)	-1,16	1,60E-02
(at5g14230): protein binding	-1,13	3,86E-06
(at1g04220): KCS2 (3-KETOACYL-COA SYNTHASE 2); fatty acid elongase	-1,10	1,28E-02
(at4g27450): unknown protein	-1,06	3,36E-05
(at3g27960): kinesin light chain-related	-1,06	1,28E-04
(at5g49360): BXL1 (BETA-XYLOSIDASE 1); hydrolase, hydrolyzing O-glycosyl compounds	-1,06	5,80E-04
(at3g19680): unknown protein	-1,05	5,84E-06
(at5g60890): MYB34 (MYB DOMAIN PROTEIN 34); DNA binding /	-1,03	2,12E-03

kinase/ transcription activator/ transcription factor		
(at2g39330): JAL23 (JACALIN-RELATED LECTIN 23)	-1,02	8,71E-04
(at3g45970): ATEXLA1 (ARABIDOPSIS THALIANA EXPANSIN-LIKE A1)	-1,00	3,33E-03

S9: Table of gene class IV (Col-0 repressed – *tga14* less expressed) at 3 hpi

Affected expression of *Pst avrRPS4*-induced genes in the *tga14* mutant at 3 hpi relative to expression in wildtype Col-0 (Col-0 repressed – *tga14* less expressed). Only genes with minimum 2 fold change and a P value < 0.005 are listed.

Description	3h Col-0 vs. tga14	P value
(at5g10030): TGA4 (TGACG MOTIF-BINDING FACTOR 4); DNA binding / calmodulin binding / transcription factor	3,02	3,16E-14
(at2g21650): MEE3 (MATERNAL EFFECT EMBRYO ARREST 3); DNA binding / transcription factor	2,51	5,00E-11
(at4g26200): ACS7; 1-aminocyclopropane-1-carboxylate synthase	1,79	1,24E-07
(at5g04950): NAS1 (NICOTIANAMINE SYNTHASE 1); nicotianamine synthase	1,70	8,65E-10
(at5g52740): heavy-metal-associated domain-containing protein	1,57	1,04E-08
(at2g37430): zinc finger (C2H2 type) family protein (ZAT11)	1,54	2,16E-06
(at5g47960): SMG1, ATRABA4C; GTP binding	1,51	1,23E-07
(at2g17740): DC1 domain-containing protein	1,29	1,22E-03
(at3g28270): FUNCTIONS IN: molecular_function unknown; INVOLVED IN: biological_process unknown; LOCATED IN: cellular_component unknown; EXPRESSED IN: 15 plant structures; EXPRESSED DURING: 9 growth stages; CONTAINS InterPro DOMAIN/s: Protein of unknown function DUF677 (InterPro:IPR007749); BEST Arabidopsis thaliana protein match is: AT14A (TAIR:AT3G28300.1); Has 443 Blast hits to 436 proteins in 133 species: Archae - 26; Bacteria - 121; Metazoa - 105; Fungi - 15; Plants - 94; Viruses - 1; Other Eukaryotes - 81 (source: NCBI BLink). | chr3:10538105-10540024 FORWARD	1,29	4,78E-07
(at2g32030): GCN5-related N-acetyltransferase (GNAT) family protein	1,27	3,02E-06
(at2g36690): oxidoreductase, 2OG-Fe(II) oxygenase family protein	1,24	1,87E-06
(at5g48430): aspartic-type endopeptidase	1,23	1,92E-02
(at3g62150): PGP21 (P-GLYCOPROTEIN 21); ATPase, coupled to transmembrane movement of substances	1,17	2,06E-07
(at4g21870): 26.5 kDa class P-related heat shock protein (HSP26.5-P)	1,15	5,62E-05
(at3g02550): LBD41 (LOB DOMAIN-CONTAINING PROTEIN 41)	1,13	5,00E-06
(at3g09520): ATEXO70H4 (exocyst subunit EXO70 family protein H4); protein binding	1,11	1,06E-07
(at3g44990): XTR8 (XYLOGLUCAN ENDO-TRANSGLYCOSYLASE-RELATED 8); hydrolase, acting on glycosyl bonds / xyloglucan:xyloglucosyl transferase	1,10	5,73E-04
(at3g55150): ATEXO70H1 (exocyst subunit EXO70 family protein H1); protein binding	1,10	4,32E-05
(at3g63440): CKX6 (CYTOKININ OXIDASE/DEHYDROGENASE 6); cytokinin dehydrogenase	1,08	2,00E-07
(at5g62280): unknown protein	1,07	1,57E-04

(at1g30370): lipase class 3 family protein	1,07	8,30E-06
(at2g26710): BAS1 (PHYB ACTIVATION TAGGED SUPPRESSOR 1); oxygen binding / steroid hydroxylase	1,07	2,98E-05
(at5g67450): AZF1 (ARABIDOPSIS ZINC-FINGER PROTEIN 1); DNA binding / nucleic acid binding / transcription factor/ transcription repressor/ zinc ion binding	1,07	1,02E-07
(at1g69526): UbiE/COQ5 methyltransferase family protein	1,05	7,64E-06
(at4g04955): ATALN (Arabidopsis allantoinase); allantoinase/ hydrolase	1,01	3,46E-04

S10: Table of gene class I (Col-0 induced – *tga14* less expressed) at 6 hpi

Affected expression of *Pst avrRPS4*-induced genes in the *tga14* mutant at 3 hpi relative to expression in wildtype Col-0 (Col-0 induced – *tga14* less expressed). Only genes with minimum 2 fold change and a P value < 0.005 are listed.

Description	6h Col-0 vs. tga14	P value
(at2g14610):PR1 (PATHOGENESIS-RELATED GENE 1)	2,78	1,91E-02
(at5g65210):TGA1; DNA binding / calmodulin binding / transcription factor	2,05	5,45E-12
MULTIPLE HITS: (at1g59500,at4g37390). at1g59500: Symbols: GH3.4 | GH3.4; indole-3-acetic acid amido synthetase | chr1:21854493-21856614 REVERSE at4g37390: Symbols: YDK1, GH3.2, BRU6, GH3-2, AUR3 | BRU6; indole-3-acetic acid amido synthetase | chr4:17579657-17582022 FORWARD	2,02	6,85E-06
(at2g14620): xyloglucan:xyloglucosyl transferase, putative	1,89	4,97E-04
(at5g40010): AATP1 (AAA-ATPase 1); ATP binding / ATPase/ nucleoside-triphosphatase/ nucleotide binding	1,81	3,28E-07
(at2g47800): ATMRP4 (ARABIDOPSIS THALIANA MULTIDRUG RESISTANCE-ASSOCIATED PROTEIN 4); ATPase, coupled to transmembrane movement of substances / folic acid transporter	1,79	2,54E-09
(at2g47000):ABCB4 (ATP BINDING CASSETTE SUBFAMILY B4); ATPase, coupled to transmembrane movement of substances / xenobiotic-transporting ATPase	1,66	1,12E-07
(at3g28510): AAA-type ATPase family protein	1,65	1,10E-02
MULTIPLE HITS: (at3g12240,at3g12230). at3g12240: Symbols: SCPL15 | SCPL15 (serine carboxypeptidase-like 15); serine-type carboxypeptidase | chr3:3902436-3904918 REVERSE at3g12230: Symbols: scpl14 | scpl14 (serine carboxypeptidase-like 14); serine-type carboxypeptidase | chr3:3899431-3901879 REVERSE	1,59	6,02E-09
(at3g60470): unknown protein	1,57	1,76E-05
(at3g09270): ATGSTU8 (GLUTATHIONE S-TRANSFERASE TAU 8); glutathione transferase	1,57	2,55E-03
(at5g45080): AtPP2-A6 (Phloem protein 2-A6); carbohydrate binding	1,54	1,16E-08
(at1g55780): metal ion binding	1,53	1,91E-06
(at3g26440): unknown protein	1,52	3,55E-04
(at5g59670): leucine-rich repeat protein kinase, putative	1,46	9,30E-05
(at5g44460): calcium-binding protein, putative	1,35	8,67E-07
(at2g43140): DNA binding / transcription factor	1,33	1,04E-06
(at5g64530): ANAC104, XND1; transcription factor	1,33	1,64E-06

(at2g26400): ATARD3 (ACIREDUCTONE DIOXYGENASE 3); acireductone dioxygenase [iron(II)-requiring]/ heteroglycan binding / metal ion binding	1,32	1,91E-02
(at5g64780): FUNCTIONS IN: molecular_function unknown; INVOLVED IN: biological_process unknown; LOCATED IN: cellular_component unknown; EXPRESSED IN: 21 plant structures; EXPRESSED DURING: 15 growth stages; CONTAINS InterPro DOMAIN/s: Uncharacterised conserved protein UCP009193 (InterPro:IPR016549); BEST Arabidopsis thaliana protein match is: unknown protein (TAIR:AT4G09830.1); Has 56 Blast hits to 56 proteins in 10 species: Archae - 0; Bacteria - 0; Metazoa - 0; Fungi - 0; Plants - 56; Viruses - 0; Other Eukaryotes - 0 (source: NCBI BLink). | chr5:25900559-25902127 REVERSE	1,31	2,30E-06
(at4g14630): GLP9 (GERMIN-LIKE PROTEIN 9); manganese ion binding / nutrient reservoir	1,30	7,09E-04
(at2g13810): ALD1 (AGD2-LIKE DEFENSE RESPONSE PROTEIN1); catalytic/ pyridoxal phosphate binding / transaminase/ transferase, transferring nitrogenous groups	1,27	4,41E-02
(at1g05560): UGT75B1 (UDP-GLUCOSYLTRANSFERASE 75B1); UDP-glucose:4-aminobenzoate acylglucosyltransferase/ UDP-glucosyltransferase/ UDP-glycosyltransferase/ abscisic acid glucosyltransferase/ transferase, transferring glycosyl groups	1,27	3,64E-04
(at5g20960): AAO1 (ARABIDOPSIS ALDEHYDE OXIDASE 1); aldehyde oxidase/ indole-3-acetaldehyde oxidase	1,25	3,26E-04
(at5g22570): WRKY38; transcription factor	1,24	1,56E-02
(at5g45090): AtPP2-A7 (Phloem protein 2-A7); carbohydrate binding	1,23	2,07E-05
(at1g17745): PGDH (3-PHOSPHOGLYCERATE DEHYDROGENASE); phosphoglycerate dehydrogenase	1,23	1,27E-03
(at5g11460): senescence-associated protein-related	1,20	2,40E-07
(at2g43000): anac042 (Arabidopsis NAC domain containing protein 42); transcription factor	1,19	8,19E-03
(at1g67810): SUFE2 (SULFUR E 2); enzyme activator	1,18	2,58E-06
(at2g34500): CYP710A1 (cytochrome P450, family 710, subfamily A, polypeptide 1); C-22 sterol desaturase/ oxygen binding	1,12	9,25E-03
(at1g03660): FUNCTIONS IN: molecular_function unknown; INVOLVED IN: biological_process unknown; LOCATED IN: cellular_component unknown; EXPRESSED IN: 15 plant structures; EXPRESSED DURING: 4 anthesis, F mature embryo stage, C globular stage, petal differentiation and expansion stage, E expanded cotyledon stage; BEST Arabidopsis thaliana protein match is: ankyrin repeat family protein (TAIR:AT1G03670.1); Has 53 Blast hits to 53 proteins in 2 species: Archae - 0; Bacteria - 0; Metazoa - 0; Fungi - 0; Plants - 53; Viruses - 0; Other Eukaryotes - 0 (source: NCBI BLink). | chr1:911436-911759 REVERSE	1,12	2,01E-04
MULTIPLE HITS: (at1g14870,at1g14880). at1g14870: FUNCTIONS IN: molecular_function unknown; INVOLVED IN: response to oxidative stress; LOCATED IN: plasma membrane; EXPRESSED IN: callus; CONTAINS InterPro DOMAIN/s: EGF-type aspartate/asparagine hydroxylation conserved site (InterPro:IPR000152), Protein of unknown function Cys-rich (InterPro:IPR006461); BEST Arabidopsis thaliana protein match is: unknown protein (TAIR:AT5G35525.1); Has 492 Blast hits to 491 proteins in 78 species: Archae - 0; Bacteria - 0; Metazoa - 93; Fungi - 76; Plants - 297; Viruses - 0; Other Eukaryotes - 26 (source: NCBI BLink). | chr1:5128375-5129523 REVERSE at1g14880: unknown protein | chr1:5132535-5133716 REVERSE	1,11	9,10E-03
(at2g37750): unknown protein	1,08	3,87E-03
(at5g55450): protease inhibitor/seed storage/lipid transfer protein (LTP) family protein	1,08	4,27E-04
(at3g51330): aspartyl protease family protein	1,08	3,15E-06
(at3g28740): CYP81D1; electron carrier/ heme binding / iron ion	1,07	2,27E-04

binding / monooxygenase/ oxygen binding		
(at1g19960): FUNCTIONS IN: molecular_function unknown; INVOLVED IN: biological_process unknown; LOCATED IN: cellular_component unknown; EXPRESSED IN: 21 plant structures; EXPRESSED DURING: 13 growth stages; BEST Arabidopsis thaliana protein match is: transmembrane receptor (TAIR:AT2G32140.1); Has 41 Blast hits to 41 proteins in 16 species: Archae - 0; Bacteria - 2; Metazoa - 25; Fungi - 0; Plants - 9; Viruses - 0; Other Eukaryotes - 5 (source: NCBI BLink). | chr1:6928039-6928463 FORWARD	1,06	1,64E-02
(at1g80110): ATPP2-B11 (ARABIDOPSIS THALIANA PHLOEM PROTEIN 2-B11); carbohydrate binding	1,05	3,71E-07
(at4g36700): cupin family protein	1,04	6,49E-05
(at1g05570): CALS1 (CALLOSE SYNTHASE 1); 1,3-beta-glucan synthase/ transferase, transferring glycosyl groups	1,04	7,44E-06

S11: Table of gene class II (Col-0 induced – *tga14* higher expressed) at 6 hpi

Affected expression of *Pst avrRPS4*-induced genes in the *tga14* mutant at 3 hpi relative to expression in wildtype Col-0 (Col-0 induced – *tga14* higher expressed). Only genes with minimum 2 fold change and a P value < 0.005 are listed.

Description	**6h Col-0 vs. tga14**	**P value**
(at5g14180): MPL1 (MYZUS PERSICAE-INDUCED LIPASE 1)	-2,56	1,18E-07
(at4g15660): glutaredoxin family protein	-1,66	1,27E-09
(at1g76790): O-methyltransferase family 2 protein	-1,47	4,14E-05
(at4g21680): proton-dependent oligopeptide transport (POT) family protein	-1,34	7,26E-04
(at3g48360): BT2 (BTB AND TAZ DOMAIN PROTEIN 2); protein binding / transcription factor/ transcription regulator	-1,23	1,21E-06
(at3g50770): calmodulin-related protein, putative	-1,10	3,94E-04
(at1g69880): ATH8 (thioredoxin H-type 8)	-1,09	6,85E-04
(at3g55970): oxidoreductase, 2OG-Fe(II) oxygenase family protein	-1,04	7,27E-06
(at5g42900): unknown protein	-1,00	7,42E-06

S12: Table of gene class III (Col-0 repressed – *tga14* higher expressed) at 6 hpi

Affected expression of *Pst avrRPS4*-induced genes in the *tga14* mutant at 3 hpi relative to expression in wildtype Col-0 (Col-0 repressed – *tga14* higher expressed). Only genes with minimum 2 fold change and a P value < 0.005 are listed.

Description	6h Col-0 vs. tga14	P value
MULTIPLE HITS: (at1g21110,at1g21120). at1g21110: O-methyltransferase, putative | chr1:7389981-7391553 REVERSE at1g21120: O-methyltransferase, putative | chr1:7395228-7396773 REVERSE	-2,96	5,99E-10
(at5g50915): basic helix-loop-helix (bHLH) family protein	-2,81	3,86E-10
(at1g21120): O-methyltransferase, putative	-2,56	6,32E-09
(at3g45060): ATNRT2.6; nitrate transmembrane transporter	-2,53	1,96E-05
(at4g25810): XTR6 (XYLOGLUCAN ENDOTRANSGLYCOSYLASE 6); hydrolase, acting on glycosyl bonds / hydrolase, hydrolyzing O-glycosyl compounds / xyloglucan:xyloglucosyl transferase	-2,17	3,11E-07
(at5g65390): AGP7	-2,13	3,43E-09
(at1g02205): CER1 (ECERIFERUM 1); octadecanal decarbonylase	-2,02	1,24E-04
(at1g02205): CER1 (ECERIFERUM 1); octadecanal decarbonylase	-1,99	6,75E-05
(at1g65390): ATPP2-A5 (ARABIDOPSIS THALIANA PHLOEM PROTEIN 2 A5); carbohydrate binding	-1,96	1,02E-04
(at4g30290): XTH19 (XYLOGLUCAN ENDOTRANSGLUCOSYLASE/HYDROLASE 19); hydrolase, acting on glycosyl bonds / hydrolase, hydrolyzing O-glycosyl compounds / xyloglucan:xyloglucosyl transferase	-1,96	4,47E-10
(at1g75750): GASA1 (GAST1 PROTEIN HOMOLOG 1)	-1,93	7,25E-10
(at5g44050): MATE efflux family protein	-1,92	2,66E-05
(at5g09440): EXL4 (EXORDIUM LIKE 4)	-1,92	1,01E-06
(at1g62510): protease inhibitor/seed storage/lipid transfer protein (LTP) family protein	-1,91	4,54E-08
(at1g19610): PDF1.4	-1,90	2,31E-05
(at3g54400): aspartyl protease family protein	-1,86	2,05E-08
(at3g62950): glutaredoxin family protein	-1,86	1,23E-08
(at5g44130): FLA13 (FASCICLIN-LIKE ARABINOGALACTAN PROTEIN 13 PRECURSOR)	-1,85	3,19E-10
(at3g45970): ATEXLA1 (ARABIDOPSIS THALIANA EXPANSIN-LIKE A1)	-1,64	3,00E-05
(at1g21910): AP2 domain-containing transcription factor family protein	-1,59	1,78E-08
(at3g27960): kinesin light chain-related	-1,58	1,01E-06
(at4g22470): protease inhibitor/seed storage/lipid transfer protein (LTP) family protein	-1,56	2,94E-05
(at2g23130): AGP17 (ARABINOGALACTAN PROTEIN 17)	-1,56	3,94E-05
(at4g32650): ATKC1 (ARABIDOPSIS THALIANA K+ RECTIFYING CHANNEL 1); cyclic nucleotide binding / inward rectifier potassium channel	-1,55	5,73E-05
(at1g35140): PHI-1 (PHOSPHATE-INDUCED 1)	-1,54	2,36E-03
(at5g61890): AP2 domain-containing transcription factor family protein	-1,53	1,81E-04
(at3g62930): glutaredoxin family protein	-1,53	1,00E-06
(at4g02330): ATPMEPCRB; pectinesterase	-1,51	5,40E-06
(at2g47550): pectinesterase family protein	-1,51	2,83E-04
(at1g19450): integral membrane protein, putative / sugar transporter family protein	-1,49	4,55E-09

(at1g21100): O-methyltransferase, putative	-1,46	3,42E-05
MULTIPLE HITS: (at1g30720,at1g30730). at1g30720: FAD-binding domain-containing protein | chr1:10898172-10899912 FORWARD at1g30730: FAD-binding domain-containing protein | chr1:10900854-10902534 FORWARD	-1,44	3,15E-05
(at1g65390): ATPP2-A5 (ARABIDOPSIS THALIANA PHLOEM PROTEIN 2 A5); carbohydrate binding	-1,43	1,14E-04
(at5g20250): DIN10 (DARK INDUCIBLE 10); hydrolase, hydrolyzing O-glycosyl compounds	-1,43	3,83E-06
(at4g37540): LBD39 (LOB DOMAIN-CONTAINING PROTEIN 39)	-1,43	3,28E-07
(at1g23205): invertase/pectin methylesterase inhibitor family protein	-1,42	7,18E-09
(at1g23800): ALDH2B7; 3-chloroallyl aldehyde dehydrogenase/ aldehyde dehydrogenase (NAD)	-1,41	6,27E-05
(at4g37450): AGP18 (ARABINOGALACTAN PROTEIN 18)	-1,40	1,91E-07
(at2g22880): VQ motif-containing protein	-1,39	4,60E-05
(at5g47330): palmitoyl protein thioesterase family protein	-1,39	2,99E-06
(at5g46050): PTR3 (PEPTIDE TRANSPORTER 3); dipeptide transporter/ transporter/ tripeptide transporter	-1,39	1,58E-05
(at2g16630): proline-rich family protein	-1,38	2,27E-06
(at5g06570): hydrolase	-1,37	1,85E-04
(at1g16370):OCT6 (ORGANIC CATION/CARNITINE TRANSPORTER 6); carbohydrate transmembrane transporter/ sugar:hydrogen symporter	-1,35	8,59E-05
(at2g34930): disease resistance family protein	-1,32	4,57E-07
(at1g51820): leucine-rich repeat protein kinase, putative	-1,32	7,12E-04
(at3g05890): RCI2B (RARE-COLD-INDUCIBLE 2B)	-1,30	7,25E-04
(at5g15350): plastocyanin-like domain-containing protein	-1,29	1,68E-08
(at4g36410):UBC17 (UBIQUITIN-CONJUGATING ENZYME 17); small conjugating protein ligase/ ubiquitin-protein ligase	-1,27	5,26E-06
(at1g03870): FLA9 (FASCICLIN-LIKE ARABINOOGALACTAN 9)	-1,25	1,78E-07
(at1g66160): CMPG1 | U-box domain-containing protein	-1,24	6,76E-04
(at2g30600): BTB/POZ domain-containing protein	-1,22	8,29E-08
(at5g11410): protein kinase family protein	-1,21	5,84E-06
(at3g27170): CLC-B (CHLORIDE CHANNEL B); anion channel/ voltage-gated chloride channel	-1,21	4,43E-06
(at3g28200): peroxidase, putative	-1,19	1,43E-06
(at5g39580): peroxidase, putative	-1,19	1,76E-02
(at3g53260): PAL2; phenylalanine ammonia-lyase	-1,19	4,74E-06
(at2g47180): AtGolS1 (Arabidopsis thaliana galactinol synthase 1); transferase, transferring glycosyl groups / transferase, transferring hexosyl groups	-1,18	1,11E-04
(at2g30600): BTB/POZ domain-containing protein	-1,18	4,40E-06
(at1g09240): NAS3 (NICOTIANAMINE SYNTHASE 3); nicotianamine synthase	-1,18	1,84E-04
(at2g34300): dehydration-responsive protein-related	-1,18	6,19E-07
(at3g14850): unknown protein	-1,17	4,42E-06
(at5g49360): BXL1 (BETA-XYLOSIDASE 1); hydrolase, hydrolyzing O-glycosyl compounds	-1,16	2,43E-04
(at3g47380): invertase/pectin methylesterase inhibitor family protein	-1,15	5,06E-05
(at1g30700): FAD-binding domain-containing protein	-1,14	1,91E-02
(at2g02990):RNS1 (RIBONUCLEASE 1); endoribonuclease/ ribonuclease	-1,13	2,32E-05
(at5g24030): SLAH3 (SLAC1 HOMOLOGUE 3); transporter	-1,11	2,02E-03
(at3g53620): AtPPa4 (Arabidopsis thaliana pyrophosphorylase 4); inorganic diphosphatase	-1,11	6,09E-08
(at5g55180): glycosyl hydrolase family 17 protein	-1,10	1,22E-03

(at5g03120): unknown protein	-1,10	1,93E-03
(at3g12700): aspartyl protease family protein	-1,09	2,77E-05
(at5g22500): FAR1 (FATTY ACID REDUCTASE 1); fatty acyl-CoA reductase (alcohol-forming)/ oxidoreductase, acting on the CH-CH group of donors	-1,09	5,35E-03
(at3g23810): SAHH2 (S-ADENOSYL-L-HOMOCYSTEINE (SAH) HYDROLASE 2); adenosylhomocysteinase/ binding / catalytic	-1,08	2,49E-08
(at1g55330): AGP21	-1,06	5,26E-07
(at5g65010): ASN2 (ASPARAGINE SYNTHETASE 2); asparagine synthase (glutamine-hydrolyzing)	-1,06	1,79E-05
(at3g23250): MYB15 (MYB DOMAIN PROTEIN 15); DNA binding / transcription factor	-1,06	4,49E-05
(at2g43520): ATTI2; serine-type endopeptidase inhibitor	-1,05	5,76E-05
(at5g15410): DND1 (DEFENSE NO DEATH 1); calcium channel/ calmodulin binding / cation channel/ cyclic nucleotide binding / intracellular cAMP activated cation channel/ intracellular cyclic nucleotide activated cation channel/ inward rectifier potassium channel	-1,05	1,36E-04
(at1g62480): vacuolar calcium-binding protein-related	-1,05	3,63E-05
(at5g05860): UGT76C2; UDP-glycosyltransferase/ cis-zeatin O-beta-D-glucosyltransferase/ cytokinin 7-beta-glucosyltransferase/ cytokinin 9-beta-glucosyltransferase/ trans-zeatin O-beta-D-glucosyltransferase/ transferase, transferring glycosyl groups	-1,05	6,66E-06
(at3g12110): Symbols: ACT11 | ACT11 (actin-11); structural constituent of cytoskeleton | chr3:3857843-3859798 FORWARD	-1,04	2,90E-06
(at2g37040): pal1 (Phe ammonia lyase 1); phenylalanine ammonia-lyase	-1,04	6,97E-04
(at3g48460): GDSL-motif lipase/hydrolase family protein	-1,02	1,15E-05
(at5g62360): invertase/pectin methylesterase inhibitor family protein	-1,01	2,32E-04
(at5g67360): ARA12; serine-type endopeptidase	-1,01	6,11E-06
(at4g09420): disease resistance protein (TIR-NBS class), putative	-1,01	4,48E-05
(at3g52450): PUB22 (PLANT U-BOX 22); ubiquitin-protein ligase	-1,00	1,24E-02

S13: Table of gene class IV (Col-0 repressed – *tga14* less expressed) at 6 hpi

Affected expression of *Pst avrRPS4*-induced genes in the *tga14* mutant at 3 hpi relative to expression in wildtype Col-0 (Col-0 repressed – *tga14* less expressed). Only genes with minimum 2 fold change and a P value < 0.005 are listed.

Description	6h Col-0 vs. tga14	P value
(at5g10030): TGA4 (TGACG MOTIF-BINDING FACTOR 4); DNA binding / calmodulin binding / transcription factor	1,99	3,90E-11
(at2g21650): MEE3 (MATERNAL EFFECT EMBRYO ARREST 3); DNA binding / transcription factor	1,72	2,07E-08
(at1g78290): serine/threonine protein kinase, putative	1,08	1,38E-05

S14: Table of gene class I (Col-0 induced – *tga14* less expressed) at 11 hpi

Affected expression of *Pst avrRPS4*-induced genes in the *tga14* mutant at 3 hpi relative to expression in wildtype Col-0 (Col-0 induced – *tga14* less expressed). Only genes with minimum 2 fold change and a P value < 0.005 are listed.

Description	11h Col-0 vs. tga14	P value
(at5g65210): TGA1; DNA binding / calmodulin binding / transcription factor	2,61	8,79E-14
(at1g17170): ATGSTU24 (GLUTATHIONE S-TRANSFERASE TAU 24); glutathione binding / glutathione transferase	1,48	9,59E-07
MULTIPLE HITS: (at1g59500,at4g37390). at1g59500: Symbols: GH3.4 | GH3.4; indole-3-acetic acid amido synthetase | chr1:21854493-21856614 REVERSE at4g37390: Symbols: YDK1, GH3.2, BRU6, GH3-2, AUR3 | BRU6; indole-3-acetic acid amido synthetase | chr4:17579657-17582022 FORWARD	1,34	5,97E-04
(at2g14620): xyloglucan:xyloglucosyl transferase, putative	1,23	1,26E-02
(at3g14440): NCED3 (NINE-CIS-EPOXYCAROTENOID DIOXYGENASE 3); 9-cis-epoxycarotenoid dioxygenase	1,16	6,26E-04
(at1g76470): 3-beta-hydroxy-delta5-steroid dehydrogenase/ binding / catalytic/ cinnamoyl-CoA reductase	1,14	6,17E-03
(at4g14630): GLP9 (GERMIN-LIKE PROTEIN 9); manganese ion binding / nutrient reservoir	1,10	2,82E-03
(at1g05100): MAPKKK18; ATP binding / kinase/ protein kinase/ protein serine/threonine kinase	1,08	1,25E-04

S15: Table of gene class II (Col-0 induced – *tga14* higher expressed) at 11 hpi

Affected expression of *Pst avrRPS4*-induced genes in the *tga14* mutant at 3 hpi relative to expression in wildtype Col-0 (Col-0 induced – *tga14* higher expressed). Only genes with minimum 2 fold change and a P value < 0.005 are listed.

Description	11h Col-0 vs. tga14	P value
(at5g14180): Symbols: MPL1 | MPL1 (MYZUS PERSICAE-INDUCED LIPASE 1); catalytic | chr5:4571337-4574462 REVERSE	-1,64	3,99E-05
(at4g15660): glutaredoxin family protein | chr4:8925806-8926310 FORWARD	-1,41	1,59E-08
(at4g37010): Symbols: CEN2 | caltractin, putative / centrin, putative | chr4:17444309-17445615 FORWARD	-1,04	7,44E-05
(at1g05880): nucleic acid binding / protein binding / structural molecule/ zinc ion binding | chr1:1775643-1778553 FORWARD	-1,03	2,68E-08
(at5g41280): FUNCTIONS IN: molecular_function unknown; INVOLVED IN: biological_process unknown; LOCATED IN: anchored to plasma membrane, anchored to membrane; EXPRESSED IN: hypocotyl, root, callus; CONTAINS InterPro DOMAIN/s: Protein of unknown function DUF26 (InterPro:IPR002902); BEST Arabidopsis thaliana protein match is: receptor-like protein kinase-related (TAIR:AT5G41290.1); Has 883 Blast hits to 865 proteins in 16 species: Archae - 0; Bacteria - 0; Metazoa - 0; Fungi - 0; Plants - 883; Viruses - 0; Other Eukaryotes - 0 (source: NCBI BLink). | chr5:16509509-16510929 FORWARD	-1,02	4,25E-05

S16: Table of gene class III (Col-0 repressed – *tga14* higher expressed) at 11 hpi

Affected expression of *Pst avrRPS4*-induced genes in the *tga14* mutant at 3 hpi relative to expression in wildtype Col-0 (Col-0 repressed – *tga14* higher expressed). Only genes with minimum 2 fold change and a P value < 0.005 are listed.

Description	11h Col-0 vs. tga14	P value
(at1g75750):GASA1 (GAST1 PROTEIN HOMOLOG 1)	-1,85	1,45E-09
(at5g65730): xyloglucan:xyloglucosyl transferase, putative / xyloglucan endotransglycosylase, putative / endo-xyloglucan transferase, putative	-1,75	1,03E-06
(at3g62950): glutaredoxin family protein	-1,58	1,41E-07
(at2g23130): AGP17 (ARABINOGALACTAN PROTEIN 17)	-1,56	3,83E-05
(at1g19610): PDF1.4	-1,50	2,86E-04
(at1g62510): protease inhibitor/seed storage/lipid transfer protein (LTP) family protein	-1,48	1,66E-06
(at3g54400): aspartyl protease family protein	-1,46	6,52E-07
(at4g22470): protease inhibitor/seed storage/lipid transfer protein (LTP) family protein	-1,37	1,31E-04
(at5g50915): basic helix-loop-helix (bHLH) family protein	-1,35	1,44E-05
(at1g09240): NAS3 (NICOTIANAMINE SYNTHASE 3); nicotianamine synthase	-1,35	4,47E-05
(at5g65390): AGP7	-1,34	2,73E-06
(at5g03120): unknown protein	-1,30	4,29E-04
(at2g10940): protease inhibitor/seed storage/lipid transfer protein (LTP) family protein	-1,29	3,49E-04
(at4g37540): LBD39 (LOB DOMAIN-CONTAINING PROTEIN 39)	-1,21	3,22E-06
(at1g23205): invertase/pectin methylesterase inhibitor family protein	-1,20	8,53E-08
(at5g22920): zinc finger (C3HC4-type RING finger) family protein	-1,13	2,64E-05
(at4g12420): SKU5; copper ion binding / oxidoreductase	-1,12	2,75E-06
(at5g65010): ASN2 (ASPARAGINE SYNTHETASE 2); asparagine synthase (glutamine-hydrolyzing)	-1,10	1,08E-05
(at1g55330): AGP21	-1,10	3,17E-07
(at1g63260): TET10 (TETRASPANIN10)	-1,05	6,35E-07
(at5g44020): acid phosphatase class B family protein	-1,03	6,35E-05
(at3g16240): DELTA-TIP; ammonia transporter/ methylammonium transmembrane transporter/ water channel	-1,02	2,23E-06
(at3g62930): glutaredoxin family protein	-1,02	1,39E-04

S17: Table of gene class IV (Col-0 repressed – *tga14* less expressed) at 11 hpi

Affected expression of *Pst avrRPS4*-induced genes in the *tga14* mutant at 3 hpi relative to expression in wildtype Col-0 (Col-0 repressed – *tga14* less expressed). Only genes with minimum 2 fold change and a P value < 0.005 are listed.

Description	11h Col-0 vs. tga14	P value
(at1g52000): jacalin lectin family protein	1,73	1,21E-06
(at3g28270): FUNCTIONS IN: molecular_function unknown; INVOLVED IN: biological_process unknown; LOCATED IN: cellular_component unknown; EXPRESSED IN: 15 plant structures; EXPRESSED DURING: 9 growth stages; CONTAINS InterPro DOMAIN/s: Protein of unknown function DUF677 (InterPro:IPR007749); BEST Arabidopsis thaliana protein match is: AT14A (TAIR:AT3G28300.1); Has 443 Blast hits to 436 proteins in 133 species: Archae - 26; Bacteria - 121; Metazoa - 105; Fungi - 15; Plants - 94; Viruses - 1; Other Eukaryotes - 81 (source: NCBI BLink). | chr3:10538105-10540024 FORWARD	1,60	1,99E-08
(at5g24420): glucosamine/galactosamine-6-phosphate isomerase-related	1,55	4,24E-05
(at3g44990): XTR8 (XYLOGLUCAN ENDO-TRANSGLYCOSYLASE-RELATED 8); hydrolase, acting on glycosyl bonds / xyloglucan:xyloglucosyl transferase	1,35	7,64E-05
(at3g50740): UGT72E1 (UDP-glucosyl transferase 72E1); UDP-glycosyltransferase/ coniferyl-alcohol glucosyltransferase/ transferase, transferring glycosyl groups	1,06	1,87E-06

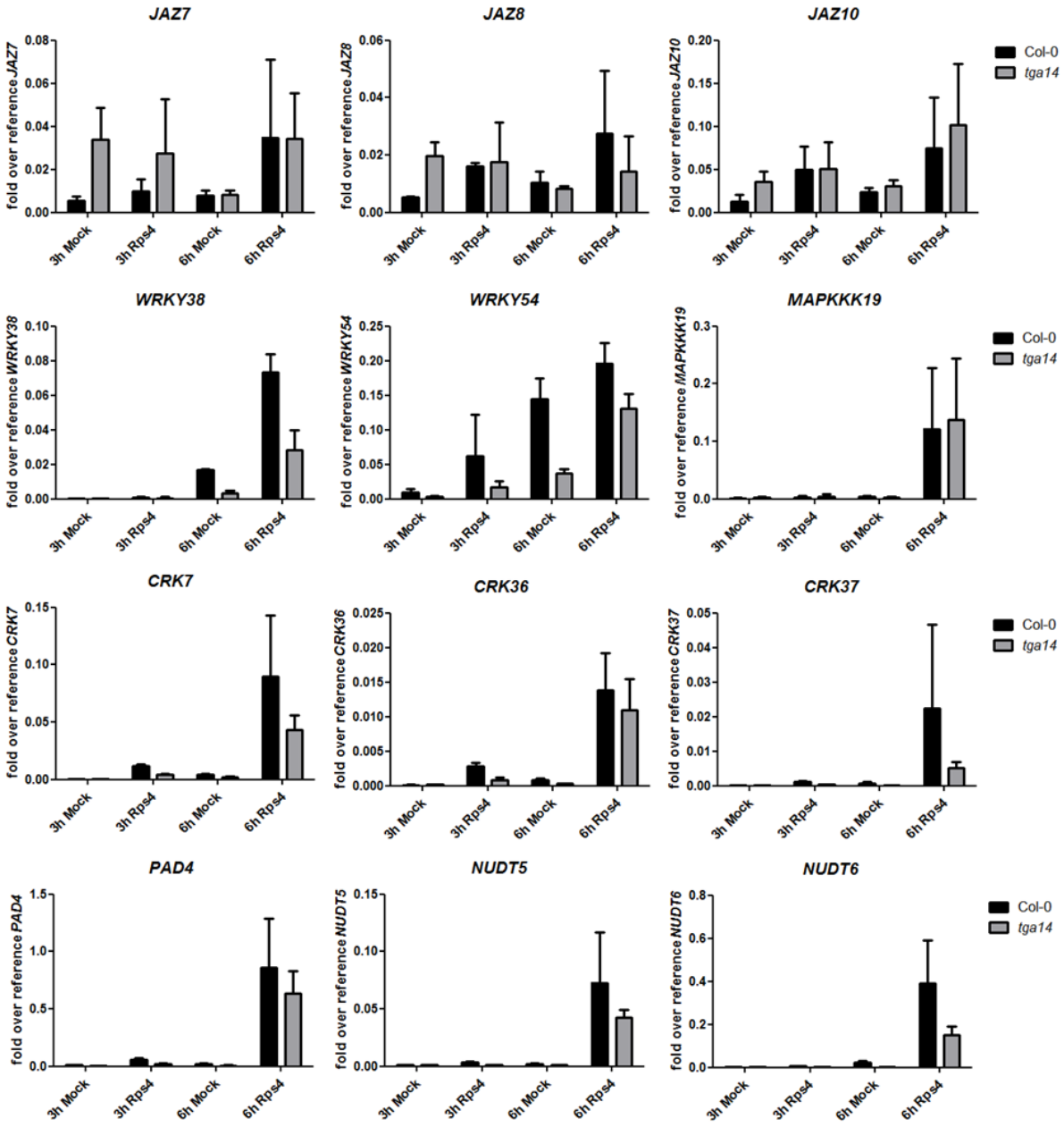

S18: Expression analysis of potential early target genes of clade I TGA TFs revealed in microarray analysis in an independent experiment

Independent samples were prepared as described befor in chapter 4.4. Transcript levels were monitored with specific primers by qRT-PCR and normalized to *UBQ5* expression.

S19: Different expression of genes induced after infection with *Pst avrRps4* in wildtype Col-0 and the *tga14* mutant at 24 hpi

Description	24 hpi Col-0 vs tga14	P value
(at3g12500): Symbols: ATHCHIB, PR3, PR-3, CHI-B, B-CHI | ATHCHIB (ARABIDOPSIS THALIANA BASIC CHITINASE); chitinase | chr3:3962382-3963964 REVERSE	0,49	3,35E-02
(at4g14630): Symbols: GLP9 | GLP9 (GERMIN-LIKE PROTEIN 9); manganese ion binding / nutrient reservoir | chr4:8392841-8393813 FORWARD	0,30	2,52E-02
(at1g55780): metal ion binding | chr1:20852685-20853310 REVERSE	0,37	7,90E-03
MULTIPLE HITS: (at1g54010,at1g54000). at1g54010: myrosinase-associated protein, putative | chr1:20158664-20160815 REVERSE at1g54000: myrosinase-associated protein, putative | chr1:20154169-20156419 REVERSE	3,45	8,58E-03
(at2g41230): unknown protein | chr2:17194926-17195674 REVERSE	0,41	1,65E-04

S20: Different expression of genes repressed after infection with *Pst avrRps4* in wildtype Col-0 and the *tga14* mutant at 24 hpi

Description	24 hpi Col-0 vs. *tga14*	P value
(at5g20630): Symbols: GLP3, GLP3A, GLP3B, ATGER3, GER3 | GER3 (GERMIN 3); oxalate oxidase | chr5:6975104-6975993 REVERSE	4,55	7,64E-04
(at1g03870): Symbols: FLA9 | FLA9 (FASCICLIN-LIKE ARABINOOGALACTAN 9) | chr1:982506-983540 REVERSE	3,10	3,14E-02
(at2g10940): protease inhibitor/seed storage/lipid transfer protein (LTP) family protein | chr2:4310412-4312103 REVERSE	2,25	3,21E-02
(at3g17170): Symbols: RFC3 | RFC3 (REGULATOR OF FATTY-ACID COMPOSITION 3); structural constituent of ribosome | chr3:5853059-5854906 REVERSE	2,96	3,04E-03
(at3g28200): peroxidase, putative | chr3:10518070-10519166 FORWARD	2,62	4,39E-02
(at3g54400): aspartyl protease family protein | chr3:20140058-20142642 REVERSE	2,93	1,58E-03
(at4g34290): SWIB complex BAF60b domain-containing protein | chr4:16410832-16412385 FORWARD	2,20	2,16E-02

(at3g53460): Symbols: CP29 | CP29; RNA binding / poly(U) binding | chr3:19819210-19821505 REVERSE	3,24	9,32E-05
(at4g26370): antitermination NusB domain-containing protein | chr4:13333724-13336230 REVERSE	2,80	2,06E-03
(at3g06980): DEAD/DEAH box helicase, putative | chr3:2201467-2204833 FORWARD	2,29	2,93E-02
(at1g69200): kinase | chr1:26015877-26018493 FORWARD	2,68	4,90E-02
(at1g55490): Symbols: CPN60B, LEN1 | CPN60B (CHAPERONIN 60 BETA); ATP binding / protein binding | chr1:20715563-20719165 REVERSE	3,15	6,59E-04
(at5g55220): trigger factor type chaperone family protein | chr5:22397616-22400842 FORWARD	2,68	8,77E-03
(at3g13470): chaperonin, putative | chr3:4389685-4392851 FORWARD	2,74	1,06E-02
(at2g03420): unknown protein | chr2:1034998-1035969 REVERSE	2,10	1,69E-02
MULTIPLE HITS: (at2g32180,at2g32650). at2g32180: Symbols: PTAC18 | PTAC18 (PLASTID TRANSCRIPTIONALLY ACTIVE 18) | chr2:13672250-13673256 REVERSE at2g32650: FUNCTIONS IN: molecular_function unknown; INVOLVED IN: biological_process unknown; CONTAINS InterPro DOMAIN/s: Cupin, RmlC-type (InterPro:IPR011051), Protein of unknown function DUF861, cupin-3 (InterPro:IPR008579), RmlC-like jelly roll fold (InterPro:IPR014710); BEST Arabidopsis thaliana protein match is: PTAC18 (PLASTID TRANSCRIPTIONALLY ACTIVE 18) (TAIR:AT2G32180.1); Has 169 Blast hits to 169 proteins in 46 species: Archae - 0; Bacteria - 71; Metazoa - 0; Fungi - 0; Plants - 81; Viruses - 0; Other Eukaryotes - 17 (source: NCBI BLink). | chr2:13851062-13852080 FORWARD	2,21	7,26E-03
(at3g44750): Symbols: HD2A, ATHD2A, HDA3, HDT1 | HDA3 (HISTONE DEACETYLASE 3); histone deacetylase/ nucleic acid binding / zinc ion binding | chr3:16297979-16299779 FORWARD	2,68	1,73E-02
(at5g46580): pentatricopeptide (PPR) repeat-containing protein | chr5:18897445-18899645 REVERSE	2,07	2,03E-02
(at2g44640): FUNCTIONS IN: molecular_function unknown; INVOLVED IN: biological_process unknown; LOCATED IN: mitochondrion, chloroplast, plasma membrane, plastid, chloroplast envelope; EXPRESSED IN: 23 plant structures; EXPRESSED DURING: 13 growth stages; BEST Arabidopsis thaliana protein match is: PDE320 (PIGMENT DEFECTIVE 320) (TAIR:AT3G06960.1); Has 25 Blast hits to 24 proteins in 8 species: Archae - 0; Bacteria - 0; Metazoa - 0; Fungi - 0; Plants - 24; Viruses - 0; Other Eukaryotes - 1 (source: NCBI BLink). | chr2:18417243-18419396 FORWARD	2,16	1,35E-02
(at3g54090): pfkB-type carbohydrate kinase family protein | chr3:20028124-20029986 FORWARD	3,23	2,97E-03

(at5g22640): Symbols: emb1211 | emb1211 (embryo defective 1211) | chr5:7529368-7533784 FORWARD	2,35	1,77E-02
(at4g12420): Symbols: SKU5 | SKU5; copper ion binding / oxidoreductase | chr4:7349662-7353074 REVERSE	2,29	4,74E-02
(at3g04550): unknown protein | chr3:1225922-1227436 FORWARD	2,22	1,35E-03

S21: Genes less expressed in the *tga14* mutant after 24 h of mock treatment

Genes less expressed in the *tga14* mutant in mock treated samples were identified by microarray analysis. Deregulated genes exhibits minimum 2 fold change and a P value < 0.05. The influence of *Pst avrRPS4* to expression in Col-0 at 24 hpi is displayed in direct comparison. Values represent log2.

Description	24 h Mock Col-0 vs. t*ga14*	P Value	24 hpi Col-0	P Value
(at3g13610): oxidoreductase, 2OG-Fe(II) oxygenase family protein | chr3:4449374-4450811 FORWARD	2,75	7,17E-03	-1,94	3,87E-02
(at4g04500): protein kinase family protein | chr4:2238411-2240865 FORWARD	2,54	2,37E-03	-0,79	2,35E-01
(at4g10500): oxidoreductase, 2OG-Fe(II) oxygenase family protein | chr4:6491017-6492476 FORWARD	2,51	6,30E-04	-0,15	7,75E-01
(at3g28510): AAA-type ATPase family protein | chr3:10685524-10687364 FORWARD	2,42	7,01E-03	-1,05	1,72E-01
(at2g26400): Symbols: ARD, ATARD3 | ATARD3 (ACIREDUCTONE DIOXYGENASE 3); acireductone dioxygenase [iron(II)-requiring]/ heteroglycan binding / metal ion binding | chr2:11231800-11233295 REVERSE	2,31	5,15E-03	-1,28	7,71E-02
(at3g11340): UDP-glucoronosyl/UDP-glucosyl transferase family protein | chr3:3556705-3558269 FORWARD	2,30	1,48E-02	-1,79	4,54E-02
(at5g05960): protease inhibitor/seed storage/lipid transfer protein (LTP) family protein | chr5:1790231-1790833 FORWARD	2,22	2,19E-07	0,77	1,63E-03
(at3g53150): Symbols: UGT73D1 | UGT73D1 (UDP-glucosyl transferase 73D1); UDP-glycosyltransferase/ transferase, transferring hexosyl groups | chr3:19697736-19699259 REVERSE	2,20	2,98E-03	-0,93	1,30E-01
(at1g67940): Symbols: ATNAP3 | ATNAP3; transporter | chr1:25477670-25478803 FORWARD	2,15	3,42E-06	0,39	1,28E-01
(at2g28190): Symbols: CSD2, CZSOD2 | CSD2 (COPPER/ZINC SUPEROXIDE DISMUTASE 2); superoxide dismutase | chr2:12014498-12016569 FORWARD	2,00	9,05E-05	0,14	6,70E-01
(at3g45160): unknown protein | chr3:16533451-16534082 REVERSE	1,97	2,20E-04	1,69	6,74E-04
(at2g35980): Symbols: YLS9, NHL10, ATNHL10 | YLS9 (YELLOW-LEAF-SPECIFIC GENE 9) | chr2:15110588-15111471 FORWARD	1,95	2,06E-02	-1,66	4,21E-02
(at5g45380): Symbols: ATDUR3, DUR3 | sodium:solute	1,88	1,04E-03	0,26	5,39E-01

symporter family protein | chr5:18391124-18395894 FORWARD				
(at5g49630): Symbols: AAP6 | AAP6 (AMINO ACID PERMEASE 6); acidic amino acid transmembrane transporter/ amino acid transmembrane transporter/ neutral amino acid transmembrane transporter | chr5:20142470-20146498 REVERSE	1,87	5,32E-09	1,01	1,74E-06
(at1g21240): Symbols: WAK3 | WAK3 (wall associated kinase 3); kinase/ protein serine/threonine kinase | chr1:7434303-7436830 FORWARD	1,85	1,90E-02	-1,96	1,41E-02
(at1g71390): Symbols: AtRLP11 | AtRLP11 (Receptor Like Protein 11); protein binding | chr1:26906453-26908807 FORWARD	1,85	2,48E-04	0,49	1,70E-01
(at4g04490): protein kinase family protein | chr4:2231957-2234638 REVERSE	1,83	2,40E-02	-2,03	1,46E-02
(at5g22570): Symbols: WRKY38, ATWRKY38 | WRKY38; transcription factor | chr5:7495539-7496784 REVERSE	1,83	1,63E-02	-1,74	2,10E-02
(at2g04430): Symbols: atnudt5 | atnudt5 (Arabidopsis thaliana Nudix hydrolase homolog 5); hydrolase | chr2:1538901-1541094 FORWARD	1,81	5,61E-03	-0,92	1,06E-01
(at3g44350): Symbols: anac061 | anac061 (Arabidopsis NAC domain containing protein 61); transcription factor | chr3:16022836-16024487 REVERSE	1,79	9,17E-04	0,21	6,06E-01
(at1g68600): unknown protein | chr1:25759842-25762934 FORWARD	1,77	2,43E-06	-1,56	7,70E-06
(at1g06830): glutaredoxin family protein | chr1:2097151-2097655 FORWARD	1,76	1,40E-05	1,48	6,01E-05
(at1g76960): unknown protein | chr1:28920457-28920956 REVERSE	1,75	1,15E-03	-0,06	8,90E-01
(at4g23150): protein kinase family protein | chr4:12125731-12128332 FORWARD	1,73	4,49E-03	-0,69	1,77E-01
(at1g76040): Symbols: CPK29 | CPK29; ATP binding / calcium ion binding / calmodulin-dependent protein kinase/ kinase/ protein kinase/ protein serine/threonine kinase/ protein tyrosine kinase | chr1:28537673-28540637 FORWARD	1,72	3,75E-03	-1,31	1,72E-02
(at2g21650): Symbols: MEE3, ATRL2 | MEE3 (MATERNAL EFFECT EMBRYO ARREST 3); DNA binding / transcription factor | chr2:9259583-9260656 FORWARD	1,72	8,05E-03	2,15	2,02E-03
(at2g18660): Symbols: EXLB3 | EXLB3 (EXPANSIN-LIKE B3 PRECURSOR) | chr2:8090658-8091656 REVERSE	1,71	5,92E-03	-0,89	1,00E-01
(at1g09080): Symbols: BIP3 | BIP3; ATP binding | chr1:2929217-2931841 REVERSE	1,68	2,85E-03	0,70	1,31E-01
(at1g35230): Symbols: AGP5 | AGP5 (ARABINOGALACTAN-PROTEIN 5) | chr1:12917149-12917763 FORWARD	1,67	7,37E-03	-0,48	3,62E-01
(at2g32990): Symbols: AtGH9B8 | AtGH9B8 (Arabidopsis thaliana glycosyl hydrolase 9B8); catalytic/ hydrolase, hydrolyzing O-glycosyl compounds | chr2:14003250-14006017 FORWARD	1,64	5,64E-04	-0,85	2,73E-02
(at4g03450): ankyrin repeat family protein | chr4:1529446-1531780 REVERSE	1,63	4,25E-03	-0,69	1,53E-01

(at1g13470): unknown protein | chr1:4620228-4621580 REVERSE	1,63	7,60E-03	-0,48	3,49E-01
(at4g00700): C2 domain-containing protein | chr4:286051-289514 FORWARD	1,61	1,08E-02	-1,07	6,48E-02
(at3g22600): protease inhibitor/seed storage/lipid transfer protein (LTP) family protein | chr3:8006508-8007471 REVERSE	1,58	4,65E-02	-1,54	5,11E-02
(at2g47130): short-chain dehydrogenase/reductase (SDR) family protein | chr2:19349536-19350539 REVERSE	1,57	6,47E-04	-0,71	5,19E-02
(at1g51890): leucine-rich repeat protein kinase, putative | chr1:19274802-19278528 REVERSE	1,57	1,59E-02	-1,40	2,68E-02
(at1g65690): harpin-induced protein-related / HIN1-related / harpin-responsive protein-related | chr1:24431430-24432953 REVERSE	1,55	4,18E-02	-1,94	1,54E-02
(at3g22910): calcium-transporting ATPase, plasma membrane-type, putative / Ca(2+)-ATPase, putative (ACA13) | chr3:8116335-8119388 REVERSE	1,55	3,95E-02	-1,01	1,55E-01
(at2g20750): Symbols: ATEXPB1, EXPB1, ATHEXP BETA 1.5 | ATEXPB1 (ARABIDOPSIS THALIANA EXPANSIN B1) | chr2:8941119-8942689 FORWARD	1,55	1,26E-02	2,34	1,02E-03
(at1g12520): Symbols: ATCCS | ATCCS (COPPER CHAPERONE FOR SOD1); superoxide dismutase/ superoxide dismutase copper chaperone | chr1:4267106-4268926 REVERSE	1,54	6,04E-04	0,02	9,46E-01
(at1g64360): unknown protein | chr1:23887870-23888533 FORWARD	1,53	2,51E-02	-1,31	4,90E-02
(at5g52390): photoassimilate-responsive protein, putative | chr5:21263936-21265264 REVERSE	1,52	1,65E-02	0,77	1,76E-01
MULTIPLE HITS: (at3g11010,at5g27060). at3g11010: Symbols: AtRLP34 | AtRLP34 (Receptor Like Protein 34); kinase/ protein binding | chr3:3450496-3453683 REVERSE at5g27060: Symbols: AtRLP53 | AtRLP53 (Receptor Like Protein 53); kinase/ protein binding | chr5:9522534-9525407 REVERSE	1,50	6,14E-03	-0,28	5,37E-01
(at3g49340): cysteine proteinase, putative | chr3:18293347-18294577 REVERSE	1,49	1,47E-02	2,37	8,65E-04
(at3g18250): unknown protein | chr3:6258067-6258417 REVERSE	1,48	7,23E-02	-2,00	2,18E-02
(at3g26960): unknown protein | chr3:9944668-9945579 REVERSE	1,48	3,79E-03	1,22	1,13E-02
(at1g22160): senescence-associated protein-related | chr1:7823149-7823971 FORWARD	1,47	3,23E-02	-0,31	6,13E-01
(at3g56710): Symbols: SIB1 | SIB1 (SIGMA FACTOR BINDING PROTEIN 1); binding / protein binding | chr3:21006750-21007565 REVERSE	1,47	1,36E-02	-1,09	5,14E-02
(at3g07390): Symbols: AIR12 | AIR12; extracellular matrix structural constituent | chr3:2365301-2366496 FORWARD	1,47	4,34E-03	-0,77	8,37E-02
(at5g45820): Symbols: CIPK20, SnRK3.6, PKS18 | CIPK20 (CBL-INTERACTING PROTEIN KINASE 20); kinase/ protein serine/threonine kinase | chr5:18586980-18588543	1,46	1,19E-03	2,49	1,76E-05

REVERSE				
(at3g25010): Symbols: AtRLP41 | AtRLP41 (Receptor Like Protein 41); kinase/ protein binding | chr3:9110103-9112748 REVERSE	1,46	8,84E-04	-0,20	5,44E-01
(at5g59670): leucine-rich repeat protein kinase, putative | chr5:24041494-24045652 FORWARD	1,45	3,84E-04	-0,24	4,08E-01
(at1g52190): proton-dependent oligopeptide transport (POT) family protein | chr1:19434509-19438971 FORWARD	1,45	1,25E-02	2,39	5,25E-04
MULTIPLE HITS: (at4g23140,at4g23160). at4g23140: Symbols: CRK6 | CRK6 (CYSTEINE-RICH RLK 6); kinase | chr4:12121383-12124205 FORWARD at4g23160: protein kinase family protein | chr4:12129485-12134187 FORWARD	1,44	8,38E-03	-0,45	3,35E-01
(at5g22580): FUNCTIONS IN: molecular_function unknown; INVOLVED IN: biological_process unknown; LOCATED IN: chloroplast; EXPRESSED IN: 22 plant structures; EXPRESSED DURING: 13 growth stages; CONTAINS InterPro DOMAIN/s: Stress responsive alpha-beta barrel (InterPro:IPR013097), Dimeric alpha-beta barrel (InterPro:IPR011008); BEST Arabidopsis thaliana protein match is: HS1 (HEAT STABLE PROTEIN 1) (TAIR:AT3G17210.1); Has 231 Blast hits to 231 proteins in 57 species: Archae - 0; Bacteria - 89; Metazoa - 0; Fungi - 4; Plants - 98; Viruses - 0; Other Eukaryotes - 40 (source: NCBI BLink). | chr5:7502674-7503449 FORWARD	1,44	6,94E-04	1,46	6,26E-04
(at5g64000): Symbols: SAL2, ATSAL2 | SAL2; 3'(2'),5'-bisphosphate nucleotidase/ inositol or phosphatidylinositol phosphatase | chr5:25616638-25618631 FORWARD	1,43	1,70E-03	0,58	1,14E-01
(at3g24900): Symbols: AtRLP39 | AtRLP39 (Receptor Like Protein 39); protein binding | chr3:9099183-9101837 REVERSE	1,42	3,41E-04	0,55	6,90E-02
(at1g26420): FAD-binding domain-containing protein | chr1:9141567-9143304 REVERSE	1,42	1,87E-02	-0,82	1,38E-01
(at5g12940): leucine-rich repeat family protein | chr5:4087712-4089004 FORWARD	1,41	6,85E-05	0,92	1,67E-03
(at1g03660): FUNCTIONS IN: molecular_function unknown; INVOLVED IN: biological_process unknown; LOCATED IN: cellular_component unknown; EXPRESSED IN: 15 plant structures; EXPRESSED DURING: 4 anthesis, F mature embryo stage, C globular stage, petal differentiation and expansion stage, E expanded cotyledon stage; BEST Arabidopsis thaliana protein match is: ankyrin repeat family protein (TAIR:AT1G03670.1); Has 53 Blast hits to 53 proteins in 2 species: Archae - 0; Bacteria - 0; Metazoa - 0; Fungi - 0; Plants - 53; Viruses - 0; Other Eukaryotes - 0 (source: NCBI BLink). | chr1:911436-911759 REVERSE	1,40	8,74E-04	-0,26	4,10E-01
(at2g32680): Symbols: AtRLP23 | AtRLP23 (Receptor Like Protein 23); kinase/ protein binding | chr2:13859769-	1,40	1,15E-02	0,05	9,18E-01

13862614 REVERSE				
(at5g38900): DSBA oxidoreductase family protein | chr5:15573505-15575618 REVERSE	1,40	3,74E-02	-1,82	1,09E-02
(at4g23610): unknown protein | chr4:12314025-12314829 FORWARD	1,39	1,45E-03	-0,08	8,17E-01
(at1g67750): pectate lyase family protein | chr1:25401588-25403503 FORWARD	1,39	5,75E-03	1,60	2,42E-03
(at2g04450): Symbols: ATNUDT6 | ATNUDT6 (Arabidopsis thaliana Nudix hydrolase homolog 6); ADP-ribose diphosphatase/ NAD or NADH binding / hydrolase | chr2:1543320-1545462 FORWARD	1,37	9,52E-03	-1,21	1,83E-02
(at5g44400): FAD-binding domain-containing protein | chr5:17886194-17888480 REVERSE	1,37	1,52E-05	-0,12	5,09E-01
(at4g15620): integral membrane family protein | chr4:8913838-8915663 FORWARD	1,37	1,49E-05	1,17	5,74E-05
(at1g56060): unknown protein | chr1:20966528-20967144 REVERSE	1,35	5,60E-03	-0,55	1,83E-01
(at5g19880): peroxidase, putative | chr5:6720384-6722475 REVERSE	1,34	1,27E-03	0,15	6,20E-01
(at5g11930): glutaredoxin family protein | chr5:3844940-3845645 REVERSE	1,32	1,30E-05	0,81	6,92E-04
(at4g28490): Symbols: RLK5, HAE | HAE (HAESA); ATP binding / kinase/ protein kinase/ protein serine/threonine kinase | chr4:14077857-14081171 FORWARD	1,32	4,21E-03	-1,13	1,04E-02
(at4g23310): receptor-like protein kinase, putative | chr4:12185737-12188763 FORWARD	1,32	4,91E-04	0,55	6,30E-02
(at1g30900): vacuolar sorting receptor, putative | chr1:10997275-11000543 FORWARD	1,32	1,41E-03	-0,06	8,40E-01
(at5g61010): Symbols: ATEXO70E2 | ATEXO70E2 (EXOCYST SUBUNIT EXO70 FAMILY PROTEIN E2); protein binding | chr5:24553898-24556749 FORWARD	1,31	1,10E-02	-0,94	5,00E-02
(at3g26210): Symbols: CYP71B23 | CYP71B23; electron carrier/ heme binding / iron ion binding / monooxygenase/ oxygen binding | chr3:9593132-9595243 REVERSE	1,31	1,74E-03	-0,26	4,12E-01
(at2g18690): unknown protein | chr2:8097420-8098827 FORWARD	1,31	3,17E-02	-1,38	2,51E-02
(at1g02450): Symbols: NIMIN1, NIMIN-1 | NIMIN1 (NIM1-INTERACTING 1); protein binding | chr1:497976-498516 REVERSE	1,30	6,25E-02	-0,71	2,79E-01
(at1g08830): Symbols: CSD1 | CSD1 (COPPER/ZINC SUPEROXIDE DISMUTASE 1); superoxide dismutase | chr1:2827061-2829315 FORWARD	1,30	4,94E-03	-0,58	1,42E-01
(at4g28250): Symbols: ATEXPB3, EXPB3, ATHEXP BETA 1.6 | ATEXPB3 (ARABIDOPSIS THALIANA EXPANSIN B3) | chr4:14000038-14002069 REVERSE	1,29	5,37E-03	1,28	5,65E-03
(at5g02490): heat shock cognate 70 kDa protein 2 (HSC70-2) (HSP70-2) | chr5:550035-552647 REVERSE	1,29	3,87E-02	-1,25	4,44E-02
(at5g02890): transferase family protein | chr5:670065-671471 REVERSE	1,29	2,91E-04	1,57	5,85E-05

(at2g37710): Symbols: RLK | RLK (receptor lectin kinase); kinase | chr2:15814718-15817004 REVERSE	1,28	2,91E-03	0,04	9,10E-01
(at4g21380): Symbols: ARK3 | ARK3 (A. THALIANA RECEPTOR KINASE 3); kinase/ transmembrane receptor protein serine/threonine kinase | chr4:11388925-11393226 REVERSE	1,28	3,50E-02	-1,50	1,73E-02
(at1g57560): Symbols: AtMYB50 | AtMYB50 (myb domain protein 50); DNA binding / transcription factor | chr1:21316828-21318064 FORWARD	1,27	3,79E-02	-1,64	1,15E-02
(at5g08240): unknown protein | chr5:2650837-2652398 REVERSE	1,27	1,85E-03	-1,14	3,67E-03
(at3g47480): calcium-binding EF hand family protein | chr3:17496354-17496947 REVERSE	1,26	4,12E-02	-1,22	4,62E-02
(at1g78410): VQ motif-containing protein | chr1:29502582-29503241 FORWARD	1,24	4,20E-02	-1,59	1,37E-02
(at1g66880): serine/threonine protein kinase family protein | chr1:24946928-24955611 FORWARD	1,24	5,87E-03	-0,75	6,06E-02
(at2g29110): Symbols: ATGLR2.8, GLR2.8 | ATGLR2.8; intracellular ligand-gated ion channel | chr2:12506880-12510552 REVERSE	1,23	1,95E-02	-0,05	9,13E-01
(at2g43570): chitinase, putative | chr2:18076224-18077463 REVERSE	1,23	3,56E-02	-1,35	2,40E-02
(at5g63180): pectate lyase family protein | chr5:25340954-25343119 REVERSE	1,23	5,43E-03	2,17	9,86E-05
(at3g48850): mitochondrial phosphate transporter, putative | chr3:18114526-18116499 REVERSE	1,23	2,94E-02	-1,70	5,56E-03
(at5g10760): aspartyl protease family protein | chr5:3400342-3402207 REVERSE	1,22	2,73E-03	1,23	2,59E-03
(at5g24530): Symbols: DMR6 | DMR6 (DOWNY MILDEW RESISTANT 6); oxidoreductase/ oxidoreductase, acting on paired donors, with incorporation or reduction of molecular oxygen, 2-oxoglutarate as one donor, and incorporation of one atom each of oxygen into both donors | chr5:8378833-8383401 FORWARD	1,22	7,81E-03	-0,21	5,83E-01
(at1g75040): Symbols: PR5, PR-5 | PR5 (PATHOGENESIS-RELATED GENE 5) | chr1:28177703-28178940 FORWARD	1,22	4,27E-02	0,33	5,46E-01
(at3g59010): pectinesterase family protein | chr3:21802805-21805214 REVERSE	1,22	4,95E-03	-0,16	6,39E-01
(at3g22400): Symbols: LOX5 | LOX5; electron carrier/ iron ion binding / lipoxygenase/ metal ion binding / oxidoreductase, acting on single donors with incorporation of molecular oxygen, incorporation of two atoms of oxygen | chr3:7926879-7931351 FORWARD	1,21	1,52E-04	-0,45	5,42E-02
MULTIPLE HITS: (at3g23120,at3g23110). at3g23120: Symbols: AtRLP38 | AtRLP38 (Receptor Like Protein 38); kinase/ protein binding | chr3:8227222-8229576 REVERSE at3g23110: Symbols: AtRLP37 | AtRLP37 (Receptor Like Protein 37); kinase/ protein binding | chr3:8222364-8224871 REVERSE	1,21	2,01E-02	-0,19	6,75E-01
(at2g29990): Symbols: NDA2 | NDA2 (ALTERNATIVE NAD(P)H DEHYDROGENASE 2); FAD binding / NADH dehydrogenase/ oxidoreductase | chr2:12793340-	1,19	2,38E-02	-1,58	5,41E-03

12795913 REVERSE				
(at5g10030): Symbols: TGA4, OBF4 | TGA4 (TGACG MOTIF-BINDING FACTOR 4); DNA binding / calmodulin binding / transcription factor | chr5:3137323-3140252 REVERSE	1,19	9,81E-07	0,29	2,79E-02
(at3g48090): Symbols: EDS1 | EDS1 (enhanced disease susceptibility 1); lipase/ signal transducer/ triacylglycerol lipase | chr3:17755374-17757780 REVERSE	1,19	1,17E-03	-0,17	5,27E-01
(at5g45800): Symbols: MEE62 | MEE62 (maternal effect embryo arrest 62); ATP binding / protein binding / protein kinase/ protein serine/threonine kinase/ protein tyrosine kinase | chr5:18575536-18579107 REVERSE	1,18	1,16E-02	0,11	7,85E-01
(at3g48080): lipase class 3 family protein / disease resistance protein-related | chr3:17752938-17755190 REVERSE	1,17	4,55E-03	-1,06	7,89E-03
(at1g70830): Symbols: MLP28 | MLP28 (MLP-LIKE PROTEIN 28) | chr1:26709947-26711462 REVERSE	1,16	4,19E-04	0,31	2,04E-01
(at5g37600): Symbols: ATGSR1, GLN1;1, GSR 1 | ATGSR1; copper ion binding / glutamate-ammonia ligase | chr5:14933336-14935841 REVERSE	1,16	3,99E-03	0,18	5,75E-01
(at5g52760): heavy-metal-associated domain-containing protein | chr5:21386824-21387703 FORWARD	1,16	4,79E-03	-1,04	9,18E-03
(at5g55450): protease inhibitor/seed storage/lipid transfer protein (LTP) family protein | chr5:22467430-22468263 FORWARD	1,16	4,11E-02	0,16	7,58E-01
(at3g01830): calmodulin-related protein, putative | chr3:296054-297133 FORWARD	1,15	5,04E-02	-1,82	5,66E-03
(at4g05590): unknown protein | chr4:2907111-2908557 FORWARD	1,14	6,45E-04	-0,22	3,63E-01
(at5g65210): Symbols: TGA1 | TGA1; DNA binding / calmodulin binding / transcription factor | chr5:26058545-26061052 FORWARD	1,14	1,20E-05	-0,95	5,52E-05
(at1g03850): glutaredoxin family protein | chr1:976097-977761 REVERSE	1,12	4,19E-02	-1,52	1,03E-02
(at3g60520): unknown protein | chr3:22361530-22362579 REVERSE	1,12	1,65E-04	-0,40	6,57E-02
(at3g51440): strictosidine synthase family protein | chr3:19089081-19090639 FORWARD	1,12	3,04E-02	-1,44	9,09E-03
(at5g45000): transmembrane receptor | chr5:18165383-18167193 FORWARD	1,11	2,12E-02	-1,41	6,22E-03
(at3g56400): Symbols: WRKY70, ATWRKY70 | WRKY70; transcription factor/ transcription repressor | chr3:20908928-20910481 REVERSE	1,11	3,18E-02	-1,25	1,87E-02
(at5g60800): heavy-metal-associated domain-containing protein | chr5:24460887-24462536 REVERSE	1,11	2,15E-02	-1,40	6,46E-03
(at4g23810): Symbols: WRKY53, ATWRKY53 | WRKY53; DNA binding / protein binding / transcription activator/ transcription factor | chr4:12392370-12393982 REVERSE	1,11	2,12E-02	-0,97	3,81E-02
(at2g17040): Symbols: anac036 | anac036 (Arabidopsis NAC domain containing protein 36); transcription factor | chr2:7407123-7408270 FORWARD	1,11	2,38E-03	0,02	9,40E-01

(at1g01560): Symbols: ATMPK11 | ATMPK11; MAP kinase/ kinase | chr1:202136-204189 FORWARD	1,11	3,30E-02	-1,71	3,38E-03
(at3g21520): unknown protein | chr3:7581959-7582793 FORWARD	1,09	3,17E-02	-2,00	1,05E-03
(at2g45600): hydrolase | chr2:18789588-18790952 FORWARD	1,09	1,17E-03	0,78	9,44E-03
(at4g11890): protein kinase family protein | chr4:7148246-7149921 FORWARD	1,09	8,13E-03	-0,65	7,79E-02
(at4g18970): GDSL-motif lipase/hydrolase family protein | chr4:10389111-10390917 REVERSE	1,08	8,63E-03	2,20	6,03E-05
(at4g28390): Symbols: AAC3, ATAAC3 | AAC3 (ADP/ATP CARRIER 3); ATP:ADP antiporter/ binding | chr4:14041288-14043278 REVERSE	1,08	6,57E-03	-0,17	5,95E-01
(at3g09270): Symbols: ATGSTU8 | ATGSTU8 (GLUTATHIONE S-TRANSFERASE TAU 8); glutathione transferase | chr3:2848289-2849289 REVERSE	1,08	2,73E-02	-0,75	1,01E-01
(at5g42830): transferase family protein | chr5:17176384-17178018 FORWARD	1,08	5,59E-03	-0,39	2,33E-01
MULTIPLE HITS: (at1g14870,at1g14880). at1g14870: FUNCTIONS IN: molecular_function unknown; INVOLVED IN: response to oxidative stress; LOCATED IN: plasma membrane; EXPRESSED IN: callus; CONTAINS InterPro DOMAIN/s: EGF-type aspartate/asparagine hydroxylation conserved site (InterPro:IPR000152), Protein of unknown function Cys-rich (InterPro:IPR006461); BEST Arabidopsis thaliana protein match is: unknown protein (TAIR:AT5G35525.1); Has 492 Blast hits to 491 proteins in 78 species: Archae - 0; Bacteria - 0; Metazoa - 93; Fungi - 76; Plants - 297; Viruses - 0; Other Eukaryotes - 26 (source: NCBI BLink). | chr1:5128375-5129523 REVERSE at1g14880: unknown protein | chr1:5132535-5133716 REVERSE	1,08	9,05E-03	-0,59	1,06E-01
(at5g60900): Symbols: RLK1 | RLK1 (RECEPTOR-LIKE PROTEIN KINASE 1); ATP binding / carbohydrate binding / kinase/ protein kinase/ protein serine/threonine kinase/ protein tyrosine kinase/ sugar binding | chr5:24498467-24501494 REVERSE	1,07	3,05E-02	-0,90	6,05E-02
(at5g46240): Symbols: KAT1 | KAT1 (POTASSIUM CHANNEL IN ARABIDOPSIS THALIANA 1); cyclic nucleotide binding / inward rectifier potassium channel | chr5:18743566-18746730 REVERSE	1,07	3,65E-02	-1,53	6,26E-03
(at5g52740): heavy-metal-associated domain-containing protein | chr5:21382530-21383180 FORWARD	1,07	9,71E-05	0,32	9,22E-02
(at5g09220): Symbols: AAP2 | AAP2 (AMINO ACID PERMEASE 2); amino acid transmembrane transporter | chr5:2866252-2869054 FORWARD	1,06	8,08E-03	0,41	2,28E-01
(at5g07690): Symbols: MYB29, ATMYB29, PMG2 | ATMYB29 (ARABIDOPSIS THALIANA MYB DOMAIN PROTEIN 29); DNA binding / transcription factor | chr5:2446764-2448543 FORWARD	1,06	2,83E-02	1,10	2,42E-02
MULTIPLE HITS: (at2g33060,at2g33050). at2g33060: Symbols: AtRLP27 | AtRLP27 (Receptor Like Protein 27);	1,06	9,36E-03	1,68	4,73E-04

kinase/ protein binding | chr2:14025483-14028196 FORWARD at2g33050: Symbols: AtRLP26 | AtRLP26 (Receptor Like Protein 26); kinase/ protein binding | chr2:14021870-14024398 FORWARD				
(at1g67810): Symbols: SUFE2 | SUFE2 (SULFUR E 2); enzyme activator | chr1:25426488-25427349 FORWARD	1,06	9,78E-02	-1,51	2,57E-02
(at1g78970): Symbols: LUP1, ATLUP1 | LUP1 (LUPEOL SYNTHASE 1); beta-amyrin synthase/ lupeol synthase | chr1:29703340-29707844 FORWARD	1,05	2,67E-04	0,80	1,85E-03
(at4g37640): Symbols: ACA2 | ACA2 (CALCIUM ATPASE 2); calcium ion transmembrane transporter/ calcium-transporting ATPase/ calmodulin binding | chr4:17682977-17686941 REVERSE	1,04	1,53E-03	-0,50	6,72E-02
(at3g51330): aspartyl protease family protein | chr3:19053368-19056224 REVERSE	1,04	6,01E-03	-0,26	4,09E-01
MULTIPLE HITS: (at5g64550,at5g64552). at5g64550: loricrin-related | chr5:25801528-25804980 REVERSE at5g64552: Symbols: CPuORF22 | CPuORF22 (Conserved peptide upstream open reading frame 22) | chr5:25801528-25804980 REVERSE	1,04	1,82E-04	0,35	7,83E-02
(at5g22740): Symbols: ATCSLA02, CSLA02, ATCSLA2 | ATCSLA02; mannan synthase/ transferase, transferring glycosyl groups | chr5:7554928-7560073 REVERSE	1,04	9,95E-05	0,08	6,50E-01
(at4g27300): S-locus protein kinase, putative | chr4:13669308-13672348 REVERSE	1,04	7,52E-03	0,88	1,73E-02
(at5g50200): Symbols: WR3 | WR3 (WOUND-RESPONSIVE 3); nitrate transmembrane transporter | chr5:20436180-20437726 FORWARD	1,04	2,74E-02	-0,12	7,62E-01
(at5g60280): lectin protein kinase family protein | chr5:24260563-24262536 FORWARD	1,03	4,14E-02	-1,34	1,27E-02
(at1g61260): unknown protein | chr1:22593465-22595069 REVERSE	1,03	8,87E-02	0,57	3,25E-01
(at5g64780): FUNCTIONS IN: molecular_function unknown; INVOLVED IN: biological_process unknown; LOCATED IN: cellular_component unknown; EXPRESSED IN: 21 plant structures; EXPRESSED DURING: 15 growth stages; CONTAINS InterPro DOMAIN/s: Uncharacterised conserved protein UCP009193 (InterPro:IPR016549); BEST Arabidopsis thaliana protein match is: unknown protein (TAIR:AT4G09830.1); Has 56 Blast hits to 56 proteins in 10 species: Archae - 0; Bacteria - 0; Metazoa - 0; Fungi - 0; Plants - 56; Viruses - 0; Other Eukaryotes - 0 (source: NCBI BLink). | chr5:25900559-25902127 REVERSE	1,03	1,41E-03	-0,18	4,57E-01
(at3g07520): Symbols: ATGLR1.4, GLR1.4 | GLR1.4 (GLUTAMATE RECEPTOR 1.4); cation channel/ intracellular ligand-gated ion channel | chr3:2394891-2398291 REVERSE	1,03	4,79E-02	0,92	7,03E-02
(at3g26230): Symbols: CYP71B24 | CYP71B24; electron carrier/ heme binding / iron ion binding / monooxygenase/ oxygen binding | chr3:9598005-9599959 REVERSE	1,03	3,36E-04	0,70	4,45E-03

(at4g20110): vacuolar sorting receptor, putative | chr4:10875289-10878730 FORWARD	1,02	2,91E-02	-1,62	2,42E-03
(at5g17760): AAA-type ATPase family protein | chr5:5860421-5862422 REVERSE	1,02	2,73E-02	-0,87	5,19E-02
(at3g25020): Symbols: AtRLP42 | AtRLP42 (Receptor Like Protein 42); protein binding | chr3:9116868-9119540 REVERSE	1,01	1,14E-03	0,14	5,53E-01
(at3g28540): AAA-type ATPase family protein | chr3:10694444-10696123 FORWARD	1,01	1,84E-02	-0,39	3,02E-01
(at2g24160): pseudogene, leucine rich repeat protein family, contains leucine rich-repeat domains Pfam:PF00560, INTERPRO:IPR001611; contains some similarity to Cf-4 (Lycopersicon hirsutum) gi|2808683|emb|CAA05268; blastp match of 37% identity and 8.4e-98 P-value to GP|2808683|emb|CAA05268.1||AJ002235 Cf-4 {Lycopersicon hirsutum} | chr2:10268008-10270612 REVERSE	1,01	2,42E-02	-0,80	6,39E-02
(at5g45650): subtilase family protein | chr5:18513431-18518868 REVERSE	1,01	3,61E-02	2,57	1,07E-04

S22: Genes stronger expressed in the *tga14* mutant after 24 h of mock treatment

Genes stronger expressed in the *tga14* mutant in mock treated samples were identified by microarray analysis. Deregulated genes exhibits minimum 2 fold change and a P value < 0.05. The influence of *Pst avrRPS4* to expression in Col-0 at 24 hpi is displayed in direct comparison. Values represent log2.

Description	24 h Mock Col-0 vs. *tga14*	P Value	24 hpiCol-0	P Value
(at4g30290): Symbols: ATXTH19, XTH19 | XTH19 (XYLOGLUCAN ENDOTRANSGLUCOSYLASE/HYDROLASE 19); hydrolase, acting on glycosyl bonds / hydrolase, hydrolyzing O-glycosyl compounds / xyloglucan:xyloglucosyl transferase | chr4:14828712-14830016 REVERSE	-3,18	4,43E-04	1,34	5,60E-02
(at4g21680): proton-dependent oligopeptide transport (POT) family protein | chr4:11517353-11519765 REVERSE	-2,89	1,65E-03	-4,29	8,59E-05
(at3g47340): Symbols: ASN1, DIN6, AT-ASN1 | ASN1 (GLUTAMINE-DEPENDENT ASPARAGINE SYNTHASE 1); asparagine synthase (glutamine-hydrolyzing) | chr3:17437884-17441243 REVERSE	-2,70	2,82E-03	-5,12	2,23E-05
(at4g15680): glutaredoxin family protein | chr4:8931652-8932295 FORWARD	-2,69	1,62E-07	0,64	1,22E-02
(at5g59310): Symbols: LTP4 | LTP4 (LIPID TRANSFER PROTEIN 4); lipid binding | chr5:23925085-23925852	-2,63	9,38E-03	-0,81	3,50E-01

REVERSE				
(at5g59320): Symbols: LTP3 | LTP3 (LIPID TRANSFER PROTEIN 3); lipid binding | chr5:23928971-23929745 FORWARD	-2,46	6,79E-03	-0,44	5,53E-01
(at1g53160): Symbols: SPL4 | SPL4 (SQUAMOSA PROMOTER BINDING PROTEIN-LIKE 4); DNA binding / transcription factor | chr1:19806419-19807608 FORWARD	-2,33	6,40E-05	0,97	2,15E-02
(at4g15690): glutaredoxin family protein | chr4:8934324-8934921 FORWARD	-2,22	1,99E-05	0,46	1,47E-01
(at5g13220): Symbols: JAZ10, TIFY9, JAS1 | JAZ10 (JASMONATE-ZIM-DOMAIN PROTEIN 10) | chr5:4218888-4220814 FORWARD	-2,21	1,05E-02	-5,46	1,56E-05
(at4g15700): glutaredoxin family protein | chr4:8937393-8937892 FORWARD	-2,13	2,10E-04	-0,95	2,97E-02
(at5g67480): Symbols: BT4 | BT4 (BTB AND TAZ DOMAIN PROTEIN 4); protein binding / transcription regulator | chr5:26930940-26932756 REVERSE	-2,07	6,04E-02	-2,29	4,13E-02
(at2g38530): Symbols: LTP2, LP2 | LTP2 (LIPID TRANSFER PROTEIN 2); lipid binding | chr2:16128378-16129158 FORWARD	-2,06	2,25E-03	1,26	3,21E-02
(at3g30775): Symbols: ERD5, PRODH, AT-POX, ATPOX, ATPDH, PRO1 | ERD5 (EARLY RESPONSIVE TO DEHYDRATION 5); proline dehydrogenase | chr3:12448636-12451248 REVERSE	-2,05	2,76E-02	-1,43	1,04E-01
(at1g03020): glutaredoxin family protein | chr1:698207-698515 REVERSE	-1,99	2,19E-05	0,00	9,89E-01
(at4g35770): Symbols: SEN1, ATSEN1, DIN1 | SEN1 (SENESCENCE 1) | chr4:16944941-16946192 FORWARD	-1,98	5,23E-04	-1,54	2,95E-03
(at3g15950): Symbols: NAI2 | NAI2 | chr3:5397569-5402652 REVERSE	-1,96	4,84E-06	-0,82	3,95E-03
(at4g15210): Symbols: ATBETA-AMY, AT-BETA-AMY, RAM1, BMY1, BAM5 | BAM5 (BETA-AMYLASE 5); beta-amylase | chr4:8666338-8669470 REVERSE	-1,89	1,20E-04	-3,43	6,54E-07
MULTIPLE HITS: (at5g24770,at5g24780). at5g24770: Symbols: VSP2, ATVSP2 | VSP2 (VEGETATIVE STORAGE PROTEIN 2); acid phosphatase | chr5:8500476-8502224 REVERSE at5g24780: Symbols: VSP1, ATVSP1 | VSP1 (VEGETATIVE STORAGE PROTEIN 1); acid phosphatase/ transcription factor binding | chr5:8507590-8508957 REVERSE	-1,73	1,25E-01	-5,45	3,75E-04
MULTIPLE HITS: (at3g28290,at3g28300). at3g28290: Symbols: AT14A | AT14A | chr3:10547504-10549367 FORWARD at3g28300: Symbols: AT14A | AT14A | chr3:10565737-10567600 FORWARD	-1,72	8,72E-05	-3,15	4,17E-07
(at4g15660): glutaredoxin family protein | chr4:8925806-8926310 FORWARD	-1,65	4,38E-07	-0,60	1,88E-03
(at2g34600): Symbols: JAZ7, TIFY5B | JAZ7 (JASMONATE-ZIM-DOMAIN PROTEIN 7) | chr2:14573080-14573856 FORWARD	-1,64	3,24E-02	-3,65	2,53E-04
(at4g18170): Symbols: WRKY28, ATWRKY28 | WRKY28;	-1,64	6,70E-03	-3,66	1,84E-05

transcription factor | chr4:10061373-10062841 FORWARD				
(at3g57520): Symbols: AtSIP2 | AtSIP2 (Arabidopsis thaliana seed imbibition 2); hydrolase, hydrolyzing O-glycosyl compounds | chr3:21288765-21293158 REVERSE	-1,61	1,95E-05	-2,35	6,49E-07
(at5g41080): glycerophosphoryl diester phosphodiesterase family protein | chr5:16441744-16443985 FORWARD	-1,61	1,10E-04	-1,79	4,49E-05
(at3g62930): glutaredoxin family protein | chr3:23261442-23261927 REVERSE	-1,61	8,30E-08	0,75	7,91E-05
(at4g12470): protease inhibitor/seed storage/lipid transfer protein (LTP) family protein | chr4:7401109-7401907 REVERSE	-1,61	2,84E-02	0,71	2,84E-01
(at2g02990): Symbols: RNS1, ATRNS1 | RNS1 (RIBONUCLEASE 1); endoribonuclease/ ribonuclease | chr2:873506-874811 FORWARD	-1,59	2,83E-02	-0,32	6,22E-01
(at4g22470): protease inhibitor/seed storage/lipid transfer protein (LTP) family protein | chr4:11840134-11841450 REVERSE	-1,58	3,63E-03	-1,18	1,83E-02
(at1g76650): Symbols: CML38 | calcium-binding EF hand family protein | chr1:28766750-28767517 REVERSE	-1,56	4,86E-02	-3,75	3,09E-04
(at3g15720): glycoside hydrolase family 28 protein / polygalacturonase (pectinase) family protein | chr3:5325290-5327537 REVERSE	-1,56	6,12E-04	0,63	7,65E-02
(at2g39030): GCN5-related N-acetyltransferase (GNAT) family protein | chr2:16298227-16299202 FORWARD	-1,53	4,49E-02	-4,24	8,55E-05
(at5g14180): Symbols: MPL1 | MPL1 (MYZUS PERSICAE-INDUCED LIPASE 1); catalytic | chr5:4571337-4574462 REVERSE	-1,51	7,12E-02	-2,16	1,64E-02
(at4g23600): Symbols: CORI3, JR2 | CORI3 (CORONATINE INDUCED 1); cystathionine beta-lyase/ transaminase | chr4:12310619-12313212 FORWARD	-1,47	7,08E-03	-3,09	3,37E-05
(at4g04330): unknown protein | chr4:2116553-2118597 REVERSE	-1,46	1,16E-03	0,73	4,81E-02
(at5g47330): palmitoyl protein thioesterase family protein | chr5:19207099-19208822 FORWARD	-1,45	2,77E-02	0,59	3,16E-01
MULTIPLE HITS: (at1g52040,at1g52030). at1g52040: Symbols: MBP1, ATMBP | MBP1 (MYROSINASE-BINDING PROTEIN 1); protein binding | chr1:19350375-19352782 REVERSE at1g52030: Symbols: MBP2, MBP1.2, F-ATMBP | MBP2 (MYROSINASE-BINDING PROTEIN 2); sugar binding / thioglucosidase binding | chr1:19345940-19348668 REVERSE	-1,45	6,36E-03	-3,20	1,92E-05
(at1g58270): Symbols: ZW9 | ZW9 | chr1:21612116-21614117 REVERSE	-1,44	2,28E-02	-2,57	7,48E-04
(at5g05600): oxidoreductase, 2OG-Fe(II) oxygenase family protein | chr5:1672120-1674739 FORWARD	-1,43	1,23E-02	-3,69	1,42E-05
(at3g14940): Symbols: ATPPC3 | ATPPC3 (PHOSPHOENOLPYRUVATE CARBOXYLASE 3); phosphoenolpyruvate carboxylase | chr3:5025238-5029710 FORWARD	-1,43	7,57E-06	1,07	8,80E-05

(at2g34930): disease resistance family protein | chr2:14737066-14739904 REVERSE	-1,35	2,34E-02	-0,45	3,95E-01
(at2g30600): BTB/POZ domain-containing protein | chr2:13037052-13041684 FORWARD	-1,32	4,25E-02	-0,54	3,61E-01
MULTIPLE HITS: (at3g16430,at3g16420). at3g16430: Symbols: JAL31 | JAL31 (JACALIN-RELATED LECTIN 31); copper ion binding | chr3:5581663-5583187 FORWARD at3g16420: Symbols: PBP1, JAL30 | PBP1 (PYK10-BINDING PROTEIN 1); copper ion binding | chr3:5579386-5580953 FORWARD	-1,30	1,07E-02	-0,78	8,94E-02
MULTIPLE HITS: (at5g49450,at5g49448). at5g49450: Symbols: AtbZIP1 | AtbZIP1 (Arabidopsis thaliana basic leucine-zipper 1); DNA binding / protein heterodimerization/ transcription factor | chr5:20051829-20052735 FORWARD at5g49448: Symbols: CPuORF4 | CPuORF4 (Conserved peptide upstream open reading frame 4) | chr5:20051829-20052735 FORWARD	-1,29	1,82E-02	-3,49	1,75E-05
(at2g27500): glycosyl hydrolase family 17 protein | chr2:11752170-11754028 REVERSE	-1,27	2,23E-02	-2,34	5,50E-04
(at1g44350): Symbols: ILL6 | ILL6; IAA-amino acid conjugate hydrolase/ metallopeptidase | chr1:16834210-16838286 REVERSE	-1,26	2,64E-02	-3,18	6,27E-05
(at5g08350): GRAM domain-containing protein / ABA-responsive protein-related | chr5:2686245-2687251 REVERSE	-1,25	2,89E-04	-0,41	1,04E-01
(at3g06500): beta-fructofuranosidase, putative / invertase, putative / saccharase, putative / beta-fructosidase, putative | chr3:2012079-2015705 FORWARD	-1,24	3,43E-02	-3,57	3,53E-05
(at5g56750): Ndr family protein | chr5:22957877-22960916 FORWARD	-1,23	2,11E-02	-2,73	1,24E-04
(at1g63180): Symbols: UGE3 | UGE3 (UDP-D-glucose/UDP-D-galactose 4-epimerase 3); UDP-glucose 4-epimerase/ protein dimerization | chr1:23427409-23429603 REVERSE	-1,20	2,30E-02	-2,79	1,01E-04
(at2g19800): Symbols: MIOX2 | MIOX2 (MYO-INOSITOL OXYGENASE 2); inositol oxygenase | chr2:8530896-8533508 REVERSE	-1,18	3,31E-02	-0,48	3,36E-01
(at2g37760): aldo/keto reductase family protein | chr2:15831854-15833920 FORWARD	-1,17	1,12E-02	-2,70	3,01E-05
(at1g19180): Symbols: JAZ1, TIFY10A | JAZ1 (JASMONATE-ZIM-DOMAIN PROTEIN 1); protein binding | chr1:6622094-6623620 FORWARD	-1,15	1,44E-02	-3,33	6,50E-06
(at1g62480): vacuolar calcium-binding protein-related | chr1:23128705-23129759 FORWARD	-1,14	3,62E-02	0,26	5,87E-01
(at2g02710): Symbols: PLP, PLPB | PLPB (PAS/LOV PROTEIN B); signal transducer/ two-component sensor | chr2:758693-760871 REVERSE	-1,14	1,20E-02	-2,59	3,83E-05
(at5g09440): Symbols: EXL4 | EXL4 (EXORDIUM LIKE 4) | chr5:2938347-2939461 FORWARD	-1,13	3,04E-02	-1,86	2,05E-03
MULTIPLE HITS: (at5g01050,at5g01040). at5g01050:	-1,11	4,64E-02	0,36	4,81E-01

laccase family protein / diphenol oxidase family protein | chr5:18086-20812 REVERSE at5g01040: Symbols: LAC8 | LAC8 (laccase 8); laccase | chr5:13128-16173 REVERSE				
MULTIPLE HITS: (at3g25760,at3g25770). at3g25760: Symbols: AOC1, ERD12 | AOC1 (ALLENE OXIDE CYCLASE 1); allene-oxide cyclase | chr3:9403883-9405250 FORWARD at3g25770: Symbols: AOC2 | AOC2 (ALLENE OXIDE CYCLASE 2); allene-oxide cyclase | chr3:9406873-9407955 FORWARD	-1,09	1,40E-03	-2,18	5,61E-06
(at1g01770): unknown protein | chr1:278615-282891 FORWARD	-1,09	2,00E-03	-1,93	2,53E-05
(at2g30040): Symbols: MAPKKK14 | MAPKKK14; ATP binding / kinase/ protein kinase/ protein serine/threonine kinase | chr2:12821710-12823169 FORWARD	-1,09	5,47E-02	-2,02	2,39E-03
(at4g33420): peroxidase, putative | chr4:16084828-16086296 FORWARD	-1,09	2,32E-02	-0,47	2,73E-01
(at2g43620): chitinase, putative | chr2:18093770-18095025 REVERSE	-1,08	2,89E-02	0,46	2,99E-01
(at2g21140): Symbols: ATPRP2 | ATPRP2 (PROLINE-RICH PROTEIN 2) | chr2:9060625-9062091 REVERSE	-1,08	1,20E-02	1,02	1,63E-02
(at1g17380): Symbols: JAZ5, TIFY11A | JAZ5 (JASMONATE-ZIM-DOMAIN PROTEIN 5) | chr1:5955488-5957212 REVERSE	-1,08	7,97E-02	-3,73	5,19E-05
(at3g20470): Symbols: GRP-5, ATGRP-5, GRP5, ATGRP5 | GRP5 (GLYCINE-RICH PROTEIN 5); structural constituent of cell wall | chr3:7140440-7141228 REVERSE	-1,07	3,53E-02	1,61	4,40E-03
(at1g56300): DNAJ heat shock N-terminal domain-containing protein | chr1:21078820-21080423 REVERSE	-1,07	2,97E-02	-3,51	8,68E-06
(at4g12480): Symbols: pEARLI 1 | pEARLI 1; lipid binding | chr4:7406105-7406937 REVERSE	-1,06	4,01E-02	1,22	2,22E-02
(at5g39580): peroxidase, putative | chr5:15847081-15849108 REVERSE	-1,06	3,21E-03	-1,29	8,60E-04
(at2g37130): peroxidase 21 (PER21) (P21) (PRXR5) | chr2:15597921-15600077 REVERSE	-1,06	9,09E-03	-1,71	3,99E-04
(at5g24160): Symbols: SQE6 | SQE6 (SQUALENE MONOXYGENASE 6); FAD binding / oxidoreductase/ squalene monooxygenase | chr5:8183075-8186640 REVERSE	-1,06	1,95E-02	-1,78	8,68E-04
(at5g43745): phosphotransferase-related | chr5:17569147-17574971 REVERSE	-1,05	5,15E-03	-1,54	3,73E-04
(at2g43820): Symbols: GT, UGT74F2 | UGT74F2 (UDP-GLUCOSYLTRANSFERASE 74F2); UDP-glucose:4-aminobenzoate acylglucosyltransferase/ UDP-glucosyltransferase/ UDP-glycosyltransferase/ transferase, transferring glycosyl groups / transferase, transferring hexosyl groups | chr2:18152227-18153908 FORWARD	-1,05	5,63E-03	-2,17	2,71E-05
(at4g19390): FUNCTIONS IN: molecular_function unknown; INVOLVED IN: biological_process unknown; LOCATED IN: chloroplast; EXPRESSED IN: 23 plant structures; EXPRESSED DURING: 13 growth stages;	-1,04	1,73E-02	-1,44	2,67E-03

CONTAINS InterPro DOMAIN/s: Uncharacterised conserved protein UCP022348 (InterPro:IPR016804), Uncharacterised protein family UPF0114 (InterPro:IPR005134); BEST Arabidopsis thaliana protein match is: unknown protein (TAIR:AT5G13720.1); Has 553 Blast hits to 553 proteins in 219 species: Archae - 18; Bacteria - 407; Metazoa - 0; Fungi - 0; Plants - 54; Viruses - 0; Other Eukaryotes - 74 (source: NCBI BLink). | chr4:10574768-10576428 REVERSE				
MULTIPLE HITS: (at1g36280,at4g18440). at1g36280: adenylosuccinate lyase, putative / adenylosuccinase, putative | chr1:13640508-13643017 FORWARD at4g18440: adenylosuccinate lyase, putative / adenylosuccinase, putative | chr4:10186131-10188909 REVERSE	-1,03	4,94E-03	-3,10	7,59E-07
(at2g43520): Symbols: ATTI2 | ATTI2; serine-type endopeptidase inhibitor | chr2:18068425-18069168 FORWARD	-1,01	1,18E-02	-1,31	2,56E-03
(at5g07440): Symbols: GDH2 | GDH2 (GLUTAMATE DEHYDROGENASE 2); ATP binding / glutamate dehydrogenase [NAD(P)+]/ glutamate dehydrogenase/ oxidoreductase | chr5:2355937-2358194 FORWARD	-1,00	6,09E-02	-3,05	7,81E-05

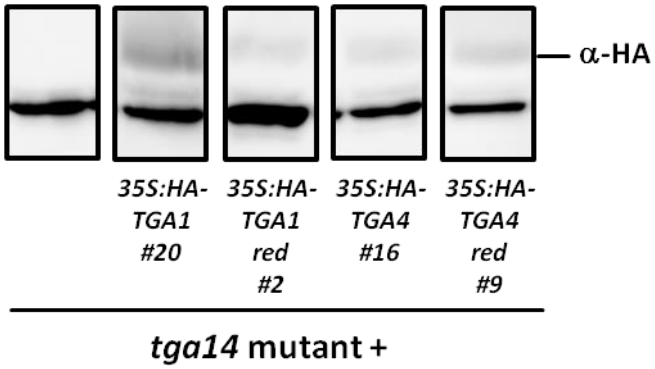

S23: Detection of clade I TGA TFs proteins ectopically expressed in the *tga14* mutant

T2 plants of the *tga14* mutant that was transformed with *35S:3xHA-TGA1*, *35S:3xHA-TGA1red*, *35S:3xHA-TGA4* or *35S:3xHA-TGA4red* were grown under LD conditions for 3 weeks. Whole proteins were extracted, separated by SDS-PAGE and the signal of the TGA TFs was detected by western blot analysis (α-HA).

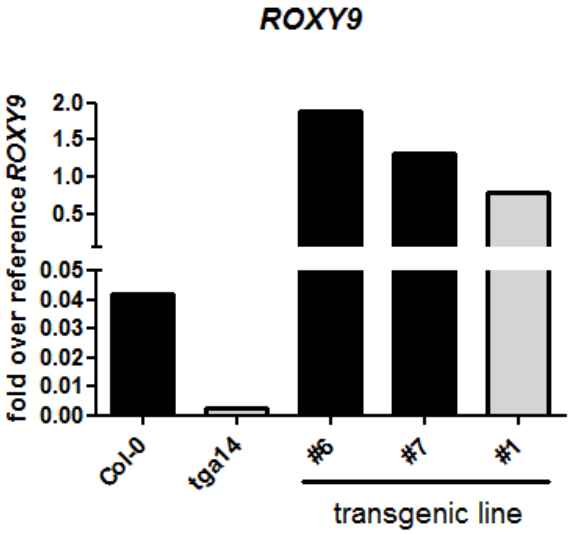

S24: Expression of *ROXY9* in transgenic plants expressing *HA-ROXY9* ectopically

ROXY9 transcript levels of wildtype Col-0, Col-0 + *35S:3xHA-ROXY9* (T1), *tga14* mutant and *tga14* + *35S:3xHA-ROXY9* (T1) plants were compared by qRT-PCR and normalized to UBQ5 expression.

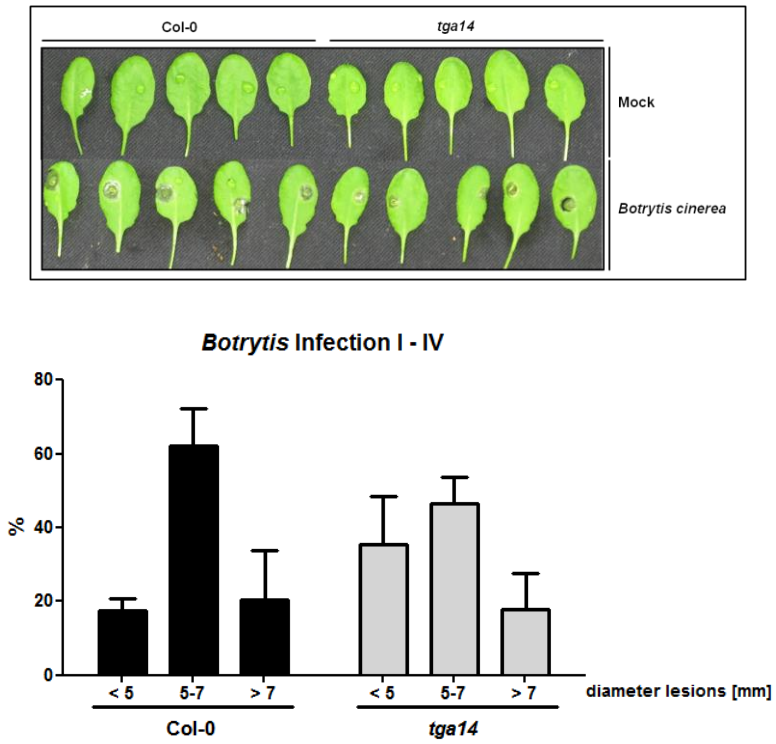

Fig. S25: Comparison of wildtype Col-0 and *tga14* mutant after infection with *B. cinerea*

Plants were grown on soil for 4 weeks under 12h/ 12h light cycle conditions. 5 leaves per plant were drop inoculated with 4 µl of *B. cinerea* spore solution (5 x 10^4 spores/ ml) or ¼ PDB media as mock control. (A) Representative pictures of wildtype Col-0 and *tga14* mutant 2 dpi with *B. cinerea*. (B) Lesion size of Col-0 wildtype and *tga14* mutant 2dpi with *B. cinerea*. At least 80 lesions per experiment were measured and grouped according to their size into the classes < 5 mm, 5-7 mm and > 7 mm. The average ± SEM represents 4 independent experiments

	conserved C-Terminus	*roxy1* mutant flowers	*ORA59* promoter activity	*B. cinerea* after over-expression	growth after over-expression
ROXY1	VMASHINGSLVPLLKDAGALWL	yes	yes	yes	yes
ROXY19	VMATHISGELVPILKEVGALWL	yes	yes	yes	no
ROXY9	VMSLHLSGSLVPLIKPYQSILY	no	no	?	yes

Fig. S26: Comparison of redundant ROXY functions

The conserved motifs in the C-Terminus are indicated in slight blue (Interaction-motif) and red (ALWL-motif). The observed functions are the complementation of affected *roxy1* flowers (Li et al., 2011), the potential to suppress *ORA59* promoter activity in transient assays (Zander et al., 2012), mediating enhanced susceptibility against *B. cinerea* after over-expression (Wang et al., 2009; Zander & Muthreich, unpublished) and mediating reduced plant growth after over-expression (Wang et al., 2009; this thesis).

7 Bibliography

Ahuja I, Kissen R and Bones AM. 2012. Phytoalexins in defense against pathogens. *Trends in Plant Science* 17(2), 73-90.

An F, Zhao Q, Ji Y, Li W, Jiang Z, Yu X, Zhang C, Han Y, He W, Liu Y, Zhang S, Ecker JR and Guo H. 2010. Ethylene-induced stabilization of ETHYLENE INSENSITIVE3 and EIN3-LIKE1 is mediated by proteasomal degradation of EIN3 binding F-box 1 and 2 that requires EIN2 in Arabidopsis. *Plant Cell* 22 (7), 2384-2401.

Aarts N, Mettz M, Holub E, Staskawicz BJ, Daniles MJ and Parker JE. 1998. Different requirements for *EDS1* and *NDR1* by disease resistance genes define at least two *R* gene-mediated signaling pathways in Arabidopsis. *Proc. Natl. Acad. Sci. USA* 95, 10306-10311.

Asai T., Tena G., Plotnikova J., Willmann MR., Chiu W., Gomez-Gomez L., Boller T., Ausubel FM. And Sheen J. 2002. MAP kinase signalling cascade in Arabidopsis innate immunity. *Nature* 415, 977-983.

Attaran E., Zeier TE., Griebel T. and Zeier J. 2009. Methyl salicylate production and jasmonate signaling are not essential for systemic acquired resistance in Arabidopsis. *Plant Cell* 21 (3), 954-971.

Axtel MJ. and Staskawicz BJ. 2003. Initiation of RPS2-specified disease resistance in Arabidopsis is coupled to the AvrRpt2-directed elimination of RIN4. *Cell* 112, 369-377.

Bartsch M, Gobbato E, Bednarek P, Debey S, Schultze JL, Bautor J and Parker JE. 2006. Salicylic Acid-Independent ENHANCED DISEASE SUSCEPTIBILITY1 Siganling in *Arabidopsis* Immunity and Cell Death Is Regulated by the Monooxygenase *FMO1* and the Nudix Hydrolase *NUDT7*. *Plant Cell* 18(4), 1038-1051.

Battepati Uma, T. Swaroopa Rani, Appa Rao Podile 2011. Warriors at the gate never sleep: Non-host resistance in plants. *Plant Physiology* 168, Issue 18, 2141-2152.

Bhattacharjee S, Halane MK, Kim SH and Gassmann W. 2011. Pathogen effectors target Arabidopsis EDS1 and alter its interactions with immune regulators. *Science* 334 (6061), 1405-1408.

Berrocal-Lobo M, Molina A and Solano R. 2002. Constitutive expressionof ETHYLENE-RESPONSE-FACTOR1 in Arabidopsis confers resistance to several necrotrophic fungi. *Plant Journal* 29 (1), 23-32.

Boch J, Verbsky ML, Robertson TL, Larkin JC and Kunkel BN. 1998. Analysis of resistance gene-mediated defense responses in Arabidopsis thaliana plants carrying a mutation in CPR5. *Molecular Plant-Microbe Interactions* 11 (12), 1196-1206.

Bowling SA, Clarke JD, Liu Y, Klessig DF and Dong X. 1997. The cpr5 mutant of Arabidopsis expresses both NPR1-dependent and NPR1-independent resistance. *Plant Cell* 9 (9), 1573-1584.

Boyle M, Le Su E, Rochon A, Shearer HL, Murmu J, Chu JY, Fobert PR and Despres C. 2009. The BTB/POZ domain of the Arabidopsis disease resistance protein NPR1 interacts with the repression domain of TGA2 to negate its function. *Plant Cell* 21 (11), 3700-13.

Cao H, Bowling SA, Gordon AS and Dong X. 1994. Characterization of an Arabidopsis Mutant That Is Nonresponsive to Inducers of Systemic Acquired Resistance. *Plant Cell* 6 (11), 1583-1592.

Cao H, Glazebrook J, Clarke JD, Volko S and Dong X. 1997. The Arabidopsis NPR1 gene that controls systemic acquired resistance encodes a novel protein containing ankyrin repeats. *Cell* 88 (1), 57-63.

Chae K, Gonong BJ, Kim S-C, Kieslich CA, Morikis D, Balasubramanian S and Lord E. 2010. A multifaceted study of stigma/style cysteine-rich adhesin (SCA)-like *Arabidopsis* lipid transfer proteins (LTPs) suggests diversified roles for these LTPs in plant growth and reproduction. *Journal of Experimental Botany* 61(15), 4277-4290.

Chanda B., Xia Y., Mandal MK., Yu K and Sekine KZ. 2011. Glycerol-3-phosphate is a critical mobile inducer of systemic immunity in plants. *Nature Genetics* 43, 421-427.

Chang JH, Rathjen JP, Bemal AJ, Staskawicz BJ and Michelmore RW. 2000. *avrPto* enhances growth and necrosis caused by *Pseudomonas syringae pv. tomato* in tomato lines lacking either *Pto* or *Prf*. *Molecular Plant-Microbe Interactions* 13 (5), 568-571.

Chatterjee S., Chaudhury S., McShan AC., Kaur K. and De Guzman RN. 2013. Structure and Biophysics of Type III Secretion in Bacteria. *Biochemistry* 52 (15), 2508- 2517.

ChaturvediR., Venables B., Petros RA., Nalam V. and Li M. 2012. An abietane diterpenoid is a potent activator of systemic acquired resistance. *Plant Journal* 71, 161-172.

Che YZ, Li YR, Zou HS, Zou LF, Zhang B and Chen GY. 2011. A novel antimicrobial protein for plant protection consisting of a *Yanthomonas oryzae* harpin and active domains of cecropin A and melittin. *Microbial Biotechnology* 4(6), 777-793.

Chen Z, Zheng Z, Huang J, Lai Z and Fan B. 2009. Biosynthesis of salicylic acid in plants. *Plant Signaling & Behaviour* 4, 493-496.

Cheng YT, Germain H, Wiermer M, Bi D, Xu F, Garcia AV, wirthmueller L, Despres C, Parker JE, Zhang Y and Li X. Nuclear pore complex component MOS7/Nup88 is required for innate immunity and nuclear accumulation of defense regulators in Arabidopsis. *Plant Cell* 21 (8), 2503-2516.

Chini A, Fonseca S, Chico JM, Fernandez-Calvo P and Solano R. 2009. The ZIM domain mediates homo- and heteromeric interactions between Arabidopsis JAZ proteins. *Plant Journal* 59 (1), 77-87.

Chisholm ST, Coaker G, Day B and Staskawicz BJ. 2006. Host-microbe interactions: shaping the evolution of the plant immune responses. *Cell* 124, no. 4 (February 24): 803-814

Chomczynski P. 1993. A reagent for the single-step simultaneous isolation of RNA, DNA and proteins from cell and tissue samples. *Biotechniques* 15 (3): 532-4, 536-7.

Chuang CF, Running MP, Williams RW and Meyerowitz EM. 1999. The PERIANTHIA gene encodes a bZIP protein involved in the determination of floral organ number in Arabidopsis thaliana. *Genes & Development* 13 (3), 334-344.

Clough SJ. 2005. Floral dip: agrobacterium-mediated germ line transformation. *Methods in Molecular Biology (Clifton, N.J.)* 286: 91-102.

Conrath U. 2011. Molecular aspects of defence priming. *Trends in Plant Science* 16 (10), 524-531.

Coppinger P, Repetti PP, Day B, Dahlbeck D, Mehlert A and Staskawicz BJ. 2004. Overexpression of the plasma membrane-localized NDR1 protein results in enhanced bacterial disease resistance in Arabidopsis thaliana. *Plant Journal* 40 (2), 225-237.

Dangl JL. And Jones JL. 2001. Plant pathogens and integrated defense responses to infection. *Nature* 411, 826-833.

Day B, Dahlbeck D and Staskawicz BJ. 2006. NDR1 interaction with RIN4 mediates the differential activation of multiple disease resistance pathways in Arabidopsis. *Plant Cell* 18 (10), 2782-2791.

Dean JV, Mohammed LA and Fitzpatrick T. 2005. The formation, vacuolar localization, and tonoplast transport of salicylic acid glucose conjugates in tobacco cell suspension cultures. *Planta* 221, 287-296.

Dempsey DA. And Lessig DF. 2012. SOS – too many signals for systemic acquired resistance? *Trends in Plant Science* 17, 538-545.

Depres C, DeLong C, Glaze S, Liu E and Fobert PR. 2000. The Arabidopsis NPR1/NIM1 Protein Enhances the DNA Binding Activity of a Subgroup of the TGA Family of bZIP Transcription Factors. *Plant Cell* 12 (2), 279-290.

Deslandes L., Olivier J., Peeters N., Feng DX., Khounlotham M., Boucher C., Somssich I., Genin S. and marco Y. 2003. Physical interaction between RRs1-R, a protein conferring resistance to bacterial wilt, and PopP2, a type III effector targeted to the plant nucleus. *Proc Natl Acad Sci USA* 100, 8024-8029.

De Torres M, Sanchez P, Fernandez-Delmond I and Grant M. 2003. Expression profiling of the host response to bacterial infection: The transition from basal to induced defense responses in *RPM1*-mediated resistance. *Plant Journal* 33(4), 665-676.

Dodds PN., Lawrence GJ., Catanzariti AM., The T., Wang CI., Ayliffe MA., Kobe B. and Ellis JG. 2006. Direct protein interaction underlies gene-for-gene specificity and coevolution of the flax resistance genes and flax rust avirulence genes. *Proc Natl Acad Sci USA* 103, 8888-8893.

Douliez JP, Michon T, Elmorjani K and Marion D. 2000. Structure, biological and technological functions of lipid transfere proteins and indulines, the major lipid binding proteins from cereal kernels. *Journal of Cereal Science* 32, 1-20

Durrant WE. And Dong X. 2004. Systemic acquired resistance. *Annual Review of Phytopathology* 42, 185-209.

Elmore JM, Lin ZJ and Coaker G. 2011. Plant NB-LRR signaling: upstreams and downstreams. *Current Opinion in Plat Biology* 14 (4), 365-371.

Fan W and Dong X. 2002. In vivo interaction between NPR1 and transcription factor TGAs leads to salicylic acid-mediated gene activation in Arabidopsis. *Plant Cell* 14 (6), 1377-1389.

Felix G., Duran JD., Volko S. and Boller T. 1999. Plants have a sensitive perception system for the most conserved domain of bacterial flagellin. *Plant Journal* 18, 265-276.

Feys BJ, Moisan LJ, Newman MA and Parker JE. 2001. Direct interaction between the Arabidopsis disease resistance signaling proteins, EDS1 and PAD4. *The EMBO Journal* 20 (19), 5400-5411.

Flor HH. 1971. Current status of the gene-for-gene concept. *Annual Review of Phytopathology* 9, 275-296.

Fode B, Siemsen T, Thurow C, Weigel R and Gatz C. 2008. The *Arabidopsis* GRAS Protein SCL14 Interacts with Class II TGA Transcription Factors and Is Essential for the Activation of Stress-Inducible Promoters. *Plant Cell* 20 (11), 3122-3135.

Fonseca S, Chini A, Hamberg M, Adie B and Porzel A. 2009. (+)-7-iso-Jasmonyl-L-isoleucine is the endogenous bioactive jasmonate. *Nature Chemical Biology* 5 (5), 344-350.

Fu ZQ. and Dong X. 2013. Systemic Acquired Resistance: Turning Local Infection into Global Defense. *Annual Review of Plant Biology* 64, 839-863.

Fu ZQ, Yan S, Saleh A, Wang W, Ruble J, Oka N, Mohan R, Spoel SH, Tada Y, Zheng N and Dong X. 2012. NPR3 and NPR4 are receptors for the immune signal salicylic acid in plants. *Nature* 486 (7402), 228-232.

Gao Z, Chen YF, Randlett MD, Zhao XC, Findell JL, Kieber JJ and Schaller GE. 2003. Localization of the Raf-like kinase CTR1 to the endoplasmic reticulum of Arabidopsis through participation in ethylene receptor signaling complexes. *The Journal of Biological Chemistry* 278 (36), 34725.34732.

Garcia AV, Blanvillain-Baufume S, Huibers RP, Wiermer M, Li G, Gobbato E, Rietz S and Parker JE. 2010. Balanced nuclear and cytoplasmic activities of EDS1 are required for a complete plant immune response. *PLoS Pathogens* 6(7), e1000970

Garcia-Brugger a., Lamotte O., Vandelle E., Bourque S.,Lecourieux D., Poinssot B., Wendehenne D. and Pugin A. 2006. Early signaling events induced by elicitors of plant defenses. *Molecular Plant Microbe Interactions* 19, 711-724.

Gassmann W, Hinsch ME and Staskawicz BJ. 1999. The *Arabidopsis RPS4* bacterial-resistance gene is member of the TIR-NBS-LRR family of disease-resistance genes. *Plant Journal* 20(3), 265-277.

Ghanta S and Chattopadhyay S. 2011. Gluathione as a signaling molecule. *Plant Signaling & Behaviour* 6(6), 783-788.

Gietz RD and Woods RA. 2002. Transformation of yeast by the LiAc/SS carrier DNA/PEG method. *Methods in Enzymology* 350: 87-96.

Gimenez-Ibanez S., Hann DR., Ntoukakis V., Petutschnig E., Lipka V. and Rathjen JP. 2009. AvrPtoB targets the LysM receptor kinase CERK1 to promote bacterial virulence on plants. *Current Biology* 19, 423-429.

Gomez-Gomez L. and Boller T. 2000. FLS2: a LRR receptor-like kinase involved in the perception of the bacterial elicitor flagellin in *Arabidopsis*. *Molecular Cell* 5, 1003-1011.

Gomez-Gomez L, Felix G and Boller T. 1999. A single locus determines sensitivity to bacterial flagellin in Arabidopsis thaliana. *Plant Journal* 18 (3), 277-284.

Gohre V., Spallek T., Haweker H., Mersmann S. and Mentzel T. 2008. Plant pattern-recognition receptor FLS2 is directed for degradation by the bacterial ubiquitin ligase AvrPtoB. *Current Biology* 18, 1824-1832.

Hanahan D. 1983. Studies on transformation of Escherichia coli with plasmids. *Journal of Molecular Biology* 166, no. 4 (June 5): 557-850.

Hauck P., Thilmony R. and he SY. 2003. A Pseudomonas syringae type III effector suppresses cell wall-based extracellular defense in susceptible Arabidopsis plants. *Proc. Natl. Acad. Sci. USA* 100, 8577-8582.

Hartley JL, Temple GF and Brasch MA. 2000. DNA cloning using in vitro site-specific recombination. *Genome Research* 10, no. 11 (November): 1788-1795.

Heidrich K, Wirtmueller L, Tasset C, Pouzet C, Deslandes L and Parker JE. 2011. Arabidopsis EDS1 connects pathogen effector recognition to cell compartiment-specific immune responses. *Science* 334 (6061), 1401-1404.

Hepworth SR, Zhang Y, McKim S, Li X and Haughn GW. 2005. BLADE-ON-PETIOLE-dependent signaling controls leaf and floral patterning in Arabidopsis. *Plant Cell* 17 (5), 1434-1448.

Hilson P, Allemeersch J, Altmann T, Aubourg S, Avon A, Beyon J, Bhalerao RP et al. 2004. Versatile Gene-Specific Sequence Tags for Arabidopsis Functional Genomics: Transcript Profiling and Reverse Genetics Applications. *Genome Research* 14(10b), 2176-2189.

Hou S., Yang Y., Wu D. and Zhang C. 2011. Evolutionary insights from PBS1, Pto and RIN4. *Plant Signaling & Behaviour* 6:6, 794-799.

Huang CF, Yamaji N and Ma JF. 2010. Knockout of a bacterial-type ATP-binding cassette transporter gene, AtSTAR1, results in increased aluminum sensitivity in Arabidopsis. *Plant Physiology* (153(4), 1669-1677.

Huang CF, Yamaji N, Mitani N, Yano M, Nagamura Y and Ma JF. 2009. A bacterial ABC transporter is involved in aluminum tolerance in rice. *Plant Cell* 21, 655-667.

Ishihama N and Yoshioka H. 2012. Post-translational regulation of WRKY transcription factors in plant immunity. *Current Opinion in Plant Biology* 15 (4), 431-437.

Jakoby M, Weisshaar B, Dröge-Laser W, Vicente-Carbajosa J, Tiedemann J, Kroj T and Parcy F 2002. bZIP transcription factors in Arabidopsis. *Trends in Plant Science* 7 (3), 106-111.

Jaskiewicz M, Conrath U and Peterhansel C. 2011. Chromatin modification acts as a memory for systemic acquired resistance in the plant stress response. *EMBO Reports* 12 (1), 50-55.

Johnson C, Boden E and Arias J. 2003. Salicylic acid and NPR1 induce the recruitment of *trans*-activating TGA factors to a defense gene promoter in Arabidopsis. *Plant Cell* 15 (8), 1846-1858.

Jones JD. and Dangl JL. 2006. The plant immune system. *Nature* 444, 323-329.

Ju C, Yoon GM, Shemansky JM, Lin DY, Ying ZI, Chang J, Garret WM, Kessenbrock WM, Groth G, Tucker ML, Cooper B, Kieber JJ and Chang C. 2012. CTR1 phosphorylates the central regulator EIN2 to control ethylene hormone signaling from ER membrane to the nucleus in Arabidopsis. *Proc. Natl. Acad. Sci. USA* 109 (47), 19486-19491.

Jung HW., Tschaplinski TJ., Wang L., Glazebrook J. and Greenberg JT. 2009. Priming in systemic plant immunity. *Science* 324, 89-91.

Kaltdorf M and Naseem M. 2013. How Many Salicylic Acid Receptors Does a Plant Cell Need? *Science Signaling* 6 (279) jc3.

Katagiri F, Lam E and Chua NH. 1989. Two tobacco DNA-binding proteins with homology to the nuclear factor CREB. *Nature* 340 (6236), 727-730.

Kesarwani M, Yoo J and Dong X. 2007. Genetic interactions of TGA transcription factors in the regulation of pathogenesis-related genes and disease resistance in Arabidopsis. *Plant Physiology* 144 (1), 336-346.

Kinkema M, Fan W and Dong X. 2000. Nuclear localization of NPR1 is required for activation of *PR* gene expression. *Plant Cell* 12 (12), 2339-2350.

Koeck M, Hardham AR and Dodds PN. 2011. The role of effectors of biotrophic and hemibiotrophic fungi in infection. *Cellular Microbiology* 13 (12), 1849-1857.

Kojer K, Bien M, Gangel H, Morgan B, Dick TP and Riemer J. 2012. Glutathione redox potential in the mitochondrial intermembrane space is linked to the cytosol and impacts the Mia40 redox state. *EMBO Journal* 31 (14), 3169-3182.

Kojima S, Bohner A, Gassert B, Yuan L and von Wiren N. 2007. AtDUR3 represents the major transporter for high-affininty urea transport across the plasma membrane of nitrogen-deficient Arabidopsis roots. *Plant Journal* 52(1), 20-40.

Köster J, Thurow C, Kruse K, Meier A, Iven T, Feussner I and Gatz C. 2012. Xenobiotic- and jasmonic acid-inducible signal transduction pathways have become interdependent at the Arabidopsis *CYP81D11* promoter. *Plant Physiology* 159(1), 391-402.

Laby RJ, Kim D and Gibson SI. 2001. The *ram1* Mutant of Arabidopsis Exhibits severly Decreased β-Amylase Activity. *Plant Physiology* 127(4), 1798-1807.

La Camera S, L`haridon F, Astier J, Zander M, Abou-Mansour E, Page G, Thurow C, Wendehenne D, Gatz C, Metraux JP anf Lamotte O. 2011. The glutaredoxin ATGRXS13 is required to facilitate Botrytis cinerea infection of Arabidopsis thaliana plants. *Plant Journal* 68 (3), 507-519.

Lam E, Benfey PN, Gilmartin PM, Fang R and Chua NH. 1989. Site-specific mutations alter in vitro factor binding and change promoter expression pattern in transgenic plants. *Proc. Natl. Acad. Sci.* 86, 7890-7894.

Lam E and Lam YK. 1995. Binding site requirements and differential representation of TGA factors in nuclear ASF-1 activity. *Nucleic Acids Research* 23(18), 3778-3785.

Lam HM, Wong P, Chan HK, Yam KM, Chen L, Chow CM, Coruzzi GM. 2003. Overexpression of the ASN1 gene enhances nitrogen status in seeds of Arabidopsis. *Plant Physiology* 132(2), 926-935.

Landy A. 1989. Dynamic, structural, and regulatory aspects of lambda site-specific recombination. *Annual Review of Biochemistry* 58: 913-949.

Lemaire SD. 2004. The glutaredoxin family in oxygenic photosynthetic organisms. *Photosynthesis research* 79 (3), 305-318.

Li S, lauri A, Ziemann M, Busch A, Bhave M and Zachgo S. 2009. Nuclear Activity of ROXY1, a Glutaredoxin Interacting with TGA Factors, Is Required for Petal Development in Arabidopsis thaliana. *Plant Cell* 21, 429-441.

Li X, Clarke JD, Zhang Y and Dong X. 2001. Activation of an EDS1-mediated R-gene Pathway in the *snc1* Mutant Leads to Constitutive, NPR1-Independent Pathogen Resistance. *Molecular Plant-Microbe Interactions* 14(10). 1131-1139.

Lillig CH and Berndt C. 2013. Glutaredoxins in Thiol/Disulfide Exchange. *Antioxidants & Redox Signaling* 18 (13), 1654-1665.

Lindermayr C, Sell S, Müller B, Leister D and Durner J. 2010. Redox regulation of the NPR1-TGA1 system of Arabidopsis thaliana nitric oxide. *Plant Cell* 22(8), 2894-2907.

Lipka U, Fuchs R and Lipka V. 2008. Arabidopsis non-host resistance to powdery mildews. *Current Opinion in Plant Biology* 11, no. 4 (August): 329-339

Louis J, Lorenc-Kukula K, Singh V, Reese J, Jander G and Shah J. 2010. Antibiosis against the green peach aphid requires the Arabidopsis thaliana MYZUS PERSICAE-INDUCED LIPASE1 gene. *Plant Journal* 64(5), 800-811.

Luna E., Bruce TJ., Roberts MR., Flors V and Ton J. 2012. Next-generation systemic acquired resistance. *Plant Physiology* 158, 844-853.

Mackey D., Holt BF. 3rd, Wiig A. and Dangl JL. 2002. RIN4 interacts with Pseudomonas syringae type III effector molecules and is required for RPM1-mediated resistance in Arabidopsis. *Cell* 108, 743-754.

Mackey D., Belkhadir Y., Alonso JM., Ecker JR. and Dangl JL. 2003. Arabidopsis RIN4 is a target of the type III virulence effector AvrRprt2 and modulates RPS2-mediated resistance. *Cell* 112, 379-389.

Maldonado AM., Doerner P., Dixon RA., Lamb CJ and Cameron RK. 2002. A putative lipid transfer protein involved in systemic acquired resistance signaling in *Arabidopsis*. *Nature* 419, 399-403.

Marathe R. and Dinesh-Kumar SP. 2003. Plant Defense: One Post, Multiple Guards?! *Molecular Cell* 11 (2), 284-286.

Mercado-Blanco J., van der Drift KM., Olsson PE., Thomas-Oates JE., van Loon LC. And Bakker PA. 2001. Analysis of the *pmsCEAB* gene cluster involved in biosynthesis of salicylic acid and the siderophore pseudomine in the biocontrol strain *Pseudomonas fluorescens* WCS374. *Journal of Bacteriology* 183, 1909-1920.

Mishina TE and Zeier J. 2006. The Arabidopsis Flavin-Dependent Monooxygenase FMO1 Is an Essential Component of Biologically Induced Systemic Acquired Resistance. *Plant Physiology* 141 (4), 1666-1675.

Mishina TE and Zeier J. 2007. Pathogen-associated molecular pattern recognition rather than development of tissue necrosis contributes to bacterial induction of systemic acquired resistance in Arabidopsis. *Plant Journal* 50 (3), 500-513.

Mou Z, Fan W and Dong X. 2003. Inducers of plant systemic acquired resistance regulate NPR1 function through redox changes. *Cell* 113, 935-944.

Murmu J, Bush MJ, DeLong C, Li S, Xu M, Khan M, Malcolmson C, Fobert PR, Zachgo S and Hepworth SR. 2010. Arabidopsis basic leucine-zipper transcription factors TGA9 and TGA10 interact with floral glutaredoxins ROXY1 and ROXY2 and are redundantly required for anther development. *Plant Physiology* 154 (3), 1492-1504.

Ndamukong I, Abdallat AA, Thurow C, Fode B, Zander M, Weigel R and Gatz C. 2007. SA-inducible Arabidopsis glutaredoxin interacts with TGA factors and suppresses JA-responsive PDF1.2 transcription. *Plant Journal* 50 (1), 128-139.

Nimchuk Z., Eulgem T., Holt BF. And Dangl JL. 2003. Recognition and response in the plant immune system. *Annual Review of Genetics* 37, 579-609.

Nürnberger T and Lipka V. 2005. Non-host resistance in plants: new insights into an old phenomenon. *Molecular Plant Pathology* 6 (3), 335-345.

Nürnberger T., Brunner F., Kemmerling B. and Piater L. 2004. Innate immunity in plants and animals: striking similarities and obvious differences. *Immunol Rev* 198, 249-266.

Park SW., Kaimoyo E, Kumar D., Mosher S. and Klessig DF. 2007. Methyl salicylate is a critical mobile signal for plant systemic acquired resistance. *Science* 318, 113-116.

Parker JE, Colemann MJ, Szabo V, Frost LN, Schmidt R, van der Biezen EA, Moores T, Dean C, Daniles MJ and Jones JDG. 1997. The Arabidopsis downy mildew resistance gene *RPP5* shares similarity to the Toll and Interleukin-1 receptors with *N* and *L6*. *Plant Cell* 9, 879-894.

Parker JE, Holub EB,Frost LN, Falk A, Gunn ND and Daniels MJ. 1996. Characterization of *eds1*, a mutation in Arabidopsis suppressing resistance to Peronospora parasitica specified by several different *RPP* genes, *Plant Cell* 8, 2033-2046.

Pauwels L, Barbero GF, Geerinck J, Tillemann S, Grunewald W, Perez AC, Chico JM, Bossche RV, Sewell J, Gil E, Garcia-Casado G, Witters E, Inze D, Long JA, De Jaeger G, Solano R and Goossens A. 2010. NINJA connects the co-repressor TOPLESS to jasmonate signaling. *Nature* 464 (7289), 788-791.

Pfund C., Tans-Kersten J., Dunning FM., Alonso JM., Ecker JR., Allen C. and Bent AF. 2004. Flagellin is not a major defense elicitor in Ralstonia solanacearum cells or extracts applied to *Arabidopsis thaliana*. *Molecular Plant-Microbe Interaction* 17, 696-706.

Pieterse CMJ, Leon-Reyes A, Van der Ent S and Van Wees SCM. 2009. Networking by small-molecule hormones in plant imunity. *Nature Chemical Biology* 5 (5), 308-316.

Postel S. and Kemmerling B. 2009. Plant systems for recognition of pathogen-associated molecular patterns. *Seminars in Cell & Developmental Biology* 20, 1025-1031.

Pre M, Atallah M, Champion A, De Vos M, Pieterse CM and Memelink J. 2008. The AP2/ERF domain transcription factor ORA59 integrates jasmonic acid and ethylene signals in plant defense. *Plant Physiology* 147 (3), 1347-1357.

Qiao H, Shen Z, Huang SS, Schmitz RJ, Urich MA, Briggs SP and JR Ecker. 2012. Processing and subcellular trafficking of ER-tethered EIN2 control response to ethylene gas. *Science* 338(6105), 390-393.

Rasmussen MW, Roux M, Petersen M and Mundy J. 2012. MAP Kinase Cascades in Arabidopsis Innate Immunity. *Frontiers in Plant Science* 3 (169).

Rate DN and Greenberg JT. 2001. The *Arabidopsis aberrant growth and death 2* mutants shows resistance to *Pseudomonas syringae* and reveals a role for NPR1 in suppressing hypersensitive cell death. *Plant Journal* 27, 203-211.

Ritter C and Dangl JL. 1995. The avrRpm1 gene of Pseudomonas syringae pv. maculicola is required for virulence on Arabidopsis. *Molecular Plant-Microbe Interactions* 8(3), 444-453.

Running MP and Meyerowitz EM. 1996. Mutations in the PERIANTHIA gene of Arabidopsis specifically alter floral organ number and initiation pattern. *Development* 122 (4), 1261-1269.

Ryals J, Lawton KA, Delaney TP, Friedrich L, Kessmann H, Neuenschwander U, Uknes S, Vernooij B and Weymann K. 1995. Signal transduction in systemic acquired resistance. *Proc. Natl. Acad. Sci.* 92 (10), 4202-4205.

Scheible WR, Morcuende R, Czechowski T, Fritz C, Osuna D, Palacios-Rojas N, Schindelasch D, Thimm O, Udvardi MK and Stitt M. Genome-wide reprogramming of primary and secondary metabolism, protein synthesis, cellular growth processes, and

regulatory infrastructure of Arabidopsis in response to nitrogen. *Plant Physiology* 136(11), 2483-2499.

Schaller A and Stintzi A. 2009. Enzymes in jasmonate biosynthesis: structure, function, regulation. *Phytochemistry* 70 (13-14), 1532-1538.

Schmid M, Uhlenhaut NH, Godard F, Demar M, Bressan R, Weigel D and Lohmann JU. 2003. Dissection of floral induction pathways using global expression analysis. *Development* 130, 6001-6012.

Schmittgen TD, Livak KJ. 2008. Analyzing real-time PCR data by comparative C(T) method. *Nature Protocols* 3 (6): 1101-1108.

Schulze-Lefert P. 2004. Knocking on the heaven´s wall. Pathogenesis of and resistance to biotrophic fungi at the cell wall. *Current Opinion in Plant Biology* 7, 377-383.

Schwessinger B. and Zipfel C. 2008. News from the frontline_ recent insights into PAMP-triggered immunity in plants. *Current Opinion in Plant Biology* 11, 389-395.

Sels J., Mathys J., De Coninck BM., Cammue BP. And De Bolle MF. 2008. Plant pathogenesis-related (PR) proteins: a focus on PR peptides. *Plant Physiology and Biochemistry* 46, 941-950.

Senthil-Kumar M and Mysore KS. 2013. Nonhost Resistance Against Bacterial Pathogens: Retrospectives and Prospects. *Annual Review of Phytopathology* 51, 407-427.

Shearer HL, Cheng YT, Wang L, Liu J, Boyle P, Despres C, Zhang Y, Li X and Fobert PR. 2012. *Arabidopsis* Clade I TGA Transcription Factors Regulate Plant Defenses in an NPR1-Independent Fashion. *Molecular Plant-Microbe Interactions* 25 (11), 1459-1468.

Shearer HL, Wang L, DeLong C, Despres C and Fobert PR. 2009. NPR1 enhances the DNA binding activity of the *Arabidopsis* bZIP transcription factor TGA7. *Botany* 87, 561-570.

Sheen J. 2001. Signal transduction in maize and Arabidopsis mesophyll protoplasts. *Plant Physiology* 127, no. 4 (December): 1466-1475.

Solano R, Stepanova A, Chao Q and Ecker JR. 1998. Nuclear events in ethylene signaling: a transcriptional cascade mediated by ETHYLENE-INSENSITIVE3 and ETHYLENE-RESPONSE-FACTOR1. *Genes & Development* 12 (23), 3703-3714.

Spoel SH and Dong X. 2008. Making sense of hormone crosstalk during plant immune responses. *Cell Host & Microbe* 3 (6), 348-351.

Srivastava MK, Dwivedi UN. 1998. Salicylic acid modulates glutathione metabolism in pea seedlings. *Plant Physiol*ogy 153, 409–414.

Stepanova AN and Alonso JM. 2009. Ethylene signaling and response: where different regulatory modules meet. *Current Opinion in Plant Biology* 12 (5), 548-555.

Strawn MA, Marr SK, Inoue K, Inada N, Zubieta C and Wildermuth MC. 2007. Arabidopsis isochorismate synthase functional in pathogen-induced salicylate biosynthesis exhibit properties consistent with a role diverse stress responses. *The Journal of Biological Chemistry* 282 (8), 5919-5933.

Sun Y., Li L., Macho AP., Han Z., Hu Z. Zipfel C.,Zhou J. and Chai J. 2013. Structural Basis for flg22-Induced Activation of the Arabidopsis FLS2-BAK1 Immune complex. *Science* 1243825.

Tada Y, Spoel Sh, Pajerowska-Mukthar K, Mou Z, Song J, Wang C, Zuo J and Dong X. Plant immunity requires conformational changes of NPR1 via S-nitrosylation and thoiredoxins. *Science* 321 (5891), 952-956.

Thines B, Katsir L, Melotto M, Niu Y, Mandaokar A, Liu G, Nomura K, He SY, Howe GA and Browse J. 2007. JAZ repressor proteins are targets of the SCF(COI1) complex during jasmonate signaling. *Nature* 448 (7154), 661-665.

Torres MA., Dangl JL. and Jones JD. 2002. Arabidopsis gp91phox homologues AtrbohD and AtrbohF are required for accumulation of reactive oxygen intermediates in the plant defense response. *Proc. Natl. Acad. Sci.* 99, 517-522.

Truman W., Bennett MH., Kubigsteltig I., Turnbull C. and Grant M. 2007. Arabidopsis systemic immunity uses conserved defense signaling pathways and is mediated by jasmonates. *Proc. Natl. Acad. Sci USA* 104, 1075-1080.

Tsuda K, Mine A, Bethke G, Igarashi D, Botanga CJ, Tsuda Y, Glazebrook J, Sato M and Katagiri F. 2013. Dual Regulation of Gene Expression Mediated by extended MAPK Activation and Salicylic Acid Contributes to Robust Innate Immuity in *Arabidopsis thaliana*. *PLoS Genetics* 9(12), e10004015.

Tsuda K, Sato M, Glazebrook J, Cohen JD and Katagiri F. 2008. Interplay between MAMP-triggered and SA-mediated defense responses. *Plant Journal* 53 (3), 763-775.

van den Burg HA. and Takken FL. 2009. Does chromatin remodeling mark systemic acquired resistance? *Trends in Plant Science* 14 (5), 286-294.

Van der Biezen EA, Freddie CT, Kahn K, Parker JE and Jones JDG. 2002. Arabidopsis *RPP4* is a member oft he *RPP5* multigene family of TIR-NB-LRR genes and confers downy mildew resistance through multiple signalling components. *Plant Journal* 29, 439-451.

Van der Hoom RAL and Kamoun S. 2008. From Guard to Decoy: A new Model for Perception of Plant Pathogen Effectors. *Plant Cell* 20 (8), 2009-2017.

Vernooij B, Friedrich L, Morse A, Reist R, Kolditz-Jawhar R, Ward E, Uknes S, Kessmann H and Ryals J. 1994. Salicylic Acid Is Not the Translocated Signal Responsible for Inducin Systemic Acquired Resistance but is Required in Signal Transduction. *Plant Cell* 6 (7), 959-965.

Vlot AC, Dempsey DA and Klessig DF. 2009. Salicylic acid, a multifaceted hormone to cambat disease. *Annual Reviews of Phytopathology* 47, 177-206.

Vogel JP., Raab TK., Schiff C. and Sommerville SC. 2002. PMR6, a pectate lyase like gene required for powdery mildew susceptibility in *Arabidopsis*. *Plant Cell* 14, 2095-2106.

Vogel-Adghough D, Stahl E, Navarpva H and Zeier J. 2013. Pipecolic acid enhances resistance to bacterial infection and primes salicylic acid and nicotine accumulation in tobacco. *Plant Signaling & Behaviour* 8 (11), e26366.

Wang L and Fobert PR. 2013. *Arabidopsis* Clade I TGA Factors Regulate Apoplastic Defences against the Bacterial Pathogen *Pseudomonnas syringae* through Endoplasmic Reticulum-Based Processes. *PLoS One* 8 (9), e77378

Wang JW, Czech B and Weigel D. 2009. *miR156*-regulated SPL transcription factors define a endogenous flowering pathway in *Arabidopsis thaliana*. *Cell* 138, 738-749.

Wang Z, Shuping X, Birenbihl RP and Zachgo S. 2009. Conserved Functions of Arabidopsis and Rice CC-Type Glutaredoxins in Flower Development and Pathogen Response. *Molecular Plant* 2 (2), 323-335.

Wen X, Zhang C, Ji Y, Zhao Q, He W, An F, Jiang L and Guo H. 2012. Activation of ethylene signaling is mediated by nuclear translocation of the cleaved EIN2 carboxyl terminus. *Cell Research* 22(11), 1613-1616.

Whalen MC, Innes RW, Bent AF and Staskawicz BJ. 1991. Identification of Pseudomonas syringae pathogens of Arabidopsis and a bacterial locus determining avirulence on both Arabidopsis and soybean. *Plant Cell* 3(1), 49-59.

Wiermer M, Feys BJ and Parker JE. 2005. Plant immunity: the EDS1 regulatory node. *Current Opinion in Plant Biology* 8(4), 383-389.

Wildermuth MC, Dewdney J, WU G and Ausubel FM. 2001. Isochorismate synthase is required to synthesize salicylic acid for plant defence. *Nature* 414, 562-565.

Wirthmüller L, Zhang Y, Jones JD and Parker JE. 2007. Nuclear accumulation of the Arabidopsis immune receptor RPS4 is necessary for triggering EDS1-dependent defense. *Current Biology* 17(23), 2023-2029.

Wu G, Poethig RS. 2006. Temporal regulation of shoot development in *Arabidopsis thaliana* by *miR156* and its target *SPL3*. *Development* 133(18), 3539-3547.

Wu Y, Zhang D, Chu JY, Boyle P, Wang Y, Brindle ID, De Luca V and Despres C. 2012. The Arabidopsis NPR1 protein is a receptor for the plant defense hormone salicylic acid. *Cell Reports* 1 (6), 639-647.

Xiang T, Zhong N, Zou Y, Wu Y, Zhang J, Xing W, Li Y, Tang X, Zhu L, Chai J and Zhou JM. 2008. *Pseudomonas syringae* effector AvrPto blocks innate immunity by targeting receptor kinases. *Current Biology* 18 (1), 74-80

Xie DX, Feys BF, James S, Nieto-Rostro M and Turner JG. 1998. COI1: and Arabidopsis gene required for jasmonate-regulated defense and fertility. *Science* 280 (5366), 1091-1094.

Xing S, Rosso MG and Zachgo S. 2008. ROXY1, a member of the plant glutaredoxin family, is required for petal development in Arabidopsis thaliana. *Development* 132 (7), 1555-1565.

Xing S, Salinas M and Huijser P. 2011. New players unveiled in early anther development. *Plant Signaling & Behaviour* 6 (7), 934-938.

Xing S and Zachgo S. 2008. ROXY1 and ROXY2, two Arabidopsis glutaredoxin genes, are required for anther development. *Plant Journal* 53 (5), 790-801.

Xin XF. And HE SH. 2013. *Pseudomonas syringae* pv. *tomato* DC3000: A Model Pathogen for Probing Disease Susceptibility and Hormone Signaling in Plants. *Annual Reviews Phytopathology* 51, 473-498.

Yamada K, Hara-Nishimura I and Nishimura M. 2011. Unique defense strategy by the endoplasmic reticulum body in plants. *Plant Cell Physiology* 52(12), 2039-2049.

Yamada K, Nagano AJ, Ogasawara K, Hara-Nishimura I and Nishimura M. 2009. The ER body, a new organelle in Arabidopsis thaliana, requires NAI2 for its formation and accumulates specific beta-glucosidases. *Plant Signaling & Behavior* 4(9), 849-852.

Zachowski A, Guerbette F, Grosbois M, Jolliot-Croquin A and Kader JC. 1998. Characterisation of acyl binding by a plant lipid-transfer protein. *European Journal of Biochemistry* 257(2), 443-448.

Zander M, Chen S, Imkampe J, Thurow and Gatz C. 2012. Repression of the Arabidopsis jasmonic acid/ethylene-induced defense pathway by TGA-interacting glutaredoxins depends on their C-terminal ALWL motif. *Molecular Plant* 5 (4), 831-840.

Zander M, La Camera S, Lamotte O, Metraux JP and Gatz C. 2010. Arabidopsis thaliana class-II TGA transcription factors are essential activators of jasmonic acid/ethylene-induced defense responses. *Plant Journal* 61 (2), 200-210.

Zhang X, Chen S and Mou Z. 2010. Nuclear accumulation of NPR1 is required for regulation of salicylate tolerance, isochorismate synthase 1 expression and salicylate accumulation in Arabidopsis. *Plant Physiology* 167 (2), 144-148.

Zhang Y, Cheng YT, Qu N, Zhao Q, Bi D and Li X. 2006. Negative regulation of defense responses in Arabidopsis by two NPR1 paralogs. *Plant Journal* 48 (5), 647-656.

Zhang Y, Fan W, Kinkema M, Li X and Dong X. 1999. Interaction of NPR1 with basic leucine zipper protein transcription factors that bind sequences required for salicylic acid induction of the *PR-1* gene. *Proc. Natl. Acad. Sci.* 96, 6523-6528.

Zhang Y, Goritschnig S, Dong X and Li X. 2003a. A gain-of-function mutation in a plant disease resistance gene leads to constitutive activation of downstream signal transduction pathways in suppressor of *npr1*-1, *constitutive 1*. *Plant Cell* 15(11), 2636-2646.

Zhang Y, Tessaro MJ, Lassner M and Li X. 2003b. Knockout analysis of Arabidopsis transcription factors TGA2, TGA5, and TGA6 reveals their redundant and essential roles in systemic acquired resistance. *Plant Cell* 15 (11), 2647-2653.

Zhou JM, Trifa Y, Silva H, Pontier D, Lam E, Shah J and Klessig DF. 2000. NPR1 differentially interacts with members of the TGA/OBF family of transcription factors that bind an element of the PR-1 gene required for induction by salicylic acid. *Molecular Plant Microbe Interactions* 13 (2), 191-202.

8 Abbreviations

Abbreviation	Description
aa	amino acids
A	Ampere
AD	activation domain
amp	ampicillin
AMS	4-acetamido-4′-maleimidylstilbene-2,2′-disulfonic acid
APS	ammoniumpersulfate
as-1	activating sequence 1
A. thaliana	*Arabidopsis thaliana*
A. tumefaciens	*Agrobacterium tumefaciens*
bp	base pairs
BSA	bovine serum albumine
bZIP	basic leucine zipper
CaMV	cauliflower mosaic virus
cDNA	copy DNA
C_T	threshold cycle
C-terminal	carboxy-terminal
Da	dalton
DNA	desoxyribonucleic acid
DNase	desoxyribonuclease

dNTPs	desoxyribonucleotides
E. coli	*Escherichia coli*
ET	Ethylene
et al.	*at alii*
F	Farad
g	Gravitation
g	gram
β-Gal	β-galactosidase
gDNA	genomic DNA
GRXs	glutaredoxins
h	Hours
HIS	marker gene for histidine prototrophy
hpi	hours past infection
HR	hypersensitive response
HSP	herring sperm DNA
JA	Jasmonic acid
kan	Kanamycine
L	litre
lacZ	gene coding for β-galactosidase
LB	Left border
LiAc	Lithium acetate
LUC	luciferase
µ	micro (10^{-6})

m	mili (10^{-3})
m	meter
M	molarity [mol/L]
min	minutes
MP	non-fat dry milk
MS	Murashige and Skoog
n	nano (10^{-9})
NPR1	NON-Expressor of PR-GENES 1
Ω	Ohm
OD	optical density
o/n	over night
ONPG	o-nitrophenyl-β-D-galactopyranoside
ONP	o-nitrophenol
p	pico
PAA	polyacrylamide
PAGE	polyacrylamide gelelectrophoresis
PCR	polymerase chain reaction
PCD	programmed cell death
PDA	potato dextrose agar
PDB	potato dextrose browth
pH	negative log10 of proton concentration
PR1	pathogenesis-related 1
RNA	ribonucleic acid

ROS	reactive oxygen species
rpm	rotations per minute
RT	room temperature
s	second
SA	salicylic acid
SAR	systemic acquired resistance
SDS	sodium dodecylsulfate
spec	spectinomycine
TEMED	N,N,N´,N´-tetraethylenediamine
TGA	TGACG motif binding bZIP transcription factor
Tris	Tris-hydroxymethylamino methane
u	unit
UV	ultra violet
V	Volt
v/v	volume per volume
wt	Wildtype
w/v	weight per volume

9 Acknowledgements

An dieser Stelle möchte ich mich zuerst bei Frau Prof. Dr. Christiane Gatz bedanken. Mit der „Aufnahme“ in Ihr Team haben Sie mir dieses Projekt in die Hände gelegt und mir damit großes Vertrauen entgegengebracht. Die doch jetzt langjährige Zusammenarbeit, gekennzeichnet durch alle Facetten der wissenschaftlichen Arbeit, hat mir aufgezeigt, dass es immer mehrere Sichtweisen auf Dinge gibt und dass man auch nach schwierigeren Phasen immer aufstehen kann. Danke für Ihre Unterstützung und Ihren Zuspruch, egal wie „ungefiltert“ ich meine Gedanken in Wort, Tat und Schrift hervorgebracht habe. Dieser Lebensabschnitt hat mich nachhaltig geprägt und charakterlich bereichert.

Meinem Korreferenten Prof. Dr Volker Lipka danke ich für die bereitwillige Unterstützung dieser Arbeit und, an dieser Stelle möchte ich mich Mark Zander anschließen, für die Einblicke in die offensive Diskussionskultur: hart aber fair und im Gespräch danach auch ein wenig herzlich. Also doch noch ein wenig mehr Ruhrgebiet als manchmal angenommen.

Mein Dank gilt auch Frau Jr. Prof. Dr. Gleason, Frau Prof. Dr. Polle, Herrn Prof. Dr. Feussner und Herrn PD Dr. Thomas Teichmann für das Beiwohnen meiner Prüfungskommission.

An dieser Stelle möchte ich Sonja von ganzem Herzen danken. Du bist während meiner Zeit in Göttingen in mein Leben getreten und hast es von Anfang an bereichert. Du hast mich während meiner Doktorarbeit in allen Situationen unterstützt und „ertragen“, egal wie meine Launen waren und ich durch die Gegend gepoltert bin. Wir haben gemeinsam schwierige Zeiten durchgestanden und Du hast mir unseren gemeinsamen Sohn Jonas geschenkt. Er ist unser größtes Glück und durch seine Geburt und unsere kleine Familie ist auch Göttingen für mich Heimat geworden. Jonas, ich hoffe, Du verstehst in ein paar Jahren und nach eventueller Lektüre dieser Doktorarbeit, warum ich nicht immer mit Dir „pielen“ und toben konnte. Ich liebe Euch!

Meinen Eltern möchte ich mich für die fortwährende und volle Unterstützung in allen Lebenslagen und Lebensphasen bedanken. Euer Rückhalt hat mir immer Kraft gegeben um weiter vorwärts zu gehen. Ich hoffe, dass ich das, was ich von euch gelernt habe, auch an Jonas weitergeben kann und so gut für Ihn sorge wie Ihr es für mich getan habt und auch noch tut. Auch meiner Schwester Sabrina, Adrian, Til und Mia möchte ich danken. Ihr habt mir besonders durch die Einblicke in eine junge Familie geholfen. Dadurch sind mir manche Dinge leichter gefallen und verständlicher gewesen um meine Arbeit und meine Familie

besser unter einen Hut zu bekommen. Ich hoffe, dass wir uns in Zukunft wieder häufiger sehen.

Jetzt möchte ich noch kurz ,aber hoffentlich nicht zu kurz, meinen Kollegen, die mir über die Jahre über den Weg gelaufen sind oder es noch immer tun, danken.

Mein Dank gilt dem „Management“ unseres Abteilung. Corinna hat mir die „Unweiten“ und die „Matrix“ der Klonierung und der Datenauswertung nähert gebracht. Sie hatte immer ein offenes Ohr für spontane „Zwischenfragen“ und hat mir verdeutlicht, dass zwei oder drei Kontrollen besser sind als nur eine und dass Thripse der Teufel sind. Guido, unser Mann für alles, hat sich durch etwaige Probleme größerer und kleinerer Ordnung nie aus der Ruhe bringen lassen und war stets zur Stelle. Wahrscheinlich hätte ich auch einen Teil des Labores in Brand setzen können, auf schnelle und inovative Lösungen war immer Verlass. Auch ein großes Danke für die konstante Versorgung mit Plätzchen der Großbäckerei Kriete zur Weihnachtszeit.

Tief verbeugen muss ich mich vor unserer „technischen Power“. Auf Anna, Larissa und Ronny war immer Verlass und Sie unterstützen mich mit ausgezeichneter Qualität made in Göttingen. Auch neben der Arbeit bereicherten Gespräche über Gott und die Welt (oder Fußball, Politik; Familie; Weltgeschehen, wirres Zeug, etc.) den Laboralltag. Besonders muss ich dabei Larissa hervorheben, mit der ich die zweite Hälfte dieser Doktorarbeit ein Labor geteilt habe und diese Zeit vermissen werde. Auch bei unseren Gärtner Feli und Herr Wedemeyer muss ich mich bedanken und „entschuldigen“, für die zeitweise konstanten Massen an Tabletts. Diese wurden auch fast alle benutzt!

Nun fällt es mir schwer, weitere Personen hervorzuheben, da der „Durchsatz“ an Personen in meiner Zeit hoch war. Trotzdem möchte ich speziell Mark nebst Ehefrau, Sebastian, Rene nebst Ehefrau, Marcel nebst Familie und Alex danken, die in der Zeit auch außerhalb der Arbeit zu Freunden geworden sind. Dies hat die Zeit in Göttingen zurückblickend auch maßgeblich geprägt. Ich gelobe hiermit auch Besserung und versuche den teilweise geringen Kontakt wieder zu erhöhen. Natürlich sollen auch alle weiteren Personen wie Anjali, Neena, Johanna, Julia, Katja, Ning, Li-Jun, Fred, Natthanon, Jan, Joachim etc nicht unerwähnt bleiben. Danke für die nette Zusammenarbeit.

Ganz am Ende möchte ich Nils danken. Du hast mir durch so ein trauriges Ereignis gezeigt, was im Leben wirklich wichtig ist. Ruhe in Frieden mein Freund.

10 Curriculum Vitae

Persönliche Daten:

Name:	Martin Muthreich
Geburtsdatum/– ort:	am 01.07.1982 in Herne
Staatsangehörigkeit:	Deutsch

Schulische Laufbahn:

Juni 1988 bis Juni 1992	Grundschule an der Claudiusstraße in Herne
August 1992 bis Mai 2001	Gymnasium Wanne in Herne, Allgemeine Hochschulreife

Zivildienst:

August 2001 bis Mai 2002	St. Anna Hospital in Herne

Studium:

WS 2002/03 bis WS 2007/08	Ruhr-Universität Bochum, Diplomstudiengang Biologie
Institut der Diplomarbeit:	Lehrstuhl für Pflanzenphysiologie
Titel der Diplomarbeit:	„Charakterisierung einer Cystinlyase (AT4G23600) und einer Tyrosinaminotransferase (AT5G53970) in *Arabidopsis thaliana*“
seit WS 2008/09	Beginn der Promotion an der Georg-August-Universität Göttingen in der Arbeitsgruppe von Prof. Dr. Christiane Gatz. Dissertationsthema: „Characterization of clade I TGA transcription factors in *Arabidopsis thaliana* with respect to biotic stress.”

Göttingen, den 19.03.2014